Universidad de Valladolid

ESCUELA TÉCNICA SUPERIOR DE INGENIEROS DE TELECOMUNICACIÓN

DEPARTAMENTO DE TEORÍA DE LA SEÑAL Y COMUNICACIONES E INGENIERÍA TELEMÁTICA

TESIS DOCTORAL:

CONTRIBUCIONES EN EL CAMPO DE LA DETECCIÓN DE LA POSICIÓN Y VELOCIDAD DE MOTORES *BRUSHED* DC Y *BRUSHLESS* DC MEDIANTE TÉCNICAS SENSORLESS

Presentada por José Carlos Gamazo Real para optar al grado de doctor por la Universidad de Valladolid

Dirigida por:
Jaime Gómez Gil

Resumen

INTRODUCCIÓN

Los **motores eléctricos** son dispositivos que convierten energía eléctrica en energía mecánica. Dentro de los motores eléctricos de corriente continua se tienen los **motores con escobillas (*brushed* DC, BDC)**, que emplean escobillas para conmutar la corriente, y los **motores sin escobillas (*brushless* DC, BLDC)**, que emplean un inversor electrónico para realizar la conmutación de fases. Tradicionalmente, en situaciones en las que se necesitaba conocer la posición y velocidad en motores eléctricos, se empleaban sensores ópticos o magnéticos de giro acoplados al motor. En los últimos años ha surgido una nueva tecnología, denominada **tecnología sin sensores** (***sensorless***), que permite detectar la posición y velocidad del motor a partir de los parámetros eléctricos del mismo, como las corrientes o las tensiones de fase.

La revisión de la literatura relacionada con motores BLDC (**Artículo 1 del compendio**) y BDC sugiere que en el control de los mismos utilizando sensores de posición, como codificadores digitales (*encoders)*, transformadores de acoplamiento variable (*resolvers*) o sondas de efecto Hall, puede reducirse el coste y aumentar la fiabilidad mediante la sustitución de dichos sensores por técnicas *sensorless*.

OBJETIVOS

El objetivo general de la tesis comprende el análisis, desarrollo y validación de diversas **técnicas *sensorless*** para la detección de la posición y velocidad de motores BDC y BLDC. Para la consecución de este objetivo se han propuesto cuatro técnicas. La primera está basada en el análisis las ondulaciones o rizado (*ripple)* de la corriente en motores BDC (**patente ES 2334551 A1)**. La segunda se fundamenta también en la componente *ripple* de la corriente para motores BDC, pero utilizando reconocimiento de patrones con clasificadores (**Artículo 2 del compendio**). La tercera está basada en la derivada de los voltajes de fase para motores BLDC (**Artículo 3 del compendio**). La cuarta aplica redes neuronales artificiales a motores BLDC (**Artículo 4 del compendio**).

MÉTODOS

La primera técnica, basada en el análisis la componente *ripple*, permite determinar la posición y velocidad de un motor BDC mediante la detección de las ondulaciones que aparecen en la corriente del motor. En esta detección se utiliza la comparación entre las muestras actuales de la corriente y las inmediatamente cercanas en tiempo, además de una ventana de tamaño variable para la observación de las mismas.

En la segunda técnica, también basada en el análisis de la componente *ripple*, se estima la posición y velocidad de motores BDC utilizando reconocimiento de patrones con clasificadores de tipo Máquina Vectores de Soporte (*Support Vector Machine*, SVM). La posición se estima contabilizando las ondulaciones que aparecen en la corriente como consecuencia de la componente *ripple*, y la velocidad mediante el inverso del tiempo transcurrido entre ondulaciones. El clasificador SVM se utiliza para detectar las ondulaciones normales, así como detectar los pulsos fantasmas y descartar los pulsos falsos en la corriente como consecuencia del ruido.

En la tercera técnica se detecta la información de posición y velocidad de un motor BLDC a través de la derivada de los voltajes de fase con respecto a un punto neutro virtual. Para la implementación de la misma se ha desarrollado un *hardware* versátil basado en una matriz de puertas programable en campo (FPGA), en un procesador en tiempo real, y en otros componentes como filtros y amplificadores. Además, se emplean algoritmos *software* de procesamiento para detectar los pulsos de la derivada de las tensiones y para filtrar los pulsos falsos que son consecuencia del ruido.

En la cuarta técnica, basada en redes neuronales artificiales (ANNs), se estima la posición y velocidad de un motor BLDC mediante dos ANNs de tipo Perceptron Multicapa (*Multilayer Perceptron*, MLP); una de ellas para estimar la posición del rotor a partir de los voltajes de fase, y la otra para estimar la velocidad a partir del resultado de posición de la primera. Para el entrenamiento y *test* de las ANNs se utilizan como referencia los datos de posición de un *encoder* incremental, y se procesan los voltajes reales del motor mediante una FPGA, un procesador en tiempo real, electrónica de acondicionamiento y un ordenador.

RESULTADOS

En la primera técnica propuesta, basada en el análisis de la componente *ripple* de la corriente, se han obtenido unos errores absolutos medios de posición y velocidad inferiores a 17,75 rad y 4,64 rpm, respectivamente, en un rango de velocidades entre 5.000 rpm y 7.000 rpm en condiciones de velocidad constante o con una variación lenta de la velocidad del motor BDC, obteniéndose los peores resultados cuando la velocidad del motor varía bruscamente. En esta técnica, se logra minimizar el coste computacional y se consigue una cierta inmunidad al ruido en la corriente que permite reducir su influencia sobre la precisión.

En la segunda técnica propuesta, basada en el reconocimiento de patrones con clasificadores aplicados a la componente *ripple*, se han obtenido unos errores absolutos medios de posición y velocidad inferiores a 19 rad y 18 rpm, respectivamente, en un rango de velocidades entre 500 rpm y 11.000 rpm. Estos resultados se han logrado bajo diferentes condiciones de operación del motor BDC, como aceleración constante y saltos abruptos de velocidad. Con esta técnica, se consigue minimizar el efecto del ruido sobre la corriente, debido a la habilidad para detectar pulsos fantasmas y descartar pulsos falsos, pero con un alto coste computacional asociado.

En la tercera técnica propuesta, basada en derivada de los voltajes de fase, se han obtenido unos errores cuadráticos medios de posición entre 10º y 30º, y de velocidad inferiores a 3 rpm con el motor BLDC sin carga. Además, se han logrado unos errores cuadráticos medios de posición entre 10º y 15º, y de velocidad inferiores a 1 rpm en condiciones de plena carga del motor. Los resultados se han obtenido en un rango de velocidades entre 5 rpm y 1.500 rpm bajo diferentes condiciones de operación, como aceleración constante y saltos bruscos de velocidad. En esta técnica, se logra una relevante inmunidad al ruido sobre los voltajes de fase del motor y un alto rendimiento con bajo coste computacional.

En la cuarta técnica propuesta, basada en redes neuronales artificiales, se ha obtenido un error de posición absoluto medio de 6,47º y un error de velocidad relativo medio de 4,87% en un rango de velocidades entre 125 rpm y 1.500 rpm con una aceleración constante del motor BLDC a plena carga. En esta técnica, se logra una relevante inmunidad al ruido sobre los voltajes de fase del motor, y una baja influencia de los errores de posición sobre la estimación de velocidad, pero con un coste computacional ligeramente elevado debido al uso de las ANNs.

CONCLUSIONES

Los resultados muestran que las cuatro técnicas propuestas permiten la detección de la posición y velocidad, tanto en motores BDC como BLDC, con una aceptable precisión, inmunidad al ruido y coste computacional sobre un amplio rango de velocidades, aunque dependiendo de la técnica considerada se tienen mayores o menores mejoras en alguno de estos factores. En base a ello, puede considerarse que las técnicas desarrolladas representan una alternativa fiable respecto a técnicas de detección basadas en sensores y frente a técnicas *sensorless* básicas.

Estos resultados han permitido alcanzar los objetivos propuestos en la tesis, a partir de los cuales se han realizado una serie de aportaciones científicas que constituyen el núcleo de esta tesis presentada como **compendio de publicaciones**.

Palabras clave: *brushed* DC (BDC), *brushless* DC (BLDC), compendio de publicaciones, corriente, detección, *driver*, posición, *sensorless*, velocidad, voltaje, tesis.

Abstract

INTRODUCTION

The **electric motors** are devices that transform the electric energy into mechanical energy. Within direct current electric motors are **motors with brushes (brushed DC, BDC)**, which use the brushes in order to accomplish the current commutation, and **motors without brushes (brushless DC, BLDC**), which use an electronic inverter for performing the phases commutation. Traditionally, in situations that require knowing the position and the speed of electric motors, optical and magnetic sensors are coupled to the motor. In recent years, a new technology has arisen, called **technology without sensors (sensorless)**, which allows to detect the position and speed of the motor from its electrical parameters like the currents or the phase voltages.

The review of the literature related to BLDC motors (**Paper 1 of the compendium**) and BDC suggests that in their control by means of position sensors, such as digital encoders, variable coupling transformers (resolvers) or Hall-effect probes, the cost could be reduced and the reliability could be increased through replacing these sensors by sensorless techniques.

OBJECTIVES

The overall objective of the thesis includes the analysis, development and validation of several **sensorless techniques** in order to detect the position and the speed of BDC and BLDC motors. For achieving this objective, four techniques have been proposed. The first is based on the analysis of the undulations or ripple of the current in BDC motors (**patent ES 2334551 A1**). The second is also based on the ripple component of the current for BDC motors, but using patterns recognition with classifiers (**Paper 2 of the compendium**). The third is founded on the derivative of the phase voltages for BLDC motors (**Paper 3 of the compendium**). The fourth applies artificial neural networks to BLDC motors (**Paper 4 of the compendium**).

METHODS

The first technique, based on the analysis of the ripple component, allows to determining the position and the speed of a BDC motor through detecting the undulations of the motor current. This detection uses the comparison between actual samples of the current and other that are close in time, along with a resizable window for monitoring them.

The second technique, also based on the analysis of the ripple component, estimates the position and the speed of BDC motors using patterns recognition with the classifier Support Vector Machine (SVM). The position is estimated by counting the undulations of the current as a result of the ripple component, and the speed is obtained from the inverse time between undulations. The classifier SVM is used to detect the normal undulations, to detect the ghost pulses and to reject false pulses in the current that appear as a consequence of the noise.

In the third technique, the position and speed information of the BLDC motor is detected through the derivative of the phase voltages regarding to a virtual neutral point. The implementation has been performed by means of a versatile hardware based on a Field Programmable Gate Array (FPGA), a real-time processor, and other components like filters and amplifiers. In addition, software processing algorithms have been used to detect the pulses of the voltages derivative and to filter the false pulses that appear due to the noise.

In the fourth technique, based on artificial neural networks (ANNs), the position and the speed of a BLDC motor is estimated through two ANNs type Multilayer Perceptron (MLP); one for estimating the rotor position from the phase voltages, and another for estimating the speed by using the result obtained from the previous one. In the training and testing of the ANNs, the reference position data from an incremental encoder are used, and the real motor voltages are processed by means of a FPGA, a real-time processor, conditioning electronics and a computer.

RESULTS

In the first proposed technique, based on the analysis of the ripple component of the current, mean absolute position and speed errors lower than 17.75 rad and 4.64 rpm, respectively, have been obtained in the speed range between 5,000 and 7,000 rpm in conditions of constant speed or with a slowly speed variation of the BDC motor, and the worse results are attained when the motor speed changes sharply. In this technique, the computational cost is minimized and some noise immunity over the current is achieved, which allows reducing its influence on the precision.

In the second proposed technique, based on the application of patterns recognition with classifiers to ripple component, mean absolute position and speed errors lower than 19 rad and 18 rpm, respectively, have been obtained in a speed range between 500 rpm and 11,000 rpm. These results have been attained under different motor operation

conditions, such as linear and sharp variations of speed. The effect of the noise over the current is minimized in this technique due to its property of detect ghost pulses and reject false pulses, but with a high computational cost.

In the third proposed technique, based on the derivative of the phase voltages, mean square position errors between 10º and 30º, and mean square speed errors lower than 3 rpm have been accomplished without a motor load. In addition, mean square position errors between 10º and 15º, and mean square speed errors lower than 1 rpm have been attained at full load. These results have been obtained in a speed range between 5 rpm and 1,500 rpm, and under different motor operation conditions, such as linear acceleration and sharp speed variations. In this technique, remarkable noise immunity over the motor phase voltages and a high performance with low computational cost are achieved.

In the fourth proposed technique, based on artificial neural networks, a mean absolute position error of 6.47º, and a mean relative speed error of 4.87% have been attained in a speed range between 125 rpm and 1,500 rpm with a constant BLDC motor acceleration at full load. In this technique, relevant noise immunity over the motor phase voltages and a low influence of position errors over the speed estimation are achieved, but with a slightly higher computational cost related to the use of ANNs.

CONCLUSIONS

The results show that the four proposed techniques allow to detect the position and the speed in BDC and BLDC motors with an acceptable precision, noise immunity, and computational cost over a wide speed range, but depending on the considered technique a larger or smaller improvement is achieved in any of these factors. On this basis it could be considered that the developed techniques represent a reliable alternative to detection techniques based on sensors and over basic sensorless techniques.

These results have allowed to achieve the objectives in the thesis, from which there have been a series of scientific publications that are the core of this thesis presented as a **compendium of publications**.

Keywords: brushed DC (BDC), brushless DC (BLDC), compendium of publications, current, detection, driver, position, sensorless, speed, voltage, thesis.

Agradecimientos

Sin más dilación, mi más sincera y profunda gratitud va dirigida a mi novia, Mayte Hernández, por su apoyo constante y desinteresado a lo largo de todo el doctorado; un largo viaje en el que me he encontrado muchos problemas y me he tropezado muchas veces, y que gracias a ella, he conseguido resurgir como el Ave Fénix para volver con fuerzas renovadas, nunca lo olvidaré. El otro pilar fundamental que ha permitido finalizar esta tesis, han sido mis padres, Antonio y Maribel, que a pesar de la distancia, siempre me han ayudado con todos sus medios disponibles para facilitarme la vida y aconsejarme para que pudiera seguir avanzando. Tampoco me puedo olvidar de los padres de Mayte, David y Teresa, quienes también han aportado su granito de arena para mi éxito, ofreciéndome siempre su hospitalidad y ayuda en momentos difíciles. Sin embargo, mi recuerdo más especial va dirigido a los miembros de mi familia con los que he pasado menos tiempo, por culpa indiscutible del doctorado, como mis hermanos, cuñados, mi abuela, aunque ya no esté, y sobre todo mis sobrinas, con énfasis especial en Alexia. Sin el sustento de todos ellos y los momentos compartidos, muy poco de este trabajo habría sido posible, o prácticamente nada, y de ahora en adelante prometo dedicarles más tiempo.

Quiero mostrar también mi agradecimiento a mi tutor, Jaime Gómez, por el soporte y consejos que me ha proporcionado a lo largo de esta etapa tan complicada, sin cuya empatía y comprensión habría sido imposible llevar a cabo un doctorado de estas características en paralelo con mi trabajo en la empresa privada y con las limitaciones de la distancia. También, me gustaría que se hicieran eco de mi gratitud algunos de los miembros del grupo de investigación de Telemática Industrial de la E.T.S. Ingenieros de Telecomunicación de la Universidad de Valladolid, por su estrecha colaboración en algunos de los temas centrales de esta tesis, tales como Ernesto Vázquez, en técnicas basadas en la componente *ripple* y reconocimiento de patrones con clasificadores, y Víctor Martínez, en redes neuronales artificiales.

Reflexionando y mirando un poco hacia atrás, me siento muy conforme y contento de haber podido llegar al final de este camino tan sinuoso. A pesar de todos los conocimientos técnicos aprendidos y toda la ingeniería aplicada, me quedo con las

personas que han formado parte de esta experiencia; los conocimientos pueden llegar a olvidarse, pero las personas y sus acciones permanecen en nuestra memoria, y transcienden más allá de estas líneas o de cualquier titulación académica.

Madrid, 28 de julio de 2015

Índice abreviado

Índice general

Índice de figuras

Listado de acrónimos

A

ABS	Antilock Brake System
AC	Alternating Current
ADC	Analog to Digital Converter
AFFO	Adaptive Full-order Flux Observer
AI	Artificial Intelligence
ANN	Artificial Neural Network
APFO	Adaptive Pseudoreduced-order Flux Observer

B

BEMF	Back-electromotive Force
BI-EKF	Bi Input-EKF
BLDC	Brushless Direct Current
BDC	Brushed Direct Current
BPM	Brushless Permanent Magnet

C

CRIM	Cauge Rotor Induction Motor

D

DC	Direct Current
DRNN	Diagonal Recurrent Neural Network
DSP	Digital Signal Processor
DTC	Direct Torque Control

DTC-SVM	DTC-Space Vector Modulation
DVD	Digital Video Disk

E

EHA	Electro-hydraulic Actuator
EKF	Extended Kalman Filter
EMA	Electro-mechanical Actuator
EMI	Electromagnetic Interference
ESA	European Space Agency

F

FFT	Fast Fourier Transform
FNN	Fuzzy Neural Network
FPGA	Field Programable Gate Array

G

GSM	Global System for Mobile Communications
GTO	Gate Turn-off

H

HDD	Hard Disk Drive
HE	Hall Effect
HVAC	Heating, Ventillation, and Air Conditioning

I

IGBT	Insulated Gate Bipolar Transistor
IPM	Interior Permanent Magnet

J

JCR	Journal Citation Reports

M

MLP	Multilayer Perceptron
MMF	Magnetomotive Force
MOSFET	Metal-oxide Semiconductor Field Effect Transistor
MPU	Motor Pump Unit
MRAS	Model Reference Adaptive System

R

RBF	Radial Basis Function

S

SMO	Sliding-mode Observer
SMPM	Surface Mounted Permanent Magnet
SRM	Switched-reluctance Motor
SVM	Support Vector Machine
SYNCREL	Synchronous Reluctance

U

UAV	Unmanned Air Vehicle

O

OACI	Organización de Aviación Civil Internacional

P

PCB	Printed Circuit Board
PLL	Phase-locked Loop
PM	Permanent Magnet
PMBLDC	Permanent Magnet Brushless Direct Current
PMID	PubMed Identifier
PMSM	Permanent Magnet Synchronous Motor
PWM	Pulse Width Modulation

W

WRIM	Wound Rotor Induction Motor
WOS	Web of Science

Z

ZCD	Zero Crossing Detection
ZCP	Zero Crossing Point

PRIMERA PARTE:
INTRODUCCIÓN AL COMPENDIO

Capítulo 1: Introducción al compendio

A lo largo de las últimas décadas ciertos países asiáticos, como Japón, han soportado la presión de los altos precios de la energía, y por ello se han dedicado muchos recursos en la implementación de ***drivers* de motores de imanes permanentes (PM)** para reducir el consumo energético en determinadas aplicaciones, como equipos de aire acondicionado y frigoríficos. Por otra parte, Estados Unidos ha mantenido el uso de *drivers* de motores de inducción, los cuales presentan una menor eficiencia que los drivers de motores PM para aplicaciones de ahorro de energía. De esta forma, el aumento de los precios de la energía unido a la rápida proliferación en la industria automovilística de *drivers* de motores para vehículos híbridos, ha generado una elevada demanda de *drivers* de motores PM de alta eficiencia. Esto ha supuesto el comienzo del interés por los **motores DC sin escobillas o *brushless* DC (BLDC)** frente a otros modelos, como los **motores DC con escobillas o *brushed* DC (BDC)** o los motores de inducción. En la actualidad los motores eléctricos desempeñan un papel muy importante como convertidores de energía electromecánica en una gran cantidad de aplicaciones, como máquinas-herramienta para la industria, fotocopiadoras, reproductores de DVD, ventanillas eléctricas de vehículos y dispositivos médicos. Con los desarrollos en semiconductores de potencia y microprocesadores con capacidad de procesado de señales, la tecnología de *drivers* de control de motores ha cambiado mucho y por ello ha aumentado su relevancia dentro del sistema que comprende un motor eléctrico.

De forma adicional a todos los aspectos indicados que propulsaron la utilización de motores eléctricos, y en concreto los de imanes permanentes, también hay que considerar todos los problemas asociados al uso de **sensores electromecánicos** para obtener la información de posición y velocidad del rotor. La respuesta ante estos inconvenientes no es sencilla, y la solución consiste en extraer indirectamente esta información mediante el desarrollo de las denominadas **técnicas *sensorless***. El término *sensorless* indica que no existen sensores adicionales para desempeñar esta tarea, pero en su lugar se utilizan métodos de acondicionamiento y procesado de los parámetros eléctricos del motor. Así se tienen normalmente circuitos de medida de las formas de onda de las corrientes y tensiones del motor, junto con el procesamiento de las mismas en dispositivos programables u ordenadores provistos con tarjetas de adquisición. En

definitiva, la mayor diferencia entre las técnicas de detección *sensorless* y el uso de sensores electromecánicos radica en que en vez de necesitarse una conexión mecánica entre el sensor y el eje del motor, sólo se emplean medidas eléctricas de las señales del mismo.

En este capítulo se consideran todos los aspectos que permiten entender la estructura y desarrollo de la tesis presentada, así como los conceptos y las tecnologías asociadas a la implementación de técnicas *sensorless* para motores BLDC y BDC. En primer lugar, en la sección 1.1 se incluye una introducción a los motores considerados, teniendo en cuenta los fundamentos, características y aplicaciones de los mismos, así como un breve análisis de las técnicas *sensorless* de detección de la posición y velocidad más relevantes para ambos tipos de motores. Como parte central de la tesis, se tienen los objetivos, los medios y la metodología de investigación empleada en las secciones 1.2, 1.3 y 1.4, respectivamente. En estas tres secciones se explican claramente los aspectos formales que justifican el desarrollo de la tesis con el fin de lograr la consecución de los objetivos. En las secciones 1.5, 1.6 y 1.7 se incluyen, respectivamente, los resultados y conclusiones, las líneas futuras de la investigación, y la relación temática de las publicaciones incluidas en el compendio de acuerdo a la línea de investigación llevada a cabo. A modo de colofón del capítulo, se presentan en las secciones 1.8 y 1.9 las contribuciones originales obtenidas y una clasificación detallada de las aportaciones científicas realizadas.

1.1 Introducción

1.1.1 Aspectos generales de los motores eléctricos

La primera máquina eléctrica que se empleó en aplicaciones de potencia fue la máquina de corriente continua en la segunda mitad del siglo XIX, no conociéndose todavía las ventajas de la corriente alterna, especialmente en la transmisión de energía eléctrica a grandes distancias. Los motores eléctricos pueden clasificarse de muchas formas, dependiendo de los parámetros considerados, tales como el tipo de alimentación (AC, DC), la provisión del flujo de trabajo (electroimanes, imanes permanentes), la velocidad o el número de fases.

Un sistema *driver* de motores típico está compuesto fundamentalmente por los bloques indicados en la Figura 1. El bloque convertidor de potencia utiliza diodos, transistores metal-oxido-semiconductor de efecto de campo (MOSFET), transistores bipolares (BJT), tiristores *gate turn-off* (GTO) o transistores bipolares de puerta aislada (IGBT) [1]. Además, los controladores pueden estar formados por varios bucles de control con el fin de regular voltaje, corriente, par, flujo, velocidad, posición, tensión u otra condición deseable de la carga, la cual podría ser una cinta transportadora o una herramienta de corte [2].

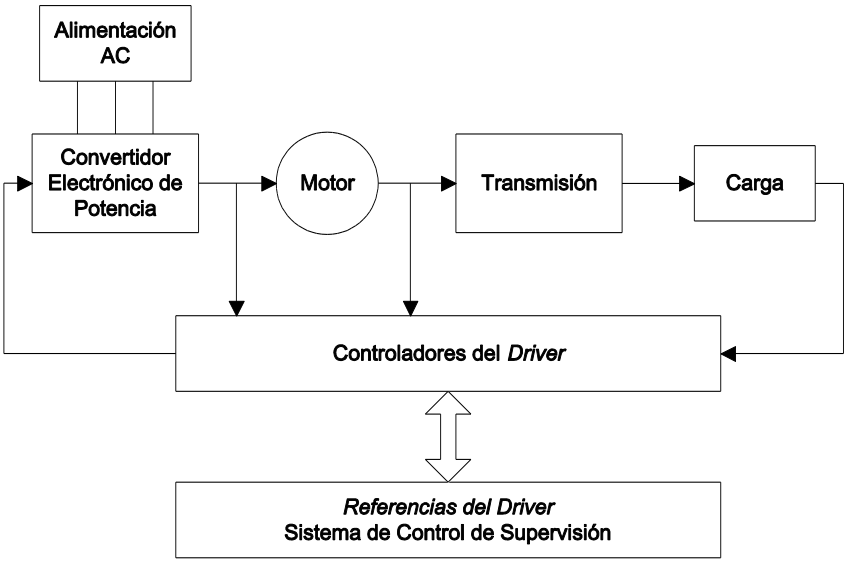

Figura 1. Diagrama de bloques típico de un sistema *driver* de motores [2].

Los principales grupos que permiten clasificar la mayoría de los motores utilizados en equipos domésticos, comerciales e industriales se indican a continuación [2-5].

- **Motor DC o *brushed* DC (BDC)**: Este motor también llamado motor DC con escobillas, se emplea frecuentemente en *drivers* de velocidad variable y en sistemas de control de posición. Las aplicaciones más frecuentes son en robótica, impresoras, máquinas-herramienta, e industrias textiles y papeleras.

- **Motor AC de Inducción**: Es el más ampliamente utilizado en la industria y se utiliza en aplicaciones de velocidad constante y variable no relacionadas con procesos dinámicos. Existen dos tipos principales: con rotor en jaula de ardilla (CRIM) y de rotor bobinado (WRIM). Las aplicaciones más frecuentes son en el ámbito doméstico, comercial e industrial, como en ventiladores y bombas.
- **Motor Síncrono**: El rotor se sincroniza con la velocidad del campo rotatorio del motor, teniendo el máximo rendimiento cuando una velocidad constante y precisa es requerida, como en aplicaciones para la industria textil y papelera. Existen dos tipos principales: velocidad variable de polos salientes o exteriores (*salient-pole*) y no salientes (*nonsalient-pole*).
- **Motor Síncrono AC de Imanes Permanentes o *Brushless* AC (PMSM)**: Desde la introducción de los materiales magnéticos de aleación, como samario-cobalto, estos motores han desplazado a los motores DC en muchas aplicaciones de alto rendimiento y baja potencia. Existen distintos tipos: de imanes superficiales (SMPM), de imanes interiores (IPM) y de imanes longitudinales [6]. Se usan en aplicaciones de velocidad variable como en máquinas-herramienta de cabezal controlado y discos duros.
- **Motor *Brushless* DC de Imanes Permanentes (BLDC)**: Proporcionan una alta eficiencia y no se necesitan escobillas para la transmisión de corriente, usándose electroimanes o imanes permanentes para generar el flujo de rotación, pero no es posible controlar de forma sencilla su velocidad usando una fuente de alimentación de frecuencia fija como en los motores BDC.
- **Motor Servo**: Históricamente se han utilizado en control de movimiento con sofisticados y costosos *drivers* y técnicas de control. Presentan un buen comportamiento dinámico, elevada fiabilidad y bajo mantenimiento. Algunos ejemplos son máquinas-herramienta, actuadores para robótica o discos duros.
- **Motor Paso a Paso**: Incrementa la posición de su rotor de forma proporcional al número de pulsos de corriente aplicados en sus bobinados, no necesitando realimentación y por tanto, con un menor coste del *driver*. Existen distintos tipos: de reluctancia variable, híbrido y de imanes permanentes.
- **Motor de Reluctancia Conmutada (SRM)**: Su funcionamiento es no lineal y se realiza mediante pulsos de corriente conmutados en cada bobinado del estátor, mientras que los polos del rotor no tienen excitación. Tienen bajo coste, construcción robusta, ausencia de escobillas y alta eficiencia.
- **Motor de Reluctancia Síncrona (SYNCREL)**: La configuración del estátor es similar a un motor de inducción o un motor síncrono, existiendo diferencias en el rotor. Existen pocos *drivers* comerciales para estos motores debido a la escasez de rotores fáciles de fabricar y con un buen rendimiento. Son utilizados en la industria del hilado de fibras y en vehículos eléctricos.

1.1.2 Motores *brushed* DC y *brushless* DC

1.1.2.1 Características

Hasta hace poco tiempo los motores *brushed* DC o BDC han sido los motores de velocidad variable más comúnmente utilizados, cuya popularidad está en descenso debido a la aparición de motores de inducción de jaula de ardilla, con un menor coste y mayor robustez. Una de sus características principales es que constan de un conmutador mecánico, el cual es un convertidor de potencia DC/AC, de forma que la corriente es alterna en las bobinas del rotor mientras que la corriente por las escobillas es continua [4]. A pesar de que este conmutador no presenta un mal comportamiento en términos de pérdidas y potencia, impone ciertos límites en corriente y velocidad, además de restricciones de uso en entornos químicamente peligrosos o propensos a explosiones, debido a la existencia de chispas y a posibles arcos eléctricos en las escobillas [7].

Por otra parte, los motores *brushless* DC o BLDC tienen una construcción similar a un motor síncrono estándar, pero al estar el campo magnético del rotor producido por un material con imantación permanente se le considera un motor de flujo constante. Este motor se parece a un motor DC convencional en diseño, teniendo una relación lineal entre la corriente y el par, así como entre el voltaje y la velocidad. Se utiliza un inversor para la conmutación electrónica de las fases en lugar de un sistema de conmutación mecánico, evitándose problemas de mantenimiento, ruido y fiabilidad. El método de conmutación comúnmente utilizado en motores de tres fases es la "secuencia de conmutación de 6 pasos" (*six-step switching sequence*), en la que sólo dos fases se activan en cada instante y la otra permanece "abierta" o "flotante" [1, 2, 8].

La Figura 2 muestra un motor típico BDC y otro BLDC, además de sus elementos más relevantes [9].

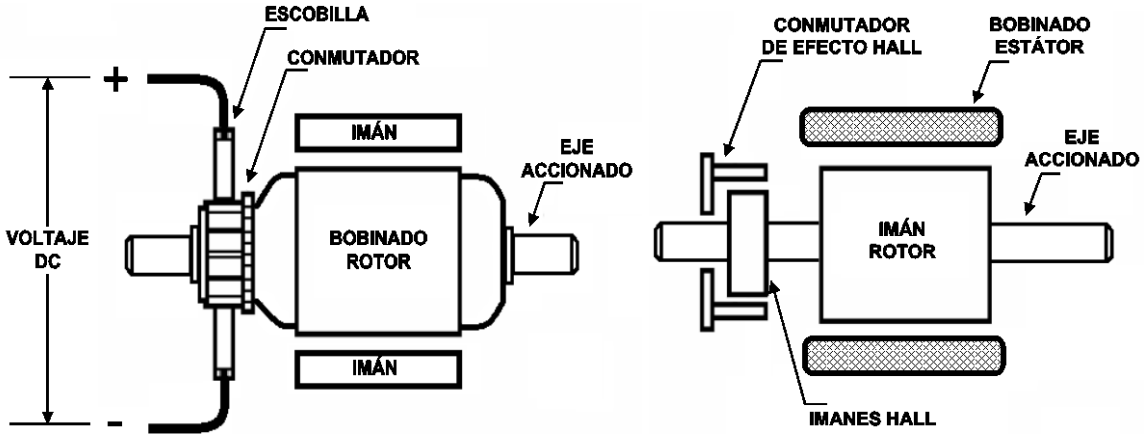

(a) (b)

Figura 2. Elementos de un motor DC: (a) Motor *brushed* DC, y (b) Motor *brushless* DC [9].

1.1.2.2 Comparativa

Teniendo en cuenta la propia construcción física de los motores BLDC, éstos presentan muchas ventajas sobre los BDC, las cuales se indican a continuación [4, 10]:

- Mejores características de velocidad frente al par, mientras que en los BDC la fricción de las escobillas es mayor a alta velocidad, influyendo en el par útil.
- Alta respuesta dinámica debido a que la inercia del rotor es menor, al estar ubicados los imanes permanentes en el rotor y no en el estátor.
- Alta eficiencia y fiabilidad; al no tener escobillas no existe caída de tensión en las mismas, no existiendo degradación eléctrica ni mecánica, y por tanto con un menor mantenimiento y una mayor vida operativa.
- Menor ruido eléctrico e interferencias electromagnéticas (EMI), al contrario que en los BDC, cuyo movimiento genera chispas y posibles arcos eléctricos.
- Operación a mayores rangos de velocidad, al no existir limitaciones mecánicas impuestas por las escobillas y el conmutador.
- Mejor relación potencia-tamaño debido a unas mejores características térmicas. Al estar el bobinado en el estátor y éste conectado a la carcasa existe una mejor disipación de calor, lo cual se consigue en los BDC a través de los huecos de aire de la carcasa.

No obstante, los motores BLDC también presentan algunas desventajas frente a los BDC, como un mayor coste de ensamblaje y un control más complejo y caro. Esto es debido a que siempre se requiere un controlador para que el motor gire, mientras que en los BDC sólo es necesario cuando se requiere variar la velocidad [5]. Además, un motor BDC tiene múltiples aplicaciones a consecuencia de que puede utilizarse en un amplio rango de velocidades ajustables con alta precisión, una característica par-velocidad variable, y una rápida aceleración, desaceleración y cambio de sentido de giro con posibilidad de frenado regenerativo. A pesar de las desventajas de los motores BLDC, la buena relación entre el par entregado y el tamaño de estos motores hace que sean útiles en aplicaciones en donde el espacio y el peso son críticos, como en aplicaciones aeroespaciales [11].

1.1.2.3 Aplicaciones

Debido a la gran cantidad de aplicaciones estos motores, se suelen clasificar en los tres categorías que se indican a continuación [10].

1.1.2.3.1 Aplicaciones con cargas constantes

En estas aplicaciones, una velocidad variable es más importante que la precisión a una velocidad dada. Se tiene un acoplamiento directo de la carga al eje del motor, como por ejemplo en ventiladores [12], bombas, compresores de aire acondicionado

[13] o extractores, demandándose controladores de bajo coste [14], generalmente en configuración de lazo abierto.

1.1.2.3.2 Aplicaciones con cargas variables

En estos casos, la carga del motor varía en un amplio margen de velocidad y se demanda una elevada precisión en el control de velocidad, además de una buena respuesta dinámica. Algunos ejemplos son aplicaciones que requieren motores de velocidad ajustable, como electrodomésticos y ventiladores para refrigeración de motores. En el sector automovilístico se utilizan para el control de bombas de combustible [15] y compresores para calefacción y aire acondicionado (HVAC) [16]. En el sector aeroespacial son utilizados en actuadores electromecánicos (EMA) y electrohidráulicos (EHA) [17], control de brazos robóticos y controles giroscópicos. En estos casos se suele realimentar la velocidad en lazo cerrado o lazo cuasi-cerrado, utilizándose algoritmos de control avanzados que incrementan la complejidad del controlador.

1.1.2.3.3 Aplicaciones de posicionamiento

La mayoría de las aplicaciones industriales y de automoción incluidas dentro de esta categoría tienen asociadas algún tipo de transmisión de potencia, como máquinas-herramienta [18], engranajes, bombas de motor (MPU) [19] o cinturones de seguridad. Las respuestas dinámicas en velocidad y par son importantes, y un ciclo típico de funcionamiento puede contener fases de aceleración, velocidad constante, deceleración y posicionamiento, además de la posibilidad de sentidos de rotación inversos. La carga en el motor puede variar durante estas fases, haciendo que el controlador sea más complejo, como en aplicaciones con discos duros (HDD) [20, 21] o discos de video digital (DVD) [22, 23]. La mayor parte de los sistemas funcionan en lazo cerrado, pudiendo existir hasta tres lazos de control para el par, la velocidad y la posición.

1.1.3 Técnicas *sensorless* de detección de la posición y velocidad

Para realizar el control eficiente de los motores BLDC o BDC se requiere la información de posición del rotor, sin embargo las limitaciones de los sensores de posición unidas a la disponibilidad de potentes y económicos microprocesadores han promovido el desarrollo de las técnicas *sensorless*. Esto abre la vía para la incorporación de este tipo de motores a aplicaciones de bajo coste, de alta fiabilidad y de grandes volúmenes de producción. Por ello, existe un interés creciente en los esquemas de control *sensorless,* de forma que la información de posición o velocidad se extrae únicamente del análisis de parámetros del motor, como las tensiones o corrientes en los bobinados, con las correspondientes ventajas asociadas:

- Las únicas conexiones *harness* con el motor son los terminales de las fases de alimentación del motor, por lo que se reducen los costes de instalación.

- La medida de posición puede incluirse junto con el resto de la electrónica de control, sin necesidad de una ubicación específica junto al motor.
- La ausencia de cableado de datos adicional para las medidas de posición o velocidad evita la degradación de los mismos por interferencias electromagnéticas, por lo que pueden simplificarse los blindajes.
- Eliminación del coste añadido al uso de un dispositivo que codifique la posición, como *encoders*, *resolvers* o sondas Hall.

1.1.3.1 Técnicas para motores *brushed* DC

Las técnicas de control *sensorless* empleadas en motores *brushed* DC pueden clasificarse tal y como se indica a continuación.

1.1.3.1.1 Técnicas básicas *sensorless* basadas en el modelo dinámico

En estas técnicas suele estimarse la velocidad del motor, con las medidas de la tensión o la corriente del motor y el modelo dinámico, y en menor medida la posición. Las más relevantes son las que se indican a continuación:

- **Uso del modelo simplificado del motor**: Utilizan directamente las ecuaciones eléctricas y en ocasiones se simplifican las ecuaciones aún más despreciando la parte inductiva [24], o implementando directamente la ecuaciones eléctricas y mecánicas [25].
- **Compensación de errores en la estimación de parámetros del motor**: Los errores de estimación en parámetros como la velocidad o el par se pueden compensar de múltiples formas, como un el uso de una ecuación diferencial de primer orden [26], o introduciendo la diferencia entre la corriente estimada y la real como nuevo término en la ecuación del motor [27, 28].
- **Técnicas adaptativas a las condiciones de funcionamiento del motor**: A través de estas técnicas se calcula en cada instante el valor real de los parámetros, por ejemplo suponiendo que éstos varían con la temperatura [24], utilizando el método de resistencia negativa [29], o midiendo la velocidad siempre en las mismas condiciones de trabajo [30].

1.1.3.1.2 Técnicas avanzadas *sensorless* basadas en el modelo dinámico

Mediante el uso del modelo dinámico y la tensión/corriente del motor se puede realizar también la estimación de la velocidad con técnicas más complejas que las anteriores, algunas de las cuales se describirán con más detalle en las técnicas de motores BLDC:

- **Filtro de Kalman Extendido (EKF)**: Mediante la caracterización de la distribución de los errores se realiza la estimación de velocidad [31, 32].

- **Redes Neuronales Artificiales (ANN)**: La red neuronal realiza el aprendizaje del modelo del motor BDC mediante ejemplos [33].
- **Observadores Adaptativos**: El observador adaptativo puede desarrollarse en base al voltaje y a la corriente del estátor para estimar la velocidad [34].

1.1.3.1.3 Técnicas *sensorless* basadas en la componente *ripple*

La componente alterna de la corriente que circula por el motor o componente *ripple* se debe a que la fuerza electromotriz (EMF) inducida en las bobinas del rotor no es constante, sino que tiene una forma sinusoidal, y a que no es rectificada de forma perfecta en el colector de delgas [35]. La posición del rotor se puede calcular contabilizando el número de ondulaciones y la velocidad a través de éstas por unidad de tiempo, teniendo en cuenta la expresión de la componente *ripple*. Estas técnicas sólo monitorizan la corriente del motor DC, y estiman la posición y velocidad con las variaciones instantáneas de la misma, resultando más adecuadas al no utilizar parámetros constantes y depender de las condiciones concretas de funcionamiento del motor DC. Debido a la influencia del ruido sobre la corriente, con estas técnicas se pretende detectar las ondulaciones producidas en la misma, incluyendo las **ondulaciones fantasma** y eliminando las **ondulaciones falsas** [36-38]. Estas técnicas se clasifican de la siguiente forma:

- **Basadas en comparador**: Son las más sencillas de implementar, realizándose la comparación de la corriente con un nivel de continua, que puede ser constante [39] o adaptado por el sistema [40]. También puede eliminarse la componente continua y realizarse la comparación con cero [41], por ejemplo mediante la estimación de su valor con un filtrado adicional [42]. Existe el problema de la distinta duración de los pulsos y el no rechazo de las falsas ondulaciones, lo cual se soluciona con un multivibrador monoestable [43] y añadiendo derivadores [36] o integradores [44].
- **Identificación de la evolución de la corriente**: Tienen una mayor inmunidad al ruido, pudiéndose utilizar un ADC para digitalizar la corriente y registrar las muestras en una memoria para las ondulaciones [45] o un filtrado paso banda empleando un *Phase-locked Loop* (PLL) [46].
- **Análisis espectral de la corriente**: Se detecta el valor de frecuencia de la componente *ripple* a partir del análisis espectral de la corriente del motor, y se usan para la detección de velocidad. Se pueden tener técnicas que funcionan en el dominio de la frecuencia, obteniéndose el espectro de la corriente a través de una FFT [47], y otras en el dominio del tiempo, trabajando directamente con la corriente usando filtrado y un derivador [48].
- **Comparación de la corriente y la tensión**: Se considera que la componente *ripple* se encuentra únicamente en la corriente del motor y el

ruido está presente en ambos parámetros, de forma que con la resta de ambas se habrá eliminado prácticamente el ruido. Se detectan las ondulaciones con un comparador [49] o se elige la componente *ripple* como la componente frecuencial presente en la corriente y no en la tensión [50].

1.1.3.1.4 Técnicas basadas en la combinación del modelo dinámico y la componente *ripple*

Intentan suplir los inconvenientes de cada uno de los dos grupos de técnicas por separado, por una parte la dependencia de los parámetros eléctricos y mecánicos del motor con las condiciones de funcionamiento, y por otra evitar la influencia del ruido para detectar ondulaciones fantasma y evitar falsas ondulaciones. Así, se puede utilizar una técnica basada en el modelo dinámico para detectar la velocidad y estimar los parámetros del motor con la componente *ripple* [51], o una técnica de la componente *ripple* para estimar inicialmente la velocidad y se realizar correcciones sobre la misma mediante el modelo dinámico teniendo en cuenta la distancia temporal entre ondulaciones [52, 53].

1.1.3.2 Técnicas para motores *brushless* DC

La Figura 3 muestra un esquema *sensorless* con un bloque estimador de posición, el cual recibe las tensiones y corrientes del motor con el fin de proporcionar información de la posición del rotor al controlador y así realizar la regulación de velocidad, posición o par del motor. Se pueden tener técnicas básicas y avanzadas, las cuales se analizan a continuación.

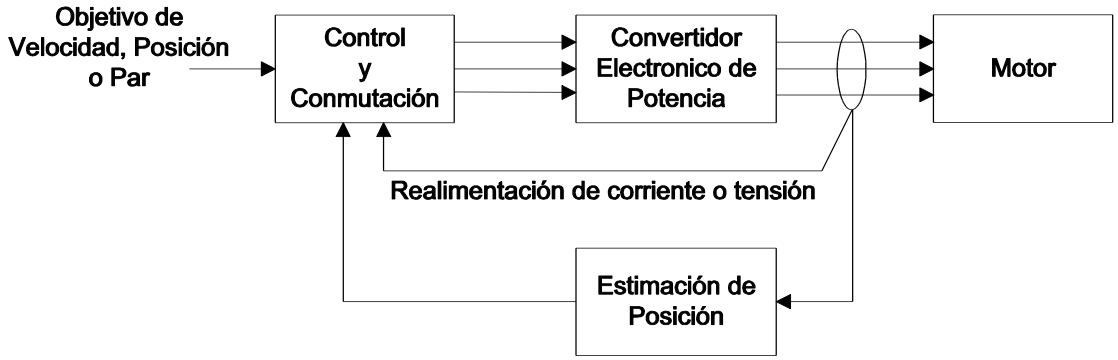

Figura 3. Estimación de posición a partir de las medidas de tensión o corriente de alimentación del motor.

1.1.3.2.1 Técnicas básicas

Estas técnicas pueden dividirse en directas e indirectas, las cuales se analizan de forma más detallada a continuación.

En las **técnicas directas** se miden los pasos por cero de la tensión BEMF de la fase inactiva, comparándola con la tensión en el punto neutro del motor. Se caracterizan por la elevada tensión en modo común y ruido de alta frecuencia debido

a las señales PWM del inversor, requiriéndose filtros y divisores de tensión. Algunas de estas técnicas son las siguientes, considerando su aplicación en un inversor de tres fases:

- **Detección del cruce por cero de BEMF (ZCD) o medida de la tensiones de fase (*Terminal Voltage Sensing*)**: Es una de las más simples y está basada en la detección del instante en el cual la tensión BEMF de la fase flotante atraviesa el punto de voltaje cero o ZCP [13], pudiéndose estimar el punto de conmutación de la corriente con un desplazamiento de 30º a partir del ZCP [19, 54]. En un inversor de tres fases, se emplea la fase flotante para la operación ZCD [55]. A cambio de la simplicidad de esta técnica, se tiene que el ZCD es sensible al ruido y un bajo rendimiento en un amplio rango de velocidad [56]. Algunas mejoras consisten en utilizar sólo una tensión de fase y filtrar para eliminar los picos de tensión (*spikes*) [20], o usar la diferencia de las tensiones de fase o de línea (*line voltages*) [57].
- **Modulación por Anchura de Pulsos (PWM)**: Existen muchos esquemas de detección basados en PWM, siendo los más relevantes:
  - PWM convencional de 120º [22, 58].
  - PWM con eliminación del punto neutro virtual [55].
  - PWM para aplicaciones de baja velocidad o baja tensión [55, 59, 60].
  - PWM para aplicaciones de alta velocidad o elevada tensión [60, 61].
  - PWM para aplicaciones de baja potencia [23, 59].
  - Control directo de corriente (*hysteresis current control*) [62].

Debido a que el filtrado en las técnicas directas introduce retardos en la conmutación a altas velocidades y la atenuación reduce la sensibilidad de la señal a bajas velocidades, se introducen las **técnicas indirectas**. Algunas de más representativas son las siguientes:

- **Integración de la fuerza contra-electromotriz**: El instante de conmutación se determina por la integración de la BEMF de la fase flotante, la cual comienza cuando BEMF de la fase flotante se hace cero [63]. Se tiene un rendimiento mejor que la técnica ZCD debido al uso de un integrador y se reduce la sensibilidad al ruido de conmutación del inversor [56].
- **Integración del tercer armónico del voltaje de fase**: Se utiliza el tercer armónico de BEMF para determinar los instantes de conmutación del motor [64]. Al requerirse sólo un filtrado reducido, los retardos son bajos, lográndose un alto rendimiento a un amplio rango de velocidades y en el arranque del motor o bajas velocidades [65].

- **Conducción de diodos de *free-wheeling* o medida de la corriente de fase (*Terminal Current Sensing*)**: La información de la posición puede obtenerse en base al estado de conducción de los diodos de *free-wheeling* conectados en paralelo con los *switches* de potencia del inversor [13], lo cual permite detectar la posición del rotor en un amplio rango de velocidades, también a baja velocidad [58].

1.1.3.2.2 Técnicas avanzadas

Otras técnicas que están centrando las investigaciones en el campo *sensorless* son los estimadores y los métodos basados en modelos. En general, un observador proporciona un modelo matemático del motor, de forma que el error entre las salidas estimadas y las magnitudes medidas se realimenta al modelo para corregir los valores estimados [65]. Las técnicas más relevantes se indican a continuación.

- **Observador *Sliding-mode* (SMO):** Es comúnmente utilizado en el campo de control de movimiento y puede ser aplicado a sistemas no lineales, como motores BLDC [66]. En la técnica de control directo de par (DTC), la observación del flujo del estátor es necesaria y la precisión del observador es afectada por la variación de la resistencia del estátor, EMI o errores de medida [67]. Un algoritmo basado en SMO junto con la teoría de hiper-estabilidad de *Popov* puede ser utilizado para calcular la velocidad y la resistencia del estátor [68]. A pesar de la robustez del observador a variaciones de parámetros y a perturbaciones como el ruido, tiene restricciones prácticas de operación [66].
- **Filtro de *Kalman* Extendido (EKF)**: Es un algoritmo de estimación recursiva óptima para sistemas no lineales y con existencia de ruido, como en motores. Procesa todas las medidas disponibles independientemente de la precisión, con el fin de proporcionar una estimación rápida y exacta de las variables de interés. Es computacionalmente intensivo [69] y puede ser utilizado para estimar la velocidad y la posición del rotor de forma estática y dinámica, siendo las variables de estado del motor estimadas con los voltajes de línea y las corrientes sin utilizarse filtrado [70]. Una técnica innovadora es EKF con dos entradas (BI-EKF) [71].
- **Observadores adaptativos**: La estimación correcta del valor de resistencia del estátor tiene una gran importancia en la estimación de la velocidad a bajas velocidades. En algunos casos esto no puede obtenerse, por ejemplo cuando el motor opera con una elevada carga variable o cuando el comando de velocidad del sistema de control cambia. En estos casos son necesarios mecanismos de estimación alternativos como los siguientes:
    - Sistema adaptable al modelo de referencia (MRAS) [68, 72].
    - Observador de flujo de orden completo adaptable (AFFO) [73, 74].

  - Observador de flujo de orden pseudo-reducido adaptable (APFO) [74, 75].

- **Redes Neuronales Artificiales (ANN)**: Consisten en la interconexión de neuronas artificiales que tienden a simular el sistema nervioso del cerebro humano, siendo el modelo de un amplificador operacional en configuración sumador el que mejor representa a una neurona biológica [1, 7]. En lo que se refiere a los motores, las ANN pueden utilizarse para estimar el flujo del rotor y el par en drivers controlados por vectores, requiriéndose el uso de DSPs debido a la alta carga computacional [76]. Una mejora son las Redes Neuronales *Fuzzy* (FNN), pudiendo estar basadas en reglas o métodos relacionales [77, 78].

1.2 Objetivos

1.2.1 Objetivo general

El objetivo general de este proyecto de tesis es el análisis, desarrollo y validación de técnicas *sensorless* para la detección de la posición y velocidad de motores *brushed* DC (BDC) y *brushless* DC (BLDC), tanto **básicas**, basadas en el procesamiento de parámetros físicos del motor como la corriente o los voltajes de fase, como **avanzadas**, basadas en observadores, clasificadores o inteligencia artificial.

1.2.2 Objetivos específicos

Debido a que el objetivo general es muy amplio, éste se ha desglosado en cinco objetivos específicos, los cuales se indican a continuación. El primer objetivo propone la realización del análisis de las técnicas *sensorless* para la detección de la posición y velocidad en motores BDC y BLDC. En el segundo objetivo se pretende desarrollar una técnica *sensorless* básica para la detección de la velocidad en motores BDC utilizando únicamente parámetros del motor, como la corriente. En el tercer objetivo se plantea el desarrollo de una técnica *sensorless* avanzada para la estimación de la posición y velocidad en motores BDC utilizando un sistema de reconocimiento de patrones estadísticos. En relación a los motores BLDC, se considera en el cuarto objetivo el desarrollo de una técnica *sensorless* básica para la detección de la posición y velocidad utilizando únicamente parámetros del motor como las tensiones de fase. Finalmente, en el quinto objetivo se contempla el desarrollo de una técnica *sensorless* avanzada para la estimación de la posición y velocidad en motores BLDC utilizando redes neuronales artificiales. A continuación, se exponen con una mayor profundidad los objetivos específicos indicados.

1.2.2.1 Objetivo 1: Análisis de las técnicas *sensorless* para motores *brushed* DC *brushless* DC

Este objetivo implica el análisis de las técnicas de detección existentes en la literatura para motores BDC y BLDC, teniendo en cuenta las ventajas e inconvenientes, así como los requisitos de implementación y aplicación práctica de las mismas. Con ello, se pretende adquirir una visión general de las técnicas **básicas** o comúnmente utilizadas, en las cuales se extrae la información de la posición y velocidad directamente a partir de parámetros del motor, como los voltajes de fase o las corrientes, y de otras técnicas más **avanzadas**, basadas en observadores, clasificadores o inteligencia artificial.

En el estudio realizado en la tesis se contemplan tanto los motores BDC como los BLDC, sin embargo, debido a la existencia de un mayor ámbito de investigación y mayor número de aplicaciones de éstos últimos, se requiere un análisis más exhaustivo de las técnicas utilizadas para este tipo de motores.

1.2.2.2 Objetivo 2: Desarrollo de una técnica *sensorless* básica para motores *brushed* DC utilizando únicamente parámetros del motor

Este objetivo consiste en el desarrollo de una técnica *sensorless* de detección de velocidad para motores BDC basada en la componente *ripple* de la corriente, utilizando únicamente la información proporcionada por ésta, e intentando minimizar el coste computacional sin afectar en exceso a la precisión. Para conseguir este objetivo, se pretende detectar las ondulaciones o pulsos que aparecen en la corriente utilizando un algoritmo simple, mediante una ventana de observación de las muestras de la corriente y un comparador. Este objetivo puede desglosarse en la siguiente forma:

- Estudio de las investigaciones más importantes dentro del campo de la detección de la posición y velocidad de motores BDC basadas en técnicas básicas, como las que utilizan el modelo dinámico del motor o la componente *ripple* de la corriente, y teniendo en cuenta la reducción del efecto del ruido para mejorar la precisión.
- Diseño de un sistema para la detección de las ondulaciones que aparecen en la corriente del motor BDC.
- Diseño de un sistema que permita detectar la velocidad de un motor BDC a partir de la información de las ondulaciones detectadas en el sistema anterior.
- Diseño e implementación de un sistema que permita adquirir los datos de un sensor de posición de tipo *encoder* incremental, con el fin de obtener la información de posición del rotor del motor BDC para ser utilizada como referencia.
- Validación de la precisión de la técnica desarrollada para diferentes motores BDC con respecto a la información de referencia obtenida del *encoder*. En esta validación se obtendrán los errores de posición y velocidad medios para cada uno de los motores considerados.
- Análisis de los resultados obtenidos.

1.2.2.3 Objetivo 3: Desarrollo de una técnica *sensorless* avanzada para motores *brushed* DC utilizando reconocimiento de patrones estadísticos

Este objetivo consiste en el desarrollo de una técnica *sensorless* de detección de la posición y velocidad para motores BDC basada en la componente *ripple* de la corriente y que permita minimizar el efecto del ruido. Para alcanzar este objetivo, se empleará un sistema de reconocimiento de patrones utilizando el clasificador *Support Vector Machine* (SVM), de forma que detecten las ondulaciones normales de la corriente, se descarten las **falsas ondulaciones** (ondulaciones no existentes en la corriente que aparecen por la presencia de ruido) y se detecten las **ondulaciones fantasmas** (ondulaciones existentes en la corriente que son enmascaradas por la presencia de

ruido). Teniendo como base las investigaciones que se realicen para lograr el objetivo 2, este objetivo puede estructurarse de la siguiente forma:

- Profundización en el estudio de las investigaciones más importantes dentro del campo de la detección de la posición y velocidad basadas en técnicas avanzadas, como los observadores *sensorless* basados en la componente *ripple* de la corriente, analizando las diferentes soluciones empleadas para reducir el efecto del ruido.
- Estudio de los sistemas de reconocimiento de patrones con énfasis especial en los que emplean patrones estadísticos.
- Estudio de los principios de los clasificadores SVM aplicados al reconocimiento de patrones.
- Diseño e implementación de un sistema para la detección de las ondulaciones que aparecen en la corriente del motor BDC utilizando técnicas de reconocimiento de patrones con clasificadores SVM.
- Diseño e implementación un sistema que permita detectar la posición y velocidad de un motor BDC con la información de las ondulaciones detectadas en el sistema anterior.
- Utilización y adaptación del sistema de adquisición para el *encoder* incremental desarrollado en el Objetivo 2, con el fin de obtener la información de posición de referencia para estos motores.
- Validación de la precisión de la técnica desarrollada para diferentes motores BDC con respecto a la información de referencia obtenida del *encoder*. En esta validación se obtendrán los errores de posición y velocidad medios para diferentes situaciones de operación de los motores considerados.
- Análisis de los resultados obtenidos.

1.2.2.4 Objetivo 4: Desarrollo de una técnica *sensorless* básica para motores *brushless* DC utilizando únicamente parámetros del motor

Este objetivo consiste en el desarrollo de una técnica *sensorless* de detección de la posición y velocidad para motores BLDC basada en la derivada de las tensiones de fase del motor con respecto a un punto neutro virtual, y en el que se reduzca el efecto del ruido. En la consecución de este objetivo representan un papel muy relevante las investigaciones que se realicen para alcanzar el Objetivo 1, puesto que representa el estudio de estado del arte de las técnicas existentes para este tipo de motores. De esta forma, se empleará un sistema *hardware* para la adquisición, acondicionamiento y cálculo de la operación derivada de las tensiones con un reducido coste computacional, para detectar posteriormente por *software* los pulsos de esta operación que proporcionan la información sobre la posición del rotor, y descartar los pulsos falsos debidos al ruido. Este objetivo puede desglosarse en los puntos que se indican a continuación:

- En línea con el Objetivo 1, se profundizará en el estudio de las investigaciones más importantes basadas en técnicas básicas dentro del campo de la detección de la posición y velocidad para motores BLDC. Por ejemplo, aquellas en las que se utilizan los voltajes de fase como los parámetros del motor a procesar.
- Estudio de las señales de los voltajes de fase de un motor BLDC y efecto de la operación matemática derivada sobre las mismas, con el fin de poder identificar pulsos o patrones que puedan relacionarse con la posición del rotor.
- Diseño e implementación un sistema *driver* para controlar distintos modelos de motores BLDC y configurar ciertos parámetros como la velocidad o el modo de arranque, así como realizar la adquisición y acondicionamiento de los voltajes del motor con cierta inmunidad al ruido. La reducción del efecto del ruido desempeña un papel importante para la adquisición de las señales del motor, y por ello es necesario tener en cuenta la minimización del ruido procedente de la conmutación del inversor y de los componentes de alta frecuencia en el terminal de masa.
- Diseño e implementación de un sistema que permita detectar la posición y velocidad de un motor BLDC con la información de los pulsos obtenidos a partir de la derivada de las tensiones de fase.
- Diseño e implementación un sistema que permita adquirir los datos de un sensor de posición de tipo *encoder* incremental para obtener información de posición de referencia del rotor del motor BLDC. En este punto se puede utilizar lo aprendido a partir de los desarrollos para motores BDC.
- Validación de la precisión de la técnica desarrollada para uno o varios motores BLDC con respecto a la información de referencia proporcionada por del *encoder*. En esta validación se obtendrán los errores de posición y velocidad medios para diferentes situaciones de operación de los motores considerados.
- Análisis de los resultados obtenidos.

1.2.2.5 Objetivo 5: Desarrollo de una técnica *sensorless* avanzada para motores *brushless* DC utilizando redes neuronales artificiales

Este objetivo consiste en el desarrollo de una técnica *sensorless* de detección de posición y velocidad para motores BLDC basada en aplicación de redes neuronales artificiales (ANNs) de tipo *Multilayer Perceptron* (MLP) a los voltajes de fase del motor con respecto a un punto neutro virtual, y en el que se reduzca el efecto de ruido. En la consecución de este objetivo representan un papel muy relevante las investigaciones realizadas para alcanzar el Objetivo 4. De esta forma, se empleará un sistema que permita la adquisición y acondicionamiento de los voltajes de fase, además de posibilitar la implementación de los algoritmos de las redes neuronales utilizadas y facilitar su entrenamiento. Este objetivo se puede estructurarse de la siguiente forma:

- Profundización en el estudio de las investigaciones dentro del campo de la detección de la posición y velocidad basadas en técnicas avanzadas, como las redes neuronales artificiales.
- Estudiar las redes neuronales artificiales con énfasis en las de tipo MLP.
- Estudio de los algoritmos de entrenamiento de redes neuronales, como por ejemplo *Backpropagation*, y su posibilidad de adaptación al uso de los voltajes de fase como señales de entrada al algoritmo. Con ello se trata de poder identificar las características de estas señales que proporcionen información de la posición del rotor.
- Diseño e implementación de un sistema que permita detectar la posición y velocidad de un motor BLDC utilizando redes neuronales entrenadas con el algoritmo seleccionado previamente.
- Utilización y adaptación del sistema *driver* desarrollado en el Objetivo 4 que permite tanto controlar distintos modelos de motores BLDC como configurar ciertos parámetros de los mismos, como la velocidad o el modo de arranque. También es necesario en esta técnica, el tener en cuenta la minimización del ruido sobre todo en el proceso de adquisición de las señales del motor.
- Utilización y adaptación del sistema de adquisición de datos para el *encoder* incremental desarrollado en el Objetivo 4, con el fin de obtener información de posición de referencia del rotor del motor BLDC.
- Validación de la precisión de la técnica desarrollada para uno o varios motores BLDC con respecto a la información de referencia proporcionada por el *encoder*. En esta validación se obtendrán los errores de posición y velocidad medios para diferentes situaciones de operación de los motores considerados.
- Análisis de los resultados obtenidos.

1.3 Medios y materiales

En la tesis se expone tanto el análisis de diversas técnicas *sensorless* para la detección de la posición y velocidad, como su implementación y prueba en plataformas con *hardware* y *software* específicos para el control de los motores, la adquisición y el procesamiento de las señales de los mismos. Debido a que los medios disponibles en el grupo de investigación de la Universidad de Valladolid, así como otros particulares del doctorando, son recursos *hardware* y *software* comerciales de uso extendido (a excepción de los específicamente desarrollados en la tesis), únicamente se enumerarán las herramientas que se ha empleado sin describir en profundidad sus funcionalidades y características.

Para poder llevar a cabo el proceso de investigación expuesto en esta tesis se han empleado los medios de tipo *hardware*, *software* y bibliográficos que se indican a continuación.

1.3.1 Medios de tipo hardware

1.3.1.1 Ordenador de desarrollo

Se ha utilizado un ordenador portátil Lenovo B560 para programar en LabVIEW el control de los motores y los algoritmos asociados a las técnicas de detección, así como diseñar en Orcad cierto *hardware* específico. También se ha empleado para la adquisición, procesado en tiempo real y post-procesado de datos, además de la representación de resultados y la redacción de la documentación relacionada con el diseño, pruebas y publicaciones. Este ordenador consta de un procesador Intel Core i3 a 2,53 GHz, memoria RAM de 4 GB y sistema operativo Windows 7 de 64 bits.

1.3.1.2 Tarjetas de adquisición y procesamiento

Estas tarjetas permiten realizar la adquisición de datos para múltiples entradas y salidas digitales y analógicas, además de proporcionar el soporte necesario para el control de los motores y el desarrollo de las técnicas de detección. A continuación se indican los modelos de tarjetas utilizados del fabricante National Instruments (NI):

- **NI USB-6008**: Tarjeta de adquisición de prestaciones bajas-medias sin recursos para tareas de tiempo real, utilizada en la implementación de técnicas para motores BDC.
- **NI USB-6251**: Utilizada al principio de las investigaciones para motores BLDC con el fin de probar distintas configuraciones en el diseño del inversor de potencia.
- NI sbRIO-9636: Una vez que se realizaron las pruebas preliminares con el inversor y los motores, se pasó a la implementación de la plataforma *driver* y el desarrollo de técnicas *sensorless*, para lo cual se utilizó esta tarjeta

procesadora debido a que tenía integrados una FPGA Xilinx Spartan-6 y un procesador de tiempo real. La disponibilidad de estos componentes en la tarjeta habilitó el uso de librerías de NI para la adquisición de señales, control del motor y diseño de los algoritmos de las técnicas para tiempo real.

1.3.1.3 Motores *brushed* DC

En el desarrollo de las técnicas *sensorless* para motores BDC se han utilizado los modelos para 12 V **Devantech EMG30** de 4,22 W y **Como Drills 719RE385** de 7,98 W, cuyas características más relevantes de indican en la Tabla II del Artículo 2 del compendio.

1.3.1.4 Motores *brushless* DC

En la tesis se han utilizado motores BLDC con distintas configuraciones, como el motor en configuración estrella **Maxon EC 45 Flat** de 12 V, 30 W y 8 pares de polos, y los motores de 24 V en configuración delta modelos **DPM 42BL41** de 5,4 A y **DPM 42BL100** de 20 A con 4 pares de polos y sensores Hall (HE) embebidos. Estos motores se han utilizado en la verificación de la plataforma *driver*, y adicionalmente el motor Maxon EC 45 Flat se ha empleado también para la validación de las técnicas *sensorless* desarrolladas. La Tabla 1 incluida en el Artículo 3 del compendio incluye las características principales de estos motores.

1.3.1.5 *Encoder* de precisión

Como referencia de posición para el análisis de la eficiencia y precisión de las técnicas sensorless desarrolladas se ha utilizado el *encoder* incremental **Kübler 05.2400.1122.1024** de 1024 pulsos por revolución.

1.3.1.6 Instrumentación de medida

La principal instrumentación de medida que se ha utilizado para el desarrollo y prueba de los diseños *hardware* implementados en la tesis son:

- Un osciloscopio digital Tektronix TDS2012 de dos canales y ancho de banda de 100 MHz con 2 GS/s.
- Un osciloscopio portátil PicoScope 2204 de dos canales y ancho de banda de 10 MHz y 50 MS/s.
- Un multímetro portátil Iso-Tech ID67.
- Una fuente de alimentación Iso-Tech IPS-3303 con dos canales 0-30 V y un canal 0-5 V con límites de corriente hasta 3 A.

1.3.1.7 Otros recursos *hardware*

En la implementación de los elementos *hardware* diseñados en la tesis se han utilizado también componentes electrónicos como semiconductores (diodos, transistores…), circuitos integrados (amplificadores operacionales, puentes en H…) y componentes pasivos (resistencias, condensadores…). También, se han utilizado algunas herramientas para la fabricación de placas de circuito impreso (PCB), como una máquina prototipadora-fresadora, una taladradora, un soldador y otros útiles como destornilladores o herramientas de corte.

1.3.2 Medios de tipo *software*

1.3.2.1 Entorno de desarrollo LabVIEW

El entorno de desarrollo LabVIEW 2012 de National Instruments se ha empleado para la programación de la plataforma de control de motores y adquisición de datos, del entorno gráfico de operación, y de los algoritmos de las técnicas de detección de posición y velocidad. Además de los *toolkits* genéricos de esta herramienta, se han utilizado los *toolkits* LabVIEW FPGA y LabVIEW Real-Time.

1.3.2.2 Entorno de desarrollo Matlab

El entorno de programación Matlab 2011a de MathWorks se ha utilizado para la implementación de algunos algoritmos de las técnicas de detección desarrolladas, como los basados en reconocimiento de patrones para motores BDC o en redes neuronales para motores BLDC, y también en el post-procesado de determinados resultados que no hayan podido ser analizados en tiempo real. También se han empleado librerías adicionales, como el *toolbox* Neural Network de Mathworks para el diseño de las dos redes neuronales de la técnica desarrollada en el Artículo 4 del compendio.

1.3.2.3 Diseño electrónico

Los programas de diseño electrónico utilizados en la tesis para el diseño del *hardware* han sido OrCAD 14 y PSpice de Cadence.

1.3.2.4 Otros recursos *software*

Para la preparación de documentación, informes de diseño, tablas de resultados, etc. se ha utilizado herramientas ofimáticas de Microsoft como Word, Excel y PowerPoint. Además, se ha utilizado Internet para la consulta de información como el acceso a bases de datos y repositorios digitales de documentación científica y de divulgación.

1.3.3 Medios bibliográficos

Los medios bibliográficos más relevantes empleados en la tesis son los que se indican a continuación:

- Fondos bibliográficos de la Universidad de Valladolid.
- Repositorios digitales de revistas científicas y bases de datos a través de la plataforma de la Biblioteca de la Universidad de Valladolid. Algunas de las más relevantes son las revistas electrónicas obtenidas de *IEEEXplore* o *ScienceDirect*, y las bases de datos *Web of Science* (WOS) o *Scopus*.

1.4 Metodología

La metodología que se expone a continuación describe de forma estructurada el procedimiento seguido en el desarrollo de las investigaciones realizadas en la tesis hasta llegar a los resultados obtenidos. Esta metodología consta de las etapas que se indican esquemáticamente en la Figura 4.

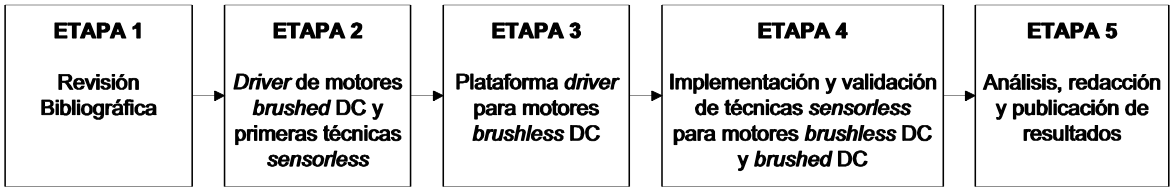

Figura 4. Etapas de la metodología seguida en la tesis.

1.4.1 Etapa 1: Revisión bibliográfica

Es la primera fase necesaria en todo estudio científico y representa un proceso transversal que se ha llevado a cabo a lo largo de toda la tesis. Por una parte, se han consultado libros de texto y revistas para el estudio de los fundamentos de los motores BDC y BLDC, así como de las técnicas comúnmente utilizadas para la detección de la posición y velocidad. Por otra parte, una vez establecida una base de conocimiento en torno al funcionamiento y la funcionalidad de los motores considerados, se han analizado publicaciones científicas más específicas y novedosas, orientadas al estudio de las técnicas de detección dentro del ámbito de la tesis. Con todo ello, se ha podido abordar el estudio del estado del arte de las técnicas de detección de la posición y velocidad de ambos tipos de motores, pudiéndose conocer las tendencias actuales dentro de la línea de investigación, así como las herramientas y tecnologías utilizadas para llevar a cabo su implementación.

1.4.2 Etapa 2: Desarrollo de un *driver* para motores *brushed* DC y primeras técnicas *sensorless*

A partir del estudio del estado del arte realizado en la etapa previa, se logró obtener un conocimiento adecuado de los fundamentos y características de los dos tipos de motores considerados en la tesis. Se comenzó a trabajar con motores BDC debido a la simplicidad de estos motores y a la necesidad de una menor cantidad de recursos para trabajar este tipo de motores con respecto a los BLDC. Con ello, se consiguió el control básico de los mismos y la adquisición de las señales más representativas en un periodo relativamente corto y con una cantidad reducida de recursos *hardware*, como una fuente de alimentación, una tarjeta de adquisición de prestaciones bajas-medias, un sencillo desarrollo hardware con un puente en H, un sensor de corriente y circuitería básica de acondicionamiento. También, se realizó un desarrollo *software* en LabVIEW (sin operación en tiempo real) para configurar parámetros del motor y poder representar

algunos de los datos adquiridos. Sobre esta base, se pudo empezar a desarrollar una técnica básica *sensorless* para la detección de velocidad en motores BDC basada en la componente *ripple* de la corriente, y se obtuvieron los primeros resultados con motores reales. En la Figura 5 se incluye el esquema de la arquitectura *hardware* utilizada para trabajar con este tipo de motores.

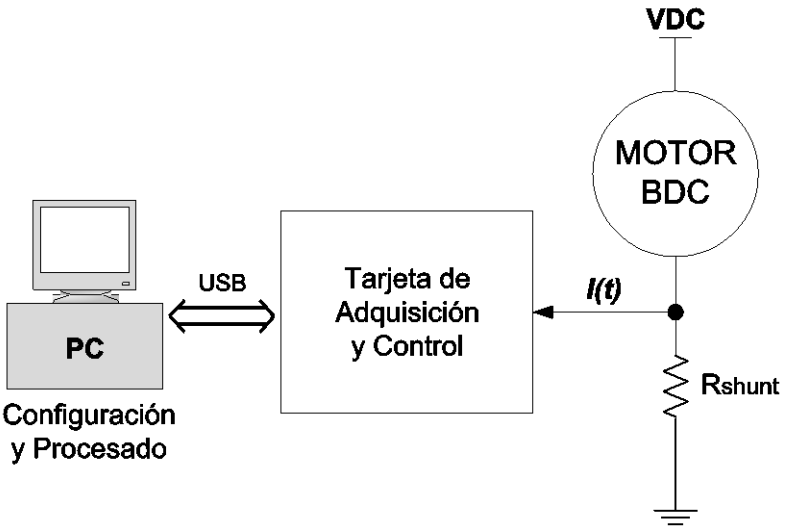

Figura 5. Esquema de la arquitectura hardware utilizada para motores *brushed* DC.

1.4.3 Etapa 3: Implementación de una plataforma *driver* para motores *brushless* DC

Una vez que se llevaron a cabo los primeros desarrollos y la propuesta de una técnica *sensorless* para motores BDC, se decidió avanzar en las investigaciones para motores BLDC teniendo en cuenta que este tipo de motores tenían asociada una complejidad más alta que los BDC, sobre todo debido a la necesidad de conmutación electrónica, un adecuado acondicionamiento de las señales para eliminar componentes espúreos, y el procesamiento de datos en tiempo real, para lo cual se necesitaron mayor cantidad de recursos y tiempo.

La principal necesidad estaba en el diseño y fabricación de un sistema o plataforma *driver* que permitiera trabajar con motores BLDC y que soportara la implementación de técnicas para ellos. En este sentido, el sistema fue diseñado con el objetivo de permitir el desarrollo y validación de técnicas de detección sin realizar prácticamente cambios en el *hardware*, solamente actuando sobre el *software* de alto nivel de la plataforma y/o reprogramando el *software* embebido en la FPGA y en el procesador de tiempo real. En la Figura 6 y en la Figura 7 se incluyen un esquema y una fotografía, respectivamente, de los elementos de que constituyen la plataforma, los cuales se describen brevemente a continuación:

- Fuente de alimentación DC de dos canales para alimentar el motor con tensión positiva (+12 V, +24 V) y para la electrónica de acondicionamiento de señales

con tensión bipolar (±12 V, ±24 V). Se incluye el condensador C_{IN} (*smoothing capacitor*) a la entrada del inversor para filtrar el ruido de alta frecuencia y picos en la corriente introducidos desde la fuente de alimentación.

- Inversor implementado con transistores BJT de potencia y diodos Schottky de *freewheeling* para proporcionar corriente y tensión al motor en las distintas fases de la secuencia de conmutación.
- Electrónica de acondicionamiento de las señales del motor para adaptar los niveles necesarios, o realizar un pre-procesamiento de las mismas, mediante el uso de amplificadores operacionales, filtros y limitadores de nivel.
- Sensor de posición de tipo *encoder* incremental, y en algunos casos sensores Hall (integrados en los motores), para proporcionar posiciones de referencia necesarias en la validación de las técnicas *sensorless* desarrolladas, junto con la respectiva electrónica de acondicionamiento.
- Electrónica de control programable para la adquisición, procesamiento de señales en tiempo real y control del motor para operar dentro de los rangos establecidos en cada caso de estudio. Se ha utilizado una FPGA y un procesador en tiempo real, cuyo *firmware* es programado como parte del controlador y del sistema de adquisición de datos.
- *Software* de alto nivel con un interfaz gráfico para la gestión del sistema completo, post-procesado de datos, representación y almacenamiento de resultados mediante LabVIEW. En el post-procesado de ciertos datos complejos se utilizó también Matlab.
- Ordenador portátil para el diseño del *software* desarrollado, control de la instrumentación y diseño del *hardware* específico, además del procesamiento y análisis de resultados.

La validación de la plataforma implementada se realizó con diferentes tipos de motores BLDC (consultar sección 1.3 de materiales y medios), tanto en configuración delta como estrella, y se realizó la detección de la posición y velocidad de los mismos utilizando un *encoder* o bien los sensores Hall integrados en algunos modelos de motores.

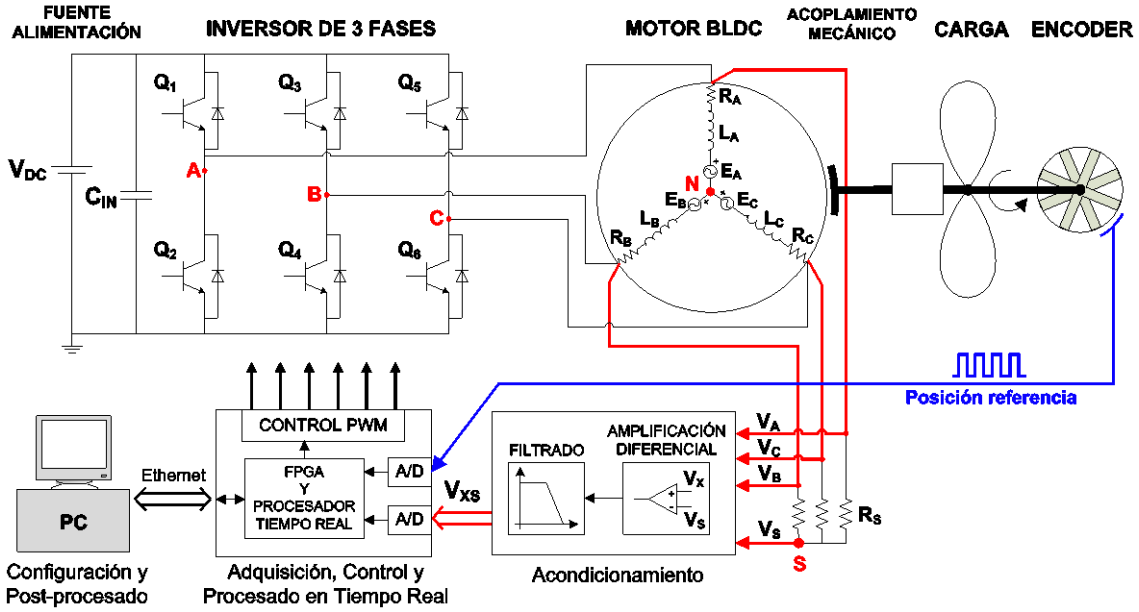

Figura 6. Esquema de la plataforma *driver* para motores *brushless* DC.

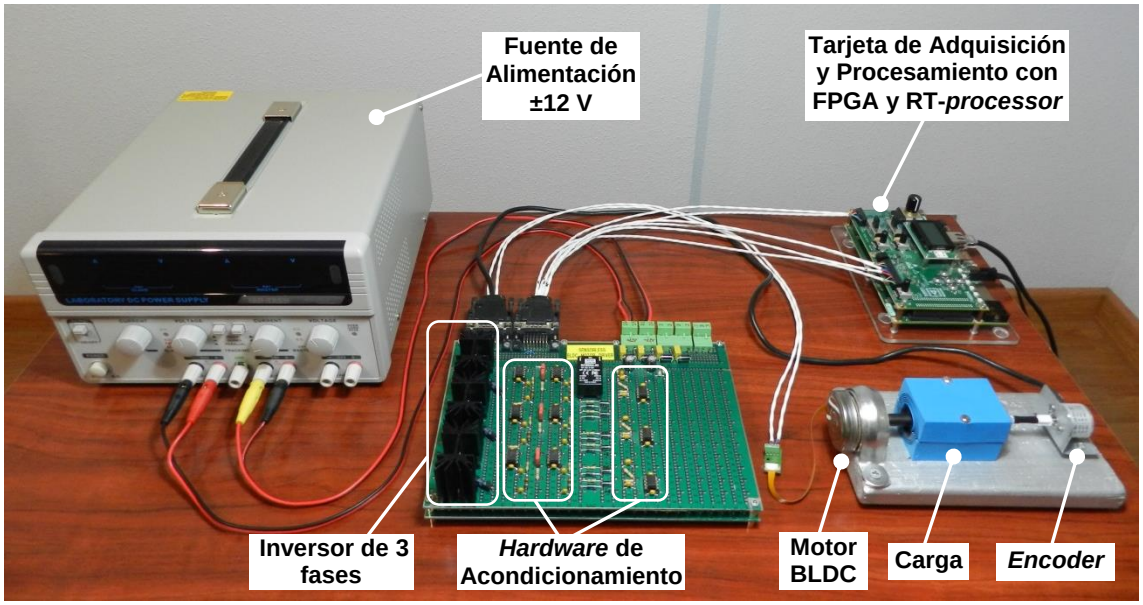

Figura 7. Fotografía de la plataforma *driver* para motores *brushless* DC.

1.4.4 Etapa 4: Diseño, implementación y validación de técnicas *sensorless* para motores *brushed* DC y *brushless* DC

Esta etapa representa la parte central de la metodología, debido a que el fin último de la tesis es el diseño de técnicas *sensorless* para detección de la posición y velocidad de motores BDC y BLDC. Las principales tareas que se han realizado en esta etapa son las siguientes:

- Adaptación del *hardware* de control para distintos tipos de motores BDC y BLDC. Sin embargo, apenas se han realizado cambios en el *hardware* utilizado en motores BDC ni la plataforma de motores BLDC, a excepción de mejoras en el acondicionamiento de ciertas señales.
- Dependiendo de la complejidad de la técnica de detección desarrollada, se ha utilizado Matlab para implementar los algoritmos de la misma para luego ser programados en LabVIEW, sobre todo en técnicas avanzadas como reconocimiento de patrones con clasificadores *Support Vector Machines* para motores BDC y redes neuronales artificiales para motores BLDC. En algoritmos más simples, se ha utilizado Matlab en menor medida y se ha empleado el *hardware* y *software* específico desarrollado para implementar el algoritmo, como en la técnica de la derivada de los voltajes de fase para motores BLDC.
- Adaptación del *software* en LabVIEW y del *firmware* de la tarjeta sbRIO-9636 (en el caso de usarse la FPGA y el procesador en tiempo real) para implementar los algoritmos específicos de cada una de las técnicas de detección consideradas.
- Realización de pruebas de validación de las técnicas de detección propuestas utilizando como referencia los datos de posición proporcionados por un *encoder* incremental.

1.4.5 Etapa 5: Análisis, redacción y publicación de resultados

En esta última fase se ha realizado la divulgación del trabajo realizado a la comunidad científica internacional, tanto en lo que se refiere a la exposición de las técnicas desarrolladas y análisis de los resultados obtenidos, como a la propuesta de líneas futuras de investigación. También, a partir del análisis de resultados se han detectado incompatibilidades y limitaciones de las técnicas desarrolladas, las cuales han servido para obtener las conclusiones del trabajo acometido y las posibles aplicaciones en sistemas reales. Con todo ello, se ha llevado a cabo la redacción del trabajo realizado tanto en forma de artículos para revistas como en la presente memoria de tesis.

1.5 Resultados y conclusiones

A partir del desarrollo de esta tesis se han obtenido los resultados y conclusiones que se indican a continuación:

- Se ha desarrollado una técnica *sensorless*, basada en la componente *ripple* de la corriente, que permite determinar la posición y velocidad de un motor BDC [37] mediante la detección del rizado u ondulaciones que aparecen en corriente del motor, la cual se realiza mediante la comparación entre las muestras actuales de la corriente y las inmediatamente anteriores y posteriores en tiempo. Esta técnica pertenece al grupo de observadores sensorless que **monitoriza la tendencia de la corriente**, y mediante una ventana de observación de las muestras de la misma de tamaño variable, dependiente de la frecuencia de la componente *ripple*, se detectan algunas ondulaciones fantasmas y se descartan algunas ondulaciones falsas. El instante utilizado para la identificación de las ondulaciones, a partir del cual se decide si se ha producido o no ondulación, es aquel en el que la corriente alcanza su valor máximo. **La estimación de la posición del motor se realiza contando el número de ondulaciones producidas, y a través de la distancia temporal entre ondulaciones se estima la velocidad**. Esta técnica ha sido validada con los motores EMG30 y 719RE385 con *tests* a velocidad constante, con una variación lenta de velocidad y con saltos de velocidad. En primer lugar, los *tests* a velocidad constante se realizaron entre 900 rpm y 3.500 rpm, obteniéndose unos resultados con unos errores absolutos medios de posición y de velocidad inferiores a 4 rad y 3,5 rpm para el EMG30, e inferiores a 2 rad y 5 rpm para el 719RE385. En segundo lugar, los *tests* con una variación lenta de velocidad se desarrollaron entre 5.000 y 7.000 rpm, obteniéndose unos resultados con unos errores absolutos medios de posición y velocidad de 10,7 rad y 4,65 rpm para el EMG30, y de 17,75 rad y 1,44 rpm para el 719RE385. En tercer lugar, se realizaron saltos de velocidad de más de 1.000 rpm con los motores girando a una velocidad superior a 2.000 rpm, obteniéndose unos resultados en los que el valor final de velocidad se logró detectar en torno a 0,5 s, y con unos errores absolutos medios de posición en torno a 30 rad y 15 rad para los motores EMG30 y 719RE385, respectivamente. A partir de estos resultados, se verifica que la técnica funciona correctamente bajo **condiciones cuasi-estáticas**, es decir cuando la velocidad del motor varía lentamente, y su funcionamiento empeora cuando la velocidad varía bruscamente o el ruido en la corriente es elevado, debido a que se incrementan el número de ondulaciones fantasmas y falsas ondulaciones. En la técnica también se ha conseguido **cierta inmunidad al ruido** en la corriente, al reducirse el efecto de ondulaciones falsas y fantasmas, y **minimizar el coste computacional sin afectar en exceso a la precisión**, debido a la simplicidad del algoritmo

empleado en la técnica. A partir del desarrollo de esta técnica se ha alcanzado el Objetivo 2 de la tesis y se ha obtenido la patente ES 2334551 A1.

- Se ha realizado una revisión detallada de las técnicas *sensorless* de detección de la posición y velocidad en motores BLDC [8] y BDC, desde las más básicas, basadas en la detección de parámetros del motor como la fuerza contraelectromotriz, la corriente o las tensiones de fase, hasta otras más avanzadas, basadas en modelos, reconocimiento de patrones o redes neuronales artificiales. También se han analizado las implementaciones de *drivers* para estos motores y sus aplicaciones. A partir de este estudio puede concluirse que el control de motores BDC y BLDC utilizando sensores, tales como *encoders*, *resolvers* o sondas Hall, puede mejorarse mediante la **sustitución de los sensores por técnicas *sensorless***. De esta forma se consigue una **reducción en el coste y un incremento de la fiabilidad**, tanto en aplicaciones de propósito general como en aquellas que son críticas o que requieren un alto rendimiento. A partir de la realización de este estudio se ha alcanzado el Objetivo 1 de la tesis y se ha escrito el Artículo 1 del compendio.

- Se ha desarrollado una técnica *sensorless*, basada en la componente *ripple* de la corriente, para estimar la posición y velocidad de motores BDC utilizando un sistema de reconocimiento de patrones con clasificadores *Support Vector Machine* (SVM) [38]. Este sistema permite detectar las ondulaciones normales en la componente *ripple*, detectar las ondulaciones fantasmas y descartar las falsas ondulaciones. Está formado por una serie de etapas entre las que se encuentran la obtención de las características de la corriente y la clasificación. El clasificador SVM tiene como entradas las características obtenidas de la corriente, de forma que a través del aprendizaje mediante ejemplos [79] permite decidir si en un instante dado existe o no una ondulación en la corriente, considerándose que el instante de identificación de las ondulaciones es aquel en el que la corriente alcanza su valor máximo. Para estimar la posición se contabilizan las ondulaciones que aparecen en la corriente como consecuencia de la componente *ripple*, y la velocidad se estima mediante el inverso del tiempo transcurrido entre ondulaciones. Esta técnica ha sido validada con los motores EMG30 y 719RE385 con *tests* a velocidad constante, aceleración constante y con saltos de velocidad. En primer lugar, los *tests* a velocidad constante se realizaron entre 500 y 11.000 rpm aproximadamente, y se obtuvieron unos resultados con unos errores de posición y velocidad absolutos medios inferiores a 6 rpm y 7,5 rad para el primer motor, y 18 rpm y 6.5 rad para el segundo, observándose que la varianza de este error es proporcional a la velocidad. En segundo lugar, los *tests* con aceleración constante se realizaron entre 3.100 y 5.100 rpm, y se consiguieron unos resultados con unos errores absolutos medios inferiores a 0.5 rpm y 2,1 rad, así como 0,2 rpm y 19 rad para el primer y segundo motor, respectivamente.

En tercer lugar, los *tests* con salto de velocidad 2.000 rpm con los motores girando a una velocidad superior a 2.000 rpm, lográndose unos resultados en los que el valor final de velocidad se consiguió detectar en un tiempo inferior a 0,2 s, y con errores de posición absolutos medios inferiores a 16 rad y 1,1 rad para el primer y segundo motor, respectivamente. Estos resultados muestran que la técnica permite la estimación de la posición y de la velocidad con unos **errores de precisión reducidos en un amplio rango de velocidades y en diferentes condiciones de operación**. Sin embargo, la técnica propuesta presenta como desventajas el **alto coste computacional**, por el uso del clasificador SVM, y una **puesta en funcionamiento ligeramente compleja** debido a la necesidad de realizar un entrenamiento adecuado del clasificador como base de su precisión. Sin embargo, debido al uso de este clasificador se logra una **minimización del efecto del ruido** sobre la señal de corriente utilizada en la detección. A partir del desarrollo de esta técnica se ha alcanzado el Objetivo 3 de la tesis y se ha escrito el Artículo 2 el compendio.

- Se ha desarrollado una técnica *sensorless* de detección de la posición y velocidad para motores BLDC utilizando la derivada de los voltajes de fase con respecto a un punto neutro virtual [80]. Esta técnica ha sido implementada utilizando una plataforma *driver* basada en una FPGA, un procesador en tiempo real, circuitería analógica (amplificadores y filtros) para el acondicionamiento y adaptación de las señales del motor, y circuitos con amplificadores operacionales en modo derivador para el cálculo de la derivada de los voltajes. También, se ha desarrollado un *software* de procesamiento basado en LabVIEW para detectar los pulsos de la derivada de las tensiones y para eliminar los pulsos falsos (*ghost pulses*) que son consecuencia del ruido. La técnica se ha validado en los rangos 5-1500 rpm y 5-150 rpm sin carga y a plena carga, respectivamente, con el motor Maxon EC 45 Flat. Se han realizado *tests* con velocidad constante, con aceleración constante y con saltos bruscos de velocidad. Por una parte, sin carga en el motor (o con una carga mínima) se han obtenido unos resultados con unos errores cuadráticos medios de posición y velocidad entre 10º y 30º e inferiores a 3 rpm, respectivamente. Por otra parte, con el motor a plena carga se han logrado unos resultados que presentan unos errores cuadráticos medios de posición entre 10º y 15º, y de velocidad inferiores a 1 rpm. Además, se observó que en condiciones de plena carga los errores de precisión eran menores que sin ella, teniendo que en cuenta que los *tests* a plena carga fueron realizados a velocidades bajas y que los errores de precisión aumentaban con la velocidad. A partir estos resultados, se verifica la efectividad de la técnica propuesta en la detección de la posición y velocidad de motores BLDC con **reducidos errores de precisión en un amplio rango de velocidades y bajo diferentes condiciones de operación** frente a otras técnicas sensorless, como las basadas en la detección del cruce por cero de la tensión BEMF (con una resolución de 30º

respecto al instante de conmutación). Además, se ha logrado un **menor coste computacional** con respecto a otras técnicas *sensorless* similares basadas en la detección de parámetros del motor. Esta técnica presenta también una **relevante inmunidad al ruido** debido al uso de un punto neutro virtual para las señales del motor y el empleo de otros recursos para su mitigación, como métodos de filtrado por *hardware* y *software*. A partir del desarrollo de esta técnica se ha alcanzado el Objetivo 4 de la tesis y se ha escrito el Artículo 3 del compendio.

- Se ha desarrollado una técnica *sensorless* para estimar la posición y velocidad de motores BLDC mediante redes neuronales artificiales de tipo *Multilayer Perceptron*, entrenadas con el algoritmo *Backpropagation*, y utilizando los voltajes de fase del motor con respecto a un punto neutro virtual. Para el entrenamiento y *test* de las ANNs se han utilizado como referencia los datos de posición de un *encoder* incremental, y se han procesado los voltajes del motor mediante una FPGA, un procesador en tiempo real, electrónica de acondicionamiento y un ordenador. Esta técnica se ha validado en el rango 125-1500 rpm con aceleración constante utilizando el motor Maxon EC 45 Flat con carga. Bajo estas condiciones, se han obtenido unos resultados con un error de posición absoluto medio de 6,47º y un error de velocidad relativo medio de 4,87%. A partir de estos resultados, se deduce que la estimación de la posición se realiza con unos **errores de precisión ligeramente inferiores** que con técnicas *sensorless* básicas (con una precisión de posición de 7,5º para un motor BLDC de 8 polos), obteniéndose que la precisión en la estimación de velocidad es poco afectada por los errores de posición. Sin embargo, debido al uso de redes neuronales el **coste computacional es relativamente más elevado** que en otras técnicas con una precisión sólo ligeramente peor. Esta técnica presenta también una **relevante inmunidad al ruido** sobre los voltajes del motor utilizados por la red neuronal, al emplearse un punto neutro virtual como referencia para las señales del motor y métodos de filtrado por *hardware*. A partir del desarrollo de esta técnica se ha alcanzado el Objetivo 5 de la tesis y se ha escrito el Artículo 4 del compendio.

De forma general, puede concluirse que se ha realizado el estudio de las técnicas *sensorless* existentes para los motores BDC y BLDC, y se han desarrollado y validado cuatro técnicas *sensorless* para ambos tipos de motores en un amplio rango de velocidades y bajo diferentes condiciones de operación. Se han logrado unos resultados con bajos errores de precisión en la detección de la posición y velocidad, además de conseguirse la reducción de la influencia del ruido sobre los voltajes o las corrientes del motor y también, en algunos casos, un bajo coste computacional.

1.6 Líneas futuras

A la partir de los resultados obtenidos se plantean una serie de posibles trabajos futuros que pueden enriquecer el campo de las tecnologías *sensorless*.

En las técnicas propuestas se realiza la detección o estimación de la posición y/o velocidad de motores *brushed* DC y *brushless* DC a partir del procesamiento de las corrientes y/o voltajes característicos de cada tipo de motor. En el caso de motores BDC, debido a los problemas que plantea el uso de elementos mecánicos para la conmutación y la transferencia de corriente de cara a la vida útil y mantenimiento del motor, se podrían utilizar las técnicas *sensorless* para monitorizar el estado de ciertos componentes fundamentales del motor, como las escobillas o las bobinas, y así predecir o evitar el fallo del motor. Para motores BLDC, podría plantearse el estimar otras magnitudes del motor como la resistencia del estátor para calcular la posición y velocidad, lo cual se realiza en algunas técnicas basadas en filtros de Kalman y observadores adaptativos como MRAS.

La experiencia obtenida de la aplicación de redes neuronales artificiales (ANN) a los los voltajes de fase del motor BLDC (Artículo 4 del compendio) puede ser extrapolada a motores BDC, teniendo en cuenta las diferencias de ambos tipos de motores. Esta aplicación de ANN a motores BDC se ha considerado en la tesis dentro del grupo de técnicas avanzadas *sensorless*, y representa una posible vía de desarrollo futuro de nuevas técnicas para este tipo de motores puesto que ya existen trabajos en esta línea.

Otra posible vía de desarrollo en motores BLDC es aplicar reconocimiento de patrones con clasificadores *Support Vector Machines*, en línea con lo aprendido a partir del desarrollo de la técnica para motores BDC incluida en el Artículo 2 del compendio. De esta forma se estaría considerando la estimación de la posición y velocidad en motores BLDC como un problema dentro de la teoría de aprendizaje estadístico, lo cual ya fue propuesto en el apartado “Future Scope” del Artículo 3 del compendio.

Con el fin de reducir el coste computacional relativamente alto de las técnicas desarrolladas basadas en el reconocimiento de patrones con clasificadores o en redes neuronales, se podrían embeber los algoritmos asociados en una matriz de puertas programable (FPGA) o en un procesador digital de señal (DSP). De esta forma, se contribuiría al uso de estas técnicas en aplicaciones con este tipo de motores, puesto que se tendría integrado en un sólo dispositivo (junto con la circuitería adicional de acondicionamiento y adquisición) la técnica de detección, y podría formar parte del *driver* de los motores de la aplicación en cuestión.

Las técnicas desarrolladas en la tesis se han validado de forma bastante exitosa para motores BDC y BLDC, lo cual avala su viabilidad y apoya el planteamiento de una posible aplicación de éstas a otros tipos de motores, como los de inducción o los paso a paso. Estos dos tipos de motores indicados son utilizados mayoritariamente a nivel industrial frente a otros, de forma que las técnicas *sensorless* aplicadas podrían tener

una alta repercusión tecnológica debido a la elevada implantación los mismos en distintos ámbitos de aplicación. En otras aplicaciones mucho más exigentes, como en el sector aeroespacial, la utilización de técnicas *sensorless* podría aplicarse a la detección de la posición del motor en actuadores electromecánicos (EMA) para el arranque y operación de los mismos. Esto supondría un gran avance de cara a las soluciones tecnológicas utilizadas actualmente en este tipo de aplicaciones, y en las cuales se busca constantemente la optimización de factores como el espacio, el peso y la fiabilidad. Lo interesante en este ámbito, a diferencia de los sectores puramente industriales, es que cualquier nueva tecnología integrada en equipos embarcados tiene asociada un exhaustivo proceso de certificación de acuerdo a estrictos estándares de seguridad (por la OACI en aeronáutica o por la ESA en espacio), lográndose alcanzar un alto nivel de mejora en las técnicas *sensorless* consideradas.

1.7 Línea de investigación y relación temática de las contribuciones

El comienzo de las investigaciones en el ámbito indicado, sobre todo en lo que se refiere al trabajo con motores DC, se llevó a cabo en la etapa como investigador en el área de Robótica Móvil, Visión Artificial y Sistemas en Tiempo Real del centro de I+D *CARTIF* (Centro de Automatización, Robótica y Tecnologías de la Información y la Fabricación). En esta etapa se colaboró en el diseño de múltiples robots para distintas aplicaciones en los que se utilizaban motores, y como principal aportación se implementó un sistema de control industrial en el que se desarrolló tanto el *hardware* y *firmware* de los microcontroladores de que constaba, además de un interfaz de gestión y control en LabVIEW. Este sistema fue aplicado para automatizar y controlar distintas máquinas y módulos industriales formados por sensores, como finales de carrera o ultrasonidos, y actuadores formados por motores BDC y servos. Algunas de las máquinas que se utilizaron como plantas bajo control fueron una máquina atadora de embutido, con múltiples motores y actuadores electrohidráulicos, y un sistema de guiado láser con dos grados de libertad implementado con motores servo. En base a todo este proceso de investigación se obtuvo el **Premio de Innovación 2004 en Ingeniería Industrial e Ingeniería Química** [81].

Posteriormente, se colaboró como investigador en el centro de I+D *CEDETEL* (Centro para el Desarrollo de las Telecomunicaciones de Castilla y León) y en el cual se trabajó en el área de radio propagación de señales, desarrollándose una plataforma móvil para automatizar las medidas de campo eléctrico de señales GSM en entornos interiores con una antena isotrópica. En este caso, el sistema robótico implementado utilizaba un motor BDC, y tanto para realizar su control como para la adquisición de las señales de la antena mediante un analizador de espectros se diseñó un programa en Visual Basic y *hardware* específico. Estas investigaciones permitieron además publicar **dos artículos en la revista *Electronics World*** [82, 83].

A partir del comienzo de los estudios de doctorado, se empezó a investigar dentro del Grupo de Telemática Industrial del Departamento de Teoría de la Señal y Comunicaciones e Ingeniería Telemática de la E.T.S.I. Telecomunicación de Valladolid. Dentro de este grupo se colaboró con Ernesto Vázquez Sánchez en una línea de investigación para el desarrollo de técnicas *sensorless* de detección de la posición y velocidad de motores BDC. Teniendo en consideración las desventajas de estos motores y las tendencias actuales, se planteó la búsqueda de otros motores DC que superaran estos problemas y tuvieran una buena perspectiva de desarrollo futuro. En este se sentido, se consideraron los motores BLDC como firme candidato para ocupar este puesto, y con ello se abrió una línea de investigación paralela centrada en estos motores con el fin de ampliar mucho más el ámbito de la tesis y enriquecer su temática, sin dejar a atrás la colaboración iniciada en motores BDC. Al principio se empezó a estudiar el funcionamiento de los motores BLDC y se realizaron experimentos preliminares

empleando motores con distintas configuraciones, como en delta o estrella, y con componentes integrados, como sondas Hall, con el fin de probar e investigar acerca del proceso de arranque y giro con o sin carga. También se probaron múltiples configuraciones *hardware*, como diferentes tipos de inversores diseñados con transistores MOSFET, BJT o IGBTs, y distintas tarjetas de adquisición de datos con una mayor o menor cantidad de recursos, como convertidores A/D o una FPGA, además de los correspondientes programas en LabVIEW para evaluar el rendimiento de cada una de ellas.

Debido a la colaboración existente en el marco de los motores BDC, se participó en la solicitud de la **patente de invención** "Método para determinar la velocidad angular en un motor conmutado mecánicamente midiendo únicamente la corriente que circula por el mismo" [37], la cual fue concedida en enero de 2011. Este trabajo se encuadra dentro de las técnicas de detección basadas en la componente *ripple*, en el cual se analiza la componente alterna de la corriente que circula por el motor, de forma que a partir de las ondulaciones de la misma se puede obtener la frecuencia *ripple* y con ella la velocidad del motor.

En lo que respecta a los motores BLDC, no solamente se continuó analizando sus principios, como las ecuaciones eléctricas y mecánicas, modelos equivalentes, configuraciones, etc., sino que también se realizó un amplio estudio de las técnicas *sensorless* básicas y avanzadas de detección de la posición y velocidad, además de sus aplicaciones. Como resultado, se publicó en julio de 2010 el artículo "Position and Speed Control of Brushless DC Motors Using Sensorless Techniques and Application Trends" [8] en la revista Sensors, incluido en la tesis como **Artículo 1 del compendio**. A medida que se siguió investigando en motores BLDC, y en línea con la metodología de la investigación expuesta, se apreció la necesidad de comenzar con el planteamiento del desarrollo de una plataforma *driver* para estos motores debido a la complejidad de su uso, la cual debía ser diseñada para soportar los desarrollos en técnicas *sensorless*. Sin embargo, en este periodo también se siguió trabajando en la investigación de técnicas *sensorless* para motores BDC y, debido al avance de las mismas, se pudieron desarrollar técnicas avanzadas de estimación de la posición y velocidad, como las basadas en reconocimiento de patrones con clasificadores.

Con todo el trabajo realizado, en marzo de 2012 fue publicado el artículo "A New Method for Sensorless Estimation of the Speed and Position in Brushed DC Motors Using Support Vector Machines" [38], en el que se presentaba la estimación de la posición y velocidad de motores *brushed* DC usando reconocimiento de patrones con clasificadores SVM. Este trabajo ha sido incluido en la tesis como **Artículo 2 del compendio**. Al igual que la técnica perteneciente la patente antes indicada, este trabajo se encuadra dentro de las técnicas de detección basadas en la componente *ripple* y supone uno de los puntos que culminan la investigación en técnicas *sensorless* para motores BDC. Los conocimientos adquiridos para el desarrollo de esta técnica se reutilizaron para avanzar con la implementación de técnicas para motores BLDC, tales

como configuraciones *hardware* para medida de corriente, utilización de *encoders* para posición de referencia del motor, así como una mejor comprensión de ciertas tecnologías, como los filtros de Kalman o Redes Neuronales Artificiales.

Debido a que en los motores BDC se utiliza la corriente para extraer información del motor, se decidió utilizar otro parámetro del motor diferente en la investigación para motores BLDC, como las tensiones de fase, con el fin de enriquecer y ampliar el ámbito del estudio presentado en la tesis. Con estas premisas se realizó la implementación de una plataforma *driver* de motores BLDC lo más versátil posible, incluyendo el *hardware* necesario para el arranque y aceleración del motor, acondicionamiento y adquisición de señales, y la programación de algoritmos en tiempo real para el desarrollo de técnicas *sensorless*. A partir de este sistema de desarrollo, se probaron distintos motores y se trabajó con técnicas PWM para el control de los motores, además de incluirse un *encoder* para las medidas de referencia de la posición y velocidad. Como resultado, se desarrolló una técnica de detección *sensorless* que utilizaba casi todos los recursos *hardware* y *software* de la plataforma con un procesamiento en tiempo real de decenas de microsegundos. En julio de 2015 se publicó el artículo de revista "Sensorless Detection of Position and Speed in Brushless DC Motors using the Derivative of Terminal Phase Voltages Technique with a Simple and Versatile Motor Driver Implementation" [80], en el que se propone una técnica *sensorless* de detección de la posición y velocidad basada en la derivada de las tensiones de fase del motor BLDC, en vez de utilizarse la información de la corriente como se hacía en motores BDC. Este trabajo figura en la tesis como **Artículo 3 del compendio**. Como línea de desarrollo futura planteada en este artículo, y en base a lo aprendido en el Artículo 2 del compendio para motores BDC, se propuso el uso de reconocimiento de patrones con clasificadores SVM para motores BLDC. De esta forma, se podría considerar la detección de la posición y velocidad en estos motores como un problema de aprendizaje estadístico para detectar los pulsos de la derivada y también descartar los pulsos falsos.

Con todo lo desarrollado, se consiguió un sistema estable y validado que permitiera desarrollar técnicas *sensorless* utilizando los voltajes de fase del motor BLDC. A partir de esto se pudo plantear la implementación de técnicas más avanzadas con el fin de alcanzar el nivel de investigación logrado antes en motores BDC. En este sentido, se comenzó a estudiar la aplicación de Redes Neuronales Artificiales (ANN) en la estimación la posición y velocidad de estos motores. Cabe destacar que las ANN también son utilizadas en motores BDC en la literatura, por lo que la utilización de las mismas ha tenido doble finalidad. Por un lado, desarrollar técnicas para motores BLDC y por otro, sentar las bases de conocimiento necesarias para poder plantear el desarrollo futuro de técnicas *sensorless* en motores BDC con otra tecnología avanzada distinta al reconocimiento de patrones con clasificadores. Como resultado, en marzo de 2015 se envió el artículo "A Sensorless Technique for Position and Speed Estimation of Brushless DC Motors with Neural Networks" a la revista *IEICE Transactions on Fundamentals of Electronics, Communications and Computer Sciences*, el cual se

encuentra actualmente en proceso de revisión. Este trabajo se referencia en la tesis como **Artículo 4 del compendio**. En este artículo se presenta una técnica para estimar la posición y velocidad de motores BLDC utilizando dos redes neuronales *Multilayer Perceptron*, en la que una de ellas estima la posición del rotor a partir de los voltajes de fase y la otra estima la velocidad utilizando la salida de posición de la primera.

Para finalizar, cabe destacar que a lo largo de la realización de la tesis se ha contribuido como revisor del Institute of Electrical and Electrical and Electronics Engineers (IEEE) para la revisión de artículos para las revistas ***IEEE Power Electronics, IEEE/ASME Transactions on Mechatronics***, e ***IEEE Sensors Journal***, cuyas publicaciones poseen una relevancia destacada dentro del ámbito de la tesis. También es importante mencionar que un aspecto fundamental en la línea de investigación seguida son las perspectivas de futuro, en base a las cuales se podría plantear la utilización total o parcial de algunas de las técnicas expuestas para otros tipos de motores, como los de inducción, masivamente utilizados a nivel industrial, además de la profundización en el desarrollo de técnicas basadas en redes neuronales o filtros de Kalman para los dos tipos de motores considerados.

1.8 Contribuciones originales

En esta sección se analiza la originalidad de las principales aportaciones científicas realizadas a partir de los resultados obtenidos para motores BDC y BLDC, haciendo mención también a las diferencias con respecto a otros trabajos dentro del mismo ámbito.

Se ha desarrollado una técnica *sensorless* para motores BDC basada en la componente *ripple* de la corriente [37] (patente de invención ES 2334551 A1), la cual permite detectar las ondulaciones que aparecen en corriente del motor mediante la comparación entre las muestras actuales de la corriente y las inmediatamente cercanas en tiempo, siendo el instante de identificación de las ondulaciones aquel en el que la corriente alcanza su valor máximo. La posición del motor se estima contando el número de ondulaciones producidas, y a través de la distancia temporal entre ondulaciones se estima la velocidad. Debido a que se emplea una ventana de observación de muestras de tamaño variable con la frecuencia *ripple*, se detectan algunas ondulaciones fantasmas y se descartan algunas ondulaciones falsas, lo cual permite reducir el efecto del ruido sobre la corriente, y por tanto mejorar la precisión. Además, debido a la simplicidad del algoritmo utilizado, se logra minimizar el coste computacional. Esta técnica, perteneciente al grupo de observadores *sensorless* que monitoriza la tendencia de la corriente, tiene en cuenta el problema del ruido de forma explícita, a diferencia de otras técnicas de este grupo y basadas en los mismos principios. Algunos ejemplos son las técnicas realizadas por Oka *et al.* [46], en la que se detecta la velocidad a partir de la frecuencia de la componente *ripple* utilizando un filtro paso bajo junto con otros componentes (como un PLL), y por Macks *et al.* [84], en la que se detecta la velocidad a partir de la frecuencia de la componente *ripple* utilizando un filtro paso alto y un comparador. Por otra parte, el bajo coste computacional también diferencia a esta técnica respecto a otras más avanzadas, en las que sí se considera el problema del ruido, pero su coste computacional es más elevado debido a requieren la realización de operaciones con cálculos intensivos, como análisis espectrales de la corriente. Algunas técnicas representativas son las desarrolladas por Gerlach [47], en la que se realiza un análisis espectral de la componente *ripple* para determinar sus componentes frecuenciales y la posición se detecta contando el número de cambios bruscos de las frecuencia *ripple*, y por Richter y Skibowski [85], en el que se la velocidad se detecta a partir de la distancia entre el mínimo y el máximo de la secuencia de autocorrelación de las muestras de la corriente.

Se ha desarrollado una técnica *sensorless* para motores BDC basada en el uso de un sistema de reconocimiento de patrones que utiliza un clasificador *Support Vector Machine* (SVM) [38] (Artículo 2 del compendio), el cual tiene como entradas las características de la corriente obtenidas por el sistema de reconocimiento de patrones, e identifica el instante en el que se ha producido una ondulación (en el que la corriente es máxima) en base al aprendizaje con ejemplos. De esta forma, se

consiguen detectar las ondulaciones normales en la componente *ripple*, así como las ondulaciones fantasmas y descartar las falsas ondulaciones para minimizar el efecto del ruido y así mejorar la precisión. Algunas técnicas similares son las realizadas por Iott y Burke [41] y Micke *et. al* [86], en las que se realiza un filtrado para eliminar la componente DC de la corriente y luego se compara la señal con un determinado nivel. A diferencia de la técnica propuesta, en estas técnicas no se lleva a cabo una reducción del efecto del ruido, debido a que no se detectan ondulaciones fantasmas ni se descartan ondulaciones falsas. En otras técnicas similares, además de emplearse un comparador, se utiliza un estimador de la distancia entre ondulaciones. Algunos ejemplos son las técnicas desarrolladas por Kessler y Schulter [52], y Lutter y Fiedrich [53], en las que se estima una ventana en donde debe encontrarse la siguiente ondulación, considerándose que hay una ondulación fantasma cuando no hay ningún pulso dentro de esta ventana, y una ondulación falsa cuando un pulso es detectado antes del inicio de la misma. A diferencia de la técnica propuesta, en estas técnicas no se consigue reducir de forma eficiente el efecto del ruido, puesto que se pueden producir errores de estimación debidos a que se descarten ondulaciones válidas y se consideren pulsos fantasmas otros que no lo son.

Se ha desarrollado una técnica *sensorless* para motores BLDC basada en el uso de la operación matemática derivada sobre las tensiones de fase del motor con respecto a un punto neutro virtual [80] (Artículo 3 del compendio). En esta técnica no es necesario utilizar comparadores de nivel (o umbral) debido a que se emplea un *hardware* específico para derivar, acondicionar y adquirir las señales del motor, basado en filtros y amplificadores, y un procesamiento *software* en tiempo-real, basado en una FPGA, para eliminar los pulsos falsos de la derivada que aparecen como consecuencia del ruido. De esta forma, se consigue minimizar el efecto del ruido sobre las tensiones del motor y se mejora la precisión al detectarse con menor error los instantes en los que se producen las conmutaciones de fase. En esta técnica, se ha empleado la operación derivada para obtener los instantes de las conmutaciones de fase, lo cual permite diferenciarla con respecto a otras que utilizan principios matemáticos diferentes, y en las cuales el uso de la derivada no es tan frecuente. Algunos ejemplos de estas técnicas han sido propuestas por Becerra *et al.* [56] o Jahns *et al.* [87], en las que se aplica la operación de integración a la tensión BEMF de la fase flotante en la conmutación, y por Moreira *et al.* [64] o Johnson *et al.* [65], en las que se emplea la integración del tercer armónico de los voltajes de fase. Otra diferencia con respecto a otros trabajos existentes es el uso de una FPGA no sólo para detectar los instantes de conmutación o ciertas características de las señales del motor, sino también para realizar un filtrado por *software* de los pulsos falsos de la derivada debidos al ruido, los cuales pueden contribuir a que se produzcan errores en la detección, y por tanto afectar a la precisión de la técnica. Algunos ejemplos representativos son los realizados por Darba *et al.* [88] y por Kuang-Yao [89], en los que se utiliza *hardware* analógico y una FPGA para muestrear los voltajes de fase del motor, y únicamente mediante la comparación del voltaje BEMF de la fase inactiva con

un cierto umbral (cruce por cero) se detectan los instantes de la conmutación, sin tener en cuenta que algunos pueden ser enmascarados por el ruido.

1.9 Aportaciones científicas

1.9.1 Aportaciones científicas relacionadas con la tesis

De acuerdo a la base de datos *Scopus* elaborada por *Elsevier* y realizando una búsqueda por autor se ha obtenido un índice personal de citas o **índice h de valor 2**. En concreto, en la Figura 8 se muestra esta base de datos [90], en la cual se indica que los artículos 1 y 2 pertenecientes al compendio son citados en otras publicaciones. El artículo 3 no tiene citas debido a que su publicación es muy reciente con respecto a la presentación de la memoria de tesis.

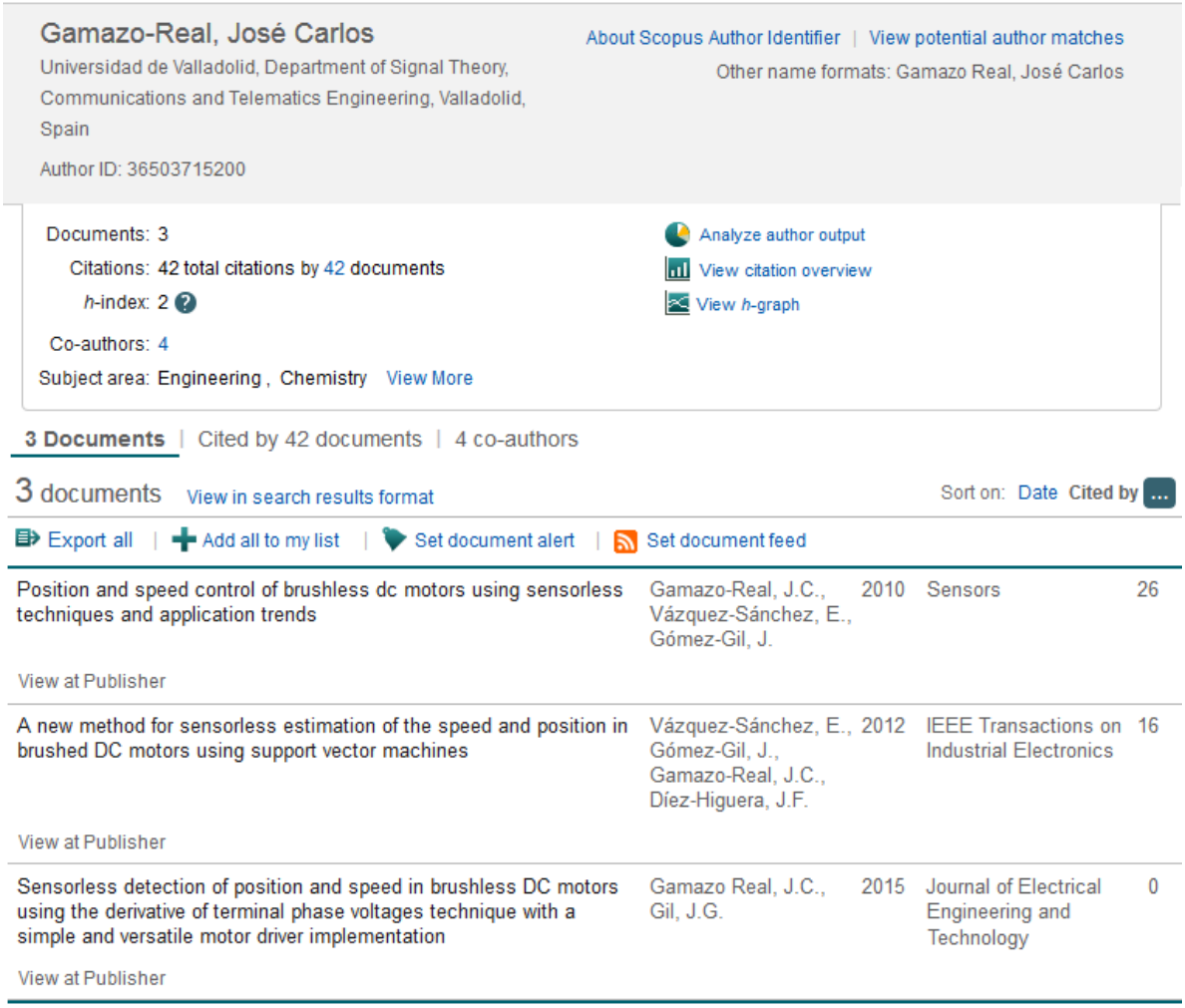

Figura 8. Índice h del autor en Scopus y artículos del compendio con citas en otras publicaciones. Fuente: Base de datos Scopus de Elsevier [90].

A continuación se incluyen de forma detallada los datos bibliográficos para cada una de las aportaciones científicas, sobre todo los artículos del compendio, en los que además se incluye más información adicional que justifica la calidad de las publicaciones, como es el **cuartil** o el **ranking** en el que se encuentra la revista dentro de cada una de las categorías o disciplinas. Además, se han consultado los *Journal Citation Reports* (JCR) de la base de datos *Web of Science* (*Institute of Scientific*

Information, ISI) para cada una de las revistas en las que se han publicado o enviado los artículos el compendio, y más en concreto el índice impacto (*Impact Factor*).

1.9.1.1 Artículo 1 compendio

Referencia: J.C. Gamazo-Real, E. Vázquez-Sánchez, and J. Gómez-Gil, "Position and Speed Control of Brushless DC Motors Using Sensorless Techniques and Application Trends," *Sensors*, vol. 10, no. 7, pp. 6901–6947, July 2010. doi: 10.3390/s100706901.

Revista: Sensors, ISSN: 1424-8220.

Factor de Impacto (JCR 2010): 1,774.

Ranking en Categorías (JCR 2010):

- Categoría Instruments & Instrumentation: 14 de 61 (Q1).
- Categoría *Chemistry, Analytical*: 38 de 73 (Q3).
- Categoría *Electrochemistry*: 16 de 26 (Q3).

Citas:

Este artículo fue publicado hace 5 años, y en la fecha de presentación de la memoria de tesis (28/07/2015) éste consta de **26 citas** según la base de datos ***Scopus*** [90], tanto por artículos publicados en la misma revista *Sensors* (factor de impacto 2,245 en JCR 2014) como por otros pertenecientes a otras revistas de cierta relevancia, como *Journal of Dynamic Systems, Measurement, and Control* (factor de impacto 1,039 en JCR 2013) o *Mathematical Problems in Engineering* (factor de impacto 1,082 en JCR 2013). También, se han consultado otras bases de datos como ***Web of Science Core Collection*** (WOS) con **9 citas** [91], o ***Google Scholar*** con **57 citas** [92]. Otro dato más a destacar es que según la revista ***BioMedUpdater*** el artículo (con el PMID 22163582) es el primero en orden de relevancia dentro su dominio o área científica desde su publicación en 2010 [93]. A continuación se incluye el listado de las publicaciones que según la base de datos *Scopus* han citado este artículo, ordenadas por fecha de antigüedad:

- S. Wang and A. C. Lee, "A 12-Step Sensorless Drive for Brushless DC Motors Based on Back-EMF Differences," *IEEE Transactions on Energy Conversion*, vol. 30, pp. 646-654, 2015.M. Gan and C. Wang, "An adaptive nonlinear extended state observer for the sensorless speed control of a PMSM," *Mathematical Problems in Engineering*, vol. 2015, 2015.
- P. Drozdowski, "Modelling of BLDCM with a double 3-phase stator winding and back EMF harmonics," *Archives of Electrical Engineering*, vol. 64, pp. 53-66, 2015.

- N. Pavan Kumar and N. Mohan Raj, "Implementation of various PWM techniques to control the speed of PMBLDC drive," *International Journal of Applied Engineering Research,* vol. 10, pp. 19867-19884, 2015.
- A. Kumar, *et al.*, "Aerodynamic simulation, thermal and fuel consumption analysis of hydrogen powered fuel cell vehicle," *International Journal of Vehicle Structures and Systems,* vol. 7, pp. 31-35, 2015.
- K. H. Zhao, *et al.*, "Online fault detection of permanent magnet demagnetization for IPMSMs by nonsingular fast terminal-sliding-mode observer," *Sensors,* vol. 14, pp. 23119-23136, 2014.
- G. J. García, *et al.*, "A survey on FPGA-based sensor systems: Towards intelligent and reconfigurable low-power sensors for computer vision, control and signal processing," *Sensors,* vol. 14, pp. 6247-6278, 2014.
- G. Szafranski, *et al.*, "Modeling and identification of electric propulsion system for multirotor unmanned aerial vehicle design," in *2014 International Conference on Unmanned Aircraft Systems, ICUAS 2014 - Conference Proceedings*, 2014, pp. 470-476.
- R. Sankarganesh and S. Thangavel, "SVPWM control based bridgeless PFC cuk converter for PMSM under dynamic conditions," *WSEAS Transactions on Circuits and Systems,* vol. 13, pp. 319-335, 2014.
- R. Jayanthi and I. Gnanambal, "Fuzzy PI controller based fault analysis and recovery in sensorless BLDC motor using High gain hybrid converter (HGHC)," *Research Journal of Applied Sciences, Engineering and Technology*, vol. 8, pp. 2195-2210, 2014.
- A. Ravi and S. Palani, "Research on sensorless control strategies for vehicle stability using fuzzy based edc," *International Journal of Engineering and Technology*, vol. 6, pp. 1017-1025, 2014.
- T. Sarkar, *et al.*, "A generalized approach to design the electrical power system of a solar electric vehicle," in *2014 IEEE Students' Conference on Electrical, Electronics and Computer Science, SCEECS 2014*, 2014.
- S. Y. Lin, *et al.*, "The study of the piston driving and position sensing for a linearly moving piston pump," in *CACS 2014 - 2014 International Automatic Control Conference, Conference Digest*, 2014, pp. 287-291.
- M. M. Nikolic, *et al.*, "FPGA based development platform for implementation of brushless DC motor control," in *2013 21st Telecommunications Forum Telfor, TELFOR 2013 - Proceedings of Papers*, 2013, pp. 632-635.

- A. Gómez-Espinosa, *et al.*, "A new adaptive self-tuning Fourier Coefficients algorithm for periodic torque ripple minimization in permanent magnet synchronous motors (PMSM)," *Sensors*, vol. 13, pp. 3831-3847, 2013.
- S. Lu, *et al.*, "Adaptive PIF control for permanent magnet synchronous motors based on GPC," *Sensors*, vol. 13, pp. 175-192, 2013.
- B. B. Li, et al., "BMP: A self-balancing mobile platform," in Proceedings - International Conference on Machine Learning and Cybernetics, 2012, pp. 868-874.
- A. Tashakori and M. Ektesabi, "Stability analysis of sensorless BLDC motor drive using digital PWM technique for electric vehicles," in *IECON Proceedings (Industrial Electronics Conference)*, 2012, pp. 4898-4903.
- B. S. K. K. Ibrahim, *et al.*, "PI-fuzzy logic control for 3 phase BLDC motor for electric vehicle application," in *Proceedings - UKSim-AMSS 6th European Modelling Symposium, EMS 2012*, 2012, pp. 84-88.
- B. Hu, *et al.*, "A novel sensorless algorithm of the trapezoidal back-electromagnetic force brushless DC motors from near-zero to high speeds," *Australian Journal of Electrical and Electronics Engineering*, vol. 9, pp. 263-274, 2012.
- I. Colak and M. Sahin, "Sensorless control of a brushless DC motor using a Self-Tuning PID," in *SPEEDAM 2012 - 21st International Symposium on Power Electronics, Electrical Drives, Automation and Motion*, 2012, pp. 1057-1062.
- S. Sukumar and M. R. Akella, "Persistence filters for estimation: Applications to control in shared-sensing reversible transducer systems," *Journal of Dynamic Systems, Measurement and Control, Transactions of the ASME*, vol. 134, 2012.
- M. A. Noroozi, *et al.*, "An improved direct torque control of brushless DC motors using twelve voltage space vectors," in *2012 3rd Power Electronics and Drive Systems Technology, PEDSTC 2012*, 2012, pp. 133-138.
- T. Bourlai, *et al.*, "On designing a SWIR multi-wavelength facial-based acquisition system," in *Proceedings of SPIE - The International Society for Optical Engineering*, 2012.
- B. Tefay, *et al.*, "Design of an integrated electronic speed controller for compact robotic vehicles," in *Proceedings of the 2011 Australasian Conference on Robotics and Automation*, 2011.

- M. I. Milanés-Montero, *et al.*, "Hall-effect based semi-fast AC on-board charging equipment for electric vehicles," *Sensors*, vol. 11, pp. 9313-9326, 2011.

1.9.1.2 Artículo 2 compendio

Referencia: E. Vazquez-Sanchez, J. Gomez-Gil, J.C. Gamazo-Real, and J.F. Diez-Higuera, "A New Method for Sensorless Estimation of the Speed and Position in Brushed DC Motors Using Support Vector Machines," *Industrial Electronics, IEEE Transactions on*, vol. 59, no. 3, pp. 1397-1408, March 2012. doi: 10.1109/TIE.2011.2161651.

Revista: IEEE Transactions on Industrial Electronics, ISSN: 0278-0046.

Factor de Impacto (JCR 2012): 5,165.

Ranking en Categorías (JCR 2012):

- Categoría *Engineering, Electrical & Electronic*: 4 de 243 (Q1).
- Categoría *Instruments & Instrumentation*: 1 de 57 (Q1).
- Categoría *Automation & Control Systems*: 1 de 59 (Q1).

Citas:

Este artículo fue publicado hace 3 años y 4 meses, y en la fecha de presentación de la memoria de tesis (28/07/2015) éste consta de **16 citas** según la base de datos ***Scopus*** [90], tanto por artículos publicados en la misma revista *IEEE Transactions on Industrial Electronics* (factor de impacto 6,500 en JCR 2013) como por otros pertenecientes a otras revistas de cierta relevancia, como *IEEE Transactions on Power Electronics* (factor de impacto 5,726 en JCR 2013), *IEEE Transactions on Industrial Informatics* (factor de impacto 8,785 en JCR 2013) o *IEEE Transactions on Vehicular Technology* (factor de impacto 2,642 en JCR 2013). También, se han consultado otras bases de datos como ***Web of Science Core Collection*** (WOS) con **7 citas** [94], o ***Google Scholar*** con **20 citas** [95]. A continuación, se incluye el listado de las publicaciones que según la base de datos *Scopus* han citado este artículo, ordenadas por fecha de antigüedad:

- C. Cui, *et al.*, "A novel drive method for high-speed brushless dc motor operating in a wide range," *IEEE Transactions on Power Electronics*, vol. 30, pp. 4998-5008, 2015.
- L. Zhang, *et al.*, "An effective video summarization framework toward handheld devices," *IEEE Transactions on Industrial Electronics*, vol. 62, pp. 1309-1316, 2015.

- L. Zhang, *et al.*, "Spatial-aware object-level saliency prediction by learning graphlet hierarchies," *IEEE Transactions on Industrial Electronics*, vol. 62, pp. 1301-1308, 2015.
- Y. Kambara, *et al.*, "Disturbance suppression method for position-sensorless motion control of DC brushed motor," in *Proceedings - 2015 IEEE International Conference on Mechatronics, ICM 2015*, 2015, pp. 194-199.
- L. Zhang, *et al.*, "A fine-grained image categorization system by cellet-encoded spatial pyramid modeling," *IEEE Transactions on Industrial Electronics*, vol. 62, pp. 564-571, 2015.
- Y. Kambara, *et al.*, "Position-sensorless motion control of DC motor," *IEEJ Transactions on Industry Applications*, vol. 135, pp. 205-211, 2015.
- Y. Tanaka and K. Kosuge, "Dynamic attack motion prediction for kendo agent," in *IEEE International Conference on Intelligent Robots and Systems*, 2014, pp. 2187-2193.
- R. Toukhtarian and S. S. Saab, "Impact of model-order reduction of a DC motor on control systems: An undergraduate laboratory module," *International Journal of Engineering Education*, vol. 30, pp. 729-737, 2014.
- X. Lu, *et al.*, "Evaluation of SVM speed and position observers for sensorless PMSM in start-up region," in *IET Conference Publications*, 2014.
- X. Lu, *et al.*, "Evaluation of SVM speed and position observers for sensorless PMSM in start-up region," in *7th IET International Conference on Power Electronics, Machines and Drives, PEMD 2014*, 2014.
- J. M. Gu, *et al.*, "Endpoint detection in low open area TSV fabrication using optical emission spectroscopy," *IEEE Transactions on Components, Packaging and Manufacturing Technology*, vol. 4, pp. 1251-1260, 2014.
- M. A. A. Mohamed, *et al.*, "Developing an Open Architecture and Intelligent System for Speed and Direction Controlling (PC-SDC) of DC Motors," *Arabian Journal for Science and Engineering*, vol. 39, pp. 8793-8810, 2014.
- A. Dadashnialehi, *et al.*, "Intelligent sensorless ABS for in-wheel electric vehicles," *IEEE Transactions on Industrial Electronics*, vol. 61, pp. 1957-1969, 2014.

- J. M. Knezevic, "Low-cost low-resolution sensorless positioning of DC motor drives for vehicle auxiliary applications," *IEEE Transactions on Vehicular Technology*, vol. 62, pp. 4328-4335, 2013.
- X. Zhu, et al., "Guest editorial special section on intelligent sensing fundamentals and applications," *IEEE Transactions on Industrial Informatics*, vol. 9, pp. 1655-1658, 2013.
- C. Cecati and F. Marignetti, "Guest editorial," *IEEE Transactions on Industrial Electronics*, vol. 59, pp. 1330-1332, 2012.

1.9.1.3 Artículo 3 compendio

Referencia: J.C. Gamazo-Real and J. Gomez-Gil, "Sensorless Detection of Position and Speed in Brushless DC Motors using the Derivative of Terminal Phase Voltages Technique with a Simple and Versatile Motor Driver Implementation," *Journal of Electrical Engineering & Technology*, vol. 10, no. 4, pp. 1540-1551, July 2015. doi: 10.5370/JEET.2015.10.4.1540.

Revista: Journal of Electrical Engineering and Technology, ISSN: 1975-0102.

Factor de Impacto (JCR 2014): 0,528.

Ranking en Categorías (JCR 2014):

- Categoría *Engineering, Electrical & Electronic*: 196 de 249 (Q4).

Citas: Este artículo fue publicado recientemente y por ello no se tienen citas, ya que su publicación es muy reciente con respecto a la presentación de la memoria de tesis (28/07/2015).

1.9.1.4 Artículo 4 compendio (enviado y pendiente de aceptación)

Título: A Sensorless Technique for Position and Speed Estimation of Brushless DC Motors with Neural Networks.

Autores: J.C. Gamazo-Real, V. Martínez-Martínez, y J. Gómez-Gil.

Revista: IEICE Transactions on Fundamentals of Electronics, Communications and Computer Sciences, ISSN: 1745-1337.

Fecha de Envío: 21 de marzo de 2015. Actualmente en estado de revisión (*Manuscript ID*: 2015EAP1049).

Factor de Impacto (JCR 2014): 0,231.

Ranking en Categorías (JCR 2014):

- Categoría *Engineering, Electrical & Electronic*: 232 de 249 (Q4).
- Categoría *Computer Science, Information Systems*: 133 de 139 (Q4).
- Categoría *Computer Science, Hardware & Architecture*: 49 de 50 (Q4).

1.9.1.5 Patente

Referencia: E. Vázquez-Sánchez, J. Gómez-Gil, J.F. Díez-Higuera, J.C. Gamazo-Real, J.C., and J. García-Martín, "Método para determinar la velocidad angular en un motor conmutado mecánicamente midiendo únicamente la corriente que circula por el mismo," ES2334551 A1 Patent, January 2011.

Extracto de publicación: Anexo A, sección A.1.

1.9.1.6 Revisión de artículos de revistas

1.9.1.6.1 Revista IEEE Transactions on Power Electronics

Esta revista tiene en **JCR 2014** un factor de impacto de **6,008** y la posición **3 de 249 (Q1)** en la categoría de interés para la tesis *Engineering, Electrical & Electronic*.

- Fuengwarodsakul, *et al.*, "Sensorless Control of Switched Reluctance Drive with small DC-link Capacitor for High-Speed Blowers," Review date: 11/07/2015.

1.9.1.6.2 Revista IEEE Sensors Journal

Esta revista tiene en **JCR 2014** un factor de impacto de **1,762** y la posición **77 de 249 (Q2)** en la categoría de interés para la tesis *Engineering, Electrical & Electronic*.

- Dadashnialehi, *et al.*, "Sensor-fusion-based ABS for Brushless In-Wheel Electric Vehicles," Review date: 27/04/2015.

1.9.1.6.3 Revista IEEE/ASME Transactions on Mechatronics

Esta revista tenía en **JCR 2012** un factor de impacto de **3,135** y la posición **18 de 243 (Q1)** en la categoría de interés para la tesis *Engineering, Electrical & Electronic*.

- Lima-Filho, *et al.*, "Embedded System Integrated Into a Wireless Sensor Network for Online Dynamic Torque and Efficiency Monitoring in Induction Motors," vol. 17, no. 3, pp. 404-414, June 2012. Review date: 29/07/2011.
- Sharma, *et al.*, "Performance Analysis of a Binary Control Technique for Brushless DC Motor Drives," Review date: 24/04/2012.
- Dwijasish, *et al.*, "Development of BLDC Motor Based Elevator System Suitable for DC Microgrid," Review date: 26/07/2015.

1.9.2 Otras aportaciones científicas no relacionadas con la tesis

1.9.2.1 Artículo 5

Referencia: J.C. Gamazo-Real, J. Blas-Prieto, R. Lorenzo-Toledo, J. Gómez-Gil, "Propagation Study of GSM Power in Two Dimensions in Indoor Environments – Part 1," *Electronics World*, vol. 116, no. 1888, pp. 28-31, March 2010.

Revista: Electronics World, ISSN: 1365-4675.

Factor de Impacto (JCR 2010): 0,047.

Ranking en Categorías (JCR 2010):

- Categoría *Engineering, Electrical & Electronic*: 243 de 247 (Q4).
- Categoría *Telecommunications*: 77 de 80 (Q4).

1.9.2.2 Artículo 6

Referencia: J.C. Gamazo-Real, J. Blas-Prieto, R. Lorenzo-Toledo, J. Gómez-Gil "Propagation Study of GSM Power in Two Dimensions in Indoor Environments – Part 2," *Electronics World*, vol. 116, no. 1889, pp. 30-34, March 2010.

Revista: Electronics World, ISSN: 1365-4675.

Factor de Impacto (JCR 2010): 0,047.

Ranking en Categorías (JCR 2010):

- Categoría *Engineering, Electrical & Electronic*: 243 de 247 (Q4).
- Categoría *Telecommunications*: 77 de 80 (Q4).

1.9.2.3 Premio de I+D

Premio: Innovación y Desarrollo 2004 en el ámbito de la Ingeniería Industrial e Ingeniería Química, Edición 11.

Entidad: Universidad de Valladolid, en colaboración con la Junta de Castilla y León, la Confederación de Empresarios de Castilla y León (CECALE), y la Cámara de Comercio e Industria de Valladolid.

Fecha Concesión: 23 de mayo de 2005 (Valladolid, España).

SEGUNDA PARTE:

ARTÍCULOS DEL COMPENDIO

Capítulo 2: Artículo 1 del compendio

En este capítulo se analiza el primer artículo del compendio, el cual incluye el estado del arte de las técnicas *sensorless* básicas y avanzadas de detección de la posición y velocidad en motores *brushless* DC (BLDC), además de los fundamentos, implementación de *drivers* y aplicaciones de estos motores. En este capítulo se incluye la información bibliográfica del artículo y su resumen, así como otros datos y análisis referidos al ámbito, motivación y originalidad del mismo. Al final del capítulo se incluye el extracto del artículo publicado en la revista *Sensors* en junio de 2010.

2.1 Datos bibliográficos

TITULO: Position and Speed Control of Brushless DC Motors Using Sensorless Techniques and Application Trends.

AUTORES: José Carlos Gamazo Real, Ernesto Vázquez Sánchez, y Jaime Gómez Gil.

REVISTA: Sensors.

EDITOR: MDPI, Multidisciplinary Digital Publishing Institute (Basel, Suiza).

FECHA PUBLICACIÓN: 19 de julio de 2010.

ISSN: 1424-8220.

DOI: 10.3390/s100706901.

VOLUMEN: 10.

NÚMERO: 7.

PÁGINAS: 6901-6947.

REFERENCIA: [8]

2.2 Resumen

Este artículo proporciona una revisión de las técnicas *sensorless* de detección de la posición y velocidad utilizadas en drivers de motores BLDC, incluyéndose además los fundamentos de las mismas utilizando sensores, junto con sus limitaciones y ventajas. El rendimiento y la fiabilidad de los *drivers* de motores BLDC han mejorado debido a que las técnicas de control se han beneficiado de la tecnología *sensorless*. De esta forma, en este artículo se revisan los avances en este campo y los desarrollos recientes, con sus ventajas e inconvenientes, así como el análisis de los aspectos relativos a la implementación práctica y las aplicaciones. Esta revisión incluye el estudio del estado del arte de las técnicas *sensorless* básicas de detección basadas en las tensiones BEMF, entre las que se incluyen la medida de los voltajes terminales de fase, integración del tercer armónico de las tensiones de fase, medida de la corriente terminal de fase, integración de la tensión back-EMF y estrategias PWM. También se consideran en el artículo algúnas técnicas más avanzadas basadas en estimadores y modelos, tales como los observadores *Sliding-mode*, el filtro de Kalman Extendido (EKF), Sistema adaptativo del modelo de referencia (MRAS), observadores adaptativos de orden completo y pseudo-reducido, y redes neuronales artificiales (ANN).

2.3 Ámbito

Dentro de la revista indicada este artículo se incluye en la sección *Physical Sensors* en la cual tienen cabida artículos teóricos y experimentales relacionados con medidas físicas y tecnología de sensores, diseño, software y nuevos principios para sensores físicos, así como artículos de revisión que cubran la temática indicada [96].

El interés de este artículo dentro del ámbito de la revista indicada, radica en el análisis exhaustivo de las técnicas *sensorless* para motores BLDC que presenta como una alternativa al uso de sensores electromecánicos en el control de la posición y velocidad de este tipo de motores. Precisamente al principio del artículo (páginas 6903-6909) se realiza una introducción al control en motores BLDC utilizando sensores, y se mencionan las características de algunos de los más relevantes como los sensores de efecto *Hall*, sensores de velocidad de reluctancia variable o los acelerómetros. Además, se indican los fundamentos de las técnicas convencionales de control utilizando sensores y algunos conceptos como la conmutación electrónica utilizando un inversor o la secuencia de conmutación de seis pasos. Una vez realizada esta introducción, se ponen de manifiesto las desventajas del uso de sensores en el control de este tipo de motores, y como el uso de las técnicas *sensorless* representa una alternativa fiable y con futuro en muchas aplicaciones.

2.4 Justificación en el marco de la tesis

La revisión de técnicas *sensorless* incluida este trabajo se encuadra dentro de la **Etapa 1 de la metodología** y permite alcanzar el **Objetivo 1** de la tesis. En este objetivo se propone la realización del análisis de las técnicas *sensorless* para la detección de la posición y velocidad de motores BLDC. En el artículo se estudian las técnicas existentes para este tipo de motores, teniendo en cuenta sus ventajas, inconvenientes y detalles de implementación práctica con énfasis especial en las aplicaciones, así como en los aspectos diferenciales más relevantes del control de estos motores utilizando sensores. Entre las técnicas analizadas se incluyen tanto las básicas basadas en métodos directos, como la detección del cruce por cero de BEMF o estrategias PWM, como en métodos indirectos para reducir el ruido de conmutación, como la integración de BEMF o detección de la conducción de los diodos de *freewheeling*. También, se han tenido en cuenta técnicas más avanzadas y actuales como las basadas en modelos, observadores, redes neuronales o filtros de Kalman, las cuales pueden proporcionar una perspectiva bastante amplia de las tendencias en este campo.

Este artículo tiene su origen en la necesidad de realizar un estudio del estado del arte detallado y actualizado de las técnicas *sensorless* para motores BLDC, debido a la gran cantidad de técnicas existentes y a la variedad de enfoques existentes para clasificarlas. En este sentido, existen trabajos similares pero no lo suficientemente completos como para tener una visión panorámica y clara de todos puntos de vista utilizados en el desarrollo de las mismas, así como de los detalles más relevantes para la implementación de *drivers* para motores BLDC. Algunos ejemplos representativos de artículos en los que se incluyen estudios del estado del arte de las técnicas *sensorless* para este tipo de motores, pero con una menor profundidad que la realizada en el artículo publicado, son los realizados por Johnson *et al.* [65], Kim *et al.* [63], Vinatha *et al.* [59], Tae-Hyung *et al.* [97], Zaky *et al.* [68], Acarnley *et al.* [98], o Jahns *et al.* [99].

2.5 Extracto de la publicación

A continuación se incluye el artículo 1 del compendio, tal y como aparece publicado en la revista *Sensors*.

Sensors **2010**, *10*, 6901-6947; doi:10.3390/s100706901

OPEN ACCESS

sensors

ISSN 1424-8220

www.mdpi.com/journal/sensors

Review

Position and Speed Control of Brushless DC Motors Using Sensorless Techniques and Application Trends

José Carlos Gamazo-Real *, Ernesto Vázquez-Sánchez and Jaime Gómez-Gil

Department of Signal Theory, Communications and Telematic Engineering, University of Valladolid (UVA), 47011 Valladolid, Spain; E-Mails: ernesto.vazquez@uva.es (E.V.-S.); jgomez@tel.uva.es (J.G.-G.)

* Author to whom correspondence should be addressed; E-Mail: jcgamazo@ribera.tel.uva.es; Tel.: +34-983-185-556; Fax: +34-983-423-667.

Received: 10 June 2010; in revised form: 30 June 2010 / Accepted: 5 July 2010 / Published: 19 July 2010

Abstract: This paper provides a technical review of position and speed sensorless methods for controlling Brushless Direct Current (BLDC) motor drives, including the background analysis using sensors, limitations and advances. The performance and reliability of BLDC motor drivers have been improved because the conventional control and sensing techniques have been improved through sensorless technology. Then, in this paper sensorless advances are reviewed and recent developments in this area are introduced with their inherent advantages and drawbacks, including the analysis of practical implementation issues and applications. The study includes a deep overview of state-of-the-art back-EMF sensing methods, which includes Terminal Voltage Sensing, Third Harmonic Voltage Integration, Terminal Current Sensing, Back-EMF Integration and PWM strategies. Also, the most relevant techniques based on estimation and models are briefly analysed, such as Sliding-mode Observer, Extended Kalman Filter, Model Reference Adaptive System, Adaptive observers (Full-order and Pseudoreduced-order) and Artificial Neural Networks.

Keywords: BLDC; back-EMF; sensorless; position; speed; estimator; Hall-effect sensors; electronic processors

1. Introduction

For the past two decades several Asian countries such as Japan, which have been under pressure from high energy prices, have implemented variable speed PM motor drives for energy saving applications such as air conditioners and refrigerators [1]. On the other hand, the U.S.A. has kept on using cheap induction motor drives, which have around 10% lower efficiency than adjustable PM motor drives for energy saving applications. Therefore recently, the increase in energy prices spurs higher demands of variable speed PM motor drives. Also, recent rapid proliferation of motor drives into the automobile industry, based on hybrid drives, generates a serious demand for high efficient PM motor drives, and this was the beginning of interest in BLDC motors.

BLDC motors, also called Permanent Magnet DC Synchronous motors, are one of the motor types that have more rapidly gained popularity, mainly because of their better characteristics and performance [2]. These motors are used in a great amount of industrial sectors because their architecture is suitable for any safety critical applications.

The brushless DC motor is a synchronous electric motor that, from a modelling perspective, looks exactly like a DC motor, having a linear relationship between current and torque, voltage and rpm. It is an electronically controlled commutation system, instead of having a mechanical commutation, which is typical of brushed motors. Additionally, the electromagnets do not move, the permanent magnets rotate and the armature remains static. This gets around the problem of how to transfer current to a moving armature. In order to do this, the brush-system/commutator assembly is replaced by an intelligent electronic controller, which performs the same power distribution as a brushed DC motor [3]. BLDC motors have many advantages over brushed DC motors and induction motors, such as a better speed *versus* torque characteristics, high dynamic response, high efficiency and reliability, long operating life (no brush erosion), noiseless operation, higher speed ranges, and reduction of electromagnetic interference (EMI). In addition, the ratio of delivered torque to the size of the motor is higher, making it useful in applications where space and weight are critical factors, especially in aerospace applications.

The control of BLDC motors can be done in sensor or sensorless mode, but to reduce overall cost of actuating devices, sensorless control techniques are normally used. The advantage of sensorless BLDC motor control is that the sensing part can be omitted, and thus overall costs can be considerably reduced. The disadvantages of sensorless control are higher requirements for control algorithms and more complicated electronics [3]. All of the electrical motors that do not require an electrical connection (made with brushes) between stationary and rotating parts can be considered as brushless permanent magnet (PM) machines [4], which can be categorised based on the PMs mounting and the back-EMF shape. The PMs can be *surface mounted on the rotor* (SMPM) or installed *inside of the rotor* (IPM) [5], and the back-EMF shape can either be sinusoidal or trapezoidal. According to the back-EMF shape, *PM AC synchronous motors* (PMAC or PMSM) have sinusoidal back-EMF and *Brushless DC motors* (BLDC or BPM) have trapezoidal back-EMF. A PMAC motor is typically excited by a three-phase sinusoidal current, and a BLDC motor is usually powered by a set of currents having a quasi-square waveform [6,7].

Because of their high power density, reliability, efficiency, maintenance free nature and silent operation, permanent magnet (PM) motors have been widely used in a variety of applications in

industrial automation, computers, aerospace, military (gun turrets drives for combat vehicles) [3], automotive (hybrid vehicles) [8] and household products. However, the PM BLDC motors are inherently electronically controlled and require rotor position information for proper commutation of currents in its stator windings. It is not desirable to use the *position sensors* for applications where reliability is of utmost importance because a sensor failure may cause instability in the control system. These limitations of using position sensors combined with the availability of powerful and economical microprocessors have spurred the development of sensorless control technology. Solving this problem effectively will open the way for full penetration of this motor drive into all low cost, high reliability, and large volume applications.

The remainder of the paper is arranged as follows. Section 2 describes the position and speed control fundamentals of BLDC motors using sensors. Next, Section 3 explains the control improvements applying sensorless techniques, describing the motor controller model and the most important techniques based on back-EMF sensing. Section 4 also briefly analyses the sensorless techniques using estimators and model-based schemes. In addition, Section 5 compares the feasibility of the control methods, and describes some relevant implementation issues, such as open-loop starting. Finally, Section 6 provides an overview for the applications of BLDC motor controllers, as well as conclusions are drawn in Section 7.

2. Position and Speed Control of BLDC Motors Using Sensors

PM motor drives require a rotor position sensor to properly perform phase commutation and/or current control. For PMAC motors, a constant supply of position information is necessary; thus a position sensor with high resolution, such as a *shaft encoder or a resolver*, is typically used. For BLDC motors, only the knowledge of six phase-commutation instants per electrical cycle is needed; therefore, low-cost *Hall-effect sensors* are usually used. Also, *electromagnetic variable reluctance* (VR) *sensors* or *accelerometers* have been extensively applied to measure motor position and speed. The reality is that angular motion sensors based on magnetic field sensing principles stand out because of their many inherent advantages and sensing benefits.

2.1. Position and Speed Sensors

As explained before, some of the most frequently used devices in position and speed applications are Hall-effect sensors, variable reluctance sensors and accelerometers. Each of these types of devices is discussed further below.

2.1.1. Hall-effect sensors

These kinds of devices are based on Hall-effect theory, which states that if an electric current-carrying conductor is kept in a magnetic field, the magnetic field exerts a transverse force on the moving charge carriers that tends to push them to one side of the conductor. A build-up of charge at the sides of the conductors will balance this magnetic influence producing a measurable voltage between the two sides of the conductor. The presence of this measurable transverse voltage is called the Hall-effect because it was discovered by Edwin Hall in 1879.

Unlike a brushed DC motor, the commutation of a BLDC motor is controlled electronically. To rotate the BLDC motor the stator windings should be energized in a sequence. It is important to know the rotor position in order to understand which winding will be energized following the energizing sequence. Rotor position is sensed using Hall-effect sensors embedded into the stator [9].

Most BLDC motors have three Hall sensors inside the stator on the non-driving end of the motor. Whenever the rotor magnetic poles pass near the Hall sensors they give a high or low signal indicating the N or S pole is passing near the sensors. Based on the combination of these three Hall sensor signals, the exact sequence of commutation can be determined. Figure 1 shows a transverse section of a BLDC motor with a rotor that has alternate N and S permanent magnets. Hall sensors are embedded into the stationary part of the motor. Embedding the Hall sensors into the stator is a complex process because any misalignment in these Hall sensors with respect to the rotor magnets will generate an error in determination of the rotor position. To simplify the process of mounting the Hall sensors onto the stator some motors may have the Hall sensor magnets on the rotor, in addition to the main rotor magnets. Therefore, whenever the rotor rotates the Hall sensor magnets give the same effect as the main magnets. The Hall sensors are normally mounted on a printed circuit board and fixed to the enclosure cap on the non-driving end. This enables users to adjust the complete assembly of Hall sensors to align with the rotor magnets in order to achieve the best performance [10].

Figure 1. BLDC motor transverse section [10].

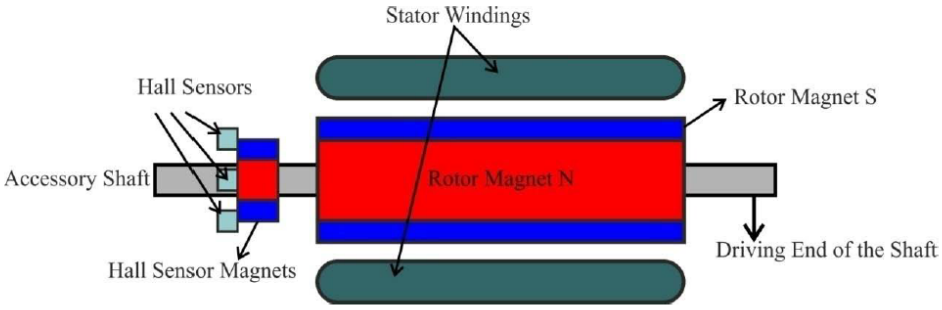

Nowadays, because miniaturized brushless motors are introduced in many applications, new position sensors are being developed, such as a three branches vertical Hall sensor [11] depicted in Figure 2a. The connecting principle between the brushless motor and this sensor is reminiscent of the miniaturized magnetic angular encoder based on 3-D Hall sensors. A permanent magnet is fixed at the end of a rotary shaft and the magnetic sensor is placed below, and the magnet creates a magnetic field parallel to the sensor surface. This surface corresponds to the sensitive directions of the magnetic sensor. Three-phase brushless motors need three signals with a phase shift of 120° for control, so a closed-loop regulation may be used to improve the motor performance. Each branch could be interpreted as a half of a vertical Hall sensor and are rotated by 120° in comparison to the other. Only a half of a vertical Hall sensor is used since little space is available for the five electrical contacts (two for the supply voltage and three to extract the Hall voltages). This sensor automatically creates three signals with a phase shift of 120°, which directly correspond to the motor driving signals, to simplify the motor control in a closed-loop configuration. A drawing of this device's use as angular position

sensor for brushless motor control is given in Figure 2b. A first alignment is between the rotor orientation and the permanent magnet, and a second alignment is between the stator and the sensor. This alignment will allow the motion information for the motor and the information about its shaft angular position.

Figure 2. (a) Schematic representation of a three branches Hall sensor. **(b)** Three branches vertical Hall device mounted as angular position sensor for brushless motor control [11].

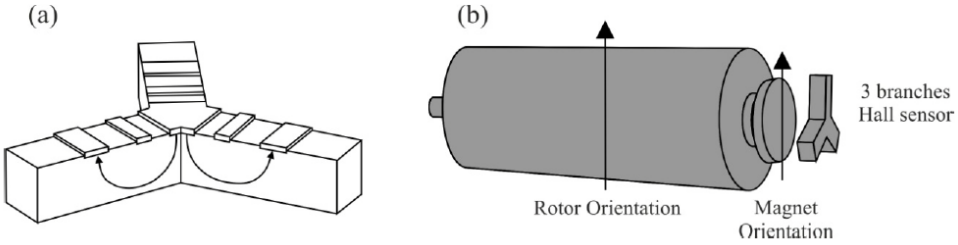

2.1.2. Variable reluctance (VR) wheel speed sensors

This kind of sensor is used to measure position and speed of moving metal components, and is often referred as a passive magnetic sensor because it does not need to be powered. It consist of a permanent magnet, a ferromagnetic pole piece, a pickup coil, and a rotating toothed wheel, as Figure 3 illustrates. This device is basically a permanent magnet with wire wrapped around it. It is usually a simple circuit of only two wires where in most cases polarity is not important, and the physics behind its operation include magnetic induction [12].

Figure 3. Variable Reluctance sensor that senses movement of the toothed wheel [12].

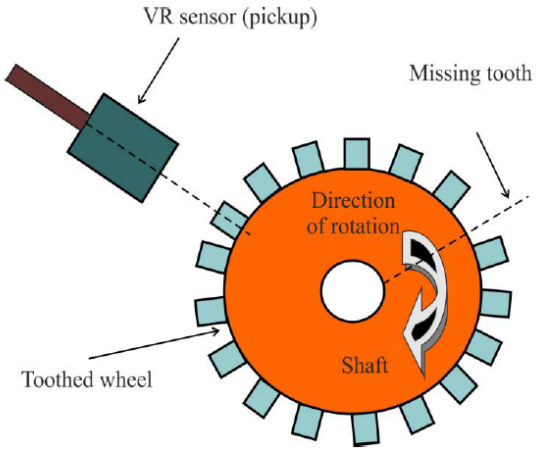

As the teeth pass through the sensor's magnetic field, the amount of magnetic flux passing through the permanent magnet varies. When the tooth gear is close to the sensor, the flux is at maximum. When the tooth is further away, the flux drops off. The moving target results in a time-varying flux that induces a voltage in the coil, producing an electrical analog wave. *The frequency and voltage of the*

analog signal is proportional to velocity of the rotating toothed wheel. Each passing discontinuity in the target causes the VR sensor to generate a pulse. The cyclical pulse train or a digital waveform created can be interpreted by the BLDC motor controller.

The advantages of the VR sensor can be summarized as follows: low cost, robust proven speed and position sensing technology (it can operate at temperatures in excess of 300 °C), self-generating electrical signal which requires no external power supply, fewer wiring connections which contribute to excellent reliability, and a wide range of output, resistance, and inductance requirements so that the device can be tailored to meet specific control requirements [12].

Due to the fact that these sensors are very small, they can be embedded in places where other sensors may not fit. For instance, when sealed in protective cases they can be resistant to high temperatures and high pressures, as well as chemical attacks [13]. Through the monitoring of the health of running motors, severe and unexpected motor failures can be avoided and control system reliability and maintainability can be improved. If the VR was integrated inside a motor case for an application in a harsh environment, sensor cables could be easily damaged in that environment. Then, a wireless and powerless sensing solution should be applied using electromagnetic pulses for passing through the motor casing to deliver the sensor signal to the motor controller [14].

The *Hall-effect sensor* explained before is an alternative but more expensive technology, so *VR sensors* are the most suitable choice to measure the rotor position and speed.

2.1.3. Accelerometers

An accelerometer is a electromechanical device that measures acceleration forces, which are related to the freefall effect. Several types are available to detect magnitude and direction of the acceleration as a vector quantity, and can be used to sense position, vibration and shock. The most common design is based on a combination of Newton's law of mass acceleration and Hooke's law of spring action [13]. Then, conceptually, an accelerometer behaves as a damped mass on a spring, which is depicted in Figure 4. When the accelerometer experiences acceleration, the mass is displaced to the point that the spring is able to accelerate the mass at the same rate as the casing. The displacement is then measured to give the acceleration.

Figure 4. Basic spring-mass system accelerometer [13].

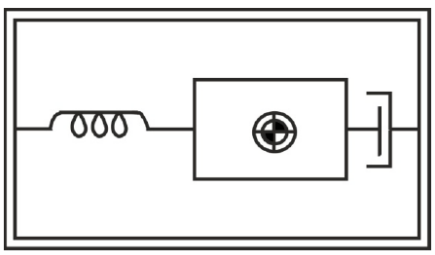

Under steady-state conditions, the measurement of acceleration is reduced to a measurement of spring extension (linear displacement) showed in Equation (1):

$$a = \frac{k}{m} \cdot \Delta x \tag{1}$$

where k is the spring constant, m is the seismic (or proof) mass, and Δx is the distance that is stretched the spring from its equilibrium position with a force given by Equation (2), which is described by Newton's and Hooke's laws:

$$F = k \cdot \Delta x \tag{2}$$

There is a wide variety of accelerometers depending on the requirements of natural frequency, damping, temperature, size, weight, hysteresis, and so on. Some of these types are piezoelectric, piezoresistive, variable capacitance, linear variable differential transformers (LVDT), potentiometric, among many others [13].

Modern accelerometers are often small micro electro-mechanical systems (MEMS), and are indeed the simplest MEMS devices possible, and consist of little more than a cantilever beam with a proof mass. The MEMS accelerometer is silicon micro-machined, and therefore, can be easily integrated with the signal processing circuits [14]. This is different when compare with a traditional accelerometer such as the piezoelectric kind.

2.2. Conventional Control Method Using Sensors

A BLDC motor is driven by voltage strokes coupled with the rotor position. These strokes must be properly applied to the active phases of the three-phase winding system so that the angle between the stator flux and the rotor flux is kept close to 90° to get the maximum generated torque. Therefore, the controller needs some means of determining the rotor's orientation/position (relative to the stator coils), such as Hall-effect sensors, which are mounted in or near the machine's air gap to detect the magnetic field of the passing rotor magnets. Each sensor outputs a high level for 180° of an electrical rotation, and a low level for the other 180°. The three sensors have a 60° relative offset from each other. This divides a rotation into six phases (3-bit code) [9].

Figure 5. Electronically commutated BLDC motor drive [16].

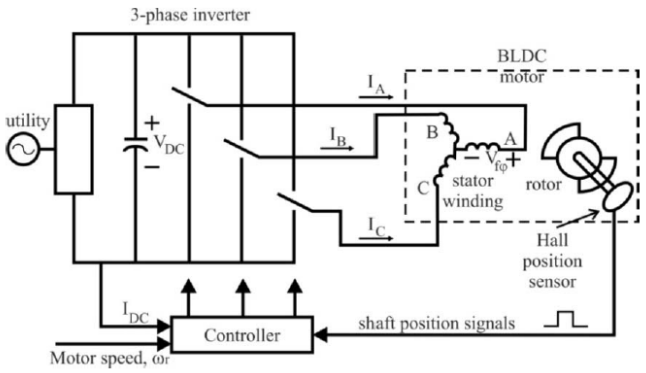

The process of switching the current to flow through only two phases for every 60 electrical degree rotation of the rotor is called *electronic commutation*. The motor is supplied from a three-phase inverter, and the switching actions can be simply triggered by the use of signals from position sensors that are mounted at appropriate points around the stator. When mounted at 60 electrical degree intervals and aligned properly with the stator phase windings these Hall switches deliver digital pulses that can be decoded into the desired three-phase switching sequence [15]. A BLDC motor drive with a six-step inverter and Hall position sensors is shown in Figure 5.

Figure 6. Hall sensor signal, back-EMF, output torque and phase current [10].

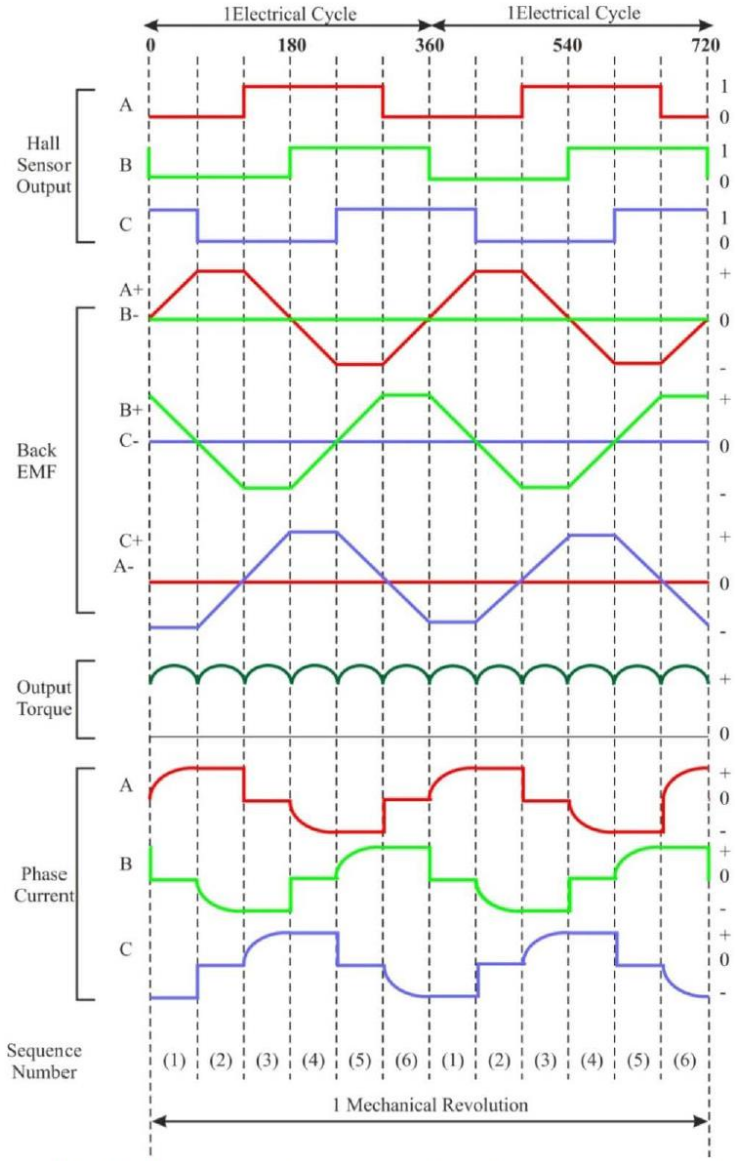

Such a drive usually also has a current loop to regulate the stator current, and an outer speed loop for speed control [16]. The speed of the motor can be controlled if the voltage across the motor is

changed, which can be achieved easily varying the duty cycle of the PWM signal used to control the six switches of the three-phase bridge.

Only two inverter switches, one in the upper inverter bank and one in the lower inverter bank, are conducting at any instant. These discrete switching events ensure that the sequence of conducting pairs of stator terminals is maintained [16]. Figure 6 shows an example of Hall sensor signals with respect to back-EMF and the phase current. One of the Hall sensors changes the state every 60 electrical degrees of rotation. Given this, it takes six steps to complete an electrical cycle. However, one electrical cycle may not correspond to a complete mechanical revolution of the rotor. The number of electrical cycles to be repeated to complete a mechanical rotation is determined by the rotor pole pairs. For each rotor pole pair, one electrical cycle is completed. *The number of electrical cycles/rotations equals the rotor pole pairs* [10]. This sequence of conducting pairs is essential to the production of a constant output torque.

In summary, permanent magnet motor drives require a rotor position sensor to properly perform phase commutation, but there are several drawbacks when such types of position sensors are used. The main drawbacks are the increased cost and size of the motor, and a special arrangement needs to be made for mounting the sensors. Further, Hall sensors are temperature sensitive and hence the operation of the motor is limited, which could reduce the system reliability because of the extra components and wiring [7]. To reduce cost and improve reliability such position sensors may be eliminated. To this end, many sensorless schemes have been reported for position (and speed) control of BLDC motors [6].

3. Techniques and Advances in Sensorless Control

Position sensors can be completely eliminated, thus reducing further cost and size of motor assembly, in those applications in which only variable speed control (*i.e.*, no positioning) is required and system dynamics is not particularly demanding (*i.e.*, slowly or, at least, predictably varying load). In fact, some control methods, such as back-EMF and current sensing, provide, in most cases, enough information to estimate with sufficient precision the rotor position and, therefore, to operate the motor with synchronous phase currents. A PM brushless drive that does not require position sensors but only electrical measurements is called a *sensorless drive* [4].

The BLDC motor provides an attractive candidate for sensorless operation because the nature of its excitation inherently offers a low-cost way to extract rotor position information from motor-terminal voltages. In the excitation of a three-phase BLDC motor, except for the phase-commutation periods, only two of the three phase windings are conducting at a time and the no conducting phase carries the back-EMF. There are many categories of sensorless control strategies [6]; however, the most popular category is based on back electromotive forces or back-EMFs [17]. Sensing back-EMF of unused phase is the most cost efficient method to obtain the commutation sequence in star wound motors. Since back-EMF is zero at standstill and proportional to speed, the measured terminal voltage that has large signal-to-noise ratio cannot detect zero crossing at low speeds. That is the reason why in all back-EMF-based sensorless methods the low-speed performance is limited, and an *open-loop starting strategy* is required [18].

Generally, a brushless DC motor consists of a permanent magnet synchronous motor that converts electrical energy to mechanical energy, an inverter corresponding to brushes and commutators, and a *shaft position sensor* [19], as Figure 7 shows. In this figure, each of the three inverter phases are highlighted in a different colour, including the neutral point: red phase *A*, green phase *B*, blue phase *C*, and pink neutral point *N*. The stator iron of the BLDC motor has a non-linear magnetic saturation characteristic, which is the basis from which it is possible to determine the initial position of the rotor. When the stator winding is energized, applying a DC voltage for a certain time, a magnetic field with a fixed direction will be established. Then, the current responses are different due to the inductance difference, and this variation of the current responses contains the information of the rotor position [20]. Therefore, *the inductance of stator winding is a function of the rotor position*.

Figure 7. Typical sensorless BLDC motor drive [19].

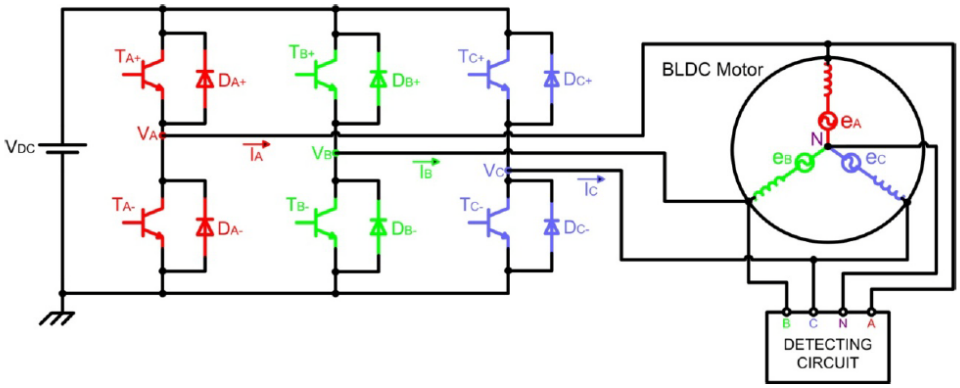

The analysis of the circuit depicted in Figure 7 is based on the motor model for phase *A* (highlighted in red colour), illustrated in Figure 8, and the following assumptions are considered [21]:

- The motor is not saturated.
- Stator resistances of all the windings are equal (R_S), self inductances are constant (L_S) and mutual inductances (M) are zero.
- Iron losses are negligible.

Figure 8. Equivalent circuit of the BLDC motor for phase *A* [21].

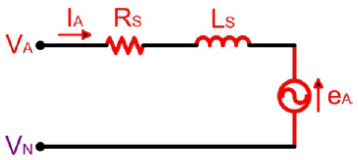

Then, the voltage function of the conducting phase winding might be expressed as indicated in Equation (3):

$$V_{DC} = I \cdot R_S + L_S \cdot \frac{dI}{dt} + e \tag{3}$$

where V_{DC} is the DC-link voltage, R_S and L_S are the equivalent resistance and inductance of stator phase winding respectively, and e is the trapezoidal shaped back-EMF.

In this paper, conventional and recent advancement of back-EMF sensing methods for the PM BLDC motors and generators are presented, which are split in two categories; direct and indirect back-EMF detection [22]:

- *Direct back-EMF detection methods*: the back-EMF of floating phase is sensed and its zero crossing is detected by comparing it with neutral point voltage. This scheme suffers from high common mode voltage and high frequency noise due to the PWM drive, so it requires low pass filters, and voltage dividers. The methods can be classified as:
  - Back-EMF Zero Crossing Detection (ZCD) or Terminal Voltage Sensing.
  - PWM strategies.
- *Indirect back-EMF detection methods*: because filtering introduces commutation delay at high speeds and attenuation causes reduction in signal sensitivity at low speeds, the speed range is narrowed in direct back-EMF detection methods. In order to reduce switching noise, the indirect back-EMF detection methods are used. These methods are the following:
  - Back-EMF Integration.
  - Third Harmonic Voltage Integration.
  - Free-wheeling Diode Conduction or Terminal Current Sensing.

3.1. Back-EMF Zero Crossing Detection method (Terminal Voltage Sensing)

The zero-crossing approach is one of the simplest methods of back-EMF sensing technique, and is based on detecting the instant at which the back-EMF in the unexcited phase crosses zero. This zero crossing triggers a timer, which may be as simple as an RC time constant, so that the next sequential inverter commutation occurs at the end to this timing interval [23].

For typical operation of a BLDC motor, the phase current and back-EMF should be aligned to generate constant torque. The current commutation point shown in Figure 9 can be estimated by the zero crossing point (ZCP) of back-EMFs and a 30° phase shift [1,4], using a six-step commutation scheme through a three-phase inverter for driving the BLDC motor. The conducting interval for each phase is 120 electrical degrees. Therefore, only two phases conduct current at any time, leaving the third phase floating. In order to produce maximum torque, the inverter should be commutated every 60° by detecting zero crossing of back-EMF on the floating coil of the motor [24], so that current is in phase with the back-EMF.

This technique of delaying 30° (electrical degrees) from zero crossing instant of the back-EMF is not affected much by speed changes [7]. To detect the ZCPs, the phase back-EMF should be monitored during the silent phase (when the particular phase current is zero) and the terminal voltages should be low-pass filtered first.

Figure 9. Zero crossing points of the back-EMF and phase current commutation points [25].

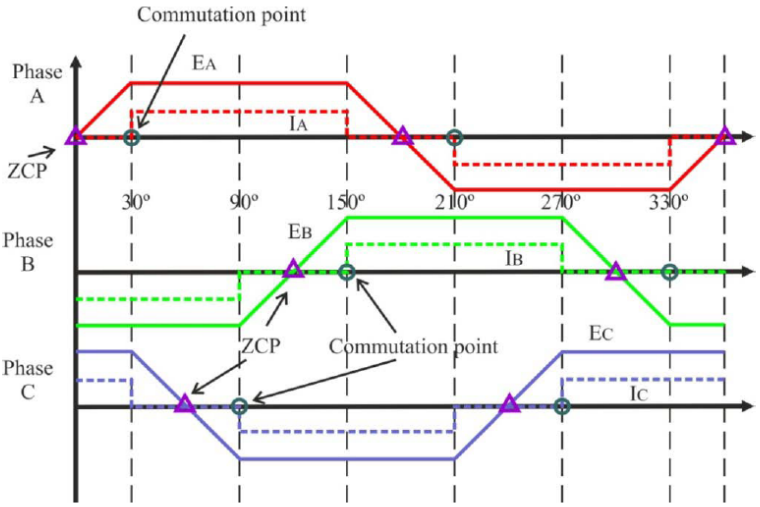

Three low-pass filters (LPFs) are utilized to eliminate higher harmonics in the phase terminal voltages caused by the inverter switching. The time delay of LPFs will limit the high speed operation capability of the BLDC machine [1,24,26]. It's necessary to point out the importance of filters when a BLDC motor drive is designed, which are used to eliminate high frequency components of the terminal voltages and to extract back-EMF of the motor.

The terminal voltage of the opened or floating phase is given by Equation (4):

$$V_C = e_C + V_N = e_C + \frac{V_{CE} - V_F}{2} - \frac{e_A + e_B}{2} \tag{4}$$

where e_C is the back-EMF of the opened phase (C), V_N is the potential of the motor neutral point, and V_{CE} and V_F are the forward voltage drop of the transistors and diodes, respectively, which implement the motor inverter of Figure 7, respectively.

As the back-EMF of the two conducting phases (A and B) have the same amplitude but opposite sign [19] the terminal voltage of the floating phase results in Equation (5):

$$e_A = -e_B \Rightarrow V_C = e_C + \frac{V_{CE} - V_F}{2} = e_C + \frac{V_B + V_A}{2} \tag{5}$$

where V_A=-V_F (forward current of diode D_{A-}) and V_B=V_{CE} (collector-emitter voltage of transistor T_{B-})

Since the zero-crossing point detection is done at the end of the PWM on-state and only the high-side of the inverter is chopped, and V_{CE} is similar to T_{A+} and T_{B-} transistors, the final detection formula can be represented by Equation (6):

$$V_{CE}^{A+} \approx V_{CE}^{B-} \Rightarrow V_C = e_C + \frac{V_{CE}^{B-} + V_{DC} - V_{CE}^{A+}}{2} \approx e_C + \frac{V_{DC}}{2} \tag{6}$$

Therefore, *the zero-crossing occurs when the voltage of the floating phase reaches one half of the DC rail voltage*. The reason why the end of the PWM on-state is selected as the zero-crossing detection point is that it is noise free to sample at that moment [20].

On the other hand, instead of using analogue LPFs, a unipolar pulse width modulation (PWM) scheme can be used to measure terminal voltages [27,28]. The difference of the ZCD method between on and off state of the PWM signal can also be taken into account [29,30]. Also, the true phase back-EMF signal could be directly obtained from the motor terminal voltage by properly choosing the PWM and sensing strategy (without the motor neutral point voltage information This would provide advantages such as no sensitivity to switching noise, no filtering required, and good motor performance a wide speed range [24,31].

The price for the simplicity of the zero-crossing method tends to be noise sensitivity in detecting the zero crossing, and degraded performance over wide speed ranges unless the timing interval is programmed as a function of rotor speed [23]. Another drawback is that it is not possible to use the noisy terminal voltage to obtain a switching pattern at low speeds since back-EMF is zero at standstill and proportional to rotor speed. Also, the estimated commutation points have position error during the transient period when the speed is accelerated or decelerated rapidly, especially for a system that has low inertia. With this method, rotor position can be detected typically from 20% of the rated speed, then a reduced speed operating range is normally used, typically around 1,000–6,000 rpm [1].

3.1.1. Optimizations

As the rotor position information can be extracted by indirectly sensing the back-EMF from only one of the three motor-terminal voltages for a three-phase motor, it is obvious that sensing each terminal voltage can provide two commutation instants. Measuring the time between these two instants, it is possible to interpolate the other four commutation instants (Figure 9 shows that six commutation points are needed), assuming motor speed does not change significantly over consecutive electrical cycles. Depending on the terminal voltage sensing locations, either a low-pass filter or a band-pass filter is used for position information retrieval. The circuit for sensing the other two terminal voltages can therefore be eliminated, leading to a significant reduction in the component count of the sensing circuit. Also, the ZCD method could be improved if a digital filtering procedure is used to identify the true and false ZCPs of phase back-EMF, which are caused by the terminal voltage spikes due to phase commutations [32].

An indirect way of detecting the ZCP of the back-EMF from the three terminal voltages without using the neutral potential is using the difference of the line voltages [33]. Another modification of the technique is to achieve the sensorless commutation by means of a Phase Locked Loop (PLL) and sensing of the phase winding back-EMF voltages [8]. This PLL has a narrow speed range due to the capabilities of the phase detector, and is sensitive to switching noise. In order to simplify the BLDC driver design, it can be built around a sensorless controller chip ML4425 from Fairchild Semiconductor [34,35].

A sensorless Field Oriented Control (FOC) of brushless motors [36], which is known to be more efficient in terms of torque generation compared to back-EMF zero crossing detection methods, is currently under development, and it could be successfully applied to the design of motor pump units for automotive applications [4].

At low speeds or at standstill, the back-EMF detection method can not be applied well because the back-EMF is proportional to the motor speed. In spite of this problem, a starting procedure can be used

to start the motor from standstill [20]. In critical applications, such as the intelligent Electro-Mechanical (EMA) and Electro-Hydraulic (EHA) actuators of aviation systems, it is necessary to ensure correct start-up of the DC motor. Electrical commutation in the first running stage is normally realized by classical PWM signal that drives a transistor power stage (see Figure 7), which is *open-loop control* without any position feedback [3].

At high speeds, the long settling time of a parasitic resonant between the motor inductance and the parasitic capacitance of power devices can cause false zero crossing detection of back-EMF. The solution to this problem is to *detect the back-EMF during on time* at high duty cycle [37], so there is enough time for the resonant transient to settle down. Then, during motor start-up and low speed, it is preferred to use the original scheme since there is no signal attenuation; while at high speed, the system can be switched to the improved back-EMF sensing scheme. With the combination of two detection schemes in one system, the motor can run very well over a *wide speed range* [24,38].

3.1.2. Applications

The terminal voltage sensing method is widely used for low cost industrial applications such as fans, pumps and compressor drives where frequent speed variation is not required. Nevertheless, BLDC motors need a *rotor position sensor*, and this reduces the system ruggedness, complicates the motor configuration and its mass production. This sensor can be has been eliminated through this sensing technique. In spite of the back-EMF being zero at standstill, this technique permits the starting of a separately controlled synchronous motor without a sensor, because the PWM signal generated in the control computer chops the motor voltage by the commutation transistors to control the motor speed [1]. An example is a motor pump unit, developed for commercial vehicle applications, in which control strategy can be based on the back-EMF zero-crossing method, and speed control loop is closed by means of the virtual feedback provided by the commutation point prediction [4].

Another important field is the super high speed motors, which are receiving increasing attentions in various applications such as machine tools, because of the advantages of their small size and light weight at the same power level [39].

3.2. Third Harmonic Voltage Integration method

This method utilises the third harmonic of the back-EMF to determine the commutation instants of the BLDC motor. It is based on the fact that in a symmetrical three phase Y-connected motor with trapezoidal air gap flux distribution, the summation of the three stator phase voltages results in the elimination of all polyphase , that is fundamental and all the harmonics components like 5th, 7th, *etc.* [40]. The resulting sum is dominated by the third harmonic component that keeps a constant phase displacement with the fundamental air gap voltage for any load and speed.

An appropriate processing of the third harmonic signal allows the estimation of the rotor flux position and a proper inverter current control. In contrast with indirect sensing methods based on the back-EMF signal, the third harmonic requires only a small amount of filtering. As a result, this method is not sensitive to filtering delays, achieving a high performance for a wide speed range. A superior motor starting performance is also achieved because the third harmonic can be detected at low speeds [41].

Referring to Figure 7, the stator voltage of the BLDC motor for phase A can be written similarly to Equation (3), where $V_{DC}=V_A$, $I=I_A$, and $e=e_A$. Equivalent expressions can be obtained for the other two stator phases. The harmonic content of the motor air gap or internal voltages e_A, e_B and e_C is a function of the rotor magnets and stator winding configurations [40]. For a full pitch magnet and full pitch stator phase winding, the internal voltages can be represented using the Fourier transform, obtaining many voltage harmonic components. If each phase inductance is constant at any rotor position, from the summation of three-terminal to neutral voltages, the third harmonic of the back-EMF can be measured by Equation (7) [25]:

$$V_{SUM} = V_{AN} + V_{BN} + V_{CN} \approx (e_A + e_B + e_C) \approx 3 \cdot E_3 \cdot \sin(3 \cdot \omega_e \cdot t) \quad (7)$$

The summed terminal voltages contain only the third and the multiples of the third harmonic due to the fact that only zero sequence current components can flow through the motor neutral. To obtain switching instants, the filtered voltage signal which provides the third harmonic voltage component is integrated to estimate the rotor flux linkage, as it is shown in Equation (8):

$$\lambda_{r3} = \int V_{SUM} \cdot dt \quad (8)$$

Figure 10 depicts the motor internal voltage corresponding to phase A, e_A, the third harmonic signal, V_{SUM}, obtained from the summation of the stator phase voltages, the rotor flux third harmonic component λ_{r3}, the rotor flux λ_r, and the stator phase currents [40]. In order to obtain maximum torque per ampere, the stator current is kept at 90 electrical degrees with respect to the rotor flux. In addition, *the zero crossings of the rotor flux third harmonic component occur at 60 electrical degrees, exactly at every desired current commutation instant.*

Figure 10. Back-EMF, third harmonic voltage, rotor flux and rotor flux fundamental components, and motor phase currents [40].

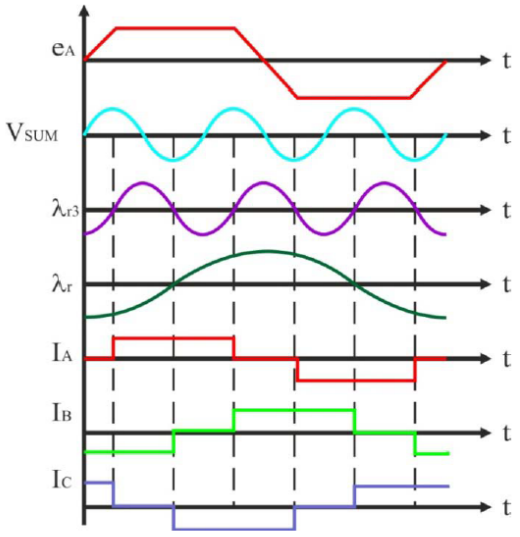

Basically, there are three methods to extract the third harmonic component of the back-EMF, using as reference a permanent-magnet brushless drive with Y-connected resistors to enable the third harmonic component of the back-EMF to be sensed [18]. These methods are the following:

- From the voltage V_{SN} between the star point S of the resistor network and the neutral point N of the stator windings [42,43].
- From the voltage V_{SH} between S and the midpoint H of the DC bus [40].
- From the voltage V_{NH} between N and H [44].

From the foregoing, *only the voltage V_{SH} is suitable for the third harmonic back-EMF sensorless operation of BLDC motors*, but as with all back-EMF based sensorless methods, an open-loop starting procedure has to be employed [18].

3.2.1. Optimizations

The improved version of this method has been developed by using a PLL [17], in which the freewheeling diode conduction period takes place right after the commutation. The inverted terminal voltage measured during the diode conduction period causes position error because of the unbalanced integration, and the commutation angle error was decreased by inverting the measured terminal voltage during the diode conduction period. The method can be integrated into the ML4425 application-specific integrated circuit (ASIC) [25,34,35].

The implementation of this improvement in an experimental system, such as an air compressor, requires low starting torque and the commutation of the BLDC drive is significantly retarded during high-speed operation [17]. To overcome the problem, the ASIC should integrate the third harmonic back-EMF instead of the terminal voltage, such that the commutation retarding is largely reduced and the motor performance is improved [45].

3.2.2. Applications

The key advantages of this technique are simplicity of implementation, low susceptibility to electrical noise, and robustness, what makes it a good option for applications requiring a wide motor speed range. Signal detection at low speeds is possible because the third harmonic signal has a frequency three times higher than the fundamental back-EMF, allowing operation in a wider speed range (100-6,000 rpm) than techniques based on sensing the motor back-EMF [40]. However, at low speed the integration process can cause a serious position error, as noise and offset error from sensing can be accumulated for a relatively long period of time [41].

3.3. Free-wheeling Diodes Conduction Detection method (Terminal Current Sensing)

Up to now, the indirect sensing algorithms explained can be applicable only to the SMPM motors whose winding inductances are almost the same and do not vary with the rotor position. These algorithms, except terminal current sensing method, utilize low pass filters or integration circuits to eliminate PWM frequency noise and to provide a phase delay for correct commutation of the stator current. But, in case of IPM motors, the inductance of stator winding varies with the rotor position. This characteristic introduces unbalance of phase impedances and variation of the potential of the

neutral point, and it is impossible to apply the terminal current sensing algorithm. IPM motors are more practical than SMPM motors because of the ruggedness of rotor structure and low inertia [28].

In this technique, the position information can be detected on the basis of the conducting state of free-wheeling diodes connected in antiparallel with power transistors because a current flows in a phase. In this phase any active drive signal is given to the positive and negative side transistors and the current results from the back-EMFs produced in the motor windings. The three-phase permanent magnet synchronous motor has the trapezoidal back-EMFs shown in Figure 9. To produce the maximum torque, the inverter commutation should be performed every 60º so that the rectangular-shaped motor line current is in phase with the back-EMF signal. A starting circuit is needed to give a commutation signal for starting. This approach makes it possible to detect the rotor position over a wide speed range, especially at a lower speed, and to simplify the starting procedure [19].

Therefore, the conducting condition of D_C. is given by Equation (9), taking into account that V_{CE} and V_F are much smaller than the back-EMFs. Then, when the back-EMF of phase C (e_C) becomes negative, the open-phase current flows through the negative-side diode D_C:

$$V_{CE}, V_F << e_A, e_B, e_C \Rightarrow e_C < -\frac{V_{CE} + V_F}{2} \approx 0 \Rightarrow e_C < 0 \quad (9)$$

Since the open-phase current results from the back-EMFs, it is impossible to detect the rotor position at a standstill. Therefore, a suitable starting procedure is necessary to the position sensorless BLDC motor drive. The procedure starts by exciting two arbitrary phases for a preset time. The rotor turns to the direction corresponding to the excited phases. At the end of the preset time, the *open-loop commutation* advancing the switching pattern by 120° is done, and the polarity of the motor line current is altered. After the starting procedure, the motor line current indicates that satisfactory sensorless commutations are performed by the free-wheeling diode conduction method [19].

3.3.1. Applications

This method has a position error of commutation points in the transient state as other back-EMF based methods. But, the most serious drawback of this method is the use of six isolated power supplies for the comparator circuitry to detect current flowing in each freewheeling diode, which prohibits this method from practical applications. However, this technique outperforms the previous back-EMF methods at low-speeds.

3.4. Back-EMF Integration Method

In this technique, the commutation instant is determined by integration of the silent phase's back-EMF (that is the unexcited phase's back-EMF). The main characteristic is that the integrated area of the back-EMFs shown in Figure 11 is approximately the same at all speeds. The integration starts when the silent phase's back-EMF crosses zero. When the integrated value reaches a pre-defined threshold value, which corresponds to a commutation point, the phase current is commutated. If flux weakening operation is required, current advance can be achieved by changing the threshold voltage. The integration approach is less sensitive to switching noise and automatically adjusts for speed changes, but low speed operation is poor due to the error accumulation and offset voltage problems

from the integration [25]. As the back-EMF is assumed to vary linearly from positive to negative (trapezoidal back-EMF assumed), and this linear slope is assumed speed-insensitive, the threshold voltage is kept constant throughout the speed range.

Figure 11. Integrated areas of the back-EMF [25].

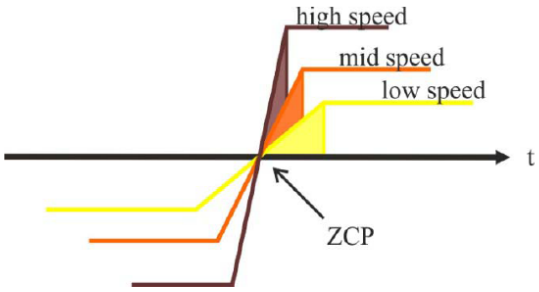

Once the integrated value reaches the threshold voltage, a reset signal is asserted to zero the integrator output. To prevent the integrator from starting to integrate again, the reset signal is kept on long enough to insure that the integrator does not start until the residual current in the open phase has passed a zero-crossing.

The use of discrete *current sensors* for each motor phase will provide complete current feedback, but the cost associated with individual current sensors (e.g., current transformers or Hall-effect sensors) is often prohibitive. An appealing alternative is the use of current sensors which are integrated into the power switches, such as power MOSFET'S and IGBT's, which are available from several device manufacturers with ratings up to several hundreds of volts and several tens of amps. However, embedded current sensors impose their own constraints; for example, the current sensing terminal is not electrically isolated from the associated power device. Also, the availability of new power integrated circuits makes it possible to take more complete advantage of these sensors for the combined purposes of current regulation and overcurrent protection [46].

Finally, the back-EMF integration approach provides significantly improved performance compared to the zero-crossing algorithm explained before. Instead of using the zero-crossing point of the back-EMF waveform to trigger a timer, the rectified back-EMF waveform is fed to an integrator, whose output is compared to pre-set threshold. The adoption of an integrator provides dual advantages of reduced switching noise sensitivity and automatic adjustment of the inverter switching instants according to changes in rotor speed [23].

3.5. Methods based on PWM strategies

There are many methods based on PWM control schemes, but the most relevant are conventional 120º, elimination of virtual neutral point, techniques for low speed, high speed and small power applications, and direct current controlled, which are explained below.

3.5.1. Conventional 120° PWM technique

The block diagram for a three-phase BLDC drive, which consists of a three-phase inverter and a BLDC motor, was shown in Figure 7. It can be controlled by the PWM technique to give proper commutations so that two of the three phases are with on states and the remaining one is with floating state. Moreover, the sequence of commutations is retained in proper order such that the inverter performs the functions of brush and commutator in a conventional DC motor, to generate a rotational stator flux [19,47]. Figure 12 shows the PWM waveforms for this conventional approach [48], which has low switching losses in the inverter side at the cost of significantly high harmonic contents. This results in increase of loss in the motor side [22].

Figure 12. PWM waveforms for a conventional approach [48].

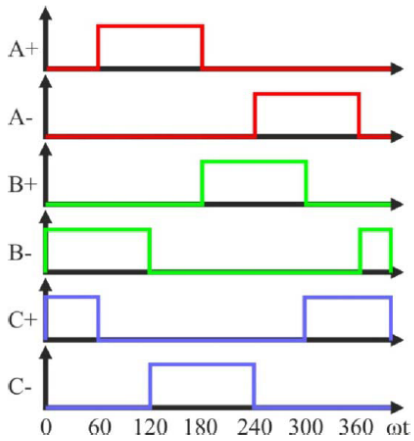

3.5.2. Technique of virtual neutral point elimination

In a typical inverter configuration, as Figure 7 illustrates, two phases are always conducting current and one phase is only available to measure back-EMF. To measure the back-EMF across a phase, the conventional method requires monitoring the phase terminal and the motor neutral point [24], as shown in Figure 13. The zero crossing of the back-EMF can be obtained by comparing the terminal voltage to the neutral point. In most cases, the motor neutral point is not available. The most commonly used method is to build a virtual neutral point that will be theoretically at the same potential as the neutral point of the wye-wound motor [38].

The conventional detection scheme is quite simple and when a PWM signal is used to regulate motor speed or torque/current, the virtual neutral point fluctuates at the PWM frequency. As a result, there is a very high common-mode voltage and high-frequency noise. Voltage dividers and low-pass filters, as shown in Figure 13, are required to reduce the common-mode voltage and minimize the high-frequency noise [38].

Figure 13. Back-EMF sensing based on virtual neutral point [38].

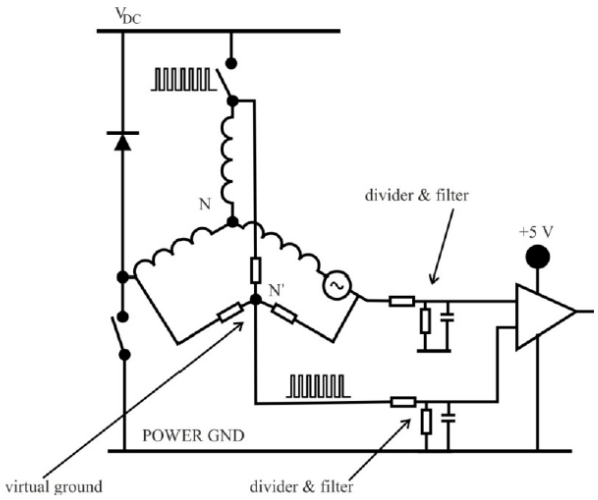

By means of eliminating the virtual neutral point when measuring back-EMF, a low amount of filtering is required, and the zero crossing of the back-EMF voltage of the floating phase can be obtained directly from the motor terminal voltage referred to ground by properly selecting the PWM and sensing strategy. Besides, the neutral point potential will be function of each phase's back-EMF, and will not be affected by any external driven voltage. Also, in this method the PWM signal is applied on high side switches only, and the back-EMF signal is synchronously detected during the PWM off time [22], as illustrated in Figure 14. The low side switches are only switched to commutate the phases of the motor. Then, the *true back-EMF can be detected during PWM off time* because the terminal voltage of the motor is directly proportional to the phase back EMF during this interval.

Figure 14. PWM applied to high side switches of a typical inverter for BLDC motors [22].

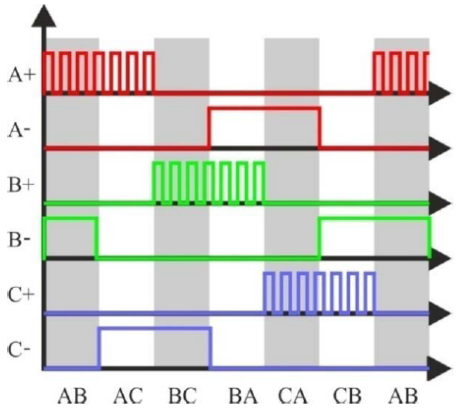

During the off time of the PWM, the terminal voltage of the floating phase is directly proportional to the back-EMF voltage without any superimposed switching noise, as Equation (10) indicates.

Besides, this terminal voltage is referenced to the ground instead of the floating neutral point, so the neutral point voltage information is not needed to detect the back-EMF zero crossing [24]:

$$V_N = \frac{e_C}{2} \Rightarrow V_C = e_C + V_N = \frac{3}{2} \cdot e_C \quad (10)$$

The resulting signal is not attenuated or filtered and it has a good signal/noise ratio, including a much wider speed range, which is beneficial at high speed operation. Then, this sensing technique has high sensitivity and it can be used in either high voltage and low voltage systems without effort to scale the voltage [22,24].

A good application for this sensorless drive system is in an automotive fuel-pump [38]. A dedicated sensorless BLDC controller can be incorporated in the fuel tank, implementing a back-EMF zero-crossing detection circuit as one of its peripherals, which simplifies the vehicle systems as well as reduces the overall system cost. This method has been also successfully applied to some home appliances for compressors, air blowers, and vacuum cleaner as well as engine cooling fan, and HVAC (Heating, Ventilating and Air Conditioning) blower motor applications.

3.5.3. Technique for low speed or low voltage applications

For low voltage applications, the voltage drop across the BJT's or MOSFET's will affect the performance. When the motor speed goes low, zero crossing is not evenly distributed. Besides, if the speed goes further low, the back-EMF amplitude becomes too low to detect [22].

There are basically two methods to correct the offset voltage of back-EMF signal [49]. One of them is to use *complementary PWM* as shown in Figure 15, which also reduces the conduction loss [22]. Another method is to eliminate the effect of diode voltage drop in order to add a constant voltage to compensate the effect of diode, and threshold voltage for avoiding the asymmetry in the distribution of zero crossing [24]. Then, in order to eliminate the non-zero voltage drop effect, a complementary PWM can be used, which will also reduce the power dissipation in the devices [49].

Figure 15. Complementary PWM algorithm [22].

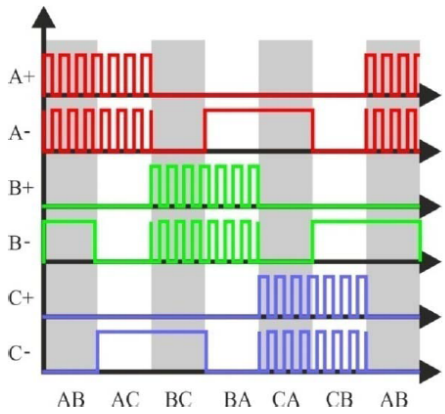

Assuming at a particular step, phase A and B are conducting current, and phase C is floating. The terminal voltage V_C is sensed when the upper switch of the half bridge is turned off, and the current goes over the freewheeling diode D. During this freewheeling period, the terminal voltage V_C is detected as phase C back-EMF. Then, the terminal voltage V_C is shown in Equation (11), considering a low voltage MOSFET, in which $R_{DS(ON)}$ is very low and V_{DS} can be ignored:

$$V_N = \frac{V_{DS} - V_D}{2} + \frac{e_C}{2} \Rightarrow V_C = e_C + V_N = \frac{3}{2} \cdot e_C - \frac{V_D}{2} \quad (11)$$

Therefore, the voltage drop on the diode will bias the terminal voltage of phase C. When the back-EMF e_C is high enough at high speed, the effect of second term of Equation (11) is negligible [24]. However, at low speed especially during the start-up, the back-EMF itself is very small, and the second term will play a significant role. This *voltage offset will cause un-evenly distributed back-EMF zero-crossings*, which causes *unexpected commutation* and will affect the performance of the system. Also, because the back-EMF signal is too weak at low speed; an amplifier can be used as a pre-conditioning circuit for adjusting the offset and amplifying the signal near the zero-crossing [49]. Finally, the motor speed can be greatly expanded with the improvements explained before. For example, if a 48 V motor is used, the speed operation range can be from 50 rpm to 2,500 rpm [49].

3.5.4. Technique for high speed or high voltage applications

One of the direct back-EMF sensing schemes analysed before could be implemented, for instance, in a hardware macro cell inside a microcontroller [49]. The three phase terminal voltages will feed into the microcontroller through resistors, which limit the injected current. When the PWM duty cycle is high, wrong zero-crossing detection occurs. This problem is caused by the large time constant of the current limit resistors. Additionally, there is some parasitic capacitance inside the microcontroller. Since the outside resistance is high enough, even though the capacitance is low, the effect of RC time constant will show up, and the falling edge of signal V_C will be long.

As the back-EMF signal is sampled at the end of PWM off time, if the PWM duty cycle is high enough such that the off time is less than the falling edge time, the sampling result is not correct because the discharging period has not finished yet. To shorten the discharging time, the RC time constant should be reduced. A possibility is to use a smaller resistor in parallel with the resistor of the time constant, and a diode to block the charging current passing through the parallel resistor [49].

Since the back-EMF is sent directly to the microcontroller through a current limit resistor, for high voltage applications the resistance value is fairly high. This resistance with the parasitic capacitance in the circuit will cause too much delay and cause false detection. Using the improvements commented before, the sensorless system can be successfully used for 300 V/30,000 rpm high-speed air blower applications [50].

3.5.5. Technique for small power applications

The basic concept for the development of this three-phase PWM technique is similar to that of synchronous rectifier for DC/DC converter. In a conventional approach [19], the switching losses are

low in the inverter side at the cost of significantly high harmonic contents, which result in increase of loss in the motor side. For small power applications of BLDC drives, for instance fan and spindle applications, due to the use of battery and limited space for heat dissipation, reduction of power consumption becomes one of the main concerns in this PWM technique [22].

The high side power device is chopped in 1/6 fundamental period and duty ratio is derived from the speed reference or error of speed. Similar control signal is applied to the low-side power device with 180º shift. These control signals are applied to the other two phases with 120° shift. Under this condition, in the circuit of Figure 7 the current flows through the anti parallel diode of power device T_{A-}, and thereby resulting in significant conduction losses, which equal to the product of forward drop voltage of diode and load current. This significant heat loss is reduced in this technique [22]. The high-side power device is chopped in fundamental period and clamped to the positive DC link rail in the consecutive fundamental period [51], which is illustrated in Figure 16. As the high-side device is with chop control, the associated low-side power device is triggered by the inverse signal of chop control.

Figure 16. PWM waveform for low power PWM technique, where ωt[60°,120°] and TA+ is "off" [51].

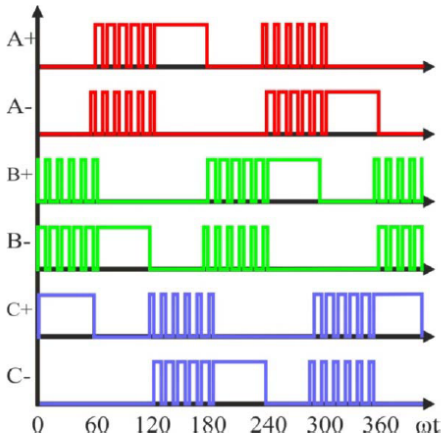

To highlight the feature of this PWM technique, the voltage drop caused by the turn-on resistance of power device and load current is significantly reduced as compared to the forward voltage drop of diode. Therefore, *the power consumption and the heat losses can be significantly reduced*.

A practical implementation of this method is in DVD spindle devices using FPGAs. Only terminal voltages of three phases are sampled and fed into the FPGA controller to calculate the commutation instants, and an external resistor and an eight-bit A/D converter are used to give the reference of duty ratio [48].

3.5.6. Direct current controlled PWM technique (hysteresis current control)

With the advantages of BLDC motor drives [2,41,52], it is possible to use a reduced converter configuration with advanced control techniques. Then one switch leg in the conventional six-switch converter, showed in Figure 7, is redundant to drive the three-phase BLDC motor, which results in the

possibility of the four-switch configuration instead of six switches [21], as shown in Figure 17. This new drive consists of two switch legs and split capacitor bank, so two phases are connected to the switch legs and the other phase to the midpoint of DC-Link capacitors. But with this configuration, the limited voltages make very difficult to obtain 120° conducting profiles. This is the well-known problem *asymmetric voltage PWM* [21], which results in the 60° phase-shifted PWM strategy to generate three-phase balanced current profiles. Also, the conventional PWM schemes cannot be directly applied for the new drive configuration.

Figure 17. Four-switch converter for driving a three-phase BLDC motor [21].

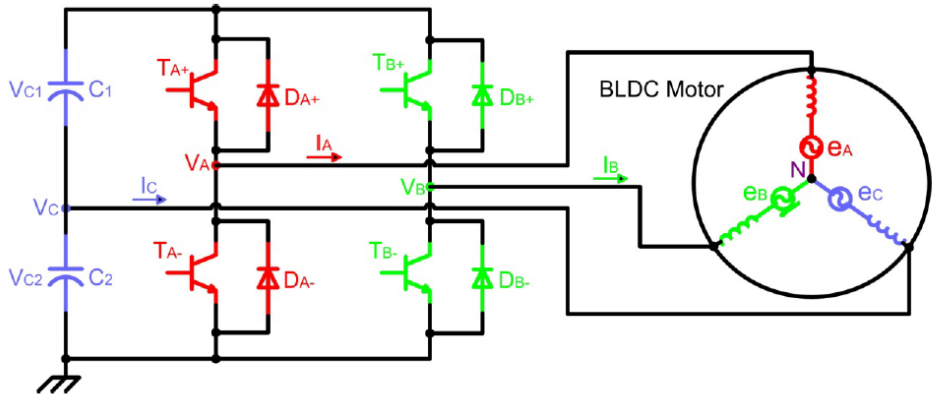

The direct current PWM control technique is based on the current controlled PWM method, instead of the voltage controlled PWM, which generates robust speed and torque responses and is simple to be implemented from the hardware and software points of view. Therefore, the four-switch three-phase BLDC motor drive, mainly applied to AC induction motor drives until now [53-55], could be a good alternative to the conventional configuration with respect to low-cost and high performance.

In a PWM control strategy for the four-switch three-phase BLDC motor drive, the three-phase currents always meet the condition of Equation (12):

$$I_C = -(I_A + I_B) \tag{12}$$

It means that control of the two-phase currents can guarantee the generation of the 120º conducting three-phase currents profiles. For completing this task, the two-phase currents are directly controlled using the *hysteresis current control* method by four switches [21].

4. Other Sensorless Techniques: Estimation and Model-Based Methods

It is convenient when designing feedback control systems, such as the motor position and speed, to assume initially that the entire state vector of the system to be controlled is available through measurement. If the entire state vector cannot be measured, as it is typical in most complex systems, the control law deduced cannot be implemented. Thus either a new approach that directly accounts for the nonavailability of the entire state vector must be devised, or a suitable approximation to the state vector that can be substituted into the control law must be determined [56]. In almost every situation,

the development and use of an approximate state vector, which will substitute the unavailable state, is vastly simpler than a direct point of view of the system design.

Adopting this perspective, a control design problem can be split into two phases. The first phase is design of the control law assuming that the state vector is available, which may be based on optimization or other design techniques, and typically results in a control law without dynamics. The second phase is the design of a system that produces an approximation to the state vector. This system, called *observer* in a deterministic setting, has as its inputs the inputs and available outputs of the system whose state is to be approximated and has a state vector that is linearly related to the desired approximation [56]. Besides the simplicity of its design, the biggest advantage of using observers is that all of the states in the system model can be estimated including states that are hard to obtain by measurements [25]. In addition to their practical utility, observers offer an associated theory, which is intimately related to the fundamental linear system concepts of controllability, observability, dynamic response, and stability, and provides a simple setting in which all of these concepts interact.

To sum up, an observer provides a mathematical model of the brushless DC motor, which takes measured inputs of the actual system and produces estimated outputs. The error between the estimated outputs and measured quantities is fed back into the system model to correct the estimated values, such as the rotor position and speed, as would be the actually measured variables in a closed-loop system control [41]. Although most of the observer-based methods are used for PMAC motors, which have sinusoidal back-EMF and need continuous rotor position, for the BLDC motors, which require just six position points for one electrical cycle, the continuous position information from the observer is not necessary typically. But, for special purposes, such as flux weakening operation based on advanced angle control, the positions between commutation points are required [25].

4.1. Sliding-Mode Observer (SMO)

For controlling BLDC motor, it is necessary to know an absolute position of the rotor, so an absolute encoder or resolver can be used for sensing the rotor position. But, these position sensors are expensive and require a special arrangement for mounting. Also, the state equation of BLDC motor is nonlinear, so it is difficult for the linear control theory to be applied and the stability of position and velocity estimation have not been clarified. To improve the mechanical robustness and to reduce the cost of the drive system, several estimation techniques eliminating the encoder or resolver can be applied [57]. Some relevant methods have been developed using the sliding-mode observer, which are briefly explained next.

In the Direct Torque Control method (DTC), the state equation of the BLDC motor is utilized to achieve a relationship between the angle of the stator current vector and the back-EMF vector angle, obtaining minimum error angle estimation and reducing the torque ripple in com-mutation regions. In this control method, the proper voltage vector is selected from a look-up table using the rotor flux vector position and torque error, which is led to the predefined hysteresis [58]. However, DTC methods based on hysteresis controllers have some serious drawbacks such as a high amount of torque and flux pulsations and variable switching frequency of the inverter [59]. Also, in the direct torque control of brushless DC motor, the stator flux linkage observation is needed, and the accuracy of the observed stator flux linkage is affected by the variation of stator resistance, electric interference,

magnetic interference, measurement error and so on [60]. These drawbacks are solved with the DTC Space Vector Modulation (DTC-SVM) scheme, which uses a constant switching frequency. However, the DTC-SVM scheme needs a transformation from stationary reference frame to stator flux field orientation frame and vice versa, therefore it has a high computation time and could be an erroneous cumulative scheme [61]. Also, with the introduction of DTC technique and the advances of speed sensorless systems, the interest in stator resistance adaptation came to scene for an optimal performance of speed sensorless systems in low speed region [62].

Recently, and commented above, low speed operation with robustness against parameter variations remains an area of research for sensorless systems, taking into account that an accurate value of stator resistance is of utmost importance for its correct operation in low speed region. As in the upper speed range, the resistive voltage drop is small as compared with the stator voltage; hence the stator flux and speed estimation can be made with good accuracy. At low speeds the stator frequency is also low, but stator's voltage reduces almost in direct proportion and the resistive voltage drop maintains its order of magnitude and becomes significant. This greatly influences the estimation accuracy of the stator flux and hence the speed estimation. An estimation algorithm based on SMO in conjunction with Popov's hyper-stability theory can be used to calculate the speed and stator resistance independently, which can guarantee the global stability and the convergence of the estimated parameters [62].

The SMO is widely studied in the field of a motion control, and it can be applied to nonlinear systems, such as BLDC motors [63]. This technique applied to control systems encounters restrictions in practice, due to the high voltage values of the power supply needed and severe stress given to the static power converters. On the other hand, the sliding mode has been shown very efficient in the state estimation due to its salient features, *i.e.*, robustness to parameter variations and disturbances including the measurement noise. The use of sliding mode in state observer does not present physical restrictions relative to the convergence condition (the estimation error moves toward zero) and does not subject the system to undesirable chattering [57]. These problems can be alleviated using a **binary observer** with continuous inertial Coordinate-Operator Feedback [63].

4.2. Extended Kalman Filter (EKF)

The extended Kalman filter algorithm is an optimal recursive estimation algorithm for nonlinear systems. It processes all available measurements regardless of their precision, to provide a quick and accurate estimate of the variables of interest, and also achieves a rapid convergence. This is done using the following factors: the knowledge of the system dynamics, statistical description of the system errors (noises, disturbances, *etc.*), and information about the initial conditions of the variables of interest. The algorithm is computationally intensive, thus an efficient formulation is needed rather than a straightforward implementation. Moreover, for a practical application of the filter in real time, different aspects of implementation have to be addressed, such as the computational requirements (processing time per filter cycle, required memory storage, *etc.*) and the computer constraints (cycle execution time, instruction set, arithmetic used, *etc.*) [64].

This method can be used to estimate the rotor position and speed. Motor state variables are estimated by means of measurements of stator line voltages and currents, and applying EKF next. During this process, voltage and current measuring signals are not filtered, and rotor position and

speed can be estimated with sufficient accuracy in both steady state and dynamic operations [22]. Unlike the deterministic base of other studies, the model uncertainties and nonlinearities in motors are well suited to the stochastic nature of EKFs, as well as the persistency of excitation due to the system and measurement noises. This is the reason why the EKF has found wide application in speed-sensorless control, in spite of its computational complexity. However, with the developments in high performance processor technology, the computational burden and speed of EKF has ceased to be a problem [65].

The block diagram of the system for speed and rotor position estimation of a BLDC motor is shown in Figure 18. The system can be functionally divided in two basic parts: the speed control system and the estimation system. The first one consists of a power circuit (DC supply, inverter and motor) and control circuits, which perform three functions: current commutation, current control and speed control. The measured speed (ω_k) and phase currents (i_k) as well as the estimated rotor position ($\hat{\theta}_{k/k}$) are used as feedback signals. The main blocks of the estimation algorithm are the EKF and the block for calculating average motor line voltages during sampling time. The average line voltages vector, defined on the basis of average line voltages in the k-sampling time (u_k), is calculated at the beginning of the sampling time by means of terminal voltages to neutral-point vector (u_{Nk}), the inverter transistors duty cycle (ϵ_k), the inverter DC voltage (U_0), the estimated speed ($\hat{\omega}_{k/k}$), the rotor position ($\hat{\theta}_{k/k}$), and measured currents vector (i_k) [66].

Figure 18. System configuration for speed and rotor position estimation of a BLDCM [66].

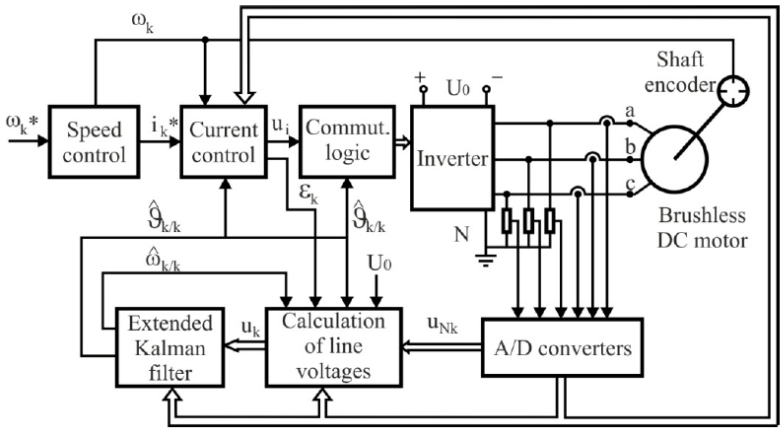

Among recent speed-sensorless studies using EKF based estimation, the simultaneous estimation of the rotor angular velocity, the rotor flux and the stator resistances, via a Kalman filter in combination with the model reference adaptive system (MRAS), have been performed, but are sensitive to variations in the stator and rotor resistances. Some innovative techniques have been currently developed, such as the *Bi Input-EKF* (BI-EKF). This method utilizes a single EKF algorithm with the consecutive execution of two different inputs, which are calculated from the two extended models based on the rotor and stator resistance estimation, respectively. These two different inputs are used for the rotor flux based speed control both in the transient and steady-state over a wide speed range. Also,

the load torque is estimated, including viscous friction term, rotor angular velocity, rotor flux, and stator current components without the need for signal injection [65].

4.3. Model Reference Adaptive System (MRAS)

In some cases, the stator and rotor resistance estimation is not applicable when the speed-sensorless control system is in transient state, such as operation under largely varying load torque and/or changes in the speed command. In other cases, the rotor time constant via high frequency signal injection, the stator resistance and the rotor angular velocity can be estimated by using MRAS. However, the stator resistance estimation is turned on for short time intervals when the rotor angular velocity estimation has reached its steady-state; that is, both the stator resistance and rotor angular velocity estimations are performed interchangeably [65].

The model reference adaptive system, developed using Popov's stability criterion, is one of many promising techniques employed in adaptive control for estimating the speed and stator resistance [62]. Among various types of adaptive system configuration, MRAS is important since it leads to a relatively easy-to-implement system with a fast adaptation for a wide range of applications. The basic principle is illustrated in Figure 19, called *parallel MRAS*. The dynamic models are represented by the block "Reference Model", which is the actual system (for example, the motor, containing all unknown parameters, *i.e.*, motor speed, stator and rotor resistances) and the block "Adjustable Model", which has the same structure as the reference one (*i.e.*, motor, but with the adjustable or estimated parameters, instead of the unknown ones). An error vector ϵ is derived using the difference between the outputs of two dynamic models and is driven to zero through an adaptation law. As a result, the estimated parameter vector will converge to its true value *X*. One of the most noted advantages of this type of adaptive system is its high speed of adaptation. This is due to the fact that a measurement of the difference between the outputs of the reference model and adjustable model is obtained directly by comparison of the states (or outputs) of the reference model with those of the adjustable model system [67]. It is remarkable that the error signal may be formulated with flux (F-MRAS), back-EMF (E-MRAS), reactive power (Q-MRAS) and active power (P-MRAS) [68].

Figure 19. Basic configuration of a MRAS [67].

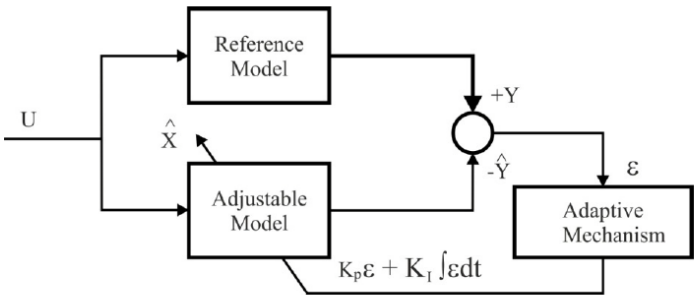

For instance, a MRAS with instantaneous *reactive power* can be used for speed estimation of sensorless vector controlled motor drive. This MRAS converts a vector quantity (*i.e.*, current vector) into a scalar quantity using the concept of reactive power, and the reference model utilizes measured

current vector. Also, the adjustable model uses the estimated stator current vector, and the current, estimated through the machine state equations, is configured in terms of reactive power [68]. An *active power* MRAS based scheme can also be used for rotor resistance identification, whose estimation is effective in wider range of variations and could be applied in real time field-oriented control (FOC) [67].

4.4. Adaptive Observers

The interest in stator resistance adaptation came to scene much recently, with the advances of speed sensorless systems and with the introduction of DTC technique. An accurate value of the stator resistance is of crucial importance for correct operation of a sensorless drive in the low speed region, since any mismatch between the actual value and the set value used within the model of speed estimation may lead not only to a substantial speed estimation error but also to instability as well. Therefore, to develop online stator resistance identification schemes are of utmost importance for accurate speed estimation in the low speed region. These estimators often use an adaptive mechanism to update the value of stator resistance. Some of the most relevant are MRAS, explained previously, and adaptive full-order flux observers (AFFO) [62].

4.4.1. Adaptive Full-order Flux Observer (AFFO)

The AFFO scheme has been developed using Lyapunov's stability criterion and allows estimating the rotor speed and stator resistance simultaneously. Using this observer, the estimated quantities converge to their real values if the persistency of excitation condition is also satisfied. Correct estimation of rotor flux space vector and rotor speed is therefore possible through this observer according to the stator and rotor resistances online adaptation [59]. Jointly with MRAS, AFFO is not computationally intensive, but with a non-zero gain matrix may become unstable. In such methods, the stator resistance adaptation mechanism is determined with the difference between the measured and observed stator currents [62]. With a maximum torque per ampere (MTPA) strategy, based on slip frequency (inverse of the rotor time constant in the rotor flux oriented reference frame) adjustment, the stator current amplitude can be minimized for each value of motor speed [59].

Apart from the variation of the stator resistance with temperature, other parameters in the AFFO will change during operation as well, such as the rotor resistance due to temperature changes, which will have an important influence on the speed accuracy of the adaptive observer. The stator and rotor self-inductance and magnetizing inductance vary due to magnetic saturation, being it possible to use a nonlinear magnetic model. In steady state, it is known that a misestimation of the rotor resistance provides correct estimations of the stator and rotor flux, but results in a misestimation of the speed [69].

This observer can be also applied in both rotor and stator-flux-vector-controlled drives, and in DTC drives. Even, it can be used in combination with the *Discrete-Time Direct Torque Control method* (DT-DTC), whose advantage over the classical DTC method is the torque-ripple-free operation in the whole speed range [69].

4.4.2. Adaptive Pseudoreduced-Order Flux Observer (APFO)

The field-oriented control (FOC) concept is widely used for high performance control of AC motors. In the case of induction or brushless drive systems, the FOC requires a speed sensor, such as shaft-mounted tachogenerator, resolver, or digital shaft position encoder, for obtaining speed information, which spoils the ruggedness and simplicity of the motor. Therefore, several speed observers have been developed to solve this problem, such as AFFO for estimating the rotor flux and speed, whose computation process is simple but it is an unstable system in some cases and unsuitable for practical applications (large speed errors may appear under heavy loads and steady-state speed disturbances may occur under light loads) [70]. Besides, the MRAS technique is applied to sensorless speed control using the field oriented reference frame. While this method is simple and always stable, its performance is poor in the low speed range, where open-loop integration may lead to instability due to stator resistance misestimation, and it is very sensitive to the offset of the voltage sensor and the stator resistance variation due to temperature [71].

An improved scheme is the Adaptive Pseudoreduced-order Flux observer (APFO), which uses the Lyapunov method and consumes less computational time with a better speed response than the AFFO over a wide speed range [70]. An innovative idea applied in this observer is a constant gain matrix, which ensures that the poles are not related to the motor speed. Then the observer poles are invariant to any speed variations, so the drive can operate at high speeds and have fast response [72].

4.5. Artificial Neural Networks (ANN)

A neural network or artificial neural network (ANN) is the interconnection of artificial neurons that tends to simulate the nervous system of a human brain. Each signal coming into a neuron along a dendrite passes through a synaptic junction. The adjustment of the impedance or conductance of the synaptic gap leads to "memory" or "learning" process in the case of brain, which is similarly required in ANN. The model of an artificial neuron that closely matches a biological neuron is given by an op-amp summer-like configuration [73].

In recent years, the use of artificial neural networks for identification and control of nonlinear dynamic systems in power electronics and motor drives have been extended, as they are capable of approximating wide range of nonlinear functions to a high degree of accuracy. If a motor drive is considered, where the essential sensor signals relating to the state of the system are fed to a neural network, the network output can interpret the "health" of the system for monitoring purposes and control. ANNs can be also used for realization of current-regulated PWM inverters, in which the network receives the phase current error signals and generates the PWM logic signals for driving the inverter devices [74].

Referring to motors, ANNs can be used to estimate rotor flux, unit vector, and torque in vector-controlled drives. The network has to be trained with a very large number of simulation data sets, so DSP-based estimators and ANN-based estimators perform comparably [73]. The capability of a neural network can be deployed to have online estimators to address the situation of similar disturbances in both stator and rotor resistances simultaneously. In this situation, the resistance observer can be realized with a recurrent neural network trained using the standard back-propagation

learning algorithm. The block diagram of a rotor flux oriented induction motor (IM) drive together with both stator and rotor resistance identifications are shown in Figure 20, which also applies to BLDC motors. A rotor flux oriented vector controller commands the motor, and the voltage model fluxes are estimated from the measured stator voltages and currents using a programmable cascaded low-pass filter (PCLPF). The stator voltages are PWM voltages, which are filtered, and only the sinusoidal voltages are taken into the PCLPF flux estimators. The RRE and SRE blocks estimate the rotor and the stator resistances, respectively, taking into consideration that the stator resistance estimation depends on the rotor resistance. The rotor flux linkages are compensated by the RRE and hence the estimation error in the stator resistance is avoided [75].

Figure 20. Block diagram of the indirect vector controlled induction motor drive with online stator and rotor resistance tracking [75].

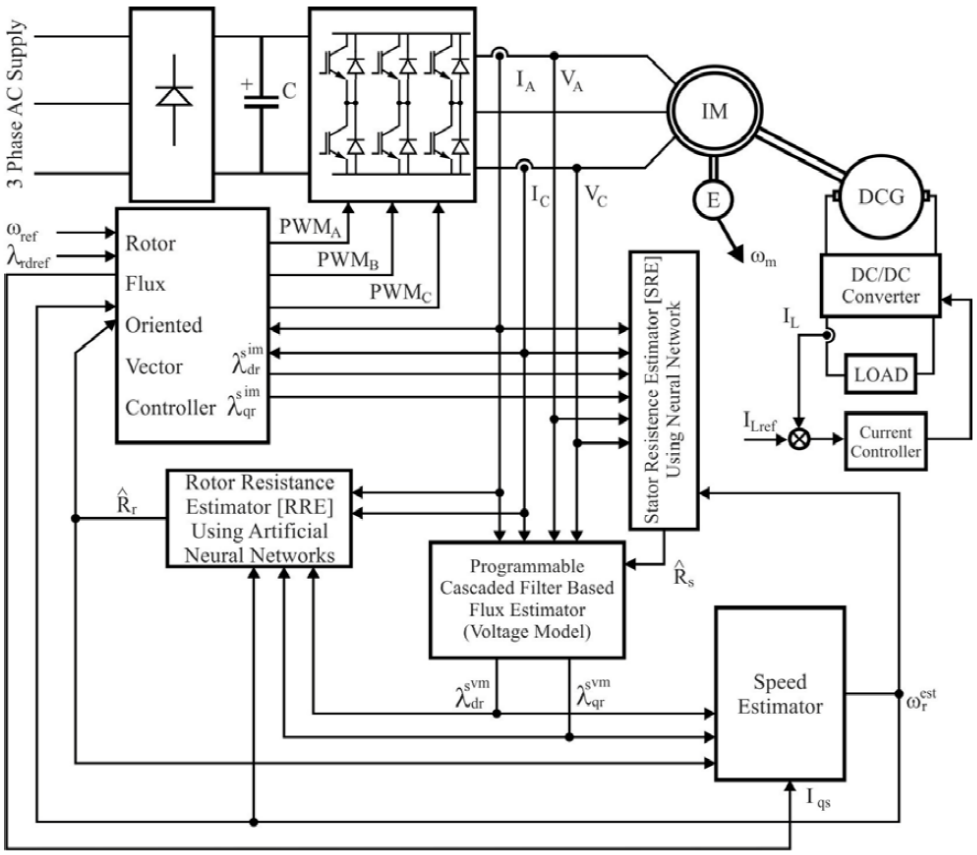

An improvement is the *Fuzzy Neural Networks* (FNN), which are systems that apply neural networks principles to fuzzy reasoning and can be based on rule or relational approaches. Basically, they emulate fuzzy logic controllers, with the advantages that it can automatically identify fuzzy rules and tune membership functions for a problem. FNNs can also identify nonlinear systems to the same precision as conventional fuzzy modelling methods, such as the development of stator flux-oriented vector-controlled drive [73].

5. Implementation of back-EMF Control Techniques

In the design and development of motor controllers based on back-EMF techniques, it is necessary to analyse the implementation options using electronic processors or ASIC. This is done by taking into account that all back-EMF sensing methods need to start the motor from standstill using an open-loop starting technique. All these issues are studied next.

5.1. Comparison of methods' feasibility

Assuming a three-phase BLDC motor as a reference model, a six-step commutation with 120º conduction time allows for current to flow in only two phases at any one time, which leaves the third phase available for sensing back-EMF. *Originally the method of sensing back-EMF* was proposed in order to build a virtual neutral point, which, in theory, will be at the same potential as the center of the wound motor. However, when using a chopping drive, the PWM signal is superimposed on the neutral voltage, inducing a large amount of electrical noise on the sensed signal [49]. To reduce the switching noise, the *back-EMF integration* [23] and *third harmonic voltage integration* [40] were introduced. The integration approach has the advantage of reduced switching noise sensitivity. However, it still has an accuracy problem at low speed. An indirect sensing of zero crossing of phase back-EMF by *detecting the conducting state of free-wheeling diodes* in the unexcited phase is complicated and costly, while its low speed operation is a problem [19]. The *back-EMF zero-crossing detection* (terminal voltage sensing) method, which does not require the motor neutral voltage, permits the extraction of the true back-EMF directly from terminal voltage by properly choosing the PWM and sensing strategy [24,76]. As a result, this sensorless BLDC driver can provide a much wider speed range from start-up to full speed than the conventional approaches.

The *third harmonic* based method is one of most relevant back-EMF sensing schemes. It has a wider speed range and smaller phase delay than the *terminal voltage sensing* method [77]. However, at low speed, the integration process can cause a serious position error, as noise and offset error from sensing can be accumulated for a relatively long period of time [25]. At lower speeds, detection of both the third harmonic and the zero-crossing of the phase voltage become difficult due to the lower signal levels. In comparison, the conventional back-EMF control scheme is able to drive the motor from 6,000 rpm to about 1,000 rpm, but the third harmonic control scheme is capable to operate the motor from rated speed (6,000 rpm) down to about 100 rpm. This does not introduce as much phase delay as the zero-crossing method and requires less filtering [41]. Then, the efficiency drop is more accentuated for the terminal voltage sensing scheme, because the delay introduced by the low pass filter decreases with the motor speed. This phase delay introduced by the filter is responsible for the loss of field orientation and loss of the quadrature condition between rotor flux and stator current. The immediate consequence is the reduction of the torque per current ratio of the motor, which implies in larger copper losses [40]. Also, the third harmonic back-EMF method is applicable for the operation in flux weakening mode, and the methods based on zero-crossing of the back-EMF are simple. However, it is only applicable under normal operating conditions (commutation advance or current decay in free-wheeling diodes lower than 30 electrical degrees) [22].

Due to most popular and practical sensorless drive methods for BLDC motors relying on speed-dependent back-EMF, and the back-EMF is zero or undetectably small at standstill and low speeds, it is not possible to use the back-EMF sensing methods in the low speed range. Then, *in all back-EMF-based sensorless techniques, the low-speed performance is limited, and an open-loop starting strategy is required* [18]. However, other control schemes such as the *PWM method eliminating the virtual neutral point* can provide a much wider speed range from start-up to full speed than the conventional schemes. Besides, this method has high sensitivity; it is good at high-speed operation due to a lack of unwanted delays in the zero-crossing detection. It can be easily used in both high-voltage or low-voltage systems, and it has a faster motor start-up because of the precise back-EMF zero-crossing detection without attenuation. Also, it is simple and easy to implement [38].

5.2. Open-Loop Starting

The back-EMF detection methods can not be applied well when the motor is at a standstill or low speed, since back-EMF is zero. A starting procedure is needed to start the motor from standstill [20]. The open-loop starting is accomplished by providing a rotating stator field which increases gradually in magnitude and/or frequency. Once the rotor field begins to become attracted to the stator field enough to overcome friction and inertia, the rotor begins to turn and the motor acts as a permanent magnet synchronous machine with the disadvantage that the initial rotor movement direction is not predictable. When the stator field becomes just strong enough, the rotor could move in either direction. If the speed of the stator field is slow enough and the load torque demanded does not exceed the pull-out torque the motor will operate synchronously in the desired direction [41]. The change over from open-loop to sensorless method is made when sufficient back-EMF is generated, so that the sensorless method should start generating the switching instants of all transistors [7].

Taking all this into account, the procedure starts by exciting two arbitrary phases for a preset time (for example, 0.5 s). At the end of the preset time, the open-loop commutation advancing the switching pattern by 120° is done, and then, the polarity of the motor line current is altered. Then, the rotor turns to the direction corresponding to the exited phases as is shown in Figure 21a. Next, the commutation signal that advances the switching pattern by 120° is given, as Figure 21b indicates, and the open-loop commutation is immediately switched to the sensorless drive. After the next commutation the position sensorless drive is attained (Figure 21c), and the motor line current indicates that satisfactory sensorless commutations are performed by the position-detecting method [19].

Figure 21. Open-loop starting procedure [19].

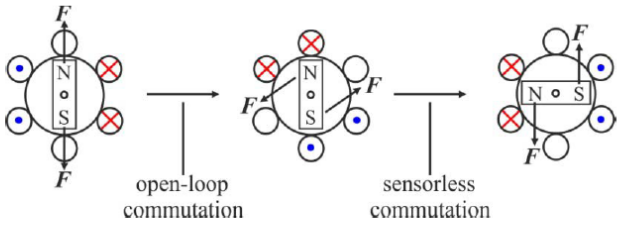

This method is simple but the reliability is affected by the load and it may cause temporarily reverse rotation of the rotor during the start-up. This is not allowed in some applications [20], such as disk drives, which strictly require unidirectional motion. However, it may be satisfactory in others such as pump and fan drives. Another problem exists if the stator field is rotating at too great a speed when the rotor field picks up. This causes the rotor to oscillate, which requires the stator field to decrease in frequency to allow starting.

The stator iron of the BLDC motor has non-linear magnetic saturation characteristic, which is the basis for determining the initial position of the rotor. In order to overcome the drawbacks mentioned above, the rotor position detecting and speed up methods based on saturation effect of the stator iron can be applied [78], such as the *short pulse sensing* technique. This scheme adopts a voltage pulse train composed of the successive short and long pulses to generate positive torque to speed up the motor, and it does not bring any reverse rotation and vibration during the start-up process [20]. The response speed of the stator current [79], and the response peak value of the current of the stator winding can be used to detect the rotor position [80,81].

5.3. Development of Controllers Using Electronic Processors and Specific Circuits

The development and implementation of different control methods for BLDC motors can be carried out by using commercial processors and specific circuits. Some of the most common electronic devices applied to back-EMF sensing techniques are explained through different implementation models and examples.

5.3.1. Digital Signal Processors (DSP)

Recently, the microprocessor technology has shown incredible improvements and the operating speed of DSPs have gotten faster and faster. Complicated control algorithms can now be easily implemented in a DSP with high sampling and calculation frequency. In addition, optimal performance of BLDC machine drive cannot be achieved with a control method based on the rotor position obtained from a position sensor such as encoders or Hall sensors, which are insensitive to parameter variation [25]. The combination of advanced DSP technology and sophisticated control will yield a better sensorless BLDC drive that has higher performance than even conventional motor drives with position Hall sensors in the near future. *In position or speed sensorless control* of drives the goal is to eliminate the sensors by powerful DSP based computation using the machine terminal voltage and current signals [82].

The Field Oriented Control (FOC) technology has been developed as a way to achieve high dynamic performance drive systems. The Universal Field Oriented (UFO) controller was introduced as a generalization for decoupling techniques for flux and torque vectors. The controller basically allows for the selection of what reference frame to use for the decoupling, depending on the operating characteristics of the drive system. The third harmonic voltage component was used solely to estimate the air gap flux of the motor, and a speed sensor was used in order to implement the complete control [83]. The acquisitions of the third harmonic voltage and rotor slot ripple signals are accomplished via the analog interface presented in Figure 22.

Figure 22. DSP and analog interface used to detect the stator phase voltages sum and the rotor slot harmonic component [83].

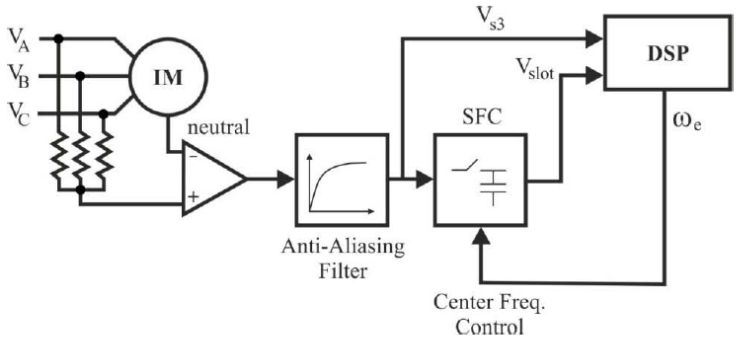

The block diagram of Figure 22 includes a DSP Texas Instruments TMS32010 [84] used to implement the control algorithms. The air gap flux and the rotor speed are detected by processing the signal obtained from the summation of the stator phase voltages, V_{s3}. The DSP performs the integration of the third harmonic voltage signal to derive the third harmonic flux. In order to detect the rotor speed the signal V_{s3} is processed by a switched capacitor band-pass filter (SCF), whose central frequency can be tuned over a wide range (from about 20 Hz to 4 kHz). *The output of the filter is a variable amplitude sinusoidal wave. This wave has the same frequency as the rotor slot ripple* [83]. Two options are to detect the frequency of the SCF output signal: a Phase Locked Loop or a frequency to voltage converter (FVC).

5.3.2. Field Programmable Gate Arrays (FPGA)

A remarkable application of DSPs or FPGAs is the sensorless control for high speed applications based on the execution of PWM control schemes, which are classified as unipolar [38] and bipolar methods [24,51]. Depending on the PWM method used the control scheme may cause a commutation delay in high speed applications since the PWM switching and the inverter commutation cannot be done independently. If the commutation instant is synchronized with the end of the PWM switching period ideal commutation occurs with any delay. But since the *commutating instant depends on the rotor position* it does not generally coincide with the end of PWM period and undesirable commutation delay is produced. This problem can be overcome by *controlling the voltage and frequency independently by DC link voltage control scheme.* This control can be implemented using a DSP or FPGA based high speed sensorless control configuration [22].

Typical high speed applications in which PWM techniques can be applied are digital video disk (DVD) spindle systems, which can be implemented using a FPGA, such as the Altera Flex EPF6024AQC240-3 [85]. The controller includes two main parts: the PWM generation circuit and the power device control circuit. Figure 23 shows the system, which consists of a FPGA, a BLDC motor, and the associated reference and sensing circuits [51]. Only terminal voltages of three phases are sampled and fed into the FPGA controller to calculate the commutation instants. This system

contributes to significant reduction of conduction losses and power consumption, which is quite essential for small power BLDCM drives powered by battery and/or with limited dissipation space.

Figure 23. Block diagram of the FPGA-based drive for DVD spindle applications [51].

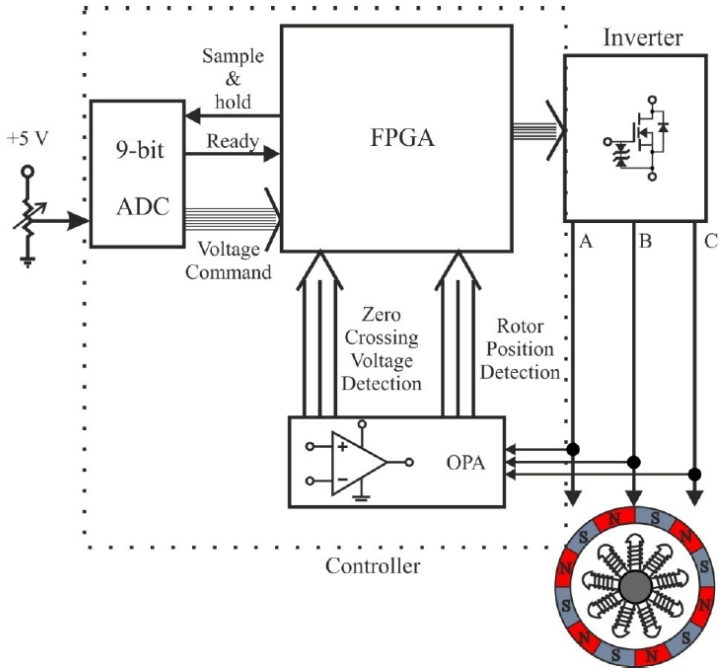

5.3.3. Microprocessors (MP)

A low-cost sensorless control scheme for BLDC motors can be implemented if rotor position information is derived by filtering only one motor-terminal-voltage, which leads to significant reduction in components count of the sensing circuit. As indicated in Figure 9, only two of the three state-windings are excited at a time, and the third phase is open during the transition periods between the positive and negative flat segments of the back-EMF [22]. Therefore, each of the motor terminal voltages contains the back-EMF information that can be used to derive the commutation instants.

Cost saving is further increased by coupling the position sensing circuit with a single-chip microprocessor or DSP for speed control. Figure 24 shows a block diagram of the position detection circuit based on sensing all three motor terminal voltages for a BLDC motor. Each of the motor terminal voltages, referred to as the negative DC bus rail V_A', V_B' and V_C' are fed into a filter through a voltage divider of a resistor network. This removes the DC component and high frequency contents that result from the PWM operation. The phase information is extracted from the back-EMF. The correction is based on measuring the elapsed time between the last two zero-crossing instants and converting it to frequency. This operation is achieved when the filtered voltage, V_A'', is passed to a comparator to detect these zero-crossing instants, which are further sent to a microprocessor for phase-delay correction and generation of commutation signals. The microprocessor produces gate control signals for the inverter and may perform closed speed control with the motor speed information measured by the frequency of the detected signals [6].

Figure 24. Block diagram of the FPGA-based drive for DVD spindle applications [6].

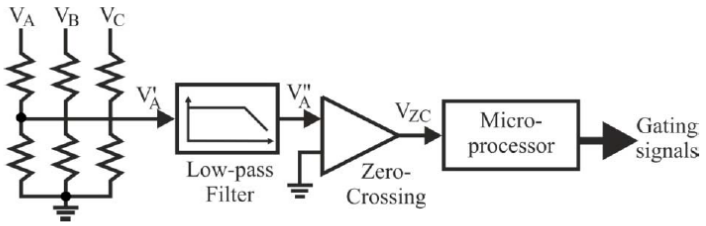

5.3.4. Microcontrollers (MC)

In recent years, with the development of mixed-signal integrated circuit technology, many system-on-chip (SOC) devices have become available. High-throughput microcontrollers with imbedded programmable memory as well as other precision analog and digital peripherals can be incorporated into a single integrated circuit. SOC devices have many advantages, including lower overall system cost and reduced board space, as well as superior system performance and reliability. Taking all these features into account, a dedicated sensorless BLDC controller implementing a back-EMF zero-crossing detection circuit as one of its peripherals, can be developed [24].

A back-EMF sensing method that requires neither a manufactured neutral voltage nor a great amount of filtering can be implemented using a microcontroller reducing the total system cost [76]. A usual microcontroller model is the ST72141 (STMicroelectronics) [50] which integrates the analog detection circuit and other motor control peripherals with a standard microcore. In this method, the true back-EMF zero crossing point can be extracted directly from the motor terminal voltage by properly choosing the PWM and sensing strategy. The motor terminal voltage is directly fed into the microcontroller through current-limiting resistors. The resulting feedback signal is not attenuated or filtered. As a result, a sensorless BLDC driver with a much wider speed range from start-up to full speed is obtained [38]. This microcontroller-based sensorless BLDC drive system could be successfully applied to automotive returnless fuel pump applications, in which a BLDC motor life span is typically around 15,000 h, extending the life of the motor almost three-fold. Once a microcontroller is used to perform the brushless commutation, other features can be incorporated into the application, such as electronic returnless, fuel system control, fuel level processing, and fuel tank pressure. These added features simplify the vehicle systems as well as drive overall system cost down.

5.3.5. Application Specific Circuits (ASIC)

Several integrated circuits have been developed to enable sensorless operation of the BLDC. These included Allegro's A8902CLBA [86] or Fairchild Semiconductor's ML4425 [87]. Each of these devices used *back-EMF methods and open-loop starting* [41].

The commercial application specific integrated circuit (ASIC) ML4425 [35] is often used for sensorless control of BLDC drives. It integrates the terminal voltage of the unenergized winding that contains the phase EMF information, and its PLL ensures that the integration result be zero. Thus, the BLDC motor can be commutated with a proper frequency and phase angle. In most cases, the ASIC provides very reliable operation, and its peripheral circuit is simple. Usually, the major problem that the ASIC encounters is the inferior starting performance as open-loop starting procedure is applied.

However, in some applications of BLDC motors, such as driving an air compressor, it requires low starting torque and the open-loop starting can be easily realized. Nevertheless, the commutation of the BLDC drive is significantly retarded during high-speed operation. This is because a relatively wide voltage pulse due to the free-wheeling diode conduction appears in the terminal voltage of the unenergized winding, and it is also integrated by the ASIC.

To overcome the problem, the ASIC should integrate the third harmonic back-EMF instead of the terminal voltage using a voltage integrator and a PLL to process the third harmonic EMF. This solution is more robust to the signal noise [17], and the power loss is reduced at high speed (*i.e.*, 120 krpm) [25].

A practical application of the ML4425 ASIC is to drive electric compressors for automotive HVAC systems. Unlike conventional vehicles that use a belt to drive air conditioner compressors, hybrid electric vehicles use an electric compressor, which is independent from the engine. Because of the requirement of sealing and cost, sensorless drive is embedded in the semi-integrated packaging compressor drive. This ASIC controller is utilized based on the terminal voltage sensing method, providing sequential commutation pulses to the inverter and, hence, *does not need a position sensor* for commutating the motor phases. The commutation is achieved by means of the PLL and speed ranges from 600 to 6,000 rpm can be reached for a 42 V automotive compressor drive [8].

6. Applications of BLDC Motor Controllers

As explained briefly in the previous sections, BLDC motors find many applications in every segment of the market, so their control techniques are very important. Automotive, appliance, industrial controls, automation, aviation and so on have applications for BLDC motors. The applications of BLDC motor control can be categorized into three major fields: constant loads, varying loads, and positioning applications [10].

6.1. Applications with Constant Loads

These are the types of applications where a variable speed is more important than keeping the accuracy at a set speed. In addition, the acceleration and deceleration rates are not dynamically changing. In these applications the load is directly coupled to the motor shaft, and this happens in fans [27], pumps, air compressors [1,28] and blowers, which demand low-cost controllers [20], mostly operating in open-loop.

A brushless DC motor built in a compressor of air conditioner is a typical application and it confirms the feasibility and the validity of some sensorless algorithms, such as a variation of the back-EMF zero crossing detection method. It is necessary to modulate the capacity of room air conditioners in proportion to the load results in energy saving and a comfortable environment. The speed of the brushless motor with a permanent magnet rotor can be easily controlled over a wide range by changing the motor voltage. Nevertheless, this type of motor needs a rotor position sensor, and this reduces the system ruggedness and complicates the motor configuration. In particular, the motor speed control and elimination of mechanical sensors are the main points of the sensorless methods, which contribute to the motor built in a completely sealed compressor and make it possible to mass produce. Mechanical sensors have low reliability in high-temperature and the need of a extra hermetic terminal of the sensor signal lead wires, and can be substituted by low-pass filters and voltage comparators [1].

An example of the Terminal Voltage Sensing algorithm can be implemented to drive an IPM BLDC motor which is in a completely sealed compressor of air conditioner. The drive works from about 500 to 7,500 rpm and at low speed, where the amplitude of back-EMF is nearly zero, taking into account that the variation of neutral voltage includes the information of rotor position [28]. Also, the control implementation of a brushless motor, which consists of a three-phase star-connected stator and a four-pole permanent magnet rotor, can be commutated using a 120-electrical-degree type inverter with a capacity of 1.5 kVA, a single-chip microcomputer and comparators [1]. This system has been used for the drive of brushless motor in compressors, and the room air conditioners that contain these control system have been mass-produced since 1982 without any particular problem since then.

6.2. Applications with Varying Loads

In these applications the load on the motor varies over a speed range and may demand high-speed control accuracy and good dynamic responses. Home appliances such as washers, dryers and refrigerators are good examples. Also, fuel pump control [38], electronic steering control, engine control and electric vehicle control [8] are examples of these in the automotive industry. In aerospace, there are a number of applications, such as centrifuges, pneumatic devices with electroactuators [3], pumps, robotic arm controls, gyroscope controls and so on. These applications may use speed feedback devices and may run in semi-closed loop or in total closed loop by using advanced control algorithms which complicates the controller and increases the price of the complete system.

The brushless DC motor is well suited for automotive returnless fuel pump applications today, because they are inherently more reliable, more efficient, and with current electronics technology, more cost effective than the standard brush-type fuel-pump motor and controller. In a returnless fuel system, the fuel pump speed is adjusted to maintain constant fuel pressure over the fuel demand/load range. It uses a sensing method that detects the true back-EMF zero crossing point, which requires neither a manufactured neutral voltage nor a great amount of filtering, and provides a wider speed range from startup to full speed. Taking into account that over the last decade, there has been a steady improvement in electronics, control algorithms, and motor technologies, BLDC motors are the preferred solution in not just automotive fuel pumps but also in a broad range of applications using adjustable speed motors, such as home appliances for compressors, air blowers, vacuum cleaners or engine cooling fans. For instance, a brush type fuel pump motor is designed to last 6,000 h, so in certain fleet vehicles this can be expended in less than one year. A BLDC motor life span is typically around 15,000 h, extending the life of the motor by almost three times. Also, because of a microcontroller is used to perform the brushless commutation other features can be incorporated into the application, such as electronic returnless fuel system control, fuel level processing, and fuel tank pressure. These added features simplify the vehicle systems as well as drive overall system cost down [38].

Another important application of BLDC motors is the aerospace field. The implementation of any new technology in the aerospace industry makes strict demands on the safety and reliability of on-board equipment. A fundamental element that drives the EHA/EMA actuator is the DC motor. Nowadays, BLDC motors are widely used, mainly because of their better characteristics and performance. In addition, the ratio of torque delivered to the size of the motor is higher, making it useful in applications where space and weight are critical factors, especially in aerospace. The

operation of an actuator is safety critical and thus the actuator requires a reliable control algorithm that ensures safe start-up and operation of the BLDC motor that drives the actuator. Intelligent EHA/EMA actuators and smart actuation systems promising technologies for future power optimised aircraft, adding important benefits in energy consumption, weight savings, easy assembly procedures and maintenance [3].

6.3. Positioning Applications

Most of the industrial and automation types of applications in this category have some kind of power transmission, which could be mechanical gears, gear pump units [4] or timer belts, or a simple belt driven system. The dynamic response of speed and torque are also important, and these applications may also have frequent reversal of rotation direction. A typical cycle will have phases of acceleration, constant speed, and deceleration and positioning. The load on the motor may vary during all of these phases, causing the controller to be complex, such as in applications with hard disk drives (HDDs) [32,79] or DVDs [48,51]. These systems mostly operate in closed loop, and there could be three control loops functioning simultaneously: torque, speed and position. *Optical encoder* or *synchronous resolvers* are used for measuring the actual speed of the motor. In some cases, the same sensors are used to get relative position information. Otherwise, separate position sensors may be used to get absolute positions. Also, computer numeric controlled machines, machines tool [39], industrial processes, and conveyer controls have plenty of applications in this category.

Hydraulic systems are commonly used in automotive applications, since they allow developing higher forces and torques compared with purely electric actuators. For example, passenger cars are equipped with hydraulically-assisted brakes, clutches and power steering systems, while in commercial vehicles hydraulic power is used to operate also lifting systems and other auxiliary machineries. If a variable speed electric motor is coupled to the hydraulic pump, a flow control valve is always necessary, and the possibility to regulate the rotational speed of the pump *i*ndependently from the engine speed allows a significant reduction of parasitic losses. However, this solution requires the design of a specific electronic controller, capable of motor speed regulation according to the hydraulic load dynamic requirements. Moreover, since the power supply of these electro-hydraulic systems must be the battery of the vehicle, to allow operation even when the engine is switched off, electric motors and power electronics must be designed for low-voltage and high-current ratings, especially in commercial vehicle applications [4]. Then, a brushless motor are the appropriate device to this purpose.

On the one hand, taking into account these considerations, the design of the electronic part of a Motor Pump Unit (MPU) is composed by a hydraulic gear pump, a permanent magnet brushless motor (chosen because of its advantages over brushed DC motors) and a power converter with a microcontroller unit, which implements the sensorless speed control scheme. For example, the key features of a MPU for commercial vehicle applications can be the following: 24 V supply, 2 kW maximum output power, 4,000 rpm maximum motor speed, 10 Nm maximum motor torque, and 150 bar maximum hydraulic pressure [4]. On the other hand, the main issues in the back-EMF zero-crossing detection method applied in the system are related to noise superimposed on both phase voltage and mid-point voltage, because of PWM modulation of the power converter and the particular

care for the implementation of start-up algorithms. A more efficient solution can be implemented if a digital controller was able to sample and digitize back-EMF measurements synchronously with PWM modulation (*i.e.*, during PWM off periods) and implement more robust zero-crossing detection algorithms [88]. Moreover, phase advance strategies will allow to extend the speed range of the motor, which could also be more easily implemented on a high-performance motor control signal processor, such as a Microchip dsPIC30F6010 Digital Signal Controller using their PWM generators and analog-to-digital converters [89].

Another important application in this category is the hard disk drives or HDDs. HDDs tend to have high spin speeds in order to reduce the access time in data reading and writing. The highest spin speed of commercial HDDs has reached 15,000 rpm and will be higher in the near future. However, for the small form factor HDDs, the back-EMF amplitudes of their spindle motors are becoming low even at the rated speed, and some methods based on the zero-crossing detection of back EMFs does not work well when the terminal voltage spikes last relatively longer at higher spin speed or the phase back- EMF amplitude is very small [32]. Recently, due to HDDs being widely used in mobile applications, the power-supply voltage has been reduced and the detection of the rotor position from the back EMF is difficult at low speed. Thus, the stable starting and acceleration to nominal operating speed, regardless of severe mechanical disturbance is the utmost concern in these applications [79]. However, since the 1970s, many methods have been developed for solving the problems in the sensorless rotor position detection, such as the back-EMF integration method or digital filtering procedures, which have been developed to identify the true and false ZCPs of phase back EMFs caused by the terminal voltage spikes due to the residual phase currents during commutations. Also, for small power applications of BLDC motor drives, such as digital video disks, due to the use of battery or/and limited space for heat dissipation, reduction of power consumption becomes one of the main concerns for the development of PWM techniques, which have been developed for controlling power devices by means of variable voltage and frequency [51].

7. Conclusions

In this paper a review of position control methods for BLDC motors has been presented. The fundamentals of various techniques have been introduced, mainly back-EMF schemes and estimators, as a useful reference for preliminary investigation of conventional methods. Advances in the position control and applications were also discussed.

To provide insight in control techniques and their benefits a classification of existing methods and newer methods were presented with their merits and drawbacks. From the above discussion, it is obvious that the control for BLDC motors using position sensors, such as shaft encoders, resolvers or Hall-effect probes, can be improved by means of the elimination of these sensors to further reduce cost and increase reliability. Furthermore, sensorless control is the only choice for some applications where those sensors cannot function reliably due to harsh environmental conditions and a higher performance is required.

Acknowledgements

This work was supported by the regional 2010 Research Project Plan of Junta de Castilla y León (Spain), reference project VA034A10-2. This work was also possible thank to the collaboration of Ernesto Vazquez-Sanchez through the Contratación de Personal Investigador de Reciente Titulación program, which was financed by Consejería de Educación of Junta de Castilla y León (Spain) and cofinanced by European Social Fund.

References and Notes

1. Iizuka, K.; Uzuhashi, H.; Kano, M.; Endo, T.; Mohri, K. Microcomputer Control for Sensorless Brushless Motor. *IEEE Trans. Ind. Appl.* **1985**, *IA-21*, 595-601.
2. Becerra, R.C.; Ehsani, M. High-Speed Torque Control of Brushless Permanent Magnet Motors. *IEEE Trans. Ind. Electron.* **1988**, *35*, 402-406.
3. Hubik, V.; Sveda, M.; Singule, V. On the Development of BLDC Motor Control Run-Up Algorithms for Aerospace Application. In *Proceedings of the 13th Power Electronics and Motion Control Conference (EPE-PEMC 2008)*, Poznan, Poland, September 2008; pp. 1620-1624.
4. Bonfe, M.; Bergo, M. A Brushless Motor Drive with Sensorless Control for Commercial Vehicle Hydraulic Pumps. In *Proceedings of the IEEE International Symposium on Industrial Electronics (ISIE 2008),* Cambridge, England, July 2008; pp. 612-617.
5. Bianchi, N.; Bolognani, S.; Jang, J.H.; Sul, S.K. Comparison of PM Motor Structures and Sensorless Control Techniques for Zero-Speed Rotor Position Detection. *IEEE Trans. Power Electron.* **2007**, *22*, 2466-2475.
6. Su, G.J.; McKeever, J.W. Low-Cost Sensorless Control of Brushless DC Motors with Improved Speed Range. *IEEE Trans. Power Electron.* **2004**, *19*, 296-302.
7. Damodharan, P.; Vasudevan, K. Indirect Back-EMF Zero Crossing Detection for Sensorless BLDC Motor Operation. In *Proceedings of the International Conference on Power Electronics and Drives Systems (PEDS 2005)*, Kuala Lumpur, Malaysia, November 2008; pp. 1107-1111.
8. Naidu, M.; Nehl, T.W.; Gopalakrishnan, S.; Wurth, L. Keeping Cool while Saving Space and Money: A Semi-Integrated, Sensorless PM Brushless Drive for a 42-V Automotive HVAC Compressor. *IEEE Ind. Appl. Mag.* **2005**, *11*, 20-28.
9. *Brushless DC Motor Control using the LPC2141 Application Note*; AN10661, NXP Semiconductors: Eindhoven, the Netherlands, October 2007.
10. *Brushless DC (BLDC) Motor Fundamentals Application Note*; AN885, Microchip: AZ, USA. 2003.
11. Burger, F.; Besse, P.A.; Popovic, R.S. New Single Chip Hall Sensor for Three Phases Brushless Motor Control. *Sens. Actuat. A-Phys.* **2000**, *81*, 320-323.
12. Bucak, I.Ö. Position Error Compensation Via a Variable Reluctance Sensor Applied to a Hybrid Vehicle Electric Machine. *Sensors* **2010**, *10*, 1918-1934.
13. Hernandez, W. Robust Multivariable Estimation of the Relevant Information Coming from a Wheel Speed Sensor and an Accelerometer Embedded in a Car Under Performance Tests. *Sensors* **2005**, *5*, 488-508.

14. Lee, D. Wireless and Powerless Sensing Node System Developed for Monitoring Motors. *Sensors* **2008**, *8*, 5005-5022.
15. *3-Phase BLDC Motor Control with Hall Sensors using 56000/E Digital Signal Controllers Application Note*; AN1916, Freescale Semiconductor: TX, USA, 2005.
16. Rajagopalan, S. *Detection of Rotor and Load Faults in Brushless DC Motors Operating Under Stationary and Non-Stationary Conditions*. Ph.D. Dissertation, Georgia Institute of Technology: Atlanta, GA, USA, August 2006.
17. Shen, J.X.; Iwasaki, S. Sensorless Control of Ultrahigh-Speed PM Brushless Motor using PLL and Third Harmonic Back EMF. *IEEE Trans. Ind. Electron.* **2006**, *53*, 421-428.
18. Shen, J.X.; Zhu, Z.Q.; Howe, D. Sensorless Flux-Weakening Control of Permanent-Magnet Brushless Machines using Third Harmonic Back EMF. *IEEE Trans. Ind. Appl.* **2004**, *40*, 1629-1636.
19. Ogasawara, S.; Akagi, H. An Approach to Position Sensorless Drive for Brushless DC Motors. *IEEE Trans. Ind. Appl.* **1991**, *27*, 928-933.
20. Lin, M.; Zhang, Z.; Lin, K. A Novel and Easy-Realizing Initial Rotor Position Detection Method and Speedup Algorithm for Sensorless BLDC Motor Drives. In *Proceedings of the International Conference on Electrical Machines and Systems (ICEMS 2008)*, Wuhan, China, October 2008; pp. 2860-2865.
21. Lee, B.K.; Kim, T.H.; Ehsani, M. On the Feasibility of Four-Switch Three-Phase BLDC Motor Drives for Low Cost Commercial Applications: Topology and Control. In *Proceedings of the Sixteenth Annual IEEE Applied Power Electronics Conference and Exposition (APEC 2001)*, Anaheim, CA, USA, March 2008; pp. 428-433; Volume 1.
22. Vinatha, U.; Pola, S.; Vittal, K.P. Recent Developments in Control Schemes of BLDC Motors. In *Proceedings of the IEEE International Conference on Industrial Technology (ICIT 2006)*, Mumbai, India, December 2006; pp. 477-482.
23. Becerra, R.C.; Jahns, T.M.; Ehsani, M. Four-Quadrant Sensorless Brushless ECM Drive. In *Proceedings of the Sixth Annual Applied Power Electronics Conference and Exposition (APEC 1991)*, Palm Springs, CA, USA, March 1991; pp. 202-209.
24. Shao, J.; Nolan, D.; Hopkins, T. A Novel Direct Back EMF Detection for Sensorless Brushless DC (BLDC) Motor Drives. In *Proceedings of the Seventeenth Annual IEEE Applied Power Electronics Conference and Exposition (APEC 2002)*, Dallas, TX, USA, March 2002; pp. 33-37; Volume 1.
25. Kim, T.; Lee, H.W.; Ehsani, M. Position Sensorless Brushless DC Motor/Generator Drives: Review and Future Trends. *IET Electr. Power Appl.* **2007**, *1*, 557-564.
26. Lin, M.; Gu, W.; Zhang, W.; Li, Q. Design of Position Detection Circuit for Sensorless Brushless DC Motor Drives. In *Proceedings of the IEEE International Electric Machines and Drives Conference (IEMDC 2007)*, Antalya, Turkey, May 2007; pp. 225-228.
27. Krishnan, R.; Lee, S. PM Brushless DC Motor Drive with a New Power-Converter Topology. *IEEE Trans. Ind. Appl.* **1997**, *33*, 973-982.
28. Yeo, H.G.; Hong, C.S.; Yoo, J.Y.; Jang, H.G.; Bae, Y.D.; Park, Y.S. Sensorless Drive for Interior Permanent Magnet Brushless DC Motors. *In Proceedings of the IEEE International Electric Machines and Drives Conference Record*, Milwaukee, WI, USA, May 1997; pp. TD1/3.1-TD1/3.3.

29. Shao, J. An Improved Microcontroller-Based Sensorless Brushless DC (BLDC) Motor Drive for Automotive Applications. *IEEE Trans. Ind. Appl.* **2006**, *42*, 1216-1221.
30. Lai, Y.S.; Lin, Y.K. Back-EMF Detection Technique of Brushless DC Motor Drives for Wide Range Control. In *Proceedings of the 32nd Annual Conference on IEEE Industrial Electronics (IECON 2006)*, Paris, France, November 2006; pp. 1006-1011.
31. Zhang, L.; Xiao, W.; Qu, W. Sensorless Control of BLDC Motors using an Improved Low-Cost Back EMF Detection Method. In *Proceedings of the 37th IEEE Power Electronics Specialists Conference (PESC 2006)*, Jeju, South Korea, June 2006; pp. 1-7.
32. Jiang, Q.; Bi, C.; Huang, R. A New Phase-Delay-Free Method to Detect Back EMF Zero-Crossing Points for Sensorless Control of Spindle Motors. *IEEE Trans. Magn.* **2005**, *41*, 2287-2294.
33. Chen, C.H.; Cheng, M.Y. A New Sensorless Commutation Drive for Brushless DC Motors and Alternators. In *Proceedings of the IEEE International Symposium on Industrial Electronics*; Montreal, Que, Canada, July 2006; pp. 2116-2121.
34. *ML4425 Sensorless BLDC Motor Controller Data Sheet*; Micro Linear: CA, USA, July 2000.
35. *Using the ML4425/ML4426 BLDC Motor Controllers Application Note*; AN42004, Fairchild Semiconductor: South Portland, ME, USA, June 1996.
36. Goetz, J.; Hu, W.; Milliken, J. Sensorless Digital Motor Controller for High Reliability Applications. In *Proceedings of the Twenty-First Annual IEEE Applied Power Electronics Conference and Exposition (APEC 2006)*, Dallas, TX, USA, March 2006; pp. 6.
37. Shao, J.; Nolan, D. Further Improvement of Direct Back EMF Detection for Sensorless Brushless DC (BLDC) Motor Drives. In *Proceedings of the Twentieth Annual IEEE Applied Power Electronics Conference and Exposition (APEC 2005)*, Austin, TX, USA, March 2005; pp. 933-937; Volume 2.
38. Shao, J.; Nolan, D.; Teissier, M.; Swanson, D. A Novel Microcontroller-Based Sensorless Brushless DC (BLDC) Motor Drive for Automotive Fuel Pumps. *IEEE Trans. Ind. Appl.* **2003**, *39*, 1734-1740.
39. Takahashi, I.; Koganezawa, T.; Su, G.; Ohyama, K. A Super High Speed PM Motor Drive System by a Quasi-Current Source Inverter. *IEEE Trans. Ind. Appl.* **1994**, *30*, 683-690.
40. Moreira, J.C. Indirect Sensing for Rotor Flux Position of Permanent Magnet AC Motors Operating Over a Wide Speed Range. *IEEE Trans. Ind. Appl.* **1996**, *32*, 1394-1401.
41. Johnson, J.P.; Ehsani, M.; Guzelgunler, Y. Review of Sensorless Methods for Brushless DC. In *Proceedings of the 1999 IEEE Industry Applications Conference (Thirty-Fourth IAS Annual Meeting)*, Phoenix, AZ, USA, October 1999; pp. 143-150; Volume 1.
42. Jufer, M.; Osseni, R. Back-EMF Indirect Detection for Self-Commutation of Synchronous Motors. In *Proceedings of the European Conference on Power Electronics and Applications (EPE 1987)*, Grenoble, France, September 1987; pp. 1125-1129.
43. Profumo, F.; Griva, G.; Pastorelli, M.; Moreira, J.; De Doncker, R. Universal Field Oriented Controller Based on Air Gap Flux Sensing Via Third Harmonic Stator Voltage. *IEEE Trans. Ind. Appl.* **1994**, *30*, 448-455.
44. Testa, A.; Consoli, A.; Coco, M.; Kreindler, L. A New Stator Voltage Third Harmonic Based Direct Field Oriented Control Scheme. In *Proceedings of the 1994 IEEE Industry Applications Society Annual Meeting*, Denver, CO, USA, October 1994; pp. 608-615; Volume 1.

45. Shen, J.X.; Iwasaki, S. Improvement of ASIC-Based Sensorless Control for Ultrahigh-Speed Brushless DC Motor Drive. In *Proceedings of the IEEE International Electric Machines and Drives Conference (IEMDC 2003)*, Madison, WI, USA, June 2003; pp. 1049-1054; Volume 2.
46. Jahns, T.M.; Becerra, R.C.; Ehsani, M. Integrated Current Regulation for a Brushless ECM Drive. *IEEE Trans. Power Electron.* **1991**, *6*, 118-126.
47. Van Hout, H.M. Brushless D.C. Motor and Switching Device for use in such a D.C. Motor. U.S. Patent 4,748,385, May 31, 1988.
48. Lai, Y.S.; Shyu, F.S.; Chang, Y.H. Novel Pulse-Width Modulation Technique with Loss Reduction for Small Power Brushless DC Motor Drives. In *Proceedings of the Industry Applications Conference (37th IAS Annual Meeting)*, Pittsburgh, PA, USA, October 2002; pp. 2057-2064; Volume 3.
49. Shao, J.; Nolan, D.; Hopkins, T. Improved Direct Back EMF Detection for Sensorless Brushless DC (BLDC) Motor Drives. In *Proceedings of the Industry Applications Conference Eighteenth Annual IEEE Applied Power Electronics Conference and Exposition (APEC 2003)*, Miami, FL, USA, February 2003; pp. 300-305; Volume 1.
50. *An Introduction to Sensorless Brushless DC Motor Drive Applications with the ST72141 Application Note*; AN1130, STMicroelectronics: Geneva, Switzerland, 2000.
51. Lai, Y.S.; Shyu, F.S.; Chang, Y.H. Novel Loss Reduction Pulsewidth Modulation Technique for Brushless DC Motor Drives Fed by MOSFET Inverter. *IEEE Trans. Power Electron.* **2004**, *19*, 1646-1652.
52. Jahns, T.M.; Soong, W.L. Pulsating Torque Minimization Techniques for Permanent Magnet AC Motor Drives-A Review. *IEEE Trans. Ind. Electron.* **1996**, *43*, 321-330.
53. Van Der Broeck, H.W.; Van Wyk, J.D. A Comparative Investigation of a Three-Phase Induction Machine Drive with a Component Minimized Voltage-Fed Inverter Under Different Control Options. *IEEE Trans. Ind. Appl.* **1984**, *IA-20*, 309-320.
54. Van der Broeck, H.W.; Skudelny, H.C. Analytical Analysis of the Harmonic Effects of a PWM AC Drive. *IEEE Trans. Power Electron.* **1988**, *3*, 216-223.
55. Blaabjerg, F.; Neacsu, D.O.; Pedersen, J.K. Adaptive SVM to Compensate DC-Link Voltage Ripple for Four-Switch Three-Phase Voltage-Source Inverters. *IEEE Trans. Power Electron.* **1999**, *14*, 743-752.
56. Luenberger, D. An Introduction to Observers. *IEEE Trans. Autom. Control* **1971**, *16*, 596-602.
57. Peixoto, Z.M.A.; Freitas Sa, F.M.; Seixas, P.F.; Menezes, B.R.; Cortizo, P.C.; Lacerda, W.S. Application of Sliding Mode Observer for Induced E.M.F., Position and Speed Estimation of Permanent Magnet Motors. In *Proceedings of the 1995 International Confererence on Power Electronics and Drive Systems (PEDS 95)*, Singapore, February 1995; pp. 599-604; Volume 2.
58. Markadeh, G.R.A.; Mousavi, S.I.; Daryabeigi, E. Position Sensorless Direct Torque Control of BLDC Motor by using Modifier. In *Proceedings of the 11th International Conference on Optimization of Electrical and Electronic Equipment, 2008 (OPTIM 2008)*, Brasov, Romania, May 2008; pp. 93-99.
59. Markadeh, G.R.A.; Hajian, M.; Soltani, J.; Hosseinia, S. Maximum Torque Per Ampere Control of Sensorless Induction Motor Drives with DC Offset and Parameter Compensation. *Energy Convers. Manage.* **2010**, *51*, 1354-1362.

60. Yang, J.; Hu, Y.; Huang, W.; Chu, J.; Gao, J. Direct Torque Control of Brushless DC Motor without Flux Linkage Observation. In *Proceedings of the IEEE 6th International Power Electronics and Motion Control Conference, 2009 (IPEMC '09)*, Wuhan, China, May 2009; pp. 1934-1937.
61. Hajian, M.; Markadeh, G.R.; Soltani, J.; Hoseinnia, S. Energy Optimized Sliding-Mode Control of Sensorless Induction Motor Drives. *Energy Convers. Manage.* **2009**, *50*, 2296-2306.
62. Zaky, M.S.; Khater, M.; Yasin, H.; Shokralla, S.S. Very Low Speed and Zero Speed Estimations of Sensorless Induction Motor Drives. *Electr. Power Syst. Res.* **2010**, *80*, 143-151.
63. Kim, Y.S.; Ahn, J.Y.; You, W.S.; Cho, K.M. A Speed Sensorless Vector Control for Brushless DC Motor using Binary Observer. In *Proceedings of the 1996 IEEE IECON 22nd International Conference on Industrial Electronics, Control, and Instrumentation*, Taipei, Taiwan, August 1996; pp. 1746-1751; volume 3.
64. Dhaouadi, R.; Mohan, N.; Norum, L. Design and Implementation of an Extended Kalman Filter for the State Estimation of a Permanent Magnet Synchronous Motor. *IEEE Trans. Power Electron.* **1991**, *6*, 491-497.
65. Barut, M. Bi Input-Extended Kalman Filter Based Estimation Technique for Speed-Sensorless Control of Induction Motors. *Energy Convers. Manage.* **2010**, *51*, 2032-2040.
66. Terzic, B.; Jadric, M. Design and Implementation of the Extended Kalman Filter for the Speed and Rotor Position Estimation of Brushless DC Motor. *IEEE Trans. Ind. Electron.* **2001**, *48*, 1065-1073.
67. Kojabadi, H.M. Active Power and MRAS Based Rotor Resistance Identification of an IM Drive. *Simulat. Pract. Theory* **2009**, *17*, 376-389.
68. Maiti, S.; Chakraborty, C. A New Instantaneous Reactive Power Based MRAS for Sensorless Induction Motor Drive. *Simulat. Pract. Theory* **2010**, In Press.
69. Maes, J.; Melkebeek, J.A. Speed-Sensorless Direct Torque Control of Induction Motors using an Adaptive Flux Observer. *IEEE Trans. Ind. Appl.* **2000**, *36*, 778-785.
70. Lin, Y.N.; Chen, C.L. Adaptive Pseudoreduced-Order Flux Observer for Speed Sensorless Field-Oriented Control of IM. *IEEE Trans. Ind. Electron.* **1999**, *46*, 1042-1045.
71. Kojabadi, H.M.; Chang, L. Model Reference Adaptive System Pseudoreduced-Order Flux Observer for very Low Speed and Zero Speed Estimation in Sensorless Induction Motor Drives. In *Proceedings of the 2002 IEEE 33rd Annual Power Electronics Specialists Conference (PESC '02)*, Madison, WI, USA, November 2002; pp. 301-305; Volume 1.
72. Kojabadi, H.M.; Chang, L. Comparative Study of Pole Placement Methods in Adaptive Flux Observers. *Control Eng. Pract.* **2005**, *13*, 749-757.
73. Bose, B.K. Fuzzy Logic and Neural Networks in Power Electronics and Drives. *IEEE Ind. Appl. Mag.* **2000**, *6*, 57-63.
74. Bose, B.K. Expert System, Fuzzy Logic, and Neural Network Applications in Power Electronics and Motion Control. *Proc. IEEE* **1994**, *82*, 1303-1323.
75. Karanayil, B.; Rahman, M.F.; Grantham, C. Online Stator and Rotor Resistance Estimation Scheme using Artificial Neural Networks for Vector Controlled Speed Sensorless Induction Motor Drive. *IEEE Trans. Ind. Electron.* **2007**, *54*, 167-176.
76. Bourgeois, J.M.; Charreton, J.M.; Guillemin, P.; Maurice, B. Control of a Brushless Motor. U.S. Patent 5,859,520, January 12, 1999.

77. Kim, T.H.; Ehsani, M. Sensorless Control of the BLDC Motors from Near-Zero to High Speeds. *IEEE Trans. Power Electron.* **2004**, *19*, 1635-1645.
78. Jang, G.H.; Park, J.H.; Chang, J.H. Position Detection and Start-Up Algorithm of a Rotor in a Sensorless BLDC Motor Utilising Inductance Variation. *IEEE Proc.-Electr. Power Appl.* **2002**, *149*, 137-142.
79. Lee, W.J.; Sul, S.K. A New Starting Method of BLDC Motors without Position Sensor. *IEEE Trans. Ind. Appl.* **2006**, *42*, 1532-1538.
80. Schmidt, P.B.; Gasperi, M.L.; Ray, G.; Wijenayake, A.H. Initial Rotor Angle Detection of a Non-Salient Pole Permanent Magnet Synchronous Machine. In *Proceedings of the 1997 IEEE Industry Applications Conference (Thirty-Second IAS Annual Meeting)*, New Orleans, LA, USA, October 1997; pp. 459-463; Volume 1.
81. Chang, Y.C.; Tzou, Y.Y. A New Sensorless Starting Method for Brushless DC Motors without Reversing Rotation. In *Proceedings of the IEEE Power Electronics Specialists Conference (PESC 2007)*, Orlando, FL, USA, June 2007; pp. 619-624.
82. Bose, B.K. Technology Advancement and Trends in Power Electronics. In *Proceedings of the 29th Annual Conference of the IEEE Industrial Electronics Society (IECON 2003)*, Roanoke, VA, USA; pp. 3019-3020; Volume 3.
83. Profumo, F.; Griva, G.; Pastorelli, M.; Moreira, J. Universal Field Oriented Controller with Indirect Speed Sensing Based on the Saturation Third Harmonic Voltage. In *Proceedings of the 24th Annual IEEE Power Electronics Specialists Conference (PESC 1993),* Seattle, WA, USA, June 1993; pp. 948-955.
84. *TMS320 Second-Generation Digital Signal Processors Data Sheet*; Texas Instruments: Dallas, TX, USA, 1990.
85. *FLEX 6000 Programmable Logic Device Family Data Sheet*; Altera: San Jose, CA, USA, March 2001.
86. *8902-A 3-Phase Brushless DC Motor Controller/Driver with Back-EMF Sensing Data Sheet*; Allegro Microsystems: Worcester, MA, USA, 1995.
87. *ML4425 Sensorless BLDC Motor Controller Data Sheet*; Fairchild Semiconductor: South Portland, ME, USA, 2001.
88. Shao, J. *Direct Back EMF Detection Method for Sensorless Brushless DC (BLDC) Motor Drives*. Ph.D. Dissertation, Faculty of the Virginia Polytechnic Institute and the State University: Blacksburg, VA, USA, September 2003.
89. *Using the dsPIC30F for Sensorless BLDC Control Application Note*; *AN901*; Microchip Technology: Chandler, AZ, USA, August 2004.

Capítulo 3: Artículo 2 del compendio

En este capítulo se analiza el segundo artículo del compendio, el cual incluye el desarrollo de una técnica *sensorless* de estimación de la posición y velocidad para motores *brushed* DC (BDC) basada en el reconocimiento de patrones con clasificadores *Support Vector Machine* (SVM), utilizando solamente la corriente del motor. En este capítulo se incluye la información bibliográfica del artículo y su resumen, así como otros datos y análisis referidos al ámbito, motivación y originalidad del mismo. Al final del capítulo se incluye el extracto del artículo publicado en la revista *IEEE Transactions on Industrial Electronics* en marzo de 2012.

3.1 Datos bibliográficos

TITULO: A New Method for Sensorless Estimation of the Speed and Position in Brushed DC Motors Using Support Vector Machines.

AUTORES: Ernesto Vázquez Sánchez, Jaime Gómez Gil, José Carlos Gamazo Real, José Fernando Díez Higuera.

REVISTA: IEEE Transactions on Industrial Electronics.

EDITOR: IEEE, Institute of Electrical and Electronics Engineers (Raleigh, NC, EE.UU.).

FECHA PUBLICACIÓN: 3 de marzo de 2012.

ISSN: 0278-0046.

DOI: 10.1109/TIE.2011.2161651.

VOLUMEN: 59.

NÚMERO: 3.

PÁGINAS: 1397-1408.

REFERENCIA: [38]

3.2 Resumen

La obtención de la información de posición y velocidad en motores BDC puede realizarse mediante la utilización de sensores mecánicos acoplados al eje del motor o empleando técnicas *sensorless*. Estas técnicas pueden clasificarse en dos grupos según están basadas en el modelo dinámico del motor o en la componente *ripple* de la corriente. En la nueva técnica *sensorless* de estimación de la posición y velocidad presentada en este artículo se aplica el reconocimiento de patrones con clasificadores SVM a la medida de los pulsos u ondulaciones de la componente *ripple* de corriente. De esta forma, la velocidad del motor se estima a partir del inverso de la distancia entre los pulsos detectados, y la posición se obtiene contando el número de pulsos. La principal ventaja de la técnica desarrollada sobre otras técnicas *sensorless* es la capacidad para detectar pulsos fantasmas y descartar pulsos falsos. Finalmente, los *tests* realizados en dos motores fraccionales BDC indican que la técnica funciona correctamente en un amplio rango de velocidades y condiciones de operación, en las cuales la velocidad se mantiene constante o se varía dinámicamente.

3.3 Fundamentos de los clasificadores SVM

El fundamento principal del artículo incluido en este artículo está en los clasificadores SVM, y por ello es interesante exponer de forma clara los fundamentos de los mismos.

Las máquinas de vectores de soporte o SVM tienen su origen en los trabajos sobre la teoría del aprendizaje estadístico y fueron introducidas en los años 90 por Vapnik y sus colaboradores, siendo pensadas originalmente para resolver problemas de clasificación binaria, sin embargo se suelen aplicar a la resolución de tareas tanto de clasificación como de regresión. Dentro de las tareas de clasificación, los SVMs pertenecen a la categoría de los **clasificadores lineales**, puesto que inducen separadores lineales o **hiperplanos**, ya sea en el espacio original de los ejemplos de entrada, si éstos son separables o cuasi-separables (ruido), o en un espacio transformado (espacio de características), si los ejemplos no son separables linealmente en el espacio original.

Mientras la mayoría de los métodos de aprendizaje se centran en minimizar los errores cometidos por el modelo generado a partir de los ejemplos de entrenamiento, el sesgo asociado a los SVM radica en la minimización del denominado "riesgo estructural". La idea es seleccionar un hiperplano de separación que equidista de los ejemplos más cercanos de cada clase para, de esta forma, conseguir lo que se denomina un margen máximo a cada lado del hiperplano. Además, a la hora de definir el hiperplano, sólo se consideran los ejemplos de entrenamiento de cada clase que caen justo en la frontera de dichos márgenes, recibiendo estos ejemplos el nombre de **vectores soporte**. Desde un punto de vista práctico, el hiperplano separador de margen máximo ha demostrado tener una buena capacidad de generalización, evitando en gran medida el problema del sobreajuste a los ejemplos de entrenamiento. Desde un punto de

vista algorítmico, el problema de optimización del margen geométrico representa un **problema de optimización cuadrático con restricciones lineales** que puede ser resuelto mediante técnicas estándar de programación cuadrática. El hiperplano que permite separar los ejemplos no es único, puesto que existen infinitos hiperplanos separables, representados por todos aquellos hiperplanos que son capaces de cumplir las restricciones impuestas. De esta forma, se hace necesario el establecimiento de un criterio para definir un hiperplano de separación óptimo, y para ello se define el "margen de un hiperplano de separación" como la mínima distancia entre dicho hiperplano y el ejemplo más cercano de cualquiera de las dos clases [100]. En la Figura 9 se aprecia el concepto de margen de un hiperplano, y las clases se identifican como "Clase Negativa" y "Clase Positiva" [38]. De esta forma, un hiperplano de separación se denomina óptimo si su margen es de tamaño máximo, y una de sus propiedades es que equidista del ejemplo más cercano de cada clase, tal y como se aprecia en la figura indicada.

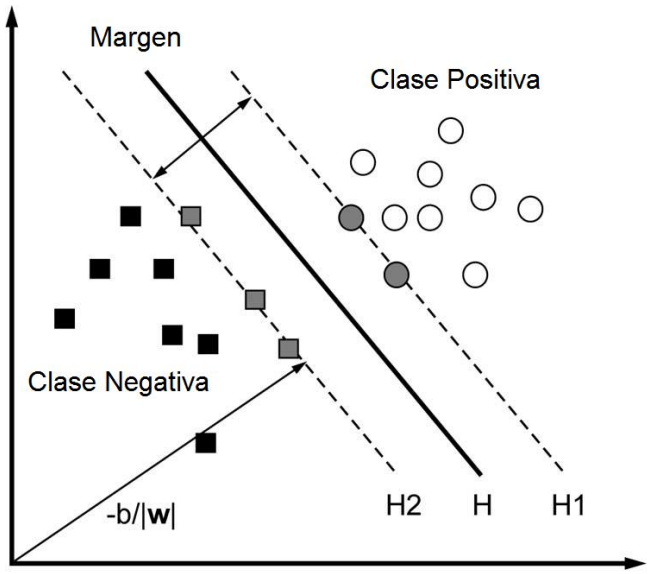

Figura 9. Separación de dos clases por un hiperplano en un SVM [38].

3.4 Ámbito

Dentro de la revista indicada este artículo pertenece a las temáticas *Power, Energy & Industry Applications* y *Signal Processing & Analysis*, y en la cual tienen cabida artículos que incluyan aplicaciones de electrónica, controles y comunicaciones, instrumentación e inteligencia computacional para la mejora de procesos y sistemas industriales [101].

El interés de este artículo dentro del ámbito de la revista se debe a la técnica que propone para medir la posición y velocidad en motores BDC utilizando la información de corriente del motor, la cual presenta ciertas ventajas para ser utilizada en entornos industriales o en aplicaciones de precisión debido a su efecto de minimización del ruido sobre las señales procesadas. Con el uso de reconocimiento de patrones con

clasificadores para el procesamiento de la corriente, la técnica *sensorless* desarrollada funciona en un amplio rango de velocidades y en diferentes condiciones de operación, como en las que hay una variación lineal o un salto salto abrupto de la velocidad, y las cuales han sido validadas en el artículo con resultados experimentales (páginas 1405-1407). Como se ha indicado, la técnica presenta una buena inmunidad al ruido, lo cual es interesante en aplicaciones industriales puesto que reduce el efecto de las fuentes de ruido y perturbaciones, al ser éstas las responsables de generar pulsos falsos o pulsos dobles en la corriente, y pulsos fantasmas como resultado de la combinación o mezcla de pulsos.

3.5 Justificación en el marco de la tesis

La técnica *sensorless* incluida en este trabajo se encuadra dentro de la **Etapa 4 de la metodología** y permite alcanzar el **Objetivo 3** de la tesis. Este objetivo considera el desarrollo de una técnica *sensorless* para motores BDC basada en la componente *ripple* de la corriente utilizando reconocimiento de patrones estadísticos y en la que se minimice el efecto del ruido. A partir de lo indicado en el objetivo, se deduce que para reducir el impacto del ruido la técnica debe ser capaz de detectar tanto las ondulaciones normales en la corriente del motor como las ondulaciones fantasmas, y además descartar las ondulaciones falsas. Para realizar la detección de las ondulaciones que aparecen en la corriente se ha utilizado un sistema de reconocimiento de patrones con el clasificador SVM. Cabe destacar que las ondulaciones fantasmas y las falsas ondulaciones aparecen mayoritariamente en la corriente cuando la velocidad del motor cambia bruscamente, lo cual ha sido probado en el *test* "*speed step*" incluido en el artículo, lográndose en éste unos resultados aceptables en la detección de la posición y velocidad del motor, debido a la adecuada detección de ondulaciones fantasmas y descarte de las ondulaciones falsas. Además, se ha utilizado un sensor de posición de tipo *encoder* incremental con el fin de evaluar el rendimiento de la técnica en motores reales. A partir de estas consideraciones, se puede decir que la técnica desarrollada cumple con el Objetivo 3 propuesto.

Este artículo se realizó con el fin de desarrollar una técnica *sensorless* de detección de la posición y velocidad para motores BDC más avanzada que la presentada en la **patente ES 2334551 A1** [37] para estos motores, pero partiendo de algunos de los conocimientos adquiridos a partir de la técnica incluida en ésta. En este sentido, al igual que en la patente, se desarrolla una técnica basada en la componente *ripple* de la corriente que circula por el motor, pero en este caso con una cierta originalidad y carácter innovador debido a la utilización de reconocimiento de patrones para detectar los pulsos en la corriente y emplear el clasificador SVM para identificarlos. En esta identificación de los pulsos, la técnica filtra, normaliza y obtiene las características más importantes de la corriente del motor, y con el clasificador SVM se decide en cada instante si se ha producido un pulso o no. Algunos trabajos representativos en los que se incluyen técnicas *sensorless* básicas basadas en la componente *ripple* son los realizados

por Ma y Weiss [102], por Iott y Burke [41] o Micke *et al.* [86], en los cuales se realiza la estimación de velocidad y posición detectando solamente variaciones instantáneas de la corriente del motor. Sin embargo, otros autores como Kessler y Schulter [52] o Lutter y Fiedrich [53] ya consideran relevante la información proporcionada por los pulsos fantasmas, los cuales pertenecen a la componente *ripple* y es el ruido el que los enmascara, pero en las técnicas que proponen se pueden producir errores en la detección de los mismos. Por ello, en el artículo propuesto se realiza de forma eficiente la detección de estos pulsos, con el fin de extraer la máxima información de la componente *ripple* y minimizar el efecto del ruido sobre la precisión.

3.6 Extracto de la publicación

A continuación se incluye el artículo 2 del compendio tal y como aparece publicado en la revista *IEEE Transactions on Industrial Electronics.*

IEEE TRANSACTIONS ON INDUSTRIAL ELECTRONICS, VOL. 59, NO. 3, MARCH 2012 1397

A New Method for Sensorless Estimation of the Speed and Position in Brushed DC Motors Using Support Vector Machines

Ernesto Vázquez-Sánchez, Jaime Gómez-Gil, José Carlos Gamazo-Real, and José Fernando Díez-Higuera

***Abstract*—Currently, for many applications, it is necessary to know the speed and position of motors. This can be achieved using mechanical sensors coupled to the motor shaft or using sensorless techniques. The sensorless techniques in brushed dc motors can be classified into two types: 1) techniques based on the dynamic brushed dc motor model and 2) techniques based on the ripple component of the current. This paper presents a new method, based on the ripple component, for speed and position estimation in brushed dc motors, using support vector machines. The proposed method only measures the current and detects the pulses in this signal. The motor speed is estimated by using the inverse distance between the detected pulses, and the position is estimated by counting all detected pulses. The ability to detect ghost pulses and to discard false pulses is the main advantage of this method over other sensorless methods. The performed tests on two fractional horsepower brushed dc motors indicate that the method works correctly in a wide range of speeds and situations, in which the speed is constant or varies dynamically.**

***Index Terms*—Brushed dc motor, current ripple, dc motor, pattern recognition, position, sensorless, speed, support vector machines (SVMs).**

I. INTRODUCTION

SENSORLESS techniques estimate the speed and position of motors without mechanical sensors coupled to the motor shaft, measuring only the current and/or the voltage of the motors. Sensorless techniques are not a recent idea, as is evidenced by the work of Allured and Strzelewigz [1]. Nevertheless, due to the complexity of these methods, they have not yet replaced conventional sensors such as encoders, potentiometers, tachometers, Hall effect sensors, or other mechanical sensors coupled to the motor shaft. The main advantages of these, compared to conventional sensors, are as follows: 1) decreased maintenance, number of connections, and cost of the final system and 2) an easier miniaturization process. In addition, mechanical elements are not coupled to the motor shaft in sensorless techniques. Sensorless techniques are particularly useful in fractional horsepower applications because they usually require a low cost and a low hardware complexity. Sensorless techniques function by monitoring the voltage and/or current of the motor to estimate the speed and position. The problem with the implementation of sensorless techniques is software complexity, since the models used and the noise in the current and voltage make it difficult to estimate the velocity and position of the motor [2].

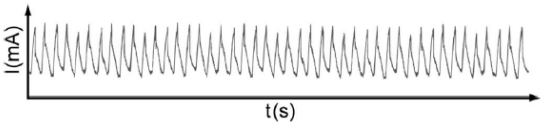

Fig. 1. Current of a brushed dc motor.

Sensorless techniques in brushed dc motors can be divided into two groups: 1) those based on the dynamic dc motor model and 2) those based on the ripple component of the motor current [3]. The first group is mainly employed to estimate the speed using the dynamic model of the brushed dc motor [4]–[9]. The dynamic model uses different parameters of the brushed dc motor such as resistance, inductance, and constant electromotive force (EMF). The problem with using the parameters of the brushed dc motor is that they depend on the operating conditions, which are changing and introduce uncertainty into the speed measurement. Although these parameters can be estimated dynamically [10], [11], this solution usually leads to a nonlinear model that increases the computational cost.

Sensorless techniques based on the ripple component only monitor the brushed dc motor current and they estimate speed and position with instantaneous variations of the current [12]–[16]. The current of a brushed dc motor, shown in Fig. 1, is mainly composed of two components: the dc component and the ripple component. The dc component is responsible for providing power to the brushed dc motor. The ripple component is an alternating component and is the direct result of two effects. The first effect is the nonideal rectification that occurs in the complex brush-commutator system that connects the rotor with the external circuit. The second effect appears in the coil of the motor and is an EMF induction, with an approximately sinusoidal shape not rectified ideally by the mechanical switching system.

Manuscript received June 1, 2010; revised September 24, 2010, February 18, 2011, March 28, 2011, and May 27, 2011; accepted June 18, 2011. Date of publication July 14, 2011; date of current version October 25, 2011. This work was supported by the Regional 2010 Research Project Plan of Junta de Castilla y León (Spain), under VA034A10-2 Project. The work of E. Vazquez-Sanchez was supported by a grant from the *Contratación de Personal Investigador de Reciente Titulación* program, which was financed by Consejería de Educación of Junta de Castilla y León (Spain) and cofinanced by the European Social Fund.

E. Vázquez-Sánchez, J. Gómez-Gil, and J. F. Díez-Higuera are with the Department of Signal Theory, Communications and Telematics Engineering, University of Valladolid, 47011 Valladolid, Spain (e-mail: ernesto.vazquez@uva.es; rnstvaz@gmail.com; jgomez@tel.uva.es; josdie@tel.uva.es).

J. C. Gamazo-Real is with the Test Facilities Department, EADS-CASA Cassidian, 28906 Madrid, Spain.

Digital Object Identifier 10.1109/TIE.2011.2161651

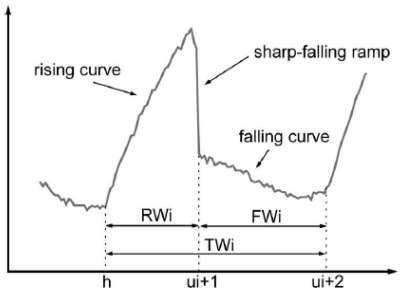

Fig. 2. Enlargement of the current of a brushed dc motor [17].

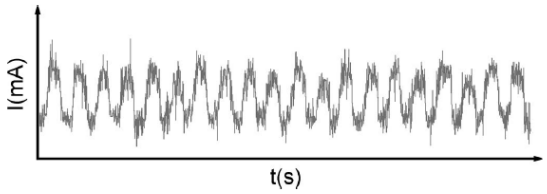

Fig. 3. Enlargement of the real current of a brushed dc motor.

Fig. 2 shows the magnification of the current signal representation of the brushed dc motor current. As this figure illustrates, the ripple component is not a sinusoidal signal but has a rise RWi, a steep fall, and another slight fall FWi [17]. Usually, those three sections of the current are not as clear, and sharp drops may not be visible in these situations. Either way, the shape of the ripple component shown in Fig. 2 is ideal, and in this figure, it is assumed that the bandwidth used for the display of the same is sufficiently high. This shape (Fig. 2) is known as an undulation, a pulse, or a commutation. The pulses that appear in the current graph are associated with the brush connection change of the commutator bar in the commutator. In this instant, the coil is short circuited. This action is also related to the instant when the EMF induced in the coil, which is connected to both commutator bars where they produce switching, is zero [18]. Thus, it is possible to measure the movement of a shaft by taking into account the number of pulses over the current signal of the brushed dc motor. In addition, if the time is monitored, the speed can be measured.

Fig. 2 shows an ideal situation without noise, but in practice, the current signal over a brushed dc motor is similar to that in Fig. 3. There are multiple noise types such as that added by the dc motor itself, that associated to the power supply, or those induced by other nearby elements. The noise sources or disturbances sometimes cause the following: 1) false pulses or double pulses in the current and 2) ghost pulses or merging pulses in the current. The false pulses are pulses that appear in the current resulting from noise and do not belong to the ripple component. The ghost pulses are pulses that belong to the ripple component, but the noise masks them in the current [19]. At a low speed, the noise becomes ever more important because the amplitude of the ripple component is smaller, and can be comparable to the noise present in the current. Consequently, to implement an effective system, it is necessary to detect false and ghost pulses. Next, the false pulses must be discarded, and the ghost pulses must be taken into account as a regular pulse ripple. This is necessary in applications where there is great amount of noise, such as noisy industrial applications, or where precision is important, such as robotic applications.

This paper proposes a method based on pattern recognition techniques to detect the pulses of the current of a brushed dc motor and, with this information, to estimate the speed and position of the brushed dc motor. Brushed dc motors are dc motors that have a mechanical commutator. Also, the proposed method is able to detect ghost pulses and to discard false pulses. The classifier support vector machine (SVM) is used for two reasons: First, it has the ability to generalize, and second, it is free of the overfitting problem [20].

In pulse detection systems for estimating speed and position, it is necessary to establish the pulse start time. Some works establish this pulse start time as the instant that the current crosses the mean current value [21]. In the proposed method, the researchers consider the pulse start time to be when the current reaches its maximum value.

Finally, this paper will evaluate the accuracy of the proposed method. Accuracy is measured by comparing the speed and the position estimated by the method with the real speed and real position collected using a high-resolution encoder.

The procedure and tests are described in more details in the following sections. Section II presents the basic theory of SVM for classification. Section III presents the proposed method and algorithm for the training method. Section IV presents a comparison of the proposed method with others used in scientific literature. Section V presents different tests to measure the accuracy and the results obtained. Finally, Section VI presents the conclusions derived from this research.

II. SVMs for Classification

SVM theory was initially developed by Vapnik [22]. It is a learning machine based on statistical theory and is used for classification and regression. Unlike traditional learning approaches, which are based on empirical risk minimization, SVM is based on structural risk minimization (SRM). The SRM principle improves the generalization ability and avoids the problem of overfitting [20].

Taylor and Cristianini [23] and Abe [24] reviewed the SVM theory. SVM is a linear classifier that establishes a hyperplane to separate two classes. This hyperplane maximizes the margin.

Given a training set or training samples $\{\boldsymbol{x}_i, y_i\}$ with $i = 1, 2, \ldots, M$, where $\boldsymbol{x}_i$ denotes the d-dimensional column vectors that are the classifier inputs, y_i denotes the class labels that are the classifier outputs and can be $+1$ or -1 to $Class + 1$ and $Class - 1$, respectively, and M is the size of the training set, the linear function that separates both classes is

$$D(\boldsymbol{x}) = \text{sign}\left(f(\boldsymbol{x})\right) \tag{1}$$

$$f(\boldsymbol{x}) = \boldsymbol{w}^{\mathrm{T}}\boldsymbol{x} + b \tag{2}$$

where $\boldsymbol{w}$ is a d-dimensional column vector which has the same dimension as the $\boldsymbol{x}$ column vector, b is a scalar, $\text{sign}(\cdot)$ is the

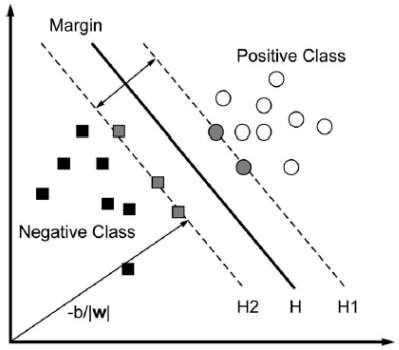

Fig. 4. Separation of two classes by an SVM.

sign function, the operator $(\cdot)^{\mathrm{T}}$ is the transpose operator, and $D(\boldsymbol{x})$ returns the label of the class that is classified $\boldsymbol{x}$. The hyperplane that separates both classes is given by $f(\boldsymbol{x}) = 0$. So, vector $\boldsymbol{w}$ and scalar b determine the position of the separating hyperplane, $\boldsymbol{w}$ determines the orientation, and b determines the hyperplane separation to the origin reference. When the training set is linearly separable, (3) must be met, and samples of the training set will be correctly classified

$$y_i f(\boldsymbol{x}_i) \geq 1 \qquad \forall\, i = 1, 2, \ldots, M. \tag{3}$$

The hyperplane that has the maximum distance between itself and the closest samples is the maximum margin hyperplane, called the optimal separating hyperplane. The classifier with the optimal hyperplane is the classifier with the greatest generalization ability. To find the optimal hyperplane, it is convenient to use three parallel hyperplanes H, H_1, and H_2 (see Fig. 4), such that

$$H : f(\boldsymbol{x}) = \boldsymbol{w}^{\mathrm{T}}\boldsymbol{x} + b = 0 \tag{4}$$

$$H_1 : f(\boldsymbol{x}) = \boldsymbol{w}^{\mathrm{T}}\boldsymbol{x} + b = +1 \tag{5}$$

$$H_2 : f(\boldsymbol{x}) = \boldsymbol{w}^{\mathrm{T}}\boldsymbol{x} + b = -1. \tag{6}$$

The hyperplanes H_1 and H_2 must contain some training samples. These training samples are known as support vectors and contain all the necessary information to build the classifier hyperplane. The distance between H_1 and H_2 is called the margin and is $2/\|\boldsymbol{w}\|$. Thus, finding the hyperplane with the maximal margin is equivalent to minimizing the following function:

$$L(\boldsymbol{w}) = \|\boldsymbol{w}\|^2/2 \tag{7}$$

also taking into account the constraint (3). This function can be minimized using the Lagrange multipliers. Then, the problem becomes to minimize (8) with respect to $\boldsymbol{w}$ and b and to maximize (8) with respect to $\boldsymbol{\alpha}$, where $\boldsymbol{\alpha}$ denotes the Lagrange multipliers

$$L(\boldsymbol{w}, b, \boldsymbol{\alpha}) = \|\boldsymbol{w}\|^2/2 - \sum_{i=1}^{M} \alpha_i \left(y_i(\boldsymbol{w}^{\mathrm{T}}\boldsymbol{x}_i + b) - 1\right). \tag{8}$$

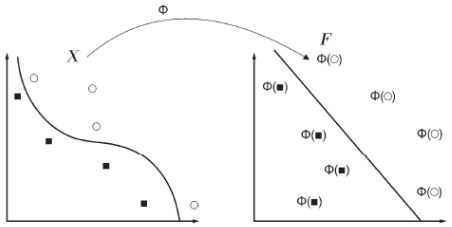

Fig. 5. Nonlinear transformation from input space to high-dimensional feature space.

TABLE I
STANDARD KERNEL FUNCTIONS

Kernel function	$K(\boldsymbol{x}_i, \boldsymbol{x}_j)$
Linear	$\boldsymbol{x}_i^T \cdot \boldsymbol{x}_j$
Polynomial	$\left(\boldsymbol{x}_i^T \cdot \boldsymbol{x}_j + 1\right)^d, d > 0$
Gaussian RBF	$\exp\left(-\|\boldsymbol{x}_i - \boldsymbol{x}_j\|^2/2\sigma^2\right)$
Sigmoid	$\tanh\left(\gamma \boldsymbol{x}_i^T \cdot \boldsymbol{x}_j + r\right)$

This problem must satisfy the Karush–Kuhn–Tuker (KKT) conditions, which are

$$\partial L(\boldsymbol{w}, b, \boldsymbol{\alpha})/\partial \boldsymbol{w} = \boldsymbol{w} - \sum_{i=1}^{M} \alpha_i y_i \boldsymbol{x}_i = 0 \tag{9}$$

$$\partial L(\boldsymbol{w}, b, \boldsymbol{\alpha})/\partial b = -\sum_{i=1}^{M} \alpha_i y_i = 0 \tag{10}$$

$$\alpha_i \left[y_i(\boldsymbol{w}^{\mathrm{T}}\boldsymbol{x}_i + b) - 1\right] = 0 \qquad \forall\, i = 1, 2, \ldots, M \tag{11}$$

$$\alpha_i \geq 0 \qquad \forall\, i = 1, 2, \ldots, M. \tag{12}$$

Substitution of the KKT conditions into (8) gives the dual problem

$$L_{\mathrm{dual}}(\boldsymbol{\alpha}) = \sum_{i=1}^{M} \alpha_i - \frac{1}{2}\sum_{i=1}^{M}\sum_{j=1}^{M} \alpha_i \alpha_j y_i y_j \boldsymbol{x}_i^{\mathrm{T}} \boldsymbol{x}_j \tag{13}$$

with the following restrictions:

$$\sum_{i=1}^{M} \alpha_i y_i = 0 \tag{14}$$

$$\alpha_i \geq 0 \qquad \forall\, i = 1, 2, \ldots, M. \tag{15}$$

Substituting (9) into (2) gives the dual form of the decision function of the following classifier:

$$f(\boldsymbol{x}) = \sum_{i=1}^{M} \alpha_i y_i \boldsymbol{x}_i^{\mathrm{T}} \boldsymbol{x} + b. \tag{16}$$

When classes are not linearly separable, the samples are transformed into a high-dimensional space, where the linear class separation is possible. The data transformation is accomplished via function $\varphi(\cdot)$, which takes the data from the input space to a feature space where classes are linearly separable. An example is shown in Fig. 5. The inner product of

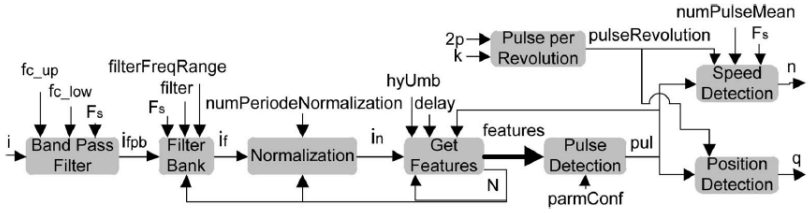

Fig. 6. Block diagram of the proposed method.

two transformed samples is replaced by the kernel function $K(\boldsymbol{x}_i, \boldsymbol{x}_j) = \phi^{\mathrm{T}}(\boldsymbol{x}_i)\phi(\boldsymbol{x}_j)$. Then, the problem given by (13) and (16) becomes

$$L_{\mathrm{dual}}(\boldsymbol{\alpha}) = \sum_{i=1}^{M} \alpha_i - \frac{1}{2} \sum_{i=1}^{M} \sum_{j=1}^{M} \alpha_i \alpha_j y_i y_j K(\boldsymbol{x}_i, \boldsymbol{x}_j) \tag{17}$$

$$f(\boldsymbol{x}) = \sum_{i=1}^{M} \alpha_i y_i K(\boldsymbol{x}_i, \boldsymbol{x}) + b \tag{18}$$

respectively.

In general, the function $\varphi(\cdot)$ is not necessary and may not be known because the kernel function is used instead. The kernel functions represent a valid inner product when they meet the Mercer conditions. The standard kernel functions are shown in Table I.

In previous ideal conditions, it was assumed that classes were separable, and therefore, (3) was always satisfied in the feature space. In real problems, however, it is not always true, and it is necessary to introduce some loss variables ξ_i. In this case, (3) becomes

$$y_i f(\boldsymbol{x}_i) \geq 1 - \xi_i \qquad \forall\, i = 1, 2, \ldots, M. \tag{19}$$

The function to optimize in this case is

$$L(\boldsymbol{w}) = \|\boldsymbol{w}\|^2/2 + C \sum_{i=1}^{M} \xi_i \tag{20}$$

where C is a penalty factor. When solving this optimization problem, the same dual problem appears as did in (13), but now subject to the following restrictions:

$$\sum_{i=1}^{M} \alpha_i y_i = 0 \tag{21}$$

$$0 \leq \alpha_i \leq C \qquad \forall\, i = 1, 2, \ldots, M. \tag{22}$$

The resolution of (13) subject to restrictions (21) and (22) is known as SVM classifier training. The training is carried out using samples of the training set in order for α_i and b to solve the dual problem. There are different training algorithms, but the most popular is sequential minimal optimization (SMO) [25].

III. Proposed Method

The main objective of this paper is to propose a new method for sensorless estimation of speed and position based on the ripple component in brushed dc motors. This method should obtain the pulse of the current, discard false pulses, and detect ghost pulses. It is based on pattern recognition techniques used to detect the pulse of the current with an SVM classifier.

This section explains the proposed method and the procedure to train the method. The method uses an SVM classifier, which needs to be trained.

A. Method

Fig. 6 shows the block diagram of the proposed method. The vertical arrows in this figure are the parameters, and the horizontal arrows are the processed data. The method processes the digitized samples of the current of a brushed dc motor and consists of the next eight blocks.

1) Bandpass Filter Block: This block filters the noise of the brushed dc motor outside the range of possible ripple frequencies. It is composed of a passband filter. The lower cutoff frequency f_{c_low} is lower than the lowest ripple frequency. The upper cutoff frequency f_{c_up} is greater than the highest ripple frequency. The parameters of this block are f_{c_low}, f_{c_up}, and F_s. The parameter F_s is the sampling frequency of the system, and it is necessary because the filter is digital (see Fig. 6).

In practice, the filter of this block is usually complemented with an antialiasing filter that operates before the A/D converter stage. In this situation, this block can sometimes be eliminated and substituted by this antialiasing filter.

The pulse width modulation (PWM) signal sometimes used to supply brushed dc motors can be considered noise. This noise can be filtered by the *Bandpass Filter Block* if the frequency of the PWM signal does not match the possible frequency ripple. Thus, the frequency of the PWM signal should be set higher than the maximum ripple frequency so that it can be filtered correctly.

2) Filter Bank Block: The *Filter Bank* block removes the noise of the current of the brushed dc motor which is within the range of possible ripple frequencies. The noise outside this range is removed by the previous block. This *Filter Bank* block is optional, and it will only be present if the range of possible ripple frequencies has significant noise. The noise in this range can be internal or external, i.e., the noise source may or may not be produced by the brushed dc motor.

The *Filter Bank* block is composed of a filter bank. Only one filter of this filter bank filters the incoming signal, and

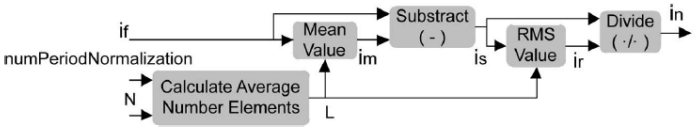

Fig. 7. Block diagram of the *Normalization* block.

the filter selection is done according to the ripple frequency detected in the previous iteration. This block has as its input the discrete period of ripple component N that is related to the ripple frequency f_r according to

$$f_r = F_s/N. \tag{23}$$

The block parameters are $filters$ and $filterFreqRange$. The $filter$ parameter is a list that indicates the number of filters in the filter bank and their lower and upper cutoff frequencies. The $filterFreqRange$ parameter indicates the range in which each filter is used according to the ripple frequency detected in the previous iteration. The configuration of this *Filter Bank* block is given by the brushed dc motor characteristics and the operating environment, i.e., it depends on how much noise the brushed dc motor current has.

3) Normalization Block: The dc component and the alternate component of the brushed dc motor current are variable signals. The variations depend on factors such as the load and speed of the brushed dc motor. The *Normalization* block removes this effect and makes the current vary between two fixed values. It also removes the dc component that the current may have after filtration.

The *Normalization* block normalizes the variance of current to $+1$ interval. This block normalizes the variance instead of the amplitude to become more robust in the presence of spurious and impulsive signals. The diagram of this block is shown in Fig. 7. The *Mean Value* block computes the mean value of the last L samples of the current according to

$$i_m[n] = \frac{1}{L[n]} \sum_{k=0}^{L[n]-1} i_f[n-k]. \tag{24}$$

The *Subtract* block removes the dc component of the current according to

$$i_s[n] = i_f[n] - i_m[n]. \tag{25}$$

The *RMS Value* block calculates the variance of the last L samples of the current without the dc component according to

$$i_r[n] = \sqrt{\frac{1}{L[n]} \sum_{k=0}^{L[n]-1} (i_s[n-k])^2}. \tag{26}$$

Finally, the *Divide* block normalizes the variance dividing the current without the dc component by its variance according to

$$i_n[n] = i_m[n]/i_r[n]. \tag{27}$$

The *Calculate Average Number Elements* block calculates the value of L according to

$$L[n] = numPeriodeNormalization \cdot N[n-1]. \tag{28}$$

The parameters of the last block are $N[n-1]$ and $numPeriodeNormalization$. The first parameter is the discrete period of the ripple component detected in the previous iteration. The second parameter is the number of periods used to calculate the mean and variance values and variance or rms value of the current. Larger values of this parameter will make the system more robust against motor noise. However, larger values make a poorer response to the speed variation of the brushed dc motor. In contrast, small values of this parameter will make the system estimate the mean and variance of the current incorrectly. An adequate value for this parameter is between five and ten.

4) Get Features Block: The *Get Features* block obtains the most important features of the current that have been filtered and normalized. Later, these features will be used by the *Pulse Detection* block.

Initially, the *Get Features* block delays the current signal according to

$$x[n] = i_n[n - delay] \tag{29}$$

where the delay parameter is the delayed sample number. This is done because it is necessary to have the present and future samples of the signal current in order to obtain some specific features. The features that this block extracts are as follows.

1) **Slope change** (sC): This feature measures the variation of the slope's current by means of

$$sC = \frac{\sum_{k=-M}^{M} (x[n] - x[n-k])}{\sum_{k=-M}^{M} |x[n] - x[n-k]|}. \tag{30}$$

In this, M is one-half of the window's size in which the feature is measured. The denominator is used to normalize the feature value, and it varies between ± 1.

2) **Maximum local** (m): This feature determines if the actual current sample is a maximum or not. The value of this feature is obtained from

$$m = \frac{\sum_{k=-M}^{M} higher\,(x[n], x[n-k])}{2M} \tag{31}$$

$$higher(y, z) = \begin{cases} 1, & \text{if } y > z \\ 0, & \text{otherwise.} \end{cases} \tag{32}$$

The denominator of (31) is used to normalize the feature value to the ± 1 range.

3) **Compare with zero** (cZ): This feature determines if the normalized current sample, from which the dc component is subtracted, is positive or negative. In order for the noise to not affect the feature measurement, the comparator is implemented with the next hysteresis function

$$cZ[n] = \begin{cases} 1, & \text{if } cZ[n-1] = 1 \ y \ x[n] > -hyUmb \\ 1, & \text{if } cZ[n-1] = 0 \ y \ x[n] > hyUmb \\ 0, & \text{if } cZ[n-1] = 1 \ y \ x[n] < -hyUmb \\ 0, & \text{if } cZ[n-1] = 0 \ y \ x[n] < hyUmb. \end{cases} \tag{33}$$

In this equation, the $hyUmb$ parameter is the hysteresis threshold, and adequate values for this parameter are between 0.3 and 0.5.

4) **Shape similarity** (s): This feature determines if the actual current sample is a maximum or not, by means of a correlation between the ideal and real shapes of the brushed dc motor current. The feature value is obtained from

$$s[n] = \frac{\sum_{k=0}^{N-1} \left(x[n-k] x_p\left[k, N[n-1]\right]\right)}{\sqrt{\sum_{k=0}^{N-1} x^2[n] \sum_{k=0}^{N-1} x_p^2\left[k, N[n-1]\right]}} \tag{34}$$

where x_p is the ideal shape of a maximum obtained from

$$x_p\left[k, N[n-1]\right] = \cos\left(\frac{2\pi k}{N[n-1]}\right). \tag{35}$$

In both equations, $N[n-1]$ is the discrete period of the ripple component detected in the previous iteration.

5) **Rising edge** (rE): This feature determines if the current has changed from a negative to a positive value since the last detected pulse. The value of this feature is obtained from

$$rE[n] = \overline{pul[n-1]} \cdot \left(fS[n-1] + cZ[n] \cdot \overline{cZ[n-1]}\right) \tag{36}$$

where $pul[n-1]$ is a logical value that indicates if a pulse was detected in the previous iteration. The operator $\bar{\cdot}$ is the negation operator; the result is zero if the input is different from zero, and it is one if the input is zero.

6) **Falling edge** (fE): This feature determines if the current has changed from a positive to a negative value since the last detected pulse. The value of this feature is obtained from

$$fE[n] = \overline{pul[n-1]} \cdot \left(fE[n-1] + cZ[n] \cdot cZ[n-1]\right). \tag{37}$$

7) **Zero crossing distance** (zCD): This feature measures the number of normalized samples since the last rising edge. If a rising edge has not yet been detected, then its value is zero. The value of this feature is obtained from

$$zCD[n] = \overline{pul[n-1]} \cdot \left(rE[n]/N[n-1] + zCD[n-1]\right). \tag{38}$$

8) **Length wave time** (Lwt): This feature measures the number of normalized samples since the last detected pulse. The value of this feature is obtained from

$$Lwt[n] = \overline{pul[n-1]} \cdot \left(1/N[n-1] + Lwt[n-1]\right). \tag{39}$$

9) **Length wave amplitude** ($Lw\alpha$): This feature measures the distance accumulated by the current amplitude since the last detected pulse. The value of this feature is obtained from

$$Lwa[n] = \overline{pul[n-1]} \cdot \left(|x[n] - x[n-1]| + Lwa[n-1]\right). \tag{40}$$

In this case, the feature is not explicitly normalized because the current was normalized by the *Normalization* block.

Many of these features give redundant information, but because they are obtained in different ways, noise will affect them differently. Therefore, all these features are used, and the *Pulse Detection* block will fuse all information contained in the features to determine if the actual sample corresponds to a pulse of the current.

Some features use the M parameter. This parameter is determined as one-half of the size of the window that is used to extract the feature. In order to eliminate noise as much as possible, this parameter should be as large as possible. This parameter has two restrictions: 1) It must be lower than one-half of the discrete period of the ripple component detected in the previous iteration, because the filter must not eliminate the current pulses, and 2) it must be lower than the delay parameter, because only delay samples will be available as samples in the future. This parameter is given according to

$$M = \min\left(0.4 \cdot N[n-1], delay\right). \tag{41}$$

The *Get Features* block also obtains N. This parameter is the number of samples in a period of the ripple component. The N value is calculated as the number of discrete samples between the last two pulses. The equations for calculating N are

$$N[n] = \overline{pul[n-1]} \cdot N[n-1] + pul[n-1] \cdot N_p[n] \tag{42}$$

$$N_p[n] = \overline{pul[n-1]} \cdot \left(N_p[n-1] + 1\right). \tag{43}$$

5) Pulse Detection Block: The *Pulse Detection* block determines with each new sample whether a current pulse appears or not. This block also discards false pulses and detects ghost pulses. The inputs of this block are the features obtained in the *Get Features* block, and the output $pul[n]$ is a Boolean value that indicates if a pulse is detected or not. This block is a classifier based on an SVM. The equations to implement the classifier are (1) and (18). In these equations, the parameters are as follows: 1) α_i, y_i from support vector set; 2) the b parameter; 3) the kernel function K; and 4) the kernel parameters. All these parameters are obtained in the training method stage, and they are passed to the *Pulse Detector* block using the $featConf$ parameter.

6) Speed Estimation Block: The *Speed Estimation* block calculates the speed of the brushed dc motor, with information

obtained from the *Pulse Detection* block. This speed n is calculated only when a new pulse has been detected. The steps of the algorithm to calculate it are as follows.

1) Update the distance or sample number to the last detected pulse d according to

$$d := d + 1 \tag{44}$$

where the operator := indicates that d is a variable of the algorithm, which is updated in each iteration.

2) If a pulse is detected, add the pulse distance to a list of distances between pulses τ_k, and reset to zero the actual distance since the last pulse. The equations that do this are

$$k := k + 1 \tag{45}$$

$$\tau_k := d \tag{46}$$

$$d := 0. \tag{47}$$

Equation (45) updates the number of pulses detected k. Equation (46) adds the distance between the last two pulses to the list of distances. Equation (47) resets the distance to the last pulse.

3) Update and output the speed. The present speed is given according to

$$n = \frac{Fs \cdot numPulseMean}{\sum_{i=0}^{numPulseMean-1} \tau_{k-i}} \cdot \frac{60}{pulseRevlolution} \tag{48}$$

where $numPulseMean$ is the number of the last distance between pulses used to calculate the speed and $pulseRevolution$ is the number of pulses produced in the current per revolution of the brushed dc motor shaft.

7) Position Estimation Block: The *Position Estimation* block calculates the position θ of the brushed dc motor. The steps of the algorithm to calculate the position are as follows.

1) Increment the number of pulses n_{pulse} if a new pulse has been detected. This is

$$n_{\text{pulse}} := n_{\text{pulse}} + 1. \tag{49}$$

2) Calculate the position of the brushed dc motor in radians according to

$$\theta = 2\pi \cdot n_{\text{pulse}}/pulseRevolution. \tag{50}$$

8) Pulses per Revolution Computation Block: The *Pulses per Revolution Computation* block determines the number of pulses of the current per revolution of the brushed dc motor shaft. This value is obtained according to

$$pulseRevolution = 2p \cdot k/\eta \tag{51}$$

where $2p$ is the number of poles, k is the number of commutation bars, and η is assumed according to

$$\eta = gcd\{2p, k\} \tag{52}$$

where gcd is the greatest common divisor. These parameters depend only on the motor construction, and they do not vary with time [18].

If the number of commutation bars and the number of poles are not known, the parameter $pulsRevolution$ can be determined experimentally. To get this parameter, the following steps should be followed. First, the brushed dc motor has to rotate at a constant speed. Second, the speed is measured by an encoder. Third, when the brushed dc motor is rotating, the τ_k that is used in (48) is measured. Finally, (48) is solved for the parameter $pulseRevolution$, where n is the speed measured with an encoder.

B. Training Method

The training method makes the SVM classifier of the proposed method learn from a training set. The classifier is implemented inside the *Pulse Detector* block (Fig. 6). This block decides for each instant of discrete time whether a current pulse has or has not happened. The inputs of the *Pulse Detector* block are the features got from the current signal by the *Get Features* block, and the output is a Boolean value that indicates if a pulse current has happened. The training sets are feature sets extracted by the *Get Features* block when a pulse happens and feature sets extracted when a pulse does not happen.

The objective of the training method is double. First, it gets training sets, and second, it trains the SVM classifier with the above training samples. Thus, the training method gets parameters of the *Pulse Detector* block. The steps to train the method are as follows.

1) **To measure signals of current related to the motor comportment**: Together with the current, the real speed and the position of the brushed dc motor are measured using a conventional sensor such as a high-resolution optical encoder. This is done on different motor conditions, as many constant speeds, many linear variations of the speed, and many speed steps.
2) **To establish a criterion to end the training process**: This criterion indicates when the training method must finish. The criterion should be established on the speed and/or position estimated by the proposed method, never if a pulse is detected or not for determinate features. For example, a criterion can be that the speed or the position does not exceed a maximum error.
3) **To set the parameters of the method**: The method has some specific parameters, and it is necessary to set the values of these parameters by the system designer. However, the values of the *Pulse Detector* block parameters are not established during this step. They are obtained at the end of the training method, and they are established in Step 7).
4) **To empty the list of training samples** S: The list of training samples is emptied. This is done in the first iteration and when a parameter of the method is modified.
5) **To get training samples**: The training samples are taken from the measured signals in Step 1). Each training sample is composed by the features taken by the *Get Features* block and by a Boolean value that indicates whether

the training samples correspond to a pulse. The designer decides if the features correspond or not to a pulse and facilitates the Boolean value in this stage. A small interval of the measured signals in Step 1) is randomly selected to get the samples when the S list is empty. However, when the S list is not empty, an interval that does not satisfy the end criterion is taken instead of a random interval.

6) **To add samples to the lists of training samples** S: The samples obtained in the previous step are added to the list of training samples S.
7) **To train the classifier**: The SVM classifier is trained with the list of training samples S. The algorithm used in this paper is the SMO, but another algorithm can be used. In this step, the parameter of the *Pulse Detector* block is obtained.
8) **To get the errors of the method**: The proposed method, with parameters obtained in the previous step, is tested with the measured signals in Step 1). The method returns an estimation of the speed and position of the brushed dc motor. The estimation is compared to the real speed and the real position to estimate the error of the method.
9) **To evaluate the error of the method**: The training end criterion is checked. Step 10) is next when the criterion is achieved. If the criterion is not yet achieved, then it is checked if it is convenient to change any parameter. If any parameter must be changed, Step 3) is the next; if not, Step 5) is the next.
10) **To return the parameters of the SVM classifier**: The parameters of the SVM classifier or *Pulse Detector* block are returned. The parameters are α_i, y_i, b, the kernel function, and the kernel parameters.

This algorithm is iterative. Each iteration adds new training samples to train the SVM classifier. The training samples added in each iteration are the samples obtained from Step 1) that measured the signal where the method did not correctly estimate the speed and position.

The kernel function with better practical results in this paper is the polynomial function. The kernel parameter is the degree, which must be below five for optimal results.

IV. Comparison With Other Methods

The more popular methods to detect the pulses of current in brushed dc motors are those that use a comparator. These methods compare the current in a brushed dc motor with the dc component of the same current signal. Implementations of these methods are as follows: 1) the one proposed by Ma and Weiss [12] that estimates the dc component as the mean value between the maximum and the minimum of the current; 2) that proposed by Iott and Burke [13] that eliminates the dc component with a high-pass filter and compares the result with zero; and 3) the proposal by Micke *et al.* [16] that obtains the dc component with a low-pass filter whose cutoff frequency is sufficiently low.

The disadvantage of these methods is that they cannot detect ghost pulses and cannot discard false pulses, as Fig. 8 shows. In this figure, (a) represents schematically the pulses of the current and its dc component, and (b) represents the output signal of a comparator that has a pulse by each detected pulse.

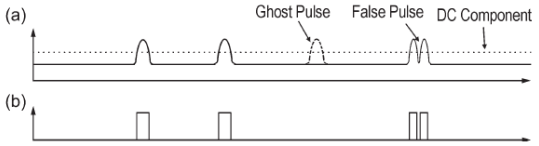

Fig. 8. False and ghost pulses. (a) Pulses of the brushed dc motor current. (b) Pulses detected by a comparator.

A solution to this problem is to combine the pulse detection with a comparator with the distance estimation between pulses through a dynamic model of the brushed dc motor. The dynamic model estimates the speed of a brushed dc motor, which is related to the frequency ripple component [18]. This means that the frequency ripple component is obtained from the estimated speed. The inverse of the frequency is the period, and the period is the temporal distance between two consecutive pulses. A temporal window that must contain the next pulse is estimated using the last temporal position of the pulse and the distance between pulses. The pulses detected before this window starts are discarded because they are estimated as false pulses. A pulse detected during the window is considered valid, and after this, the system starts from the beginning to detect the next pulse. If no pulse is detected during the window, the system determines that a ghost pulse has occurred and a pulse is added. This solution was applied, for example, by Kessler and Schulter [19] and Lutter and Fiedrich [26].

However, the aforementioned solution has the same problems as the sensorless techniques based on the dynamic model of the brushed dc motor. The dynamic model of a brushed dc motor uses some parameters whose values depend on the operating conditions of the brushed dc motor. If these operating conditions vary, these parameters vary in value. If the estimated parameter values are very different from the real parameter values, the method is not able to correctly estimate the distance between pulses or the temporal window. This causes the method to 1) discard some true pulses detected by the comparator and 2) erroneously indicate that a ghost pulse has occurred.

According to the proposed method by Ohishi *et al.* [11], a second solution to the aforementioned problem is the dynamic estimation of dc parameters in the brushed dc motor. However, it leads to a difficult-to-solve nonlinear model that also has a high computational cost. Also, in this solution, the dynamic model of the brushed dc motor needs to monitor the current and the voltage of the brushed dc motor simultaneously. This causes the system to require an additional A/D converter, therefore increasing the system cost.

The proposed method in this paper solves the previous problems with the monitoring of only the current of the brushed dc motor. In this case, the SVM classifier detects current pulses, detects ghost pulses, and discards false pulses. A correct SVM training is essential to allow the system to detect ghost pulses and to discard false pulses. To achieve the objective, the elapsed time since the last detected pulse is introduced in the obtained features. Real examples of the detection of a ghost pulse and the discarding of a false pulse are shown in Figs. 9 and 10, respectively. These figures also show the brushed dc motor current whose variance is normalized to ± 1, the pulses detected

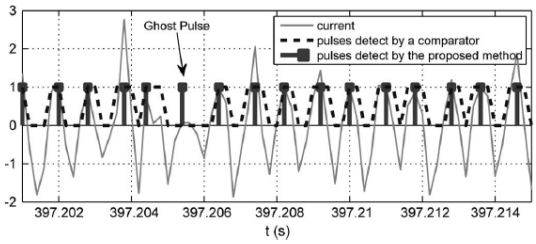

Fig. 9. Real example of the detection of a ghost pulse using the proposed method. The method that uses a comparator does not detect the ghost pulse. In this example, the speed of the brushed dc motor is high.

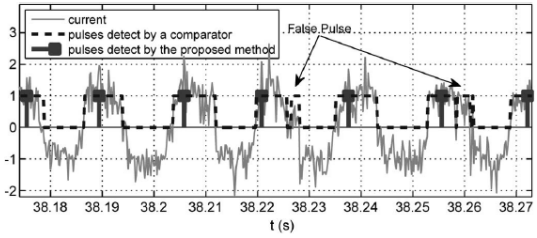

Fig. 10. Real example of the detection of a false pulse using the proposed method. The method that uses a comparator does not discard the false pulse. In this example, the speed of the brushed dc motor is low.

by the proposed method, and the pulses detected by a method that uses a comparator.

Modern microcontrollers or DSP devices can support the computational cost of the proposed method if the method is parallelized. In addition, there are some techniques that decrease the number of operations that need to be realized by the SVM [23], [24]. Also, in order to decrease the hardware cost, the sensorless processing hardware can be shared by several brushed dc motors or by other devices.

V. Experimental Results

This section presents the procedure for measuring the accuracy of the proposed method and presents the results obtained from the two brushed dc motors that were tested.

A. Experiment

The accuracy of the proposed methods is measured by comparing the estimated speed and position with the real speed and position of a brushed dc motor in different situations of work: 1) a constant speed; 2) a linear variation of the speed or a constant acceleration; and 3) a speed step.

Fig. 11 shows the architecture hardware. The architecture consists of a brushed dc motor, a current sensor, a data acquisition card, and a PC.

Tests were done with two brushed dc motors, the EMG30 and the 719RE385, whose characteristics are shown in Table II. The sensor of the current was a small resister with only 20 mΩ, usually called a shunt resistor. A low-cost data acquisition card (National Instruments USB-6008) was used to measure and digitalize the signal of the current by means of one of

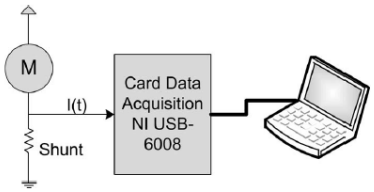

Fig. 11. Architecture hardware.

TABLE II
Motor Specifications

Parameter / Motor	EMG30	719RE385
Manufacturer	Devantech Ltd.	Como Drills
Nominal Voltage	12 V	12 V
No Load Current	530 mA	250 mA
Nominal Speed	6000 r.p.m.	5000 r.p.m.
Poles ($2p$)	2	2
Commutator Bars (k)	3	5
Resistance (R_a)	1.8 Ω	1.5 Ω
EMF Constant (c)	0.0178 V/r.p.m.	0.00101 V/r.p.m.

its four differential analog inputs. The sampling frequency was 5 kHz. The data acquisition card was connected to a PC. This processed the signal of the current in order to estimate the speed and the position of the brushed dc motor according to the proposed method. The PC was a laptop with a T8300 microprocessor, 3 GB of RAM, and 320 GB of hard disk space. The operating system was Windows 7, and the development environment was Matlab R2009a. The PC was configured to work in soft real time, and the data acquisition card was configured to acquire the current in a continuous mode. In order to estimate the real speed and position of the brushed dc motor and to compare it with the proposed method, a high-resolution incremental encoder attached to the motor shaft was used. The encoder was connected to the 32-bits counter of the data acquisition card. Fig. 11 does not show the encoder and its connections.

B. Results

The results obtained in the tests are shown separately for the three different behaviors of the brushed dc motors.

1) Constant Speed: In this situation, the two brushed dc motors are turned at different constant speeds. In this test, the average error and deviation error of speed, with respect to real speed and position, were obtained. The deviation error is shown in absolute value (in revolutions per minute) and in relative value (in percent). Also, shown are the estimated positions and real positions for several constant speeds.

Tables III and IV show the results obtained in the estimation of the brushed dc motor speed for the EMG30 and 719RE385 dc motors. The average error of the estimate speed is low and constant. However, the absolute error variance increases as the speed increases. However, the relative error variance is always constant. This indicates that absolute error variance is proportional to the speed. Figs. 12 and 13 show the estimated and real positions for the EMG30 and 719RE385 dc motors. For the EMG30 dc motor, the position is shown at the constant

TABLE III
SPEED MEASUREMENT ERRORS WITH THE EMG30 DC MOTOR

Real Speed (r.p.m.)	Average error		Deviation	
	Absolute (r.p.m.)	Relative (%)	Absolute (r.p.m.)	Relative (%)
501	1.03	0.21	3.51	0.70
807	1.09	0.14	5.86	0.73
1044	0.88	0.08	6.72	0.64
1526	1.79	0.12	8.62	0.56
2028	0.28	0.01	12.22	0.60
3082	5.72	0.19	7.22	0.23
4051	1.01	0.02	20.45	0.50
5055	3.26	0.06	21.51	0.43
6088	2.39	0.04	19.11	0.31
8041	4.01	0.05	32.14	0.40
9017	3.96	0.04	34.62	0.38
10117	1.96	0.02	36.13	0.36
11097	5.79	0.05	29.74	0.27

TABLE IV
SPEED MEASUREMENT ERRORS WITH THE 719RE385 DC MOTOR

Real Speed (r.p.m.)	Average error		Deviation	
	Absolute (r.p.m.)	Relative (%)	Absolute (r.p.m.)	Relative (%)
592	0.18	0.03	2.41	0.41
858	0.36	0.04	2.52	0.29
1029	0.43	0.04	2.45	0.24
1499	0.40	0.03	3.36	0.22
1971	0.74	0.04	4.73	0.24
3010	0.07	0.002	7.50	0.25
3949	2.86	0.07	10.82	0.27
5012	7.51	0.15	21.25	0.42
6084	5.64	0.09	28.82	0.47
7062	12.18	0.17	36.96	0.52
8017	11.49	0.14	49.48	0.62
8964	11.12	0.12	49.71	0.55
9994	17.54	0.18	76.67	0.77

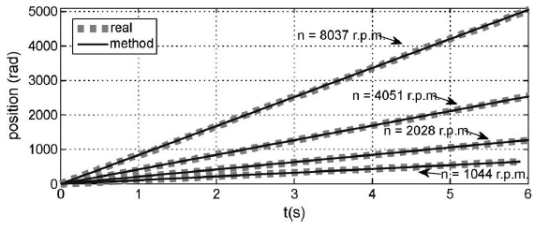

Fig. 12. Position at different constant speeds in the EMG30 dc motor.

speeds 1044, 2028, 4051, and 8037 r/min, and the average errors of position were 1.81, 7.49, 3.35, and 2.52 rad, respectively. For the 719RE385 dc motor, the positions at the constant speeds 934, 1970, 3482, and 5012 r/min are shown. The average position errors were 3.19, 1.44, 0.47, and 6.50 rad, respectively. These data indicate that the proposed method works correctly in a wide range of speeds.

2) Constant Acceleration: In this situation, the speed of the brushed dc motor varies linearly or with a constant acceleration. The results shown are the estimated speeds and positions with respect to the real speeds and positions.

For the EMG30 dc motor, the speed varies linearly from 4100 to 5100 r/min, and for the 719RE385 dc motor, it varies linearly from 3100 to 5100 r/min. Figs. 14 and 15 show the speed results

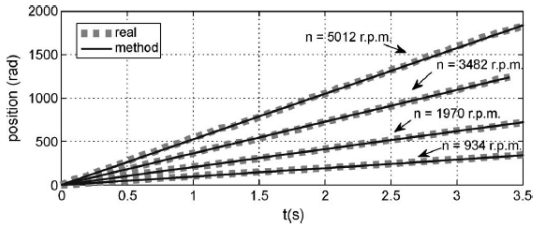

Fig. 13. Position at different constant speeds in the 719RE385 dc motor.

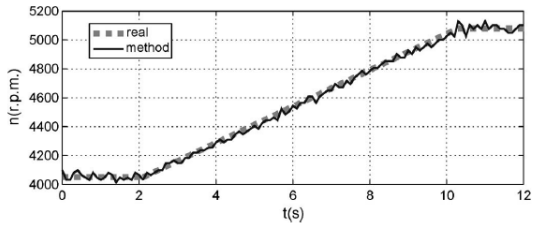

Fig. 14. Speed with linear variation of speed in the EMG30 dc motor.

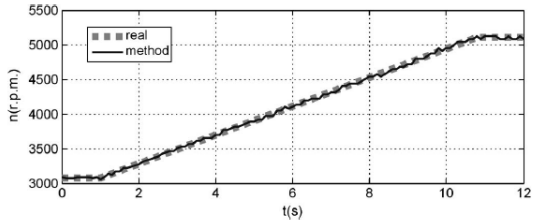

Fig. 15. Speed with linear variation of speed in the 719RE385 dc motor.

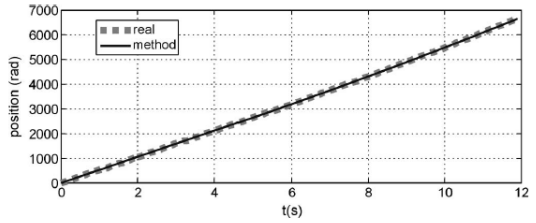

Fig. 16. Position with linear variation of speed in the EMG30 dc motor.

for each dc motor. For the EMG30 dc motor, the average error of the speed was 0.49 r/min, and the variance was 20.03 r/min. For the 719RE385 dc motor, the average error of the speed was 0.16 r/min, and the error variance was 10.57 r/min. Figs. 16 and 17 show the position results for the two dc motors. The average error of position was 2.09 rad for the EMG30 dc motor, and it was 18.98 for the 719RE385 dc motor. All these data indicate that the error is low and that the proposed method correctly estimates the speed and position of a brushed dc motor when the speed varies slowly.

3) Speed Step: In the third work situation, a speed step is produced in the speed of the brushed dc motor. The results

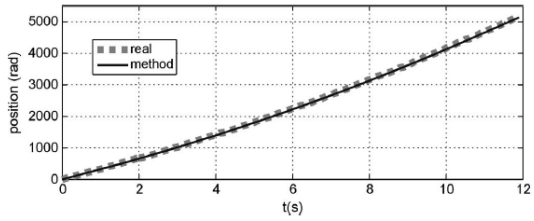

Fig. 17. Position with linear variation of speed in the 719RE385 dc motor.

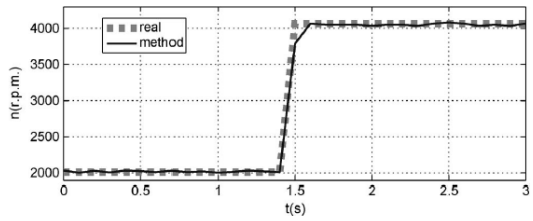

Fig. 18. Speed with speed step in the EMG30 dc motor.

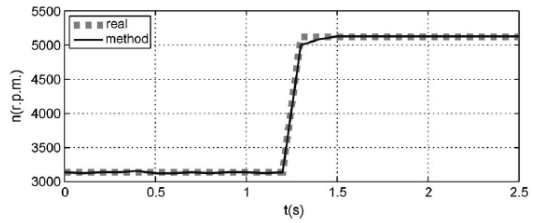

Fig. 19. Speed with speed step in the 719RE385 dc motor.

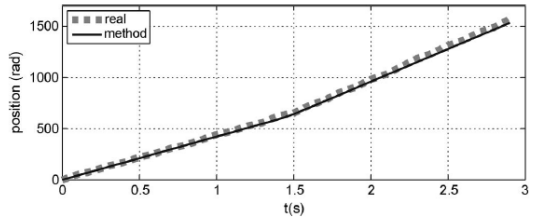

Fig. 20. Position with speed step in the EMG30 dc motor.

shown are the estimated speed and position with respect to the real speed and position.

For the EMG30 dc motor, the step speed was from 2000 to 4000 r/min, and for the 719RE385 dc motor, it was from 3100 to 5100 r/min. Figs. 18 and 19 show the estimated and real speeds for the two brushed dc motors. The proposed method took 0.1 s to reach the final value of the speed for the EMG30 dc motor and 0.2 s for the 719RE385 dc motor. Figs. 20 and 21 show the position results for the two dc motors. The average error of position was 15.90 for the EMG30 dc motor, and it was 1.02 for the 719RE385 dc motor. These results indicate that the error is low and that the proposed method is able to estimate correctly the speed and position.

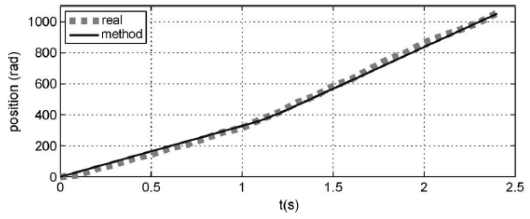

Fig. 21. Position with speed step in the 719RE385 dc motor.

VI. CONCLUSION

This paper has presented a new sensorless method for estimating the speed and position of brushed dc motors using SVMs. The method uses sensorless techniques based on the ripple component. The method employs pattern recognition techniques to detect the pulse in brushed dc motor current signals, and it uses SVMs to classify the pulse. To identify the pulses, the method filters, normalizes, and obtains the more important features of the current in a brushed dc motor. Then, the SVM decides in each instance if a pulse has been produced. Finally, the method counts the detected pulses in order to estimate the position and takes the inverse temporal distance between pulses in order to estimate the speed.

This method has an advantage over other existing methods: the ability to detect ghost pulses and to discard false pulses. This is achieved by introducing the time that has elapsed since the last detected pulse into the feature set and by using an SVM as a classifier to detect the pulses.

The experimental results, obtained to validate the proposed method, show that the method works in a wide range of speeds and in different operating conditions, such as linear speed variation and abrupt jumps of speed in a brushed dc motor.

REFERENCES

[1] R. B. Allured and A. S. Strzelewigz, "Commutator pulse counting apparatus," U.S. Patent 346 725, Oct. 10, 1967.
[2] P. Vas, *Sensorless Vector and Direct Torque Control*. Oxford, UK: Oxford Univ. Press, 1998.
[3] M. Hilairet and F. Auger, "Speed sensorless control of a DC-motor via adaptive filters," *IET Elect. Power Appl.*, vol. 1, no. 4, pp. 601–610, Jul. 2007.
[4] P. Chevrel and S. Siala, "Robust DC-motor speed control without any mechanical sensor," in *Proc. IEEE Int. Conf. Control Appl.*, 1997, pp. 244–246.
[5] J. Scott, J. McLeish, and W. H. Round, "Speed control with low armature loss for very small sensorless brushed dc motors," *IEEE Trans. Ind. Electron.*, vol. 56, no. 4, pp. 1223–1229, Apr. 2009.
[6] Z. Z. Liu, F. L. Luo, and M. H. Rashid, "Speed nonlinear control of dc motor drive with field weakening," *IEEE Trans. Ind. Appl.*, vol. 39, no. 2, pp. 417–423, Mar./Apr. 2003.
[7] G. S. Buja, R. Menis, and M. I. Valla, "Disturbance torque estimation in a sensorless dc drive," *IEEE Trans. Ind. Electron.*, vol. 42, no. 4, pp. 351–357, Aug. 1995.
[8] S. M. R. Kazmi, H. Goto, H.-J. Guo, and O. Ichinokura, "A novel algorithm for fast and efficient speed-sensorless maximum power point tracking in wind energy conversion systems," *IEEE Trans. Ind. Electron.*, vol. 58, no. 1, pp. 29–36, Jan. 2011.
[9] S. R. Bowes, A. Sevinc, and D. Holliday, "New natural observer applied to speed-sensorless dc servo and induction motors," *IEEE Trans. Ind. Electron.*, vol. 51, no. 5, pp. 1025–1032, Oct. 2004.
[10] F. Genduso, R. Miceli, C. Rando, and G. R. Galluzzo, "Back EMF sensorless-control algorithm for high-dynamic performance PMSM," *IEEE Trans. Ind. Electron.*, vol. 57, no. 6, pp. 2092–2100, Jun. 2010.

[11] K. Ohishi, Y. Nakamura, Y. Hojo, and H. Kobayashi, "High-performance speed control based on an instantaneous speed observer considering the characteristics of a DC chopper in a low speed range," *Elect. Eng. Jpn.*, vol. 130, no. 3, pp. 77–87, Feb. 2000.
[12] J. Ma and S. Weiss, "Motor pulse extraction system," U.S. Patent 4 684 858, Aug. 1987.
[13] J. Iott and D. Burke, "Brushed motor position control based upon back current detection," U.S. Patent 2006/0261763 A1, Nov. 23, 2006.
[14] W. S. Ra, H. J. Lee, J. B. Park, and T. S. Yoon, "Practical pinch detection algorithm for smart automotive power window control system," *IEEE Trans. Ind. Electron.*, vol. 55, no. 3, pp. 1376–1384, Mar. 2008.
[15] K. R. Geldhof, A. P. M. Van den Bossche, and J. A. Melkebeek, "Rotor-position estimation of switched reluctance motors based on damped voltage resonance," *IEEE Trans. Ind. Electron.*, vol. 57, no. 9, pp. 2954–2960, Sep. 2010.
[16] M. Micke, H. Sievert, J. Hachtel, and G. Hertlein, "Method and device for measuring the rotational speed of a pulse-activated electric motor based on a frequency of current ripples," U.S. Patent 7 265 538 B2, Sep. 4, 2007.
[17] T. Figarella and M. H. Jansen, "Brush wear detection by continuous wavelet transform," *Mech. Syst. Signal Process.*, vol. 21, no. 3, pp. 1212–1222, Apr. 2007.
[18] B. Yuan, Z. Hu, and Z. Zhou, "Expression of sensorless speed estimation in direct current motor with simplex lap winding," in *Proc. ICMA*, 2007, pp. 816–821.
[19] E. Kessler and W. Schulter, "Method for establishing the rotational speed of mechanically commutated DC motors," U.S. Patent 6 144 179 A, Nov. 7, 2000.
[20] V. Vapnik, *The Nature of Statistical Learning Theory*. New York: Springer-Verlag, 1995.
[21] J. Ma and S. Weiss, "Motor pulse extraction system," U.S. Patent 4 684 858, Aug. 4, 1987.
[22] B. E. Boser, I. M. Guyon, and V. N. Vapnik, "A training algorithm for optimal margin classifiers," in *Proc. 5th Annu. Workshop Comput. Learn. Theory*, 1992, pp. 144–152.
[23] J. S. Taylor and N. Cristianini, *An Introduction to Support Vector Machines and Other Kernel-Based Learning Methods*. Cambridge, U.K.: Cambridge Univ. Press, 2000.
[24] S. Abe, *Support Vector Machines for Pattern Classification*. London, U.K.: Springer-Verlag, 2005.
[25] J. C. Platt, "Fast training of support vector machines using sequential minimal optimization," in *Advances in Kernel Methods: Support Vector Learning*, B. Schölkopf, C. J. C. Burges, and A. J. Smola, Eds. Cambridge, MA: MIT Press, 1999, pp. 185–208.
[26] T. Lutter and T. Fiedrich, "Method for detecting the rotational position of the drive shaft a DC motor," U.S. Patent 67 680 282 B2, Jul. 27, 2004.

Ernesto Vázquez-Sánchez was born in Plasencia, Spain, in 1985. He received the M.S. degree in telecommunication engineering and the M.S. degree in electronic engineering from the University of Valladolid, Valladolid, Spain, in 2008 and 2010, respectively.

Since 2009, he has been as a Researcher with the Department of Signal Theory, Communications and Telematics Engineering, University of Valladolid. His current research interests are communications and sensorless technology for motors.

Jaime Gómez-Gil was born in Aguilar de Bureba, Spain, in 1971. He received the M.S. degree in telecommunication engineering and the Ph.D. degree in signal theory, communications and telematics engineering from the University of Valladolid, Valladolid, Spain, in 2001 and 2005, respectively.

From 2001 to 2002, he was with the Center for the Development of Telecommunication in Castilla y León (CEDETEL), Valladolid. Since 2002, he has been a full-time Professor with the Department of Signal Theory, Communications and Telematics Engineering, University of Valladolid. His current research is centered on GPS and machine vision applied to agricultural engineering. His other interest areas are sensorless technology and human–computer interface technology.

José Carlos Gamazo-Real was born in Valladolid, Spain, in 1979. He received the B.S. and two M.S. degrees in electronics and telecommunications engineering from the University of Valladolid, Valladolid, in 2001, 2004, and 2007, respectively.

From 2003 to 2004, he was with the Robotics, Artificial Vision and Real-time Systems Department, Cartif Technology Centre, Valladolid, as an Associate Researcher. From 2006 to 2009, he was with the R&D and Electronics Department, Enerman, S.A., as the Chief Coordinator and the Principal Research Engineer. Since 2009, he has been with the Test Facilities Department, EADS-CASA Cassidian, Madrid, Spain, where he is a Design and Integration Engineer of Avionics Military Air Systems. His current research interests are sensorless control of brushless machines using power electronics and their applications for flight control systems of aircraft aerodynamic surfaces.

José Fernando Díez-Higuera was born in Bercero, Spain, in 1963. He received the M.S. degree in industrial engineering and Ph.D. degree in telecommunications engineering from the University of Valladolid, Valladolid, Spain, in 1991 and 1996, respectively.

From 1991 to 1999, he was an Assistant Professor with the Higher School of Telecommunications Engineering, University of Valladolid, where he has been a Professor of computer programming since 1999 and a Researcher with the Industrial Telematics Group, Department of Signal Theory, Communications and Telematics Engineering, since 1996. His main research interests are biologically inspired visual models, development, business intelligence, intelligent transport systems, and games-based computer science learning.

Capítulo 4: Artículo 3 del compendio

En este capítulo se analiza el tercer artículo del compendio, el cual incluye el desarrollo de una técnica *sensorless* de detección de la posición y velocidad para motores *brushless* DC (BLDC) basada en la derivada de las tensiones de fase del motor, cuyo *hardware* y *software* se ha implementado sobre en una plataforma *driver* específicamente diseñada en la tesis para este tipo de motores. En este capítulo se incluye la información bibliográfica del artículo, así como otros datos y análisis referidos al ámbito, motivación y originalidad del mismo. Al final del capítulo se incluye el extracto del artículo publicado en la revista *Journal of Electrical Engineering and Technology* en julio de 2015.

4.1 Datos bibliográficos

TITULO: Sensorless Detection of Position and Speed in Brushless DC Motors using the Derivative of Terminal Phase Voltages Technique with a Simple and Versatile Motor Driver Implementation.

AUTORES: José Carlos Gamazo Real y Jaime Gómez Gil.

NOMBRE DE REVISTA: Journal of Electrical Engineering and Technology.

EDITOR: KIEE, Korean Institute of Electrical Engineers (Seúl, Korea del Sur).

FECHA DE PUBLICACIÓN: 1 de julio de 2015.

ISSN: 1975-0102.

DOI: 10.5370/JEET.2015.10.4.1540.

VOLUMEN: 10.

NÚMERO: 4.

PÁGINAS: 1540-1551.

REFERENCIA: [80]

4.2 Resumen

El objetivo de este artículo es desarrollar una técnica *sensorless* para la detección de la posición y velocidad en motores BLDC, así como superar los inconvenientes de las técnicas basadas en el uso de sensores de posición, y la mejora del rendimiento de enfoques de detección tradicionales que utilizan los voltajes de fase del motor. En la técnica desarrollada, la posición y velocidad del motor se obtiene mediante el cálculo de la derivada de los voltajes de fase con respecto a un punto neutro virtual. Para implementar el proceso de arranque del motor BLDC y desarrollar los algoritmos de la técnica de detección, se ha utilizado una tarjeta con una FPGA y un procesador en tiempo real. También, se ha desarrollado un hardware específico para accionar este tipo de motores mediante el uso de señales con modulación de anchura de pulsos (PWM). En la evaluación del rendimiento de *hardware* y *software* diseñados se han empleado motores tanto en configuración delta como estrella, y los *tests* se han realizado con una carga acoplada al motor y sin ella. Los resultados experimentales para validar la técnica de detección se llevaron a cabo en los rangos 5-1500 rpm y 5-150 rpm en condiciones de ausencia de carga y a plena carga, respectivamente. Específicamente, en los resultados se obtuvieron unos errores cuadráticos de velocidad y posición inferiores a 3 rpm y entre 10º y 30º, respectivamente, sin carga en el motor. Además, en condiciones de plena carga, los resultados se obtuvieron con unos errores de velocidad y posición en torno a 1 rpm y entre 10º y 15º, respectivamente. Estos resultados proporcionan la evidencia de que la técnica desarrollada permite detectar la posición y velocidad de motores BLDC con reducidos errores de precisión tanto en el arranque del motor como en un amplio rango de velocidades, además de reducirse la influencia del ruido en la detección de posición. Esto sugiere que la técnica puede ser utilizada como una alternativa fiable respecto a las técnicas basadas en sensores posición para aplicaciones de precisión.

4.3 Ámbito

Dentro de la revista indicada este artículo se incluye en la sección *Electric Machinery and Power Electronics*, cuya temática comprende desde maquinas eléctricas, como motores de inducción o motores de imanes permanentes, electrónica de potencia, tecnologías para el transporte del electricidad, energías renovables, controladores y *drivers* de motores [103].

El interés de este artículo dentro del ámbito de la revista radica en la técnica *sensorless* propuesta para motores *brushless*, los cuáles pueden englobarse dentro del grupo de motores síncronos de imanes permanentes. Para realizar la implementación de técnica mencionada, en el artículo se profundiza tanto en el *hardware* de acondicionamiento, adquisición y procesamiento de las señales del motor, como en los algoritmos *software* que constituyen la plataforma *driver* utilizada para su desarrollo, lo cual cubre otra de las líneas dentro de la sección de la revista como son los

controladores y *drivers* de motores. Cabe destacar que en el artículo además de realizarse la implementación y *test* de la técnica *sensorless* propuesta, se incluye una descripción del sistema controlador y *driver* de potencia desarrollado para llevar a cabo la actuación sobre motor BLDC.

4.4 Justificación en el marco de la tesis

La técnica *sensorless* incluida en este trabajo se encuadra dentro de las **Etapas 3 y 4 de la metodología**, y permite alcanzar el **Objetivo 4** de la tesis. Este objetivo consiste en el desarrollo de una técnica *sensorless* de detección de la posición y velocidad para motores BLDC basada en la derivada de las tensiones de fase del motor con respecto a un punto neutro virtual, y en el que se reduzca el efecto del ruido. En línea con lo indicado en el objetivo, se ha empleado una plataforma *driver* diseñada para distintos tipos de motores BLDC con el fin de realizar el control y adquirir las señales de los mismos. El *hardware* de acondicionamiento de señales de este sistema proporciona cierta inmunidad al ruido debido al empleo de punto neutro virtual para las señales del motor y determinadas configuraciones *hardware* basadas en amplificadores de instrumentación y filtros. Además, al haberse implementado la operación derivada en *hardware* y los algoritmos de detección de pulsos de la derivada en una FPGA, se logra un procesamiento en tiempo real con un coste computacional relativamente bajo. Para la validación de la técnica, se han realizado *tests* con un motor real con y sin carga bajo diferentes condiciones de operación, como velocidad constante y saltos bruscos de velocidad, y se ha empleado un *encoder* incremental como referencia de posición para los *tests*, obteniéndose en todos ellos unos resultados con unos errores de precisión reducidos. Esto evidencia que la detección de los pulsos de la derivada se realiza de forma adecuada para obtener la posición y velocidad del motor, junto con el rechazo de los pulsos falsos debidos al ruido. En base a lo comentado, se puede considerar que la técnica cumple con el Objetivo 4.

El presente artículo se obtuvo a partir de la finalización de implementación de la plataforma *driver* de motores BLDC y la intención de desarrollar una técnica que explotara al máximo los recursos proporcionados por ésta. En esta idea radica la originalidad del artículo y en la cual se buscaban cubrir básicamente dos necesidades. Por una parte, probar con una implementación real el *hardware* de acondicionamiento y adquisición, la tarjeta de procesamiento, el entorno de programación *software*, y la utilización del *encoder* incremental de posición con un motor BLDC real con carga. Por otra parte, la implementación de una técnica *sensorless* en línea con los objetivos de la tesis y relacionada con el procesamiento más o menos directo algún parámetro físico del motor, lo cual es típico de las técnicas básicas. En este sentido, algunos trabajos representativos en los que se incluyen técnicas *sensorless* básicas basados en parámetros físicos del motor son los presentados por Damodharan y Vasudevan [104] y Becerra *et al.* [56], con la detección del cruce por cero del voltaje BEMF, por Moreira [64] y Shen *et al.* [105], que presentan la detección del tercer armónico del voltaje BEMF, por Jahns

et. al [87], con la integración del voltaje BEMF, o por Cham y Samad [106] la medida las corrientes de fase del motor.

4.5 Extracto de la publicación

A continuación se incluye el artículo 3 del compendio tal y como aparece publicado en la revista *Journal of Electrical Engineering and Technology*.

J Electr Eng Technol.2015; 10(4): 1540-1551
http://dx.doi.org/10.5370/JEET.2015.10.4.1540

ISSN(Print) 1975-0102
ISSN(Online) 2093-7423

Sensorless Detection of Position and Speed in Brushless DC Motors using the Derivative of Terminal Phase Voltages Technique with a Simple and Versatile Motor Driver Implementation

José Carlos Gamazo Real† and Jaime Gómez Gil*

Abstract – The detection of position and speed in BLDC motors without using position sensors has meant many efforts for the last decades. The aim of this paper is to develop a sensorless technique for detecting the position and speed of BLDC motors, and to overcome the drawbacks of position sensor-based methods by improving the performance of traditional approaches oriented to motor phase voltage sensing. The position and speed information is obtained by computing the derivative of the terminal phase voltages regarding to a virtual neutral point. For starting-up the motor and implementing the algorithms of the detection technique, a FPGA board with a real-time processor is used. Also, a versatile hardware has been developed for driving BLDC motors through pulse width modulation (PWM) signals. Delta and wye winding motors have been considered for evaluating the performance of the designed hardware and software, and tests with and without load are performed. Experimental results for validating the detection technique were attained in the range 5-1500 rpm and 5-150 rpm under no-load and full-load conditions, respectively. Specifically, speed and position square errors lower than 3 rpm and between 10º-30º were obtained without load. In addition, the speed and position errors after full-load tests were around 1 rpm and between 10º-15º, respectively. These results provide the evidence that the developed technique allows to detect the position and speed of BLDC motors with low accuracy errors at starting-up and over a wide speed range, and reduce the influence of noise in position sensing, which suggest that it can be satisfactorily used as a reliable alternative to position sensors in precision applications.

Keywords: BLDC motor, Phase voltage derivative, Position and speed detection, PWM control with FPGA, Sensorless.

1. Introduction

BLDC motors are increasingly being used in different areas such as industry, residential and automotive applications, mainly because of their advantages over traditional brushed DC and induction motors. Better speed and torque characteristics, high efficiency and reliability, long operating life and noiseless operation are their most relevant features [1]. Different types of position sensors such as encoders, resolvers and Hall sensors are used for achieving a proper motor commutation in these applications. Sensors are commonly mounted inside the motor, so they are subjected to stressful operating conditions, and position measurements could be deteriorated. In order to overcome the disadvantages of rotor position sensors, sensorless techniques have arisen in recent years [2].

There are many categories of sensorless methods [1], such as zero crossing detection of back electromotive force (BEMF) [3, 4], third harmonic voltage sensing of BEMF [5, 6; 7], detection of free-wheeling diodes [8], integration of BEMF [9] and phase current sensing [10]. Advanced sensorless techniques are estimation and model-based methods such as sliding-mode observer [11], Extended Kalman Filter [12], adaptative observers [13, 14] and artificial neural networks [15]. The most common signals considered in position sensing and commutation techniques are the line to line motor voltages, motor terminal voltages in respect to the half of the DC bias, and terminal motor voltages regarding a virtual neutral point [2].

BEMF techniques have been traditionally considered for detecting the rotor position or speed [16]. However, it is difficult to detect the BEMF in a lower speed range because these signals are proportional to the rotor speed. For that reason, new detection algorithms with a simple starting procedure and high quality-cost ratio are needed for overcoming the problems of conventional techniques. In the proposed method, the position information is detected by processing the derivative of phase terminal voltages regarding to a virtual neutral point, and its precision is verified using an incremental shaft encoder.

† Corresponding Author: Dept. of Signal Theory, Communications and Telematics Engineering, University of Valladolid, Spain. (jcgamazo @ribera.tel.uva.es)
* Dept. of Signal Theory, Communications and Telematics Engineering, University of Valladolid, Spain. (jcgamazo@ribera.tel.uva.es)
Received: July 4, 2014; Accepted: January 29, 2015

This approach makes it possible to detect the rotor position over a wide speed range, solving the problems of BEMF methods at low speeds, and to use a simple starting procedure. The effectiveness of the proposed detection technique is analyzed through the implementation of a prototype with general purpose real-time hardware and software. Experimental results are obtained in order to confirm its practical validity.

The description of the motor driver and detection system is included in section 2. In this section, all the relevant elements considered in the system are analyzed, such as the BLDC motor, three-phase inverter, controller, motor signals conditioning circuitry, and the encoder used as reference. The methodology for motor starting-up and driving are explained in section 3. Section 4 describes the detection technique, including the developed hardware and algorithms for signal conditioning and processing. Experimental results at different speeds show the validity of the method in section 5 using an encoder. Finally, paper conclusions are presented in section 6.

2. Detection System Description

The control and detection system is composed of different modules for motor signals acquisition, conditioning and processing. The main elements are depicted in Fig. 1, such as the equivalent circuit of a BLDC motor, a three-phase inverter with power transistors and free-wheeling diodes, the conditioning circuitry for motor phase voltages, and the processing hardware for PWM control and rotor position / speed detection through a FPGA and a real-time processor. Hardware also includes shunt resistors (R_{sa}, R_{sb} and R_{sc}) and conditioning circuitry for analyzing phase currents if necessary, and an encoder for position reference. An image

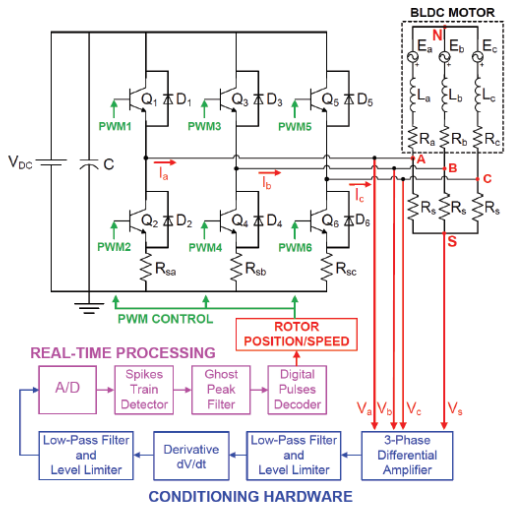

Fig. 1. Control and detection system

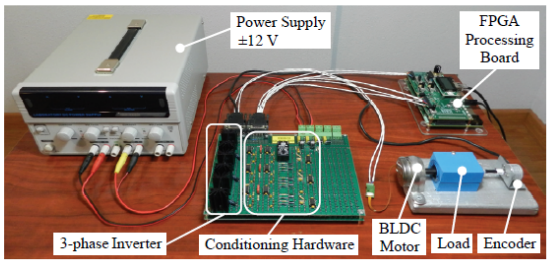

Fig. 2. Image of the experimental set-up

of the developed prototype is shown in Fig. 2.

2.1 BLDC motors

The implementation has been performed using BLDC motors with iron-core and star or wye winding configuration. The selected device is Maxon EC 45 Flat with a nominal voltage of 12 V, 8 pole pairs, and without Hall sensors embedded. Additionally, two BLDC motors with a delta winding configuration, that is the neutral point is not available, have been also considered in the analysis for evaluating the performance of the inverter. These models are DPM 42BL41 and DPM 42BL100, both with a nominal voltage of 24 V, 4 pole pairs and internal Hall sensors. Their main parameters are shown in Table 1.

A typical brushless motor with a star configuration respect to a neutral point N is shown in Fig. 1. It is considered that the motor is not saturated, iron losses are negligible, stator resistances (R) of all windings are equal, self inductances (L) are constant and mutual inductances (M) are zero [1]. Taking into account these assumptions, the motor is characterized with Eqs. (1)-(3).

$$V_{an} = R \cdot I_a + L \cdot \frac{dI_a}{dt} + E_a \tag{1}$$

$$V_{bn} = R \cdot I_b + L \cdot \frac{dI_b}{dt} + E_b \tag{2}$$

$$V_{cn} = R \cdot I_c + L \cdot \frac{dI_c}{dt} + E_c \tag{3}$$

Table 1. Parameters of BLDC motors

Parameter	Maxon EC 45 Flat	DPM 42BL41	DPM 42BL100
Number of pole pairs	8	4	4
Number of phases	3	3	3
Nominal speed	2850 rpm	4000 rpm	4000 rpm
Nominal voltage	12 V	24 V	24 V
Maximum current	1.96 A	5.4 A	20 A
Nominal torque	53.2 mNm	62.5 mNm	250 mNm
Terminal resistance phase to phase	1.4 Ω	1.8 Ω	0.28 Ω
Terminal inductance phase to phase	0.56 mH	2.23 mH	0.54 mH
Torque constant	25.5 mNm/A	35 mNm/A	36 mNm/A
Rotor inertia	92.5 gcm^2	240 gcm^2	960 gcm^2

where E is the trapezoidal shaped BEMF and I is the armature current through a specific phase.

However, for reducing the common mode noise that affects to terminal phase voltages [2], a virtual neutral point S has been provided with three star-connected resistors R_s, as Eqs. (4)-(6) show.

$$V_{as} = V_{an} + V_{ns} \quad (4)$$

$$V_{bs} = V_{bn} + V_{ns} \quad (5)$$

$$V_{cs} = V_{cn} + V_{ns} \quad (6)$$

According to Eq. (7), only two motor terminal voltages regarding to the virtual neutral point are necessary for position and speed detection.

$$V_{as} + V_{bs} + V_{cs} = 0 \quad (7)$$

During motor operation the current flows through two phases at any instant, which leaves the third phase opened or floating. If the motor is running at a constant speed, due to the magnetic field of the motor is uniformly distributed in the air gap, this results in a BEMF with a trapezoidal shape with a magnitude proportional to the rotor speed. Considering that phases A and B are conducting and phase C is opened, I_a=–I_b, I_c=0 and E_a=–E_b [17]. Terminal voltages regarding to the virtual neutral potential are shown in Eqs. (8)-(10).

$$V_{as} = R \cdot I_a + L \cdot \frac{dI_a}{dt} + E_a + V_{ns} \quad (8)$$

$$V_{bs} = -R \cdot I_a - L \cdot \frac{dI_a}{dt} - E_a + V_{ns} \quad (9)$$

$$V_{cs} = E_c + V_{ns} \quad (10)$$

The voltage between neutral and virtual neutral points is proportional to the BEMF of the floating phase, as Eq. (11) shows, which is obtained with the combination of Eqs. (7)-(10). It explains the influence of the virtual neutral potential over the terminal voltages of the conducting phases.

$$V_{ns} = -\frac{1}{3} E_c \quad (11)$$

2.2 Three-phase inverter

The inverter is based on a six-step sequence for stator winding commutation. At any moment, there is always a phase with its upper or lower leg in a disconnected state [18], which can be used for predicting the six rotor position instants of an electrical cycle. A mechanical cycle is proportional to a number of electrical cycles according to Eq. (12).

$$T_M = K_P \cdot T_E \quad (12)$$

where T_M is the mechanical period, K_P is the number of rotor pole pairs, and T_E is the electrical period. The proposed detection technique is validated using the motor Maxon EC 45 with K_P=8, so a mechanical cycle is composed of 8 electrical cycles.

Different types of devices could be used for implementing the inverter, such as MOSFETs, IGBTs or bipolar transistors. However, the integrated half-bridge bipolar switch Texas Instruments UC2950T has been selected due to the high-current provided with low saturation voltages and low-level logic signals for enabling the device. Also, high-speed flyback diodes with a forward voltage of 1.4 V are embedded inside the bridge for the free-wheeling operation. The main switching characteristics of the device taken into account for setting the processing tasks of the controller, and generating the PWM duty cycles are included in Table 2. Another relevant advantage is the versatility of the device because of the wide range of nominal motor voltages (8 V to 35 V) that can be driven, like the 12 V and 24 V BLDC motors included in Table 1.

Table 2. Switching characteristics of the UC2950T half-bridge for 12V supply voltage

Parameter	Value
Source turn-on delay	300 ns
Source turn-off delay	1 µs
Sink turn-on delay	200 ns
Source turn-off delay	100 ns

2.3 Motor signals conditioning

The proposed detection technique can use two or three terminal voltages with respect to the virtual neutral point, so hardware requirements are reduced. The common mode noise due to the virtual node S can influence on acquired signals, which is avoided by using differential amplifiers, such as Burr-Brown INA126 with a high common mode rejection ratio (94 dB) and low voltage noise (35 nV/√Hz at 1 kHz).

The use of filters is required to remove high switching frequency signals caused by the PWM inverter operation, which could result in a time delay that depends on the rotor speed and affect the dynamic performance of the drive [2]. These effects are not relevant in the developed prototype, so motor signals acquisition have been optimized using low pass filters for limiting the high frequency noise, voltage-level limiters based on Schottky Barrier diodes, and current limiting resistors.

Once each motor phase voltage is conditioned for being acquired, a specific conditioning is implemented according to the derivation method. Operational amplifiers Texas Instruments LM258AP and low-pass filters have been used for reducing the effects of high frequency components.

2.4 Controller

The core processing is based on a FPGA Xilinx Spartan-

6 LX45 and a real-time processor running up to 400 MHz. Both are embedded in the board National Instruments sbRIO-9636 with high signal integrity characteristics. For interfacing with the motor driver, the controller includes 16 analog inputs, 4 analog outputs and 24 digital I/O lines.

The system runs in open-loop for motor starting and in closed-loop for precision applications, such as rotary mechanical tools, robotics arms or aerodynamic surfaces. In these cases a PI or fuzzy controller could be introduced for improving the system stability [19].

2.5 Position sensor

An incremental encoder Kübler 2400 with 1024 pulses per revolution has been included in the prototype. It is only used as a reference for analyzing and contrasting the position and speed precision errors of the proposed detection method, where 1024 pulses corresponds to 360 mechanical degrees and the resolution is 360º/1024=0.35º.

3. Motor Driving and Starting Procedure

This section describes the procedure for starting the motor from standstill and driving until a reference speed is reached.

3.1 Description of sequential motor control

The three phase motor is driven through a six-step switching sequence. However, one electrical cycle may not correspond to a complete mechanical revolution of the rotor. This is determined with the number of rotor pole pairs according to Eq. (12). Considering the Maxon EC 45 motor, one mechanical cycle is equivalent to 8 electrical cycles and the resolution of detection method is 7.5º (mechanical degrees), which is demonstrated in Eqs. (13)-(14).

$$R_E = \frac{360^\circ}{N_C} \tag{13}$$

$$R_T = \frac{R_E}{N_S} \tag{14}$$

where R_E is the resolution per electrical cycle, N_C is the electrical cycles per mechanical revolution, R_T is the resolution of the proposed detection technique and N_s is the switching steps per electrical cycle. For the implemented prototype with Maxon EC 45 motor: N_C=8, N_S=6, R_E=45º and R_T=7.5º.

The sequence for activating the power switches *Q1* to *Q6* for clockwise motor rotation is shown in Table 3. The rotor position in electrical and mechanical degrees for Maxon EC 45 motor is only included for the first electrical cycle of one mechanical revolution.

Table 3. Sequence for clockwise rotation and rotor position in electrical and mechanical degrees

Sequence Number	Phase to Phase Voltage	Active PWM		Motor phases			Rotor position (1/8 mechanical cycle)	
		High switch	Low switch	A	B	C	Electrical degrees	Mechanical degrees
1	V_{ab}	PWM1	PWM4	On	On	Off	0-60º	0-7.5º
2	V_{ac}	PWM1	PWM6	On	Off	On	60º-120º	7.5º-15º
3	V_{bc}	PWM3	PWM6	Off	On	On	120º-180º	15º-22.5º
4	V_{ba}	PWM3	PWM2	On	On	Off	180º-240º	22.5º-30º
5	V_{ca}	PWM5	PWM2	On	Off	On	240º-300º	30–37.5º
6	V_{cb}	PWM5	PWM4	Off	On	On	300º-360º	37.5º-45º

3.2 PWM motor driving

PWM signals (*PWM1* to *PWM6*) are connected to the base of the power transistors in Fig. 1, and are switched on/off according to the sequence indicated in Table 3. For varying the speed, the voltage across the motor must be modified, which could be achieved by changing the duty cycle of the PWM signals or configuring the commutation period between phases T_C with a fixed PWM frequency and duty cycle. When the duty cycle is modified, the average voltage supplied to the stator changes, thus affecting the speed. However, the variation of PWM duty cycle is limited by the switching characteristics of active power devices, whose switching period is determined by turn-on and turn-off delays. These restrictions can be overcome if the device switching period is fixed at the minimum level and the speed is controlled by changing the commutation period between phases.

One advantage of using PWM signals for controlling the motor is the flexibility for hooking up motors with different rated voltages. It is achieved owing to the average voltage output of the controller can be matched to the motor rated voltage by limiting the percent of PWM duty cycle. With this consideration, PWM techniques are very important in the controller design for a low noise operation and running at higher speeds [1]. Because of only two out of three phases are excited at any instant time, the BLDC motor can be driven with different PWM configurations [20]. PWM signals could be only applied on the high side switch and the low side is active during the step, PWM applied on the low side switch and high side enabled during the step, or PWM applied on both sides and switched on / off together [21, 22]. Other special PWM techniques could be applied for reducing the influence of the switching noise in the position sensing and optimizing the rotor position tracking at low speeds. This improvement can be achieved by splitting the active period of each switch into two intervals, so each switch is held in on state during the first interval and PWM switching is executed during the second [4].

The controller has been designed for applying PWM signals on both sides. Frequency and duty cycle configuration of PWM signals has been optimized according to the switching characteristics of UC2950T devices summarized

in Table 2. A PWM frequency of 20 kHz and a duty cycle of 50% have been selected after different evaluation tests. The rotor speed ω_R is configured by changing the commutation period between phases T_C, so for a higher speed a lower period is needed. PWM signals have been designed for being generated with the FPGA processing board sbRIO-9636 with an output high level of 3.3 V. Fig. 3 illustrates this procedure with a duty cycle $D=T_{ON}/T_{PWM}$; where T_{ON} is fixed at the optimum switching time of power devices and T_C is varied for different speeds.

3.3 Starting from standtill

The problem of conventional open-loop start-up methods exists when the motor is at standstill or operates at low speeds. In this situation, phase voltages have not an enough level and the signal-to-noise ratio is too small, so it is very difficult to get the position information from the motor. The most common method for solving this problem is the open-loop start-up with three states: alignment, open-loop starting and open-loop speed control mode [23]. When the motor is running at a minimum speed, motor signals have a detectable level and a closed-loop control mode can be applied [24]. Other methods are based on the saturation effect of the stator iron core [25] or in a 180-degree commutation scheme [26] for improving the use of machine capacity regarding to the 120-degree method.

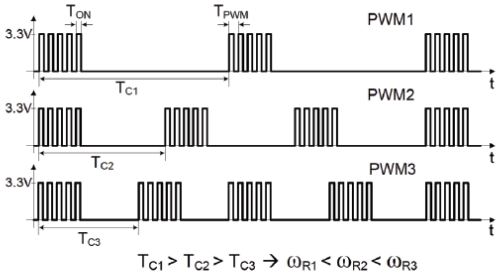

Fig. 3. PWM procedure for configuring the rotor speed ω_R in the experimental set-up.

The estimation of the rotor initial position plays a relevant role for a stable starting with maximum torque in order to reduce the start-up time. A simplified open-loop starting is accomplished by providing switching signals to motor with a frequency ramp model based on the sequence shown in Table 3. The rotor is linearly accelerated up to a reference speed, which is more effective and easier to implement than other techniques for similar applications [2]. Some of the traditional drawbacks of this type of techniques, such as the oscillation of the rotor speed with a temporary reverse rotation [25], are not relevant enough in the current implementation.

In a traditional BEMF-based method, a minimum speed level is needed before position detection since the BEMF voltage is proportional to the rotating speed [17]. However,

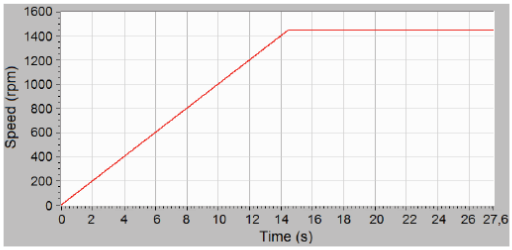

Fig. 4. Starting speed ramp up to 1450 rpm

the proposed detection technique does not depend on the BEMF level and only phase voltage changes are considered. In this paper, an open-loop ramping control scheme is adopted to accelerate the motor without using a previous alignment, which simplifies the starting. The rotor position and speed are detected with enough precision at very low speeds, so the commutation signal could be estimated accurately near to standstill and a closed-loop scheme can be applied. Fig. 4 illustrates the speed ramp used in the experimental set-up for accelerating up to a reference speed of 1450 rpm.

The start-up algorithm has been implemented in the processing board sbRIO-9636 in order to achieve a real-time and deterministic behavior. The generation of PWM signals is embedded in a FPGA Spartan 6 with a clock frequency of 40 MHz, obtaining a precise PWM cycle with setup and hold times lower than 50 ns. The control sequence of power switches indicated in Table 3 is integrated in a real-time processor.

The flow chart of the starting algorithm is included in Fig. 5. The motor is accelerated by increasing the speed according to a ramp shape, whose slope determines the acceleration up to the limit speed. The prototype is configured for a slope with unit value, as Fig. 4 shows. Depending upon the application, other slopes could be selected for starting the motor faster or slower. When the speed limit is reached, the motor rotates at this speed in steady mode. A pink circle indicates the loop for generating PWM signals at 20 kHz and 50% duty cycle using the FPGA. These signals are transmitted to the inverter switches for performing the commutation. A new electrical cycle starts if the sequence counter reaches N_S-1 iterations, and the instantaneous switching loop period is computed according to the rotor speed, as Eq. (15) indicates.

$$T_{SW}(us) = \frac{60 \cdot 10^6 \, \mu s / \min}{K_P \cdot N_S \cdot \omega_i} \tag{15}$$

where ω_i is the instantaneous motor speed in rpm.

4. Detection Technique Implementation

The derivative technique is based on applying the

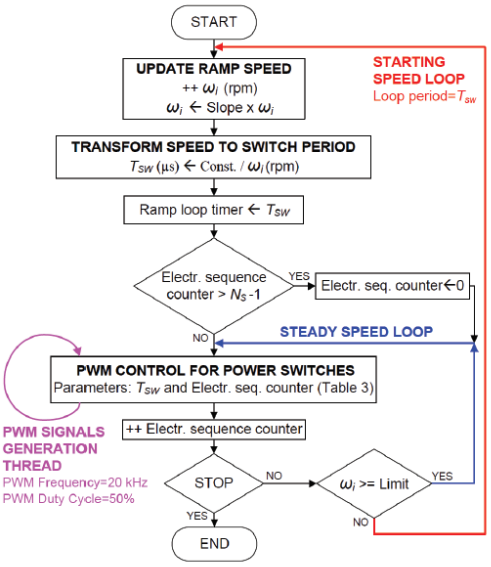

Fig. 5. Flow chart of starting algorithm and steady running mode

mathematical operation of differentiation to the phase motor voltages with a virtual neutral point as reference. The points when the motor voltage varies due to a phase commutation are detected as voltage peaks or spikes. With this approach, it is not necessary to sense noise-sensitive zero crossing points as the conventional BEMF method, so the hardware and software implementation is cost effective and less complex. In addition, two phase voltages are only needed for detecting speed and position, and the third voltage can be obtained due to the structure of the six-step sequence used for driving the motor.

4.1 Conditioning of motor signals

In order to obtain the derivative of phase voltages in real-time without the influence of processing delays, specific conditioning hardware has been developed. Based on the general scheme of Fig. 1, the hardware stages for conditioning motor phase voltages V_a, V_b and V_c regarding to the virtual neutral point S and derivation spikes train are depicted in Fig. 6. Taking as reference the phase A (similar to phases B and C), the differential voltage V_{as} is amplified. However, switching noise is also amplified with the phase voltage, so filtering is necessary for reducing the influence of high frequency components. Voltage limiters are also included for adapting the signal to the input levels of processing board. Next, the derivative operation is applied to the amplified phase voltage, and "ghost" spikes that could be obtained from undesirable voltage level changes are filtered. This filter must be designed in order to obtain voltage spikes narrow enough (low rise and fall times) for a precise detection of phase commutations. An additional

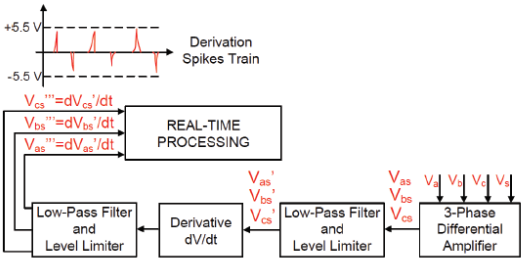

Fig. 6. Block diagram of conditioning hardware

voltage level limiter is included before sending the signal dV_{as}/dt to the processing card.

The voltages V_{as}, V_{bs} and V_{cs} are used in the measurement process according to Eqs. (4)-(6), so the motor neutral reference is not considered and a relevant amount of switching noise is avoided. Due to motor voltages are differential amplified, the three motor phase voltages V_a, V_b and V_c and the virtual neutral potential V_s. are assumed as inputs of the conditioning hardware module, as Eqs. (16)-(18) demonstrate.

$$V_{as} = V_{an} + V_{ns} = V_a - V_n + V_n - V_s = V_a - V_s \quad (16)$$

$$V_{bs} = V_{bn} + V_{ns} = V_b - V_n + V_n - V_s = V_b - V_s \quad (17)$$

$$V_{cs} = V_{cn} + V_{ns} = V_c - V_n + V_n - V_s = V_c - V_s \quad (18)$$

The development of accurate and low noise signal conditioning stages is based on precision differential amplifiers Texas Instruments INA126. Fig. 7 shows only the required circuitry for the phase A (similar for phases B and C). Decoupling capacitors has been included close to the device power pin for avoiding the effect of noisy power supplies. The power supply voltage V_{DC} is 12 V or 24 V depending on the BLDC motor nominal voltage (12 V for Maxon EC45). The gain G is set to 5 V/V for an appropriate amplification within the permissible levels. A good common-mode rejection with a low-impedance connection to reference ground terminal is ensured with this implementation. Fig. 9(a) depicts the phase voltage V_a and the differential voltage V_{as}'. It has been verified that the voltage waveforms depicted in Fig. 9 are very similar using the prototype set-up with or without load.

After the amplification process, phase voltages are filtered

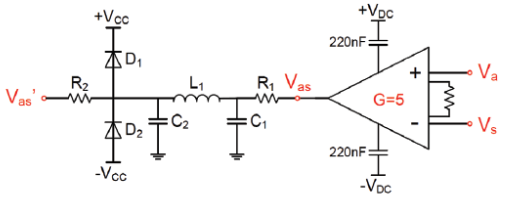

Fig. 7. Differential amplification of the phase A voltage with low-pass filters and a voltage/current limiter

for reducing the voltage ripple, the inverter switching noise and other high frequency components on the ground terminal owing to motor currents. Filtering is composed of a conventional low-pass filter and a PI-low-pass filter in cascade. The first one reduces voltage ripples and the second one enables a fine adjustment for smoothing the current provided to the load. Eqs. (19) and (20) indicate the cut-off frequency of the first low-pass filter (f_{c1}) and PI-low-pass filter (f_{c2}), respectively, both with a voltage gain of 1. A spectral analysis through FFT has been performed for selecting both cut-off frequencies. The first filter is more restrictive, so its cut-off frequency is lower (7 kHz to 20 kHz), and the second filter has a greater frequency for attenuating spurious high-frequency components (100 kHz to 200 kHz).

$$f_{c1} = \frac{1}{2 \cdot \pi \cdot R_1 \cdot C_1} \tag{19}$$

$$f_{c2} = \frac{1}{2 \cdot \pi \cdot \sqrt{L_1 \cdot C_2}} \tag{20}$$

Before transmitting signals to the processing board, the filtered differential voltages must be limited for avoiding damages due to overvoltages, undervoltages and over-currents. A current limiting resistor (R_2) is included and a diode clamping circuit with Schottky rectifiers 1N5817 (D_1, D_2) is used as overvoltage / undervoltage protection (V_{CC}=5V). Taking into account that the maximum current for measuring each voltage is 10 mA and the forward voltage (V_F) of 1N5817 devices is 0.22 V for 25 ºC operation, the valid range of V_{as}' is between $V_{CC}+V_{FD1}$ and $-(V_{CC}+V_{FD2})$ which is 5.22 V and -5.22 V respectively.

4.2 Derivative operation

This process is the key of the detection method and a train of voltage spikes for each phase is obtained after its application. Each spike indicates when a phase commutation occurs, so after an adequate processing the rotor position and speed is extracted. The implementation is performed for obtaining real-time results and eliminating processing delays. The operational amplifier Texas Instruments LM258AP is used owing to its good characteristics of common-mode rejection ratio (80 dB) and slew rate (0.3 V/µs at unity gain) with a low input noise voltage (40 nV/√Hz). Fig. 8 illustrates the hardware implementation for the phase A (similar for phases B and C). Based on this circuit, Eq. (21) represents the derivative operation.

$$V_{as}'' = -R_3 \cdot C_3 \cdot \frac{dV_{as}'}{dt} \tag{21}$$

where the constant $R_3 \cdot C_3$ is low enough ($\approx 10^{-3}$) for compensating the high level of voltage spikes due to phase commutations. Fig. 9(b) shows the waveforms of V_{as}' and

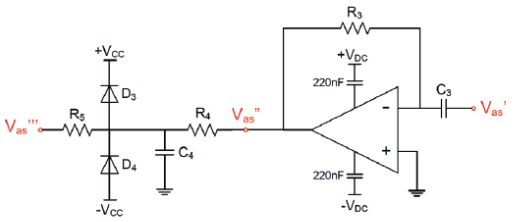

Fig. 8. Derivation of the differential phase voltage A with a filter and a voltage / current limiter

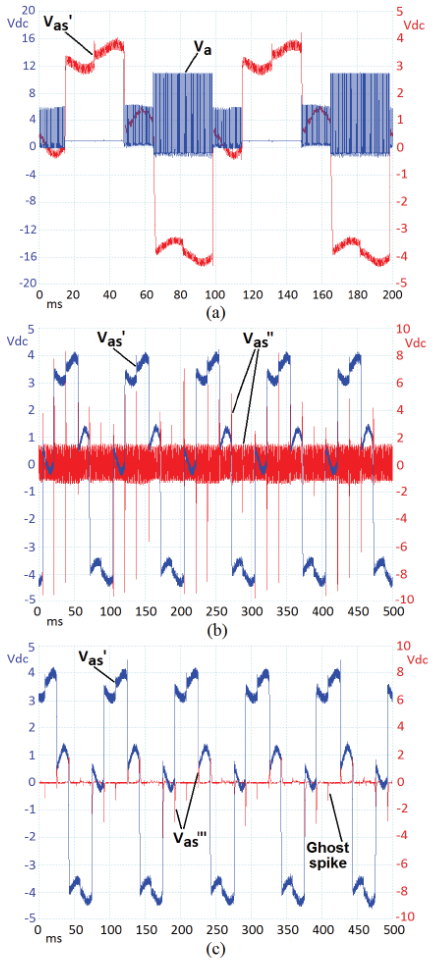

Fig. 9. Measured waveforms with the motor running at 75 rpm. (a) Phase voltage V_a and differential filtered voltage V_{as}'; (b) V_{as}' and derivative voltage V_{as}''; (c) V_{as}' and filtered derivative voltage V_{as}'''.

V_{as}'' with the motor running at 75 rpm.

The derivation voltage spikes train must have an adequate level for the subsequent FPGA processing, so filtering and level limiting are needed. The cut-off

frequency of the low-pass filter (f_{c3}) must be matched to the maximum detectable rotor speed, so in the current implementation for medium-high speeds the cut-off frequency is between 300 Hz and 1000 Hz, according to Eq. (19) with *R4* and *C4* instead of *R1* and *C1*. Fig. 9(c) shows the waveforms of V_{as}' and V_{as}'''' at 75 rpm. The comparison of this figure regarding to Fig. 9(b) demonstrates the efficiency of filtering for removing high-frequency spurious from derivative voltage spikes.

In a similar way to the previous design, a current limiting resistor (R_5) and a diode clamping circuit (D_3, D_4) for overvoltage/undervoltage protection are included in Fig. 8. Considering a maximum current 30 mA for transmitting the spikes train, the diode forward voltage is near to 0.25 V, so the valid range of V_{as}'' is between −5.25 V and 5.25 V.

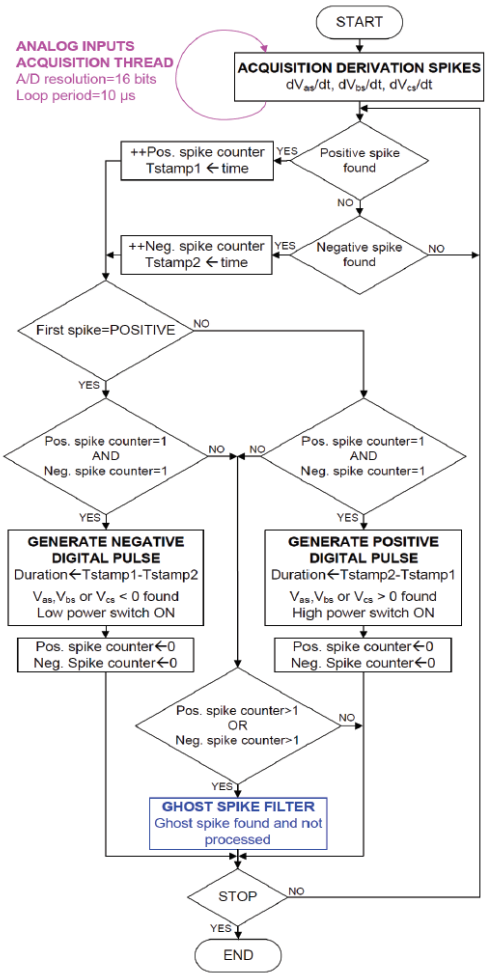

Fig. 10. Flow chart of the algorithm for processing the phase voltage derivation

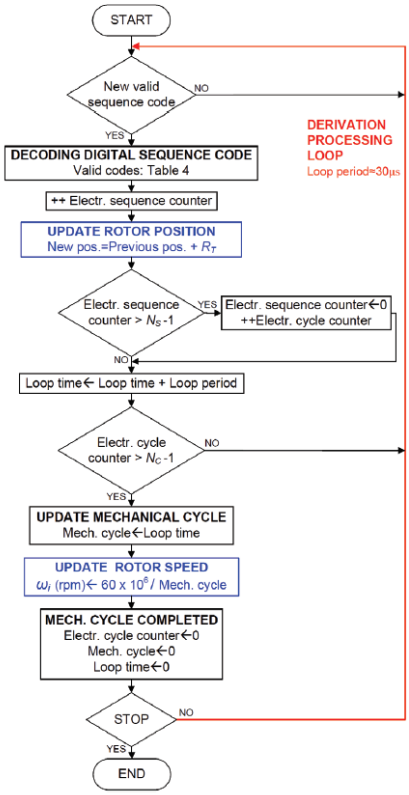

Fig. 11. Flow chart of the decoding algorithm for updating the rotor position and speed

4.3 Processing software and algorithms

The algorithms embedded in FPGA and real-time processor for computing the rotor position and speed are explained through two flow charts.

The processing of the derivation voltage is depicted in Fig. 10. Analog voltages are acquired with an execution thread of 10 µs rate period (half of the minimum signal period as Nyquist sampling theorem exposes) with a 16-bit resolution. Voltage detectors are used for obtaining positive and negative digital pulses according to the spikes train of the derivative operation. A positive digital pulse is generated when a negative and a positive voltage spikes are detected successively. By contrast, a negative pulse is obtained if a positive and a negative voltage spikes appear, as see Fig. 12(a) depicts. For each electrical cycle six pulses are obtained, so six digital codes must be considered for the rotor position detection, as Table 4 indicates.

The commented flow chart includes a Ghost Peak Filter for rejecting the derivation spikes that are not compliant with the digital pulse generation criteria. For instance, if two negative spikes are detected successively, the second is removed because the algorithm waits a positive spike for

obtaining a positive digital pulse. The origin of ghost peaks is fluctuations in the differential phase voltage that induces incorrect derivation spikes.

The flow chart of the position/speed decoding algorithm is illustrated in Fig. 11, where the processing loop lasts 30 µs. When a new sequence code is detected, if it is validated, a new electrical sequence step is identified. The rotor position is updated according to the previous position and the resolution of Eq. (14), and the rotor speed is computed with the elapsed time for completing a mechanical cycle.

The operation of the derivation technique for phase A is illustrated in Fig. 12(a), where negative digital pulses are included for remarking the sign of the phase voltage detected, but they are processed as '0' or '1'. Derivation spikes are shown, and a ghost spike is also depicted, which is filtered by the processing algorithm. Fig. 12(b) depicts the processed voltages V_{as} and V_{bs} and their associated digital pulses for position detection. Pulses of phase C can be obtained taking into the voltage of phases A and B, which contributes to reduce the computing requirements. The waveforms obtained after derivation processing are very similar with or without a motor load, obviously within the admissible speed ranges. With these considerations, the performance at full-load is only analyzed at low speed.

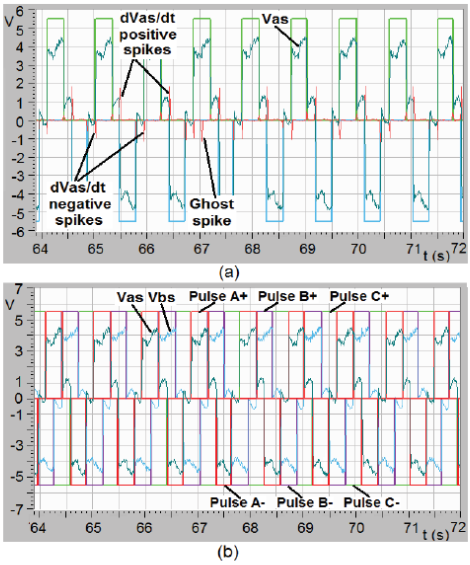

Fig. 12. Waveforms of derivation technique processing at 75 rpm. (a) V_{as}, derivative voltage V_{as}''' and digital pulses for phase A. (b) Sequence pulses for phases A, B and C

Table 4. Digital sequences for clockwise rotation

Sequence number	Phase to phase voltage	High switches			Low switches		
		A	B	C	A	B	C
		Q1	Q3	Q5	Q2	Q4	Q6
1	Vab	1	0	0	0	1	0
2	Vac	1	0	0	0	0	1
3	Vbc	0	1	0	0	0	1
4	Vba	0	1	0	1	0	0
5	Vca	0	0	1	1	0	0
6	Vcb	0	0	1	0	1	0

5. Experimental Results and Discussion

For evaluating the performance of the detection technique, an encoder has been used for establishing speed and position references. The rotor speed and position are analyzed through tests at different speeds in order to compare the values obtained with the detection technique and the encoder. No-load tests are aimed at low-medium speeds (5-1500 rpm) due to the most relevant limitations of conventional detection methods are located in these ranges, taken into account the specific limitations under no-load or full-load conditions. The load included in the prototype set-up behaves as a motor brake, and it has been configured in full-load tests for being equivalent to a torque between 52 and 53 mNm that opposes the motor rotation (maximum continuous torque of Maxon EC 45 motor is 53.2 mNm, see Table 1). Full-load tests are only analyzed at low speeds (under 150 rpm) due to the influence of the load over the maximum torque/speed ratio of the BLDC motor.

Fig. 13 shows the evaluation of the technique with sharp speed changes with no-load (or low load). At low speeds the detected speed is similar the reference. However, when speed is increased, the technique needs a stabilization time that causes an oscillation around the reference, such

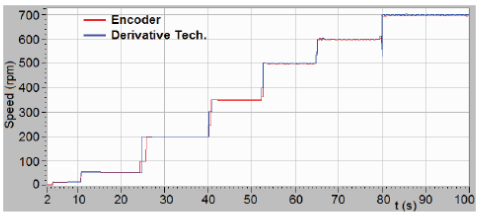

Fig. 13. Speed detection without load at 10 rpm, 50 rpm, 200 rpm, 350 rpm, 500 rpm, 600 rpm and 700 rpm

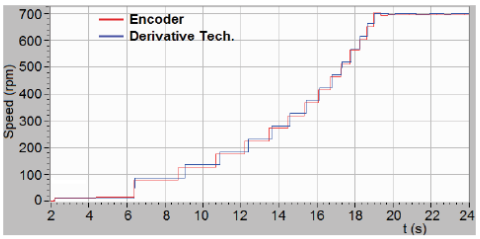

Fig. 14. Speed detection without load at 700 rpm from standstill

as the undershoot that appears in the change from 600 rpm to 700 rpm. Fig. 14 depicts the system response from standstill to 700 rpm, and it clearly illustrates how the detection technique tracks the reference speed line with a minimum error (square error lower than 3 rpm) and small oscillations.

Some tests have been accomplished for testing the position detection, as Fig. 15 and Fig. 16 illustrate. Normally, the detection system needs two mechanical periods for engaging with encoder position using a linear acceleration ramp from standstill. Considering the detection case of 700 rpm, Fig. 5 indicates that reference position is reached in 6 s with this acceleration scheme. With other starting configurations, like an exponential curve, the encoder position could be reached around 1-2 s. During the reference reaching time, the rotor speed is lower than 100 rpm (around 10-20 rpm according to Fig. 14), which demonstrates that the method is fast enough for a wide range of positioning applications. If the rotor speed is relatively low, the position reference is reached faster (under 1 s) and position oscillations in steady state are reduced, as Fig. 16 shows for 125 rpm. The position square error is between 10º-30º, which improves the performance of some complex estimation methods with resolution of 30º.

Fig. 17 and Fig. 18 depict the speed and position tracking of the technique in the range 5-150 rpm, respectively. Multiple speeds within this range have been considered for validating the accuracy and precision at full-load. As a result, the technique follows the reference speed with a square error lower than 1 rpm, the stabilization times between speed changes are reduced, and undershoots/ overshoots of speed are avoided regarding to no-load tests (see Fig. 13). The position tracking error with these conditions is between 10º-15º, according to Fig. 18.

In addition, Fig. 19 and Fig. 20 illustrate in detail that under full-load conditions the position ramps are more linear (slopes are almost constant from 0º to 360º), and the position/speed tracking of the technique is more stable against sharp speed changes (for instance, transition from 45 rpm to 8 rpm), due to the steps of motor sequences are also more progressive and less impulse owing to the "filter" effect that provides the load, which opposes motor inertia.

A detail of Fig. 17 and Fig. 19 must be clarified, where the speed tracking is only updated after finishing a full rotor mechanical cycle. This could be improved by modifying the algorithm of Fig. 11 in order to update the speed after each electrical cycle, which would provide a faster speed response. This is a common behavior with or without load, and that is the reason why the first speed step of 5 rpm starts in 13 s in both figures.

The experimental results indicate that the accuracy errors are lower with full-load tests than under no-load conditions. However, it must be taken into account than full-load tests are performed at low speeds, and position / speed errors tend to increase when the speed is higher due to the appearance of tracking faults, such as oscillations and under/over-shoots that influence over the accuracy and precision. In summary, the tests results in this section provide the evidence that the developed technique allows the estimation of the position and speed of BLDC motors (at no-load and full-load conditions) with relatively low

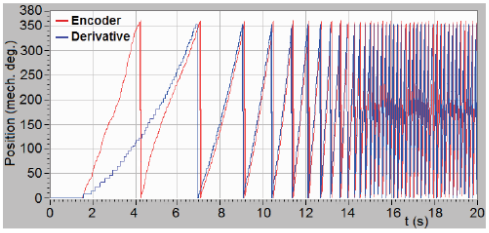

Fig. 15. Position detection without load at 700 rpm

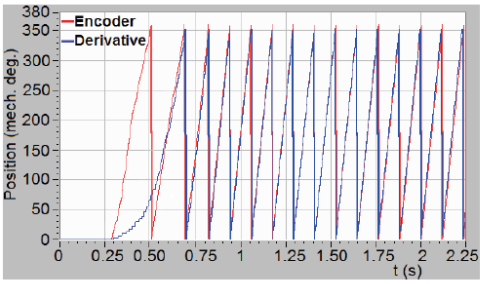

Fig. 16. Position detection without load at 125 rpm

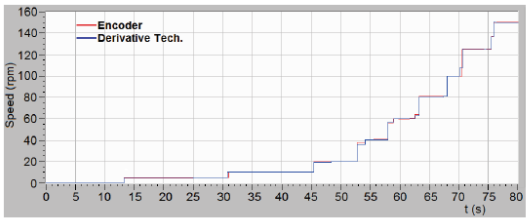

Fig. 17. Speed detection with full-load at 5 rpm, 10 rpm, 20 rpm, 40 rpm, 60 rpm, 80 rpm, 100 rpm, 125 rpm, and 150 rpm

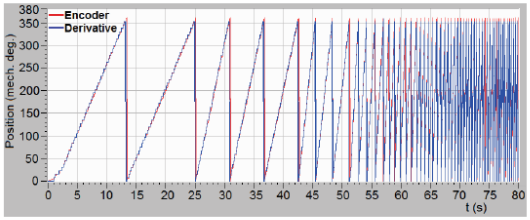

Fig. 18. Position detection with full-load at 5 rpm, 10 rpm, 20 rpm, 40 rpm, 60 rpm, 80 rpm, 100 rpm, 125 rpm, and 150 rpm

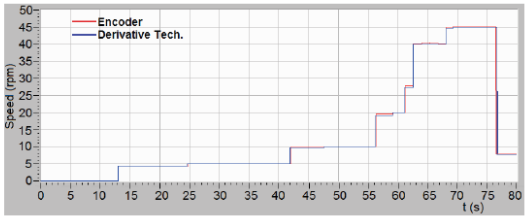

Fig. 19. Speed detection with full-load at 5 rpm, 10 rpm, 20 rpm, 28 rpm, 40 rpm, and 45 rpm, with a sharp speed change from 45 to 8 rpm

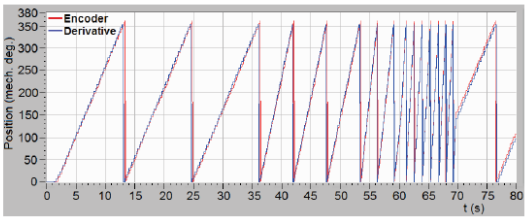

Fig. 20. Position detection with full-load at 5 rpm, 10 rpm, 20 rpm, 28 rpm, 40 rpm, and 45 rpm, with a sharp speed change from 45 to 8 rpm

accuracy errors over a wide speed range.

6. Future scope

An optimization of the proposed technique is the digital implementation of the derivative operation, including the low-pass filtering, inside the FPGA. A more advanced improvement is to pattern recognition techniques with the classifier Vector Machines (SVM) in order to consider the position and speed detection of BLDC motors as a problem of statistical learning theory, which will allow to map motor voltages to commutation signals.

7. Conclusion

An efficient position and speed detection technique for BLDC motors has been developed in this paper with a simple motor driver implementation and without using position sensors. Common disadvantages of methods based on sensors, such as high development and maintenance costs, are overcome with the new technique. It is based on the derivative of two or three motor terminal voltages regarding to a virtual neutral potential, and the implementation cost is minimized due to its reduced requirements with the use of general-purpose devices and a FPGA processing board. Though filters are used for avoiding the influence of inverter switching PWM signals, their effects over the dynamic performance are not relevant. Different models of motors have been considered for verifying the system, and the proposed technique has been validated in open-loop mode for starting-up in order to reach a reference speed using an improved position tracking, with and without load, over a wide speed range. In closed loop mode, it can be combined with a controller, such as PI or Fuzzy, for providing the feedback speed or position. Experimental results were performed in the range 5-1500 rpm and 5-150 rpm at no-load and full-load conditions, respectively. Speed and position square errors lower than 3 rpm and between 10º-30º were attained after no-load tests. The results with full-load tests improve the performance under no-load criteria, whose square errors are under 1 rpm and between 10º-15º for speed and position detection, respectively. Analyses performed throughout the paper and experimental results verify the effectiveness of the proposed technique for position and speed detection of BLDC motors under no-load and full-load conditions, and its operational performance regarding to similar techniques based on phase voltage sensing. The results were obtained with low accuracy errors over a relatively wide speed range, which suggest that the proposed technique is a reliable alternative to traditional sensorless detection approaches.

References

[1] J.C. Gamazo Real, E. Vázquez Sánchez, J. Gómez Gil, "Position and Speed Control of Brushless DC Motors Using Sensorless Techniques and Application Trends," *Sensors*, 10, July 2010.

[2] S. Tsotoulidis, A. Safacas, "A sensorless commutation technique of a brushless DC motor drive system using two terminal voltages in respect to a virtual neutral potential," *in Proceedings of 20th Int. Conf. Elect. Mach. (ICEM)*, pp. 830-836, 2-5 Sept. 2012.

[3] P. Damodharan, K. Vasudevan, "Sensorless Brushless DC Motor Drive Based on the Zero-Crossing Detection of Back Electromotive Force (EMF) From the Line Voltage Difference," *IEEE Trans. Energy Convers.*, vol. 25, no 3, pp. 661-668, Sept. 2010.

[4] R. C. Becerra, T. M. Jahns, M. Ehsani, "Four-quadrant sensorless brushless ECM drive," *in Proceedings of 6th Annu. Appl. Power Electron. Conf. and Expo. (APEC)*, pp. 202-209, 10-15 Mar 1991.

[5] J. Moreira, "Indirect sensing for rotor flux position of permanent magnet AC motors operating over a wide speed range," *IEEE Trans. Ind. Appl.*, vol. 32, no. 6, pp. 1394-1401, Nov./Dec. 1996.

[6] J. X. Shen, S. Iwasaki, "Sensorless control of ultrahigh-speed PM brushless motor using PLL and third harmonic back EMF", *IEEE Trans. Ind. Electron.*, vol. 53, no. 2, pp. 421-428, April 2006.

[7] P. P. Acarnley, J. F. Watson, "Review of position-sensorless operation of brushless permanent-magnet machines", *IEEE Trans. Ind. Electron.*, vol. 53, no. 2, pp. 352-362, April 2006.

[8] S. Ogasawara, H. Akagi, "An approach to position sensorless drive for brushless dc motors," *IEEE Trans. Ind. Appl.*, vol. 27, no. 5, pp. 928-923, Sep./Oct. 1991.
[9] T. M. Jahns, R. C. Becerra, M. Ehsani, "Integrated current regulation for a brushless ECM drive," *IEEE Trans. Power Electron.*, vol. 6, no. 1, pp. 118-126, Jan 1991.
[10] Chin-Long Cham, Z. B. Samad, "Brushless DC Motor Electromagnetic Torque Estimation with Single-Phase Current Sensing," *J. Electr. Eng. Technol.*, vol. 9, no. 3, pp. 866-872, May 2014.
[11] M. S. Zaky, M. Khater, H. Yasin, S. S. Shokralla, "Very low speed and zero speed estimations of sensorless induction motor drives," *Electr. Power Syst. Res.*, vol. 80, Issue 2, pp. 143-151, February 2010.
[12] M. Barut, "Bi Input-extended Kalman filter based estimation technique for speed-sensorless control of induction motors," *Energy Conv. Manag.*, vol. 51, Issue 10, pp. 2032-2040, October 2010.
[13] J. Maes, J. A. Melkebeek, "Speed-sensorless direct torque control of induction motors using an adaptive flux observer," *IEEE Trans. Ind. Appl.*, vol. 36, no. 3, pp. 778-785, May/Jun 2000.
[14] Yih-Neng Lin, Chern-Lin Chen, "Adaptive pseudo reduced-order flux observer for speed sensorless field-oriented control of IM," *IEEE Trans. Ind. Electron.*, vol. 46, no. 5, pp. 1042-1045, October 1999.
[15] B. K. Bose, "Fuzzy logic and neural networks in power electronics and drives," *IEEE Ind. Appl. Mag.*, vol. 6, no. 3, pp. 57-63, May/June 2000.
[16] I. Kenichi, U. Hideo, K. Minoru, E. Tsunehiro, M. Katsuo, "Microcomputer Control for Sensorless Brushless Motor," *IEEE Trans. Ind. Appl.*, vol. 21, no. 3, pp. 595-601, 1985.
[17] Kuang-Yao Cheng, Ying-Yu Tzou, "Design of a sensorless commutation IC for BLDC motors," *IEEE Trans. Power Electron.*, vol. 18, no. 6, pp. 1365-1375, Nov. 2003.
[18] Y. Gao, Y. Liu, "Research of sensorless controller of BLDC motor," *in Proceedings of 10th IEEE Int. Conf. Ind. Inform. (INDIN)*, pp. 725-728, 25-27 July 2012.
[19] Sang-Hoon Song, Yong-Ho Yoon, Byoung-Kuk Lee, Chung-Yuen Won, "Autonomous Underwater Vehicles with Modeling and Analysis of 7-Phase BLDC Motor Drives," *J. Electr. Eng. Technol.*, vol. 9, no. 3, pp. 932-941, May 2014.
[20] Yen-Shin Lai, Fu-San Shyu, Yung-Hsin Chang, "Novel loss reduction pulsewidth modulation technique for brushless dc motor drives fed by MOSFET inverter," *IEEE Trans. Power Electron.*, vol. 19, no. 6, pp. 1646-1652, Nov. 2004.
[21] J. Shao, D. Nolan, M. Teissier, D. Swanson, "A novel microcontroller-based sensorless brushless DC (BLDC) motor drive for automotive fuel pumps," *IEEE Trans. Ind. Appl.*, vol. 39, no. 6, pp. 1734-1740, Nov./Dec. 2003.
[22] M. Shanmugapriya, P. A. Michael, "Sensorless control of an four switch three phase inverter using FPGA," *in Proceedings of Int. Conf. Adv. in Eng., Sci. and Manage. (ICAESM)*, pp. 689-693, 30-31 March 2012.
[23] Kai-Sheng Kan, Ying-Yu Tzou, "Adaptive soft starting method with current limit strategy for sensorless BLDC motors," *in Proceedings of IEEE Int. Symp. Ind. Electron. (ISIE)*, pp. 605-610, 28-31 May 2012.
[24] Hung-Chi Chen, Chang-Ming Liaw, "Current-mode control for sensorless BDCM drive with intelligent commutation tuning," *IEEE Trans. Power Electron.*, vol. 17, no. 5, pp. 747-756, Sep. 2002.
[25] M. Tursini, R. Petrella, F. Parasiliti, "Initial rotor position estimation method for PM motors," *IEEE Trans. Ind. Appl.*, vol. 39, no. 6, pp. 1630-1640, Nov.-Dec. 2003.
[26] M. A. Noroozi, J. S. Moghani, J. Mili Monfared, H. Givi, "Sensorless starting method for Brushless DC Motors using 180 degree commutation," *in Proceedings of 3rd Power Electron. and Drive Syst. Technol. (PEDSTC)*, pp. 57-61, 15-16 Feb. 2012.

José Carlos Gamazo Real He received M.S. degree in Telecommunications engineering from University of Valladolid. His research interests are sensorless technology, mechatronics, and aerospace systems engineering.

Jaime Gómez Gil He received M.S. degree in electrical engineering from University Valladolid. His research interests are sensorless technology and agricultural engineering.

Capítulo 5: Artículo 4 del compendio

En este capítulo se analiza el cuarto artículo del compendio, el cual incluye el desarrollo de una técnica *sensorless* de estimación de la posición y velocidad para motores *brushless* DC (BLDC), utilizando dos redes neuronales artificiales tipo *Multilayer Perceptron* en base a la información proporcionada por los voltajes de fase del motor, y con el uso de la plataforma *driver* de motores desarrollada en la tesis para este tipo de motores. En este capítulo se incluye la información bibliográfica del artículo, así como otros datos y análisis referidos al ámbito, motivación y originalidad del mismo. Al final del capítulo se incluye el extracto del artículo enviado a la revista *IEICE Transactions on Fundamentals of Electronics, Communications and Computer Sciences* en marzo de 2015, y el cual se encuentra en proceso de revisión.

5.1 Datos bibliográficos

TITULO: A Sensorless Technique for Position and Speed Estimation of Brushless DC Motors with Neural Networks.

AUTORES: José Carlos Gamazo-Real, Víctor Martínez-Martínez, Jaime Gómez-Gil.

REVISTA: IEICE Transactions on Fundamentals of Electronics, Communications and Computer Sciences.

EDITOR: IEICE, Institute of Electronics, Information and Communication Engineers (Tokio, Japón).

FECHA DE ENVÍO: 21 de marzo de 2015. Actualmente se encuentra en estado de revisión (*Manuscript ID*: 2015EAP1049).

ISSN: 1745-1337.

5.2 Resumen

Este artículo presenta una técnica *sensorless* para estimar la posición y velocidad de motores BLDC mediante el uso de Redes Neuronales Artificiales (ANN). La técnica desarrollada está compuesta de dos redes neuronales *Multilayer Perceptron* (MLP); una de las cuales se utiliza para estimar la posición del rotor a partir de los voltajes del motor, y la otra para estimar la velocidad a partir del resultado de posición de la red anterior. En el entrenamiento y *test* de las redes neuronales, se han utilizado como referencia los datos de posición de un *encoder* incremental, y se han procesado los voltajes de fase del motor por medio de una matriz de puertas programable en campo (FPGA), un procesado en tiempo real, electrónica específica de acondicionamiento de señales y un ordenador. En los *tests* experimentales se ha obtenido unos resultados con un error de posición absoluto medio de 6,47º y un error de velocidad relativo medio de 4,87% en el rango de velocidades 125-1500 rpm. De esta forma, los resultados indican que la técnica propuesta permite la estimación de la posición y velocidad de motores BLDC con una precisión aceptable en un amplio rango de velocidades, lo cual representa una alternativa fiable con respecto a otros enfoques *sensorless* de detección tradicionales.

5.3 Fundamentos de las redes neuronales MLP

El Perceptrón Multicapa o MLP constituye el modelo de ANN más utilizado en la práctica, tanto para la resolución de problemas de clasificación como de regresión, al haber demostrado su condición de aproximación para la mayor parte de las funciones existentes. Este modelo de ANN surgió en los años 80 como una solución para superar el problema detectado en el Perceptron Simple, es decir, la imposibilidad de aprender clases de funciones no linealmente separables. Se caracteriza por su organización en capas de celdas disjuntas, de forma que ninguna salida neuronal constituye una entrada para las neuronas de la misma capa o de capas previas, evitándose así las conexiones autorecurrentes. De esta forma, la arquitectura del Perceptrón Multicapa coincide con el Perceptrón Simple, con la única diferencia de la inclusión de una o varias capas ocultas [107], tal y como se puede apreciar en la Figura 10. Mediante la aplicación del Teorema de Kolmogorov, Hetch-Nielsen demostró que una arquitectura de características similares al MLP y con una única capa oculta resultaba ser un aproximador universal de funciones.

Otro aspecto importante de las redes MLP lo representa el aprendizaje, el cual constituye un caso especial de aproximación funcional, donde no existe ninguna consideración previa acerca del modelo correspondiente a los datos analizados. De esta forma, el proceso de aprendizaje supone encontrar una función que represente correctamente los patrones de aprendizaje, además de llevar a cabo un proceso de generalización que permita tratar de forma eficiente casos no analizados durante el este proceso. En este sentido, dado un conjunto de pares de patrones de aprendizaje y una

función de error, el proceso de entrenamiento implica la búsqueda de un conjunto de pesos que **minimiza el error de aprendizaje**, es decir, el error entre los valores estimados y los valores medidos procedentes del conjunto de muestras. Existen múltiples algoritmos de aprendizaje, los cuales pueden clasificarse según distintos criterios, como el orden de la función de error, el tipo de actualización de los pesos, o el tipo de minimización local o global. Entre ellos destaca el algoritmo *Backpropagation*, que es el algoritmo de aprendizaje supervisado de gradiente descendiente más usado (es decir, **el aprendizaje busca un mínimo global de la función de error**), a pesar de que posee una convergencia muy lenta y puede provocar la caída en un mínimo local. Otros algoritmos son el de Quasi-Newton y el de Levenberg-Marquardt.

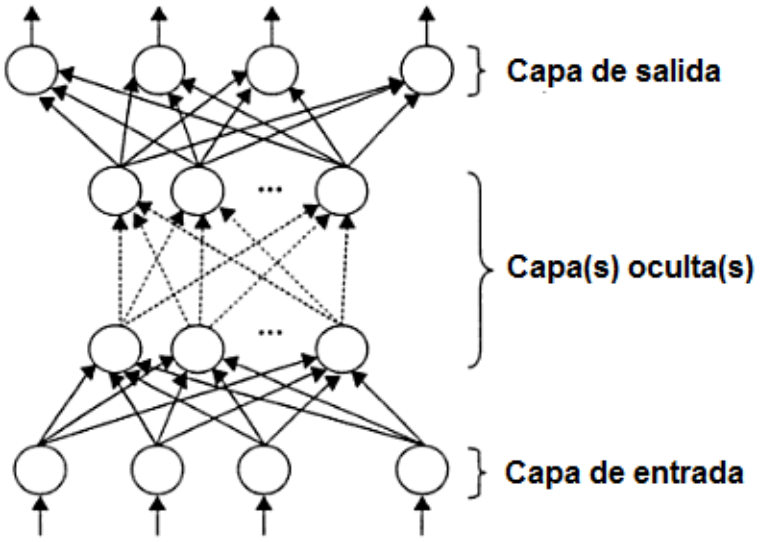

Figura 10. Arquitectura del Perceptrón Multicapa (MLP) [107].

5.4 Ámbito

Dentro de la revista indicada este artículo se incluye en la sección *Systems and Control*. Esta revista cubre diferentes áreas como el procesamiento de señales analógico y digital, teoría de circuitos, análisis numérico y optimización, señales y teoría de comunicaciones, tecnologías de medida o redes neuronales [108].

El interés de este artículo dentro del ámbito de la revista radica en la aplicación de la tecnología de redes neuronales a la estimación parámetros en motores eléctricos como son la velocidad y la posición, lo cual cubre varias ramas de la temática de la revista como son redes neuronales, procesamiento analógico de señales, tecnologías de medida y sistemas de control.

5.5 Justificación en el marco de la tesis

La técnica *sensorless* incluida en este trabajo se encuadra dentro de la **Etapa 4 de la metodología**, y permite alcanzar el **Objetivo 5** de la tesis. En este objetivo se plantea el

desarrollo de una técnica *sensorless* de detección de la posición y velocidad para motores BLDC basada en aplicación de redes neuronales artificiales MLP a los voltajes de fase del motor con respecto a un punto neutro virtual. En esta técnica se profundiza en el estudio de técnicas *sensorless* avanzadas, puesto que la extracción de información de los voltajes de fase del motor se realiza con una tecnología relativamente más compleja que únicamente la aplicación de conversiones básicas a los voltajes o corrientes del motor y detectar pulsos o niveles de señales. Se han utilizado dos redes neuronales MLP, la primera estima la posición con la información de los voltajes y la segunda utiliza la información de posición para estimar la velocidad. Para la adquisición y acondicionamiento de los voltajes de fase del motor utilizados para el entrenamiento con el algoritmo *Backpropagation* de las redes neuronales y validación de la técnica se ha empleado la plataforma *driver* de motores considerada en la Etapa 4 de la metodología, la cual ha sido aplicada también en el **Artículo 3 del compendio**. Debido a esto se consigue reducir el ruido que afecta a las señales del motor por la propia configuración del *hardware* que constituye el *driver*, basado en amplificadores de instrumentación, filtros y el uso de un punto neutro virtual para las señales del motor. Debido también al uso de la plataforma *driver* se ha empleado un *encoder* incremental para proporcionar referencias de posición fiables en los *tests* de validación. En estos *tests* se han analizado las estimaciones de posición y velocidad en un amplio rango de velocidades, obteniéndose unos resultados con una precisión sólo ligeramente mejor que otras técnicas con una resolución típica de 7,5º para un motor de 8 polos, y con una baja influencia sobre la estimación de velocidad de los errores de posición. Sin embargo, el coste computacional de la técnica es relativamente elevado debido al uso de redes neuronales. Tal y como muestran los resultados, la técnica permite estimar la posición y velocidad de motores BLDC con errores bajos y un rendimiento adecuado usando únicamente los voltajes de fase del motor, por lo cual puede concluirse que la técnica cumple con el objetivo impuesto.

Este artículo evidencia de forma relevante la profundización que se ha realizado en la investigación en técnicas *sensorless* para motores BLDC. De esta forma, el artículo constituye la culminación en la investigación para motores BLDC, al incluir una técnica *sensorless* avanzada. Teniendo esto en cuenta, la originalidad del mismo radica en explotar los conocimientos obtenidos a partir del Artículo 3 del compendio, en el cual se prueba el adecuado funcionamiento de la plataforma *driver* con la capacidad para controlar el motor, adquirir señales del mismo y procesar información del sensor de posición. De esta manera, al haber abordado con éxito todos estos aspectos, se puede plantear la aplicación de tecnologías mucho más complejas en la estimación de la posición y velocidad para motores BLDC, como es la inteligencia artificial (AI). Entre todas las disciplinas que engloba la AI, se han seleccionado las ANN a consecuencia de su creciente impacto en los últimos años en el área de la electrónica de potencia y *drivers* de motores, sobre todo debido a la capacidad de aproximar una amplia cantidad de funciones no lineales con exactitud [78, 109]. Adicionalmente, las ANN presentan características importantes como la tolerancia a fallos, la capacidad de procesamiento

paralelo, la habilidad de aprendizaje o la flexibilidad, que las convierten en un firme candidato para resolver problemas de *drivers* de motores. Algunos trabajos representativos son los realizados por Krishnan *et al.* [110] y por El-Sharkawi [111], en los que se aplican las ANNs de forma específica a *drivers* de motores PMSM y motores BLDC, respectivamente. Más concretamente, existen algunos trabajos más orientados a la temática del artículo propuesto, en los cuales se proponen técnicas *sensorless* para realizar la estimación de la posición y velocidad en motores PMSM, como los BLDC, pero a diferencia del artículo presentado (con ANNs de tipo MLP) se utilizan varias redes neuronales de otro tipo. Algunos artículos característicos de esta temática son los presentados por Li *et al.* [112] para motores PMSM utilizando una ANN de tipo recurrente diagonal (DRNN), por Juan *et. al* [113] para motores BLDC empleando dos ANNs de tipo *Radial Basis Function* (RBF), o por Fengtai y Dapeng [114] en el que la información de posición del motor BLDC se obtiene a partir de la estimación del vector de flujo de fase del estátor, y la red neuronal se usa para minimizar la suma de los errores cuadráticos entre los valores estimados y los actuales.

5.6 Extracto del documento

A continuación se incluye el Artículo 4 del compendio tal y como ha sido enviado a la revista *IEICE Transactions on Fundamentals of Electronics, Communications and Computer Sciences.*

PAPER

A Sensorless Technique for Position and Speed Estimation of Brushless DC Motors with Neural Networks

José Carlos GAMAZO-REAL[†a)], ***Student Member,*** **Víctor MARTÍNEZ-MARTÍNEZ**[†] **and Jaime GOMEZ-GIL**[†], ***Nonmembers***

SUMMARY This paper presents a sensorless technique for estimating the position and speed of BLDC motors by using Artificial Neural Networks (ANNs). The developed technique is composed of two Multilayer Perceptron (MLP) ANNs: one for estimating the rotor position from the motor voltages, and another one for rotor speed estimation from the position output of the previous one. In the training and testing of the ANNs, the position data of a shaft encoder was used as a reference and the real motor voltages were processed by means of a Field Programmable Gate Array (FPGA), a real-time processor, ad-hoc conditioning electronics, and a PC. A mean absolute position error of 6.47° and a mean relative speed error of 4.87% in the 125-1500 rpm range were achieved in the experimental tests. The results show that the proposed technique with two neural networks MLP allows the estimation of position and speed of BLDC motors with an acceptable precision over a wide speed range, which represents a reliable alternative to traditional sensorless detection approaches.

key words: *artificial neural network, brushless DC, multilayer perceptron, position/speed detection, sensorless.*

1. Introduction

Brushless DC (BLDC) motors, also called Permanent Magnet DC Synchronous motors (PMSM), are one of the motor types that have gained popularity more rapidly, mainly because of their better characteristics [1] and architecture suitable for any safety-critical applications. The application of BLDC motors to different areas, such as industry or automotive, has increased also because of their advantages over traditional brushed DC and induction motors: better speed and torque performance, high efficiency and reliability, long operating life and noiseless operation [2]. Due to the measurement of rotor position and speed is necessary for properly perform motor phases commutations, sensors are traditionally mounted inside the motor (Hall sensors) or externally attached on shaft (resolvers and encoders). However, these devices are subjected to stressful operating conditions, so position and speed measurements could be deteriorated. In order to overcome these disadvantages, sensorless techniques have arisen in recent years [3]. A brushless drive that does not require position sensors but only electrical measurements is called sensorless drive. The BLDC motors provides an attractive candidate for sensorless operation because the nature of its excitation offers a low-cost way to extract rotor position information from the motor terminal voltages.

In the last decades, many efforts have been made for rotor position and speed detection using sensorless techniques. There are many categories of sensorless detection strategies [4], but the most popular category is based on back electromotive forces (BEMF) [5], [6]. This category is split into two groups of techniques: *Direct and Indirect BEMF* detection. In Direct BEMF techniques, the back-EMF of floating phase is sensed and its zero crossing is detected by comparison with the neutral point voltage. This scheme suffers from high common mode voltage and high frequency noise, so low pass filters and voltage dividers are needed. Some of these techniques are Zero Crossing Detection (ZCD) of BEMF [7]-[9], and Pulse Width Modulation (PWM) strategies, such as the conventional 120º PWM technique [10] and the Direct Current controlled PWM technique [11]. Because of filtering introduces commutation delay at high speeds and attenuation causes reduction in signal sensitivity at low speeds, the speed range is narrowed in the Direct BEMF techniques. In order to reduce these effects, Indirect BEMF detection techniques are used, and the most popular are the following: BEMF Integration [12], Third Harmonic Voltage Integration [13], and Free-wheeling Diode Conduction State Detection [14].

However, owing to the importance of these types of motors in many applications, the limited low-speed performance of BEMF-based techniques, and that an open-loop starting strategy is required [15], advanced sensorless techniques based on *models and estimators*

†The authors are with the Department of Signal Theory, Communications and Telematics Engineering, University of Valladolid, Valladolid, 47011 Spain.
a)E-mail: jcgamazo@ribera.tel.uva.es

have arisen in recent years for improving the BLDC motors operation. Some of the most relevant are: Sliding-mode Observers (SMO), Extended Kalman Filter (EKF), Adaptative Observers, and Artificial Intelligence (AI) techniques. The *Sliding-mode Observers* are widely applied to nonlinear systems, such as BLDC motors, but several restrictions are found in the practice [16]. However, these observers are not restricted due to the convergence condition of estimation error towards zero [17]. An optimal estimation algorithm for nonlinear systems is the *Extended Kalman Filter*. It processes all available measurements regardless of their precision, and provides a quick and accurate estimation of the variables of interest with a rapid convergence [18]. The model uncertainties and nonlinearities in motors are well suited to the stochastic nature of EKF, as well as the measurement noises. Some innovative techniques are the Bi Input-EKF (BI-EKF) or the combination of EKF with the Model Reference Adaptative System (MRAS) [19]. Among Adaptative Observers, MRAS is one of many promising techniques employed in adaptative control for estimating the speed and stator resistance [17], such as in Field Oriented Control (FOC) [20]. Other Adaptative Observers are Adaptative Full-order Flux Observer (AFFO) [21] and Adaptative Pseudoreduced-Order Flux Observer (APFO) [22]. However, despite the progress of the advanced sensorless techniques previously commented, the use of *Artificial Intelligence techniques* for identification and control of nonlinear dynamic systems has been extended [23], such as Artificial Neural Networks (ANN), Expert Systems, Fuzzy Logic, or Genetic Algorithms [24].

Among all the branches of AI, ANNs seem to have a maximum impact on power electronics and motor drives area. The use of ANNs for identification and control has been extended as they are capable of approximating a wide range of nonlinear functions with a high degree of accuracy [23], [25]. An improvement in the field of ANNs is Fuzzy Neural Networks (FNN), which are techniques that apply neural networks principles to fuzzy reasoning and are based on rule or relational approaches [26]. Other modern powerful estimation methods can be developed for PMSM by applying hybrid artificial intelligence, neuro-genetic systems, or pattern recognition techniques like Support Vector Machines (SVM) [27]. Due to the relevance of their characteristics, like a parallel distributed structure, ability to learn, fault tolerance, nonlinearity and flexibility, ANNs are confirmed as a good candidate for solving problems of motor drivers [28], [29], and specifically the estimation of position and speed in PMSM motors [30]-[32] that is under interest on this paper.

The purpose of this paper is to develop a sensorless technique for estimating the position and speed of BLDC motors by using ANNs. In the developed technique, the rotor position and speed information are estimated with two Multilayer Perceptron (MLP) ANNs. The training of the ANNs are accomplished through the real motor voltages and the precise position data of an incremental shaft encoder, which are acquired and processed by means of a real-time motor driver prototype based on a Field Programmable Gate Array (FPGA). The testing of the estimation technique is performed with a real BLDC motor by comparing the rotor position and speed tracking regarding to the reference provided by the encoder. The description of the motor driver and the acquisition system is explained in section 2. The neural network algorithm and the training method are covered in section 3. In order to analyze the validity of the proposed technique, experimental results at different speeds are exposed in section 4. Finally, paper conclusions and contributions are considered in section 5.

2. Motor Driver and Data Acquisition System

The processing system is composed of modules for Pulse Width Modulation (PWM) control, motor signals conditioning, and acquisition, including the gathering of encoder position data used as reference for training and testing the ANNs. Its main elements are depicted in Fig. 1. In this paper, the motor data control and processing are based on a FPGA Xilinx Spartan-6 and a real-time processor. In addition, ad-hoc hardware has been developed for implementing the motor driver, such as a three-phase inverter with power transistors and free-wheeling diodes, and conditioning circuitry for amplification and filtering the motor phase voltages.

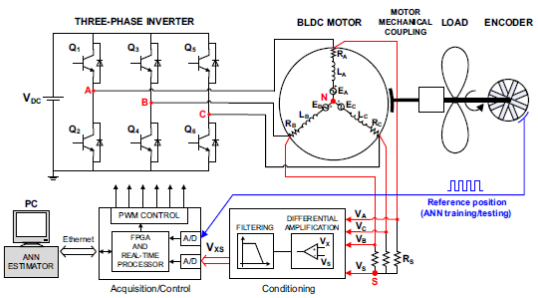

Fig. 1 Hardware used for BLDC motor driving, motor signals conditioning/acquisition, and testing the proposed technique.

In a conventional open-loop start-up scheme, the phase voltages do not have an enough level and the signal-to-noise ratio is too small when the motor is at standstill or operates at low speeds, so it is very difficult

to get the position information from the motor [33]. With these considerations, the estimation of the rotor initial position represents a relevant role for a stable starting with a maximum torque and a low start-up time. A simplified open-loop ramping model based on the activation sequence of Table 1 has been adopted to accelerate the motor without using a previous alignment. When the speed limit is reached, the motor rotates at this speed in steady mode with the coupled load. The implementation of the ANN model is performed with Matlab in a PC, and the motor data is transmitted from the real-time processor through an Ethernet link.

Table 1 Sequence for clockwise motor rotation and correspondence with the rotor position (*Kp*: rotor pole pairs).

Seq. number	Active transistors		Active phases			Rotor position	
	High	Low	A	B	C	Electrical	Mechanical
1	Q1	Q4	on	on	off	0-60°	0°-60°/K_P
2	Q1	Q6	on	off	on	60°-120°	60°/K_P -120°/K_P
3	Q3	Q6	off	on	on	120°-180°	120°/K_P -180°/K_P
4	Q3	Q2	on	on	off	180°-240°	180°/K_P -240°/K_P
5	Q5	Q2	on	off	on	240°-300°	240°/K_P -300°/K_P
6	Q5	Q4	off	on	on	300°-360°	300°/K_P -360°/K_P

The operation of the motor-phase inverter is based on a six-step sequence for stator winding commutation, as Table 1 shows. At any electrical sequence position, there is always a phase with its upper o lower leg in a disconnected state. Therefore, only two transistors of different phases are switched on at the same time, and any transistor of the open phase is enabled [14]. This performance can be used for predicting the six rotor position instants in an electrical cycle. A mechanical cycle is proportional to a number of electrical cycles according to Eq. (1).

$$T_M = K_P \cdot T_E \tag{1}$$

where T_M is the mechanical period, K_P is the number of rotor pole pairs, and T_E is the electrical period.

A typical brushless motor with a star configuration with respect to the neutral point N was previously shown in Fig. 1. Motor phase voltages regarding to the point N are characterized with Eq. (2) [32]. It could be considered that the motor is not saturated, iron losses are negligible, stator resistances (R) of all windings are equal, self-inductances (L) are constant, and mutual inductances (M) are near to zero [2].

$$V_{XN} = R \cdot I_X + (L - M) \cdot \frac{dI_X}{dt} + E_X \tag{2}$$

where x indicates the motor phase (A, B or C), E is the trapezoidal shaped BEMF, and I is the armature current.

In order to decrease the common mode noise that affects to terminal phase voltages, a virtual neutral point S has been provided in Fig. 1 with three star-connected resistors R_S [1], according to Eq. (3).

$$V_{XS} = V_{XN} + V_{NS} \tag{3}$$

where V_{NS} is the voltage between the neutral point N and the virtual point S.

The common mode noise due to the virtual node S can affect the acquired signals, which is avoided by using differential amplifiers with high common mode rejection ratio and low voltage noise. The use of filters is required to remove high frequency switching components of PWM inverter operation. Voltage level limiters are also included for adapting motor data to the input levels of the acquisition and control board.

With these assumptions, voltages V_{XS} are measured according to Eq. (3), so the motor neutral reference is not considered and a relevant amount of switching noise is avoided. However, due to the noise of the virtual node S can affect the acquired signals, differential amplifiers are used for avoiding this effect. Then, three motor phase voltages V_X and the virtual neutral potential V_S are assumed as inputs of the conditioning stage, as Eq. (4) indicates on the basis of the Eq. (3).

$$V_{XS} = V_X - V_S \tag{4}$$

After the amplification process, motor phase voltages are filtered for reducing the voltage ripple, the inverter switching noise, and other high frequency components on the ground terminal, without any relevant influence on the dynamic performance of the drive.

3. Neural Network Technique

3.1 Principles

ANNs are processing tools inspired in human neural systems that consist of a number of interconnected artificial neurons. They are widely used in the literature because of their input-output mapping capability, which consists of relating input and output variables without the need to understand the process that relates them [34].

Artificial neurons are simple processing units with an output value as a function of some input values. Perceptron is one of the most common neurons, which basically have a structure of an operational amplifier in adder mode. Firstly, each input signal of a perceptron (x_i) flows through a gain or weight (w_i). After that, all inputs signals are added with a bias value (b). The resultant signal passes to the output through a nonlinear or linear

transfer function called activation function (φ) [26]. Eq. (5) shows the characteristic equation of a perceptron.

$$y = \varphi \cdot \left(\sum_{n=1}^{N} x_i \cdot w_i + b \right) \quad (5)$$

The impact of ANNs in power electronics is significant on account of they can generate a nonlinear mapping between the inputs and outputs of an electric drive without the need for a predetermined model. Several issues must be considered in order to select the ANNs for practical applications, where the most relevant are the selection of the ANN structure, learning algorithm, activation functions, and the correlation, size and range of the training data [26], [29], [35].

In the proposed article, the designed ANN structure is a fully connected Multilayer Perceptron with 3 layers. The number of neurons at the input and output layers is selected depending on the number of input and output variables, respectively. A *trial-and-error* algorithm is used to obtain the neurons of the hidden layer, selecting the number of neurons which maximizes the success rate of the method after processing the validation samples dataset. The activation functions of the MLP neurons are the *tan-sigmoid* function for the hidden-layer neurons and a *linear* function for the output neurons. Tan-sigmoid functions have been specifically selected owing to they provide the capability for establishing non-linear relations among input and output variables, and their output values are limited to the range (-1, 1). On another side, linear functions allow a continuous non-limited output.

3.2 Algorithm

The proposed detection technique includes two methods for estimating the BLDC rotor position and speed, respectively, which are described next.

The position estimation method is developed with a 3-layer MLP-ANN that consists of 10 inputs, 5 hidden neurons, and 2 outputs, whose structure is depicted in Fig. 2. Due to the relationship between the motor phase voltages VXS and the rotor position (see Table 1), the inputs of the ANN are: 3 phase voltages in the actual acquisition time, 3 phase voltages of the previous time, 3 values obtained from the product of the voltages in the actual and previous acquisition times, and the acquisition timestamp difference between the previous and actual voltages. These inputs provide to the ANN the information about the actual rotor mechanical position and its change from the previous one. By processing these data, the proposed ANN estimates the mechanical position angle associated to the provided inputs. This angle is obtained by the ANN with the values of its sine and cosine components, and owing to the position angle is a periodic variable, two neurons are needed to encode it. The commented codification provides information to the ANN about the distance between the first and the last rotor position, so if both positions are near, the numeric difference is low [34]. The result is two ANN outputs that represent the encoded rotor position.

By means of the information included in Table 1, the position angle provided by the ANN is associated to one of the six electrical positions or sequence numbers (from 1 to 6) of the rotor. Moreover, the proposed algorithm considers also other six rotor positions that are associated to the transition between two consecutive electrical rotor positions, but starting in zero. For instance, a sequence number 2-3 indicates a rotor position that corresponds to a transition between the sequence numbers 2 and 3. These new positions provide a better resolution as they are used in the speed estimation ANN. The correspondence between an angle provided by the position-estimation ANN and the electrical rotor position (also called *equivalent sequence number*) is presented in Table 2.

Table 2 Correspondence between the electrical rotor positions and ANN outputs used for position estimation.

ANN estimated position	Equivalent seq. number	ANN output sin(θ)	ANN output cos(θ)
0°	0	0	1
30°	0-1	0.5	sqrt(3)/2
60°	1	sqrt(3)/2	0.5
90°	1-2	1	0
120°	2	sqrt(3)/2	-0.5
150°	2-3	0.5	-sqrt(3)/2
180	3	0	-1
210°	3-4	-0.5	-sqrt(3)/2
240°	4	-sqrt(3)/2	-0.5
270°	4-5	-1	0
300°	5	-sqrt(3)/2	0.5
330°	5-6	-0.5	sqrt(3)/2
360°	6 (=0)	0	1

The second method estimates the rotor speed on the basis of the position output of the previous method. This method is split into two parts. The first part is used for computing speed ratio values as a function of the rotor position that is provided by the position method. The second part is applied for estimating the motor speed using the different speed ratio values computed in the first part.

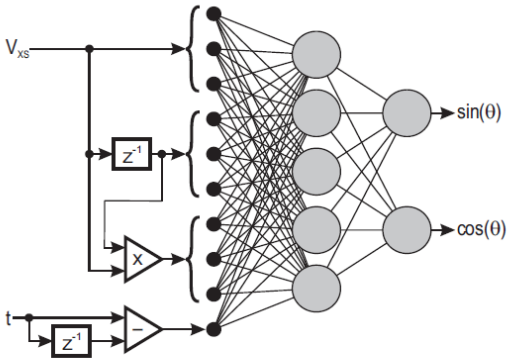

Fig. 2 Structure of the proposed position estimation ANN.

In order to calculate the speed ratio values in the first part of the second method, the position differentials were divided into time differentials according to the following conditions:

a) 1st condition of speed ratio: Assuming that the last sample is n^{th}, the speed is obtained respect to the n^{th} sample versus the n^{th}-1, n^{th}-2,…n^{th}-d. Eq. (6) shows the expression to calculate this speed ratio.

$$\text{speed\_ratio}_{1\text{st cond}}[i] = \frac{\boldsymbol{\theta}[n] - \boldsymbol{\theta}[n-i]}{t[n] - t[n-i]} \qquad (6)$$

where $\theta[n]$ refers to the angle position and $t[n]$ the time for the n^{th} sample.

b) 2nd condition of speed ratio: Considering the last and the previous samples with the same rotor position. Eq. (7) shows the expression to calculate this speed ratio.

$$\text{speed\_ratio}_{2\text{nd cond}}[j] = \frac{\boldsymbol{\theta}_j[n] - \boldsymbol{\theta}_j[n-1]}{t_j[n] - t_j[n-1]} \qquad (7)$$

where $\theta_j[n]$ and $t_j[n]$ are respectively the n^{th} sample of the angle position and the time vectors associated to the position j.

The second part of the method is developed with a 3-layer MLP-ANN that is composed of 21 inputs, 10 hidden neurons, and 1 output. The inputs consist of 9 speed ratio values in the first condition and 12 speed ratio values, which are related to the 12 rotor positions shown in Table 2, in the second one. The structure of the ANN proposed to estimate the speed of the rotor is shown in Fig. 3, where some neurons of the input and hidden layers have been omitted for simplicity. The output speed value obtained from the ANN is post-processed to avoid data outliers and to improve the accuracy of the proposed estimation technique. This post-processing is done by calculating the median value of the actual speed and other 499 previous speed values obtained by the ANN.

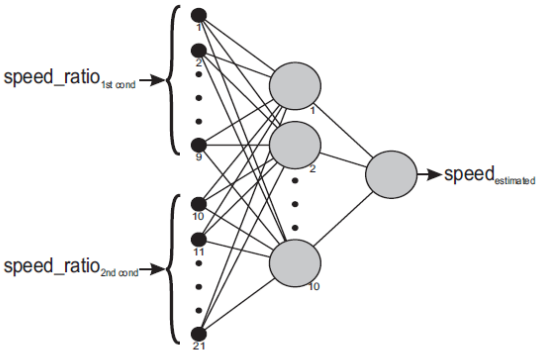

Fig. 3 Structure of the proposed speed estimation ANN, including the position number of each neuron in the layer.

In addition, a general block diagram of the proposed detection technique has been included in Fig. 4, which includes the methods to estimate both position and speed.

3.3 Data training

A shaft encoder has been used for obtaining the rotor position reference in order to train the ANNs and evaluate the technique performance. The incremental encoder included in the system provides 1024 pulses per mechanical revolution, which enables the analysis of position errors with a resolution of 0.35º.

During the training phase, the measured motor phase voltages with respect to the virtual neutral point (V_{XS}) and encoder mechanical positions are provided to the ANNs, so the networks are trained offline by associating: (i) the voltage values with the position obtained from the encoder for position estimation; and (ii) the speed ratio values computed from the encoder data with the speed reference set for speed estimation. Taking into account these details, the proposed ANNs are trained with the *Backpropagation* algorithm by employing 40% of the available data as the training dataset and other 10% as the validation dataset. The 50% remaining are the dataset used in the testing phase.

4. Experimental Results

The verification of the proposed estimation technique could be performed by embedding the ANNs algorithm in the FPGA-based prototype. However, this setup has been only applied for acquiring the motor phase voltages and the encoder data (and driving the motor), which are used for training and testing the network offline.

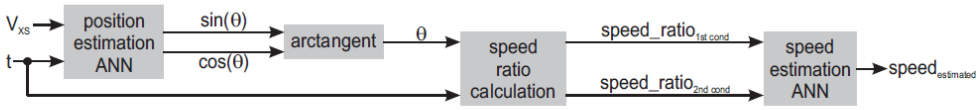

Fig. 4 Block diagram of the proposed detection technique.

The training of the ANNs has been deeply explained in the subsection 3.3. In the testing phase, experimental results have been obtained by using a BLDC motor Maxon EC 45 Flat with a load of 35 mNm. The parameters of the mentioned BLDC motor are listed in Table 3.

Table 3 BLDC motor parameters.

Parameter	Value
Number of pole pairs	8
Number of phases	3
Nominal voltage	12 V
Maximum current	1.96 A
Nominal torque	53.2 mN·m
Terminal resistance phase to phase	1.4 Ω
Terminal inductance phase to phase	0.56 mH
Rotor inertia	92.5 g·cm^2

The verification was performed with the mentioned motor, whose resolution per electrical cycle is 45° and each mechanical cycle is composed of 8 electrical cycles. Rotor position and speed estimations have been analyzed through tests at different speeds in order to compare the results with the detection technique and the reference encoder. The performance testing has been carried out in the range between 125 rpm and 1500 rpm. The results of the position tracking using the neural network technique regarding to the reference position of the encoder are given in Fig. 5 and Fig. 6 for 175 rpm and 850 rpm, respectively. The results of the speed tracking are included in Fig. 7 and Fig. 8 for 175 rpm and 850 rpm, respectively. The position waveform is only depicted in one mechanical cycle for analyzing in detail the tracking precision of the ANN regarding to the encoder. However, speed is showed in a wide range of acquired samples for validating the steady-state performance of the technique. Both estimated position and speed track the encoder reference waveform with low accuracy errors, and the behavior of the transients around the reference in steady-state is stable and predictable.

Due to the objective of the ANNs is to minimize the squared error between estimated and measured values, a position mean absolute error of 6.47° (mechanical degrees) and a speed mean relative error of 4.87% have been obtained in the range 125-1500 rpm. The Table 4 includes position and speed errors at different speeds in the mentioned range. Considering these results, the developed technique is accurate and precise enough for a wide speed range, and improves the performance of traditional detection approaches with a typical resolution of 7.5° for 8-pole motors. The speed is also estimated with precision enough on the basis of the estimated position, so the position errors have a low influence on the speed estimation.

Table 4 Estimation of performance at different speeds.

Motor speed (rpm)	Position mean absolute error	Speed mean relative error
175	5.72	4.19
325	6.25	5.47
475	6.38	2.69
600	6.37	3.85
725	6.35	4.55
850	5.85	2.66

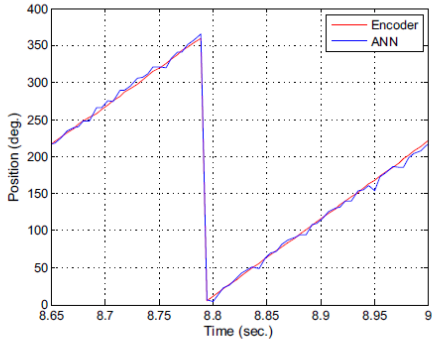

Fig. 5 Position estimation regarding to reference encoder at 175 rpm.

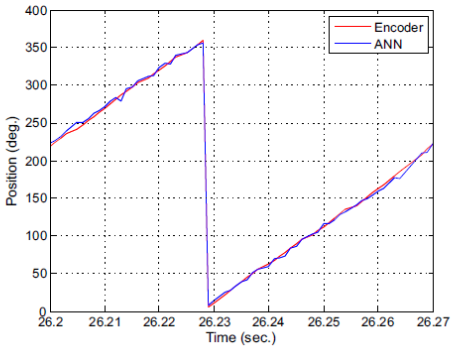

Fig. 6 Position estimation regarding to reference encoder at 850 rpm.

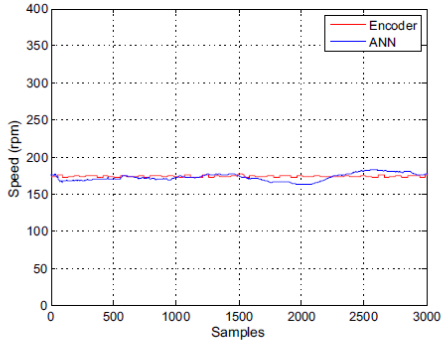

Fig. 7 Speed estimation regarding to reference encoder at 175 rpm.

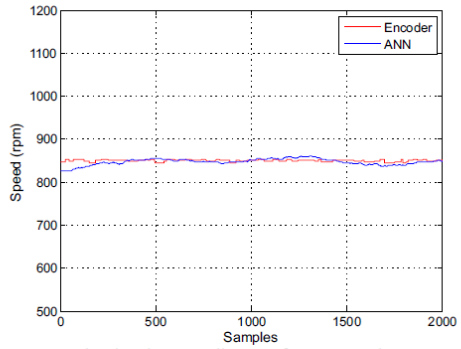

Fig. 8 Speed estimation regarding to reference encoder at 850 rpm.

5. Conclusion

A technique composed of two neural networks MLP was developed for estimating the position and speed of BLDC motors. The neural networks were trained using the Backpropagation algorithm, and tested with a real BLDC motor and the reference position information of an encoder, which were processed with a FPGA-based prototype. Experimental results were performed in the range 125-1500 rpm, and mean position and speed errors of 6.47° and 4.87%, respectively, were attained. The results show that the proposed technique with two neural networks MLP allows the estimation of position and speed of BLDC motors with an acceptable precision over a wide speed range, which represents a reliable alternative to traditional sensorless detection approaches

Acknowledgements

The Víctor Martínez-Martínez's work was supported by a *Formación de Personal Investigador* program grant. This program was financed by the University of Valladolid (Spain) and co-financed by Banco Santander.

References

[1] R.C. Becerra and M. Ehsani, "High-speed torque control of brushless permanent magnet motors," IEEE Trans. Ind. Electron., vol.35, no.3, pp.402-406, Aug. 1988.

[2] J.C. Gamazo, E. Vázquez, and J. Gómez, "Position and speed control of brushless DC motors using sensorless techniques and application trends," Sensors, vol.10, no.7, pp.6901-6947, July 2010.

[3] S. Tsotoulidis and A. Safacas, "A sensorless commutation technique of a brushless DC motor drive using two terminal voltages in respect to a virtual neutral potential," IEEE Proc. Int. Conf. Elect. Mach., pp.830-836, Sept. 2012.

[4] J.W. McKeever and G.J. Su, "Low-cost sensorless control of brushless DC motors with improved speed range," IEEE Trans. Power Electron., vol.19, no.2, pp.296-302, March 2004.

[5] S. Tsotoulidis, A. Safacas, E. Mitronikas, "A sensorless commutation strategy for a brushless DC motor drive system based on detection of back electromagnetic force," IEEE Proc. Elect. Mach. and Power Electron., pp.32-37, Sept. 2011.

[6] J.X. Shen and S. Iwasaki, "Sensorless control of ultrahigh-speed PM brushless motor using PLL and third harmonic back EMF," IEEE Trans. Ind. Electron., vol.53, no.2, pp.421-428, April 2006.

[7] R.C. Becerra, T.M. Jahns, and M. Ehsani, "Four-quadrant sensorless brushless ECM Drive," IEEE Proc. Appl. Power Electron., pp. 202-209, March 1991.

[8] R. Krishnan and S. Lee, "PM brushless DC motor drive with a new power-converter topology," IEEE Trans. Ind. Applicat., vol.33, no.4, pp.973-982, Jul/Aug 1997.

[9] P. Damodharan and K. Vasudevan, "Sensorless brushless DC motor drive based on the zero-crossing detection of back electromotive force (EMF) from the line voltage difference," IEEE Trans. Energy Convers., vol.25, no.3, pp.661-668, Sept. 2010.

[10] L. Yen-Shin, S. Fu-San, and C. Yung-Hsin, "Novel pulse-width modulation technique with loss reduction for small power brushless DC motor drives," IEEE Proc. Ind. Applicat., vol.3, pp.2057-2064, Oct. 2002.

[11] L. Byoung-kuk, K. Tae-Hyung, and M. Ehsani, "On the feasibility of four-switch three-phase BLDC motor drives for low cost commercial applications: topology and control," IEEE Trans. Power Electron., vol.18, no.1, pp.164-172, Jan. 2003.

[12] T. Kim, H.W. Lee, and M. Ehsani, "Position Sensorless Brushless DC Motor/Generator Drives: Review and Future Trends," IET Electr. Power Applicat., vol.1, no.4, pp.557-564, July 2007.

[13] J.C. Moreira, "Indirect sensing for rotor flux position of permanent magnet AC motors operating over a wide speed range," IEEE Trans. Ind. Applicat., vol.32, no.6, pp.1394-1401, Nov./Dec. 1996.

[14] S. Ogasawara and H. Akagi, "An approach to position sensorless drive for brushless DC motors," IEEE Trans. Ind. Applicat., vol.27, no.5, pp.928-933, Sep./Oct. 1991.

[15] J.X. Shen, Z.Q. Zhu, and D. Howe, "Sensorless flux-weakening control of permanent magnet brushless machines using third-harmonic back-EMF," IEEE Proc. Elect. Mach. and Drives, vol.2, pp.1229-1235, June 2003.

[16] K. Young-Seok, A. Jun-Young, Y. Wan-Sik, and C. Kyu-Min, "A speed sensorless vector control for brushless DC motor using binary observer," IEEE Proc. Ind. Electron., Control, and Instrum., vol.3, pp.1746-1751, Aug. 1996.

[17] M.S. Zaky, M. Khater, H. Yasin, and S.S. Shokralla, "Very Low Speed and Zero Speed Estimations of Sensorless Induction Motor Drives," Electr. Power Syst. Res., vol.80, no.2, pp.143-151, Feb. 2010.

[18] R. Dhaouadi, N. Mohan, and L. Norum, "Design and implementation of an extended Kalman filter for the state

estimation of a permanent magnet synchronous motor," IEEE Trans. Power Electron., vol.6, no.3, pp.491-497, Jul. 1991.
[19] M. Barut, "Bi input-extended Kalman filter based estimation technique for speed-sensorless control of induction motors," Energy Convers. Manage., vol.51, no.10, pp.2032-2040, Oct. 2010.
[20] H.M. Kojabadi, "Active power and MRAS based rotor resistance identification of an IM drive," Simulat. Model. Pract. And Theory, vol.17, no.2, 376-389, Feb. 2009.
[21] J. Maes and J.A. Melkebeek, "Speed-sensorless direct torque control of induction motors using an adaptive flux observer," IEEE Trans. Ind. Applicat., vol.36, no.3, pp.778-785, May/Jun. 2000.
[22] L. Yih-Neng and C. Chern-Lin, "Adaptive pseudoreduced-order flux observer for speed sensorless field-oriented control of IM," IEEE Trans. Ind. Electron., vol.46, no.5, pp.1042-1045, Oct. 1999.
[23] B.K. Bose, "Expert system, fuzzy logic, and neural network applications in power electronics and motion control," IEEE Proc., vol.82, no.8, pp.1303-1323, Aug. 1994.
[24] B.K. Bose, "Neural network applications in power electronics and motor drives-an Introduction and perspective," IEEE Trans. Ind. Electron., vol.54, no.1, pp.14-33, Feb. 2007.
[25] M. Yasser, A. Trisanto, J. Lu, and T. Yahagi, "A method for simple adaptive control of nonlinear systems using neural networks," IEICE Trans. Fundam. Electron. Commun. Comput. Sci., vol.E89-A, no.7, pp.2009-2018, July 2006.
[26] B.K. Bose, "Fuzzy logic and neural networks in power electronics and drives," IEEE Ind. Applicat. Mag., vol.6, no.3, pp.57-63, May/Jun. 2000.
[27] E. Vazquez-Sanchez, J. Gomez-Gil, J.C. Gamazo-Real, and J.F. Diez-Higuera, "A New Method for Sensorless Estimation of the Speed and Position in Brushed DC Motors Using Support Vector Machines," IEEE Trans. Ind. Electron., vol.59, no.3, pp.1397-1408, March 2012.
[28] R. Krishnan, R. Monajemy, and N. Tripathi, "Neural control of high performance drives: an application to the PM synchronous motor drive," IEEE Proc. Ind. Electron., Control, and Inst., vol.1, pp.38-43, Nov. 1995.
[29] M.A. El-Sharkawi, "Neural network application to high performance electric drives systems," IEEE Proc. Ind. Electron., Control, and Inst., vol.1, pp.44-49, Nov. 1995.
[30] L. Hongru, W. Jianhui, G. Shusheng, and Y. Tao, "A neural-network-based adaptive estimator of rotor position and speed for permanent magnet synchronous motor," IEEE Proc. Elect. Mach. and Sys., vol.2, pp.735-738 , Aug. 2001.
[31] F. Huang and D. Tien, "A neural network approach to position sensorless control of brushless DC motors," IEEE Proc. Ind. Electron., Control, and Inst., vol.2, pp.1167-1170, Aug. 1996.
[32] J. Wang, H. Liu, Y. Zhu, B. Cui, and H. Duan, "A new minimum torque-ripple and sensorless control scheme of BLDC motors based on RBF networks," IEEE Proc. Power Electron. and Motion Control, vol.2, pp.1-4, Aug. 2006.
[33] K. Kai-Sheng and T. Ying-Yu, "Adaptive soft starting method with current limit strategy for sensorless BLDC motors," IEEE Proc. Ind. Electron., pp.605-610, May 2012.
[34] S. Haykin, 2nd ed., "Neural networks: a comprehensive foundation", Prentice Hall, New Jersey, 1999.
[35] C.M. Bishop, "Neural networks for pattern recognition", Oxford University Press, Oxford, 2007.

José Carlos Gamazo-Real was born in Valladolid, Spain, in 1979. He received the B.S. degree in Telecommunication Engineering (Electronic Systems specialty), the M.S. degree in Electronics Engineering, and the M.S. degree in Telecommunication Engineering from the University of Valladolid, Valladolid, Spain, in 2001, 2004 and 2007, respectively. He was researcher with the Center of Automation, Robotics, Information, and Manufacturing Technologies (CARTIF) between 2003 and 2004, and with the Center for Development of Telecommunication in Castilla y León (CEDETEL) in 2006, Valladolid. Since 2006, he combines the PhD as student of the Dept. of Signal Theory, Communications and Telematics Engineering, University of Valladolid, with the work at companies like Enerman, S.A. (2006-2009), and Thales Alenia Space (2013-2015), and Airbus DS (2009-2013, 2015-onwards). His research interests are sensorless technology, signal processing and mechatronics. Other interest areas are aerospace systems and avionics.

Víctor Martínez-Martínez was born in León, Spain, in 1987. He received the B.S. degree in Telecommunication Engineering and the M.S. degree in Information and Communications Technologies Research from the University of Valladolid, Valladolid, Spain, in 2010 and 2011, respectively. Since 2009 to 2011, he has been a part-time researcher with the Dept. of Signal Theory, Communications and Telematics Engineering and with the Dept. of Agricultural and Forestry Engineering, University of Valladolid. Since 2011, he has been a full-time researcher and PhD student of the Dept. Signal Theory, Communications and Telematics Engineering, University of Valladolid. His current research interests are signal processing and data analysis applied to agro-industrial processes.

Jaime Gomez-Gil was born in Aguilar de Bureba, Spain, in 1971. He received the M.S. degree in telecommunication engineering and the Ph.D. degree in Signal Theory, Communications and Telematics Engineering from the University of Valladolid, Valladolid, Spain, in 2001 and 2005, respectively. From 2001 to 2002, he was with the Center for the Development of Telecommunication in Castilla y León (CEDETEL), Valladolid. Since 2002, he has been a full-time Professor with the Dept. of Signal Theory, Communications and Telematics Engineering, University of Valladolid. His current research is GPS and machine vision for agricultural engineering. Other interest areas are sensorless and human–computer interface technology.

Referencias*

[1] B. Bose, *Power Electronics and Motor Drives: Advances and Trends*, First ed. U.S.A., 2006.

[2] M. H. Rashid, *Power Electronics Handbook: Devices, Circuits, and Applications.*, Third ed. U.S.A., 2011.

[3] D. F. Warne, *Electrical Engineer's Handbook*, First ed. United Kingdom, 2000.

[4] P. Moreton, *Industrial Brushless Servomotors*, First ed. United Kingdom, 2000.

[5] R. Crowder, *Electric Drives and Electromechanical Systems*, First ed. United Kingdom, 2006.

[6] N. Bianchi, *et al.*, "Comparison of PM Motor Structures and Sensorless Control Techniques for Zero-Speed Rotor Position Detection," *Power Electronics, IEEE Transactions on*, vol. 22, pp. 2466-2475, 2007.

[7] S. Haykin, *Neural Networks: A Comprehensive Foundation*, Second ed. India, 2001.

[8] J. C. Gamazo-Real, *et al.*, "Position and Speed Control of Brushless DC Motors Using Sensorless Techniques and Application Trends," *Sensors*, vol. 10, pp. 6901-6947, 2010.

[9] D. Choppa, "Performance of Torus-type Brushless DC Motor with Winding Connected in Two and Three-phase System," Master of Science in Electrical Engineering, Department of Electrical & Computer Engineering, Andhra University, India, 2006.

[10] Microchip, "Brushless DC (BLDC) Motor Fundamentals Application Note," *AN885*, 2003.

[11] R. C. Becerra and M. Ehsani, "High-speed torque control of brushless permanent magnet motors," *Industrial Electronics, IEEE Transactions on*, vol. 35, pp. 402-406, 1988.

[12] R. Krishnan and S. Lee, "PM brushless DC motor drive with a new power-converter topology," *Industry Applications, IEEE Transactions on*, vol. 33, pp. 973-982, 1997.

[13] Y. Hyeong-Gee, *et al.*, "Sensorless drive for interior permanent magnet brushless DC motors," in *Electric Machines and Drives Conference Record, 1997. IEEE International*, 1997, pp. TD1/3.1-TD1/3.3.

[14] m. Lin, *et al.*, "A novel and easy-realizing initial rotor position detection method and speedup algorithm for sensorless BLDC motor drives," in *Electrical Machines and Systems, 2008. ICEMS 2008. International Conference on*, 2008, pp. 2860-2865.

[15] S. Jianwen, *et al.*, "A novel microcontroller-based sensorless brushless DC (BLDC) motor drive for automotive fuel pumps," *Industry Applications, IEEE Transactions on*, vol. 39, pp. 1734-1740, 2003.

[16] M. Naidu, *et al.*, "Keeping cool while saving space and money: a semi-integrated, sensorless PM brushless drive for a 42-V automotive HVAC compressor," *Industry Applications Magazine, IEEE*, vol. 11, pp. 20-28, 2005.

---

* *Bibliografía en formato IEEE ordenada en orden de aparición en el documento.*

[17] V. Hubik, *et al.*, "On the development of BLDC motor control run-up algorithms for aerospace application," in *Power Electronics and Motion Control Conference, 2008. EPE-PEMC 2008. 13th*, 2008, pp. 1620-1624.

[18] I. Takahashi, *et al.*, "A super high speed PM motor drive system by a quasi-current source inverter," *Industry Applications, IEEE Transactions on*, vol. 30, pp. 683-690, 1994.

[19] M. Bonfe and M. Bergo, "A brushless motor drive with sensorless control for commercial vehicle hydraulic pumps," in *Industrial Electronics, 2008. ISIE 2008. IEEE International Symposium on*, 2008, pp. 612-617.

[20] J. Quan, *et al.*, "A new phase-delay-free method to detect back EMF zero-crossing points for sensorless control of spindle motors," *Magnetics, IEEE Transactions on*, vol. 41, pp. 2287-2294, 2005.

[21] L. Wook-Jin and S. Seung-Ki, "A New Starting Method of BLDC Motors Without Position Sensor," *Industry Applications, IEEE Transactions on*, vol. 42, pp. 1532-1538, 2006.

[22] L. Yen-Shin, *et al.*, "Novel pulse-width modulation technique with loss reduction for small power brushless DC motor drives," in *Industry Applications Conference, 2002. 37th IAS Annual Meeting. Conference Record of the*, 2002, pp. 2057-2064 vol.3.

[23] L. Yen-Shin, *et al.*, "Novel loss reduction pulsewidth modulation technique for brushless dc motor drives fed by MOSFET inverter," *Power Electronics, IEEE Transactions on*, vol. 19, pp. 1646-1652, 2004.

[24] M. Kessler and K.-H. Preis, "Procedimiento y Disposición de Circuito para la Detección del Número de Revoluciones de un Motor de Corriente Continua," ES 2205028 T3 Patent, 2004.

[25] A. Bobbio, "Método y Sistema de Circuitos para Detectar la Velocidad de Rotación en Motores CC," ES 2135002 T3 Patent, 1999.

[26] M. Guerreiro, *et al.*, "A Microcontroller Sensorless Speed Control of a Direct Current Motor," in *Industrial Electronics, 2007. ISIE 2007. IEEE International Symposium on*, 2007, pp. 1143-1146.

[27] S. Yachiangkam, *et al.*, "Speed-sensorless Separately Excited DC Motor Drive with an Adaptive Observer," in *TENCON 2004. 2004 IEEE Region 10 Conference*, 2004, pp. 163-166 Vol. 4.

[28] V. M. Hernandez and H. Sira-Ramirez, "Position Control of an Inertia-spring DC-motor System Without Mechanical Sensors: Experimental Results," in *Decision and Control, 2001. Proceedings of the 40th IEEE Conference on*, 2001, pp. 1386-1391 vol.2.

[29] J. Scott, *et al.*, "Speed Control With Low Armature Loss for Very Small Sensorless Brushed DC Motors," *Industrial Electronics, IEEE Transactions on*, vol. 56, pp. 1223-1229, 2009.

[30] H. Johnson, "Electric Motor Speed Sensing," US 3708737 Patent, 1973.

[31] R. Won-Sang, *et al.*, "Practical Pinch Detection Algorithm for Smart Automotive Power Window Control Systems," *Industrial Electronics, IEEE Transactions on*, vol. 55, pp. 1376-1384, 2008.

[32] O. Aydogmus and M. F. Talu, "Comparison of Extended-Kalman- and Particle-Filter-Based Sensorless Speed Control," *Instrumentation and Measurement, IEEE Transactions on*, vol. 61, pp. 402-410, 2012.

[33] F. Farkas, *et al.*, "Speed Sensorless Neuro-Fuzzy Controller for Brush type DC Machines " presented at the 5th International Symposium of Hungarian Researchers on Computational Intelligence, Hungary, 2004.

[34] T. Son Nguyen, *et al.*, "Improved Performance of a Sensorless DC Motor Control Using Fuzzy Logic," in *Intelligent and Advanced Systems (ICIAS), 2014 5th International Conference on*, 2014, pp. 1-6.

[35] Y. Baoguo, *et al.*, "Expression of Sensorless Speed Estimation in Direct Current Motor with Simplex Lap Winding," in *Mechatronics and Automation, 2007. ICMA 2007. International Conference on*, 2007, pp. 816-821.

[36] R. B. Allured, *et al.*, "Commutator Pulse Counting Apparatus " US3346725 Patent, 1967.

[37] E. Vazquez-Sanchez, *et al.*, "Método para Determinar la Velocidad Angular en un Motor Conmutado Mecánicamente Midiendo Únicamente la Corriente que Circula por el Mismo," ES 2334551 A1 Patent, 2010.

[38] E. Vazquez-Sanchez, *et al.*, "A New Method for Sensorless Estimation of the Speed and Position in Brushed DC Motors Using Support Vector Machines," *Industrial Electronics, IEEE Transactions on*, vol. 59, pp. 1397-1408, 2012.

[39] N. Katsumura, "Apparatus for Measuring Motor Rotation Position and Speed," US 4788497 Patent, 1988.

[40] C. C. Lo, "Motor Control System," US 6653810 Patent, 2003.

[41] J. Iott and D. Burke, "Brushed Motor Position Control Based Upon Back Current Detection," US 20060261763 Patent, 2006.

[42] T. Bertolini, *et al.*, "Method and Apparatus for Counting Revolutions of a Mechanically Commutated DC-Motor," EP 0689054 Patent, 1999.

[43] K. Mourad and L. Castellar, "Process and Device for Detecting the Speed of Rotation of a DC Electric Motor Controlled by a PWM Control Signal " US 6236175 Patent, 2001.

[44] A. Seino, *et al.*, "Rotation Signal Detection Device of DC Motor with Brushes," US 4443745 Patent, 1985.

[45] T. Gerlach, "Method for Determining the Rotational Position of the Drive Shaft of a Commutated DC Motor," US 6847914 Patent, 2005.

[46] T. Oka, *et al.*, "Device for Determining Rotational Number of DC Motors," US 6172473 Patent, 2001.

[47] T. Gerlach, "Method for Correcting the Determination of the Rotational Position of a Commutated DC Motor Drive Shaft," US 6839653 Patent, 2005.

[48] M. Hilairet and F. Auger, "Speed Sensorless Control of a DC-motor Via Adaptive Filters," *Electric Power Applications, IET*, vol. 1, pp. 601-610, 2007.

[49] K. Berland, *et al.*, "Intelligent Commutation Pulse Detection System to Control Electric DC Motors Used with Automobile Accesories," US 5497326 Patent, 1996.

[50] T. Gerlach, "Method for Determining the Frequency of the Current Ripple in the Armature Current of a Commutated DC Motor," US 7079964 Patent, 2006.

[51] S. W. Brooks, "Apparatus for Detecting the Speed of an Electric Motor," US 4227129 Patent, 1980.

[52] E. Kessler and W. Schulter, "Method for Establishing the Rotational Speed of Mechanically Commutated DC Motors," US 6144179 Patent, 2000.

[53] T. Lutter and T. Fiedrich, "Method for Detecting the Rotational Position of the Drive Shaft a DC Motor," US 6768282 Patent, 2004.

[54] K. Iizuka, *et al.*, "Microcomputer Control for Sensorless Brushless Motor," *Industry Applications, IEEE Transactions on*, vol. IA-21, pp. 595-601, 1985.

[55] S. Jianwen, *et al.*, "A novel direct back EMF detection for sensorless brushless DC (BLDC) motor drives," in *Applied Power Electronics Conference and Exposition, 2002. APEC 2002. Seventeenth Annual IEEE*, 2002, pp. 33-37 vol.1.

[56] R. C. Becerra, *et al.*, "Four-quadrant sensorless brushless ECM drive," in *Applied Power Electronics Conference and Exposition, 1991. APEC '91. Conference Proceedings, 1991., Sixth Annual*, 1991, pp. 202-209.

[57] C. Cheng-Hu and C. Ming-Yang, "A New Sensorless Commutation Drive for Brushless DC Motors and Alternators," in *Industrial Electronics, 2006 IEEE International Symposium on*, 2006, pp. 2116-2121.

[58] S. Ogasawara and H. Akagi, "An approach to position sensorless drive for brushless DC motors," *Industry Applications, IEEE Transactions on*, vol. 27, pp. 928-933, 1991.

[59] U. Vinatha, *et al.*, "Recent Developments in Control Schemes of BLDC Motors," in *Industrial Technology, 2006. ICIT 2006. IEEE International Conference on*, 2006, pp. 477-482.

[60] S. Jianwen, *et al.*, "Improved direct back EMF detection for sensorless brushless DC (BLDC) motor drives," in *Applied Power Electronics Conference and Exposition, 2003. APEC '03. Eighteenth Annual IEEE*, 2003, pp. 300-305 vol.1.

[61] STMicroelectronics, "An Introduction to Sensorless Brushless DC Motor Drive Applications with the ST72141 Application Note," *AN1130*, 2000.

[62] L. Byoung-kuk, *et al.*, "On the feasibility of four-switch three-phase BLDC motor drives for low cost commercial applications: topology and control," *Power Electronics, IEEE Transactions on*, vol. 18, pp. 164-172, 2003.

[63] T. Kim, *et al.*, "Position sensorless brushless DC motor/generator drives: review and future trends," *Electric Power Applications, IET*, vol. 1, pp. 557-564, 2007.

[64] J. C. Moreira, "Indirect sensing for rotor flux position of permanent magnet AC motors operating over a wide speed range," *Industry Applications, IEEE Transactions on*, vol. 32, pp. 1394-1401, 1996.

[65] J. P. Johnson, *et al.*, "Review of sensorless methods for brushless DC," in *Industry Applications Conference, 1999. Thirty-Fourth IAS Annual Meeting. Conference Record of the 1999 IEEE*, 1999, pp. 143-150 vol.1.

[66] K. Young-Seok, *et al.*, "A speed sensorless vector control for brushless DC motor using binary observer," in *Industrial Electronics, Control, and Instrumentation, 1996., Proceedings of the 1996 IEEE IECON 22nd International Conference on*, 1996, pp. 1746-1751 vol.3.

[67] M. Hajian, *et al.*, "Energy optimized sliding-mode control of sensorless induction motor drives," *Energy Conversion and Management*, vol. 50, pp. 2296-2306, 2009.

[68] M. S. Zaky, *et al.*, "Very low speed and zero speed estimations of sensorless induction motor drives," *Electric Power Systems Research*, vol. 80, pp. 143-151, 2010.

[69] R. Dhaouadi, *et al.*, "Design and implementation of an extended Kalman filter for the state estimation of a permanent magnet synchronous motor," *Power Electronics, IEEE Transactions on*, vol. 6, pp. 491-497, 1991.

[70] B. Terzic and M. Jadric, "Design and implementation of the extended Kalman filter for the speed and rotor position estimation of brushless DC motor," *Industrial Electronics, IEEE Transactions on*, vol. 48, pp. 1065-1073, 2001.

[71] M. Barut, "Bi Input-extended Kalman filter based estimation technique for speed-sensorless control of induction motors," *Energy Conversion and Management*, vol. 51, pp. 2032-2040, 2010.

[72] S. Maiti and C. Chakraborty, "A new instantaneous reactive power based MRAS for sensorless induction motor drive," *Simulation Modelling Practice and Theory*, vol. 18, pp. 1314-1326, 2010.

[73] J. Maes and J. A. Melkebeek, "Speed-sensorless direct torque control of induction motors using an adaptive flux observer," *Industry Applications, IEEE Transactions on*, vol. 36, pp. 778-785, 2000.

[74] H. M. Kojabadi, *et al.*, "A MRAS-based adaptive pseudoreduced-order flux observer for sensorless induction motor drives," *Power Electronics, IEEE Transactions on*, vol. 20, pp. 930-938, 2005.

[75] H. M. Kojabadi and L. Chang, "Comparative study of pole placement methods in adaptive flux observers," *Control Engineering Practice*, vol. 13, pp. 749-757, 2005.

[76] B. K. Bose, "Fuzzy logic and neural networks in power electronics and drives," *Industry Applications Magazine, IEEE*, vol. 6, pp. 57-63, 2000.

[77] M. N. Cirstea, *et al.*, *Neural and Fuzzy Logic Control of Drives and Power Systems*, First ed. United Kingdom, 2002.

[78] B. K. Bose, "Expert system, fuzzy logic, and neural network applications in power electronics and motion control," *Proceedings of the IEEE*, vol. 82, pp. 1303-1323, 1994.

[79] H. Wang, *et al.*, "A Brief Review of Machine Learning and Its Application," in *Information Engineering and Computer Science, 2009. ICIECS 2009. International Conference on*, 2009, pp. 1-4.

[80] J. C. Gamazo-Real and J. Gomez-Gil, "Sensorless Detection of Position and Speed in Brushless DC Motors using the Derivative of Terminal Phase Voltages Technique with a Simple and Versatile Motor Driver Implementation," *Journal of Electrical Engineering & Technology*, vol. 10, pp. 1540-1551, 2015.

[81] DiCYT. (Mayo 2005, Acceso: 14/07/2015). *Premio: Innovación 2004 en Ingeniería Industrial e Ingeniería Química*. Available: http://www.dicyt.com/noticias/la-universidad-premia-tres-proyectos-fin-de-carrera-innovadores

[82] J. C. Gamazo-Real, *et al.*, "Propagation Study of GSM Power in Two Dimensions in Indoor Environments – Part 1," *Electronics World*, vol. 116, pp. 28-31, 2010.

[83] J. C. Gamazo-Real, *et al.*, "Propagation Study of GSM Power in Two Dimensions in Indoor Environments – Part 2," *Electronics World*, vol. 116, pp. 30-34, 2010.

[84] H. R. Macks, *et al.*, "Method and Apparatus for DC Motor Speed Monitoring," US 5524168 Patent, 1996.

[85] I. Richter and K. Skibowski, "Method of and Device for Contactless Measurement of Rotary Speed of Direct Current motor by Forming Autocorrelation Sequence," US 5581178 Patent, 1996.

[86] M. Micke, *et al.*, "Method and Device for Measuring the Rotational Speed of a Pulse-activated Electric Motor Based on a Frequency of Current Ripples," US 7265538 Patent, 2007.

[87] T. M. Jahns, *et al.*, "Integrated current regulation for a brushless ECM drive," *Power Electronics, IEEE Transactions on*, vol. 6, pp. 118-126, 1991.

[88] A. Darba, *et al.*, "FPGA-based implementation of the back-EMF symmetric-threshold-tracking sensorless commutation method for Brushless DC-machines," in *Sensorless Control for Electrical Drives and Predictive Control of Electrical Drives and Power Electronics (SLED/PRECEDE), 2013 IEEE International Symposium on*, 2013, pp. 1-6.

[89] C. Kuang-Yao, "Novel Architecture of a Mixed-Mode Sensorless Control IC for BLDC Motors with Wide Speed Ranges," in *Applied Power Electronics Conference and Exposition, 2009. APEC 2009. Twenty-Fourth Annual IEEE*, 2009, pp. 2022-2027.

[90] Scopus. (Acceso: 14/07/2015). *Citas Artículos 1, 2 y 3 del Compendio de Publicaciones*. Available: http://www.scopus.com/authid/detail.url?authorId=36503715200

[91] WebOfScience. (Acceso: 14/07/2015). *Citas Artículo 1 del Compendio de Publicaciones*. Available: https://apps.webofknowledge.com/full_record.do?product=UA&search_mode=GeneralSearch&qid=2&SID=T12w3LZrbl5ZH6dREgH&page=1&doc=1

[92] GoogleScholar. (Acceso: 14/07/2015). *Citas Artículo 1 del Compendio de Publicaciones*. Available: https://scholar.google.com/scholar?cites=14971704385503934772&as_sdt=2005&sciodt=0,5&hl=en

[93] BioMedUpdater. (Acceso: 14/07/2015). *Citas Artículo 1 del Compendio de Publicaciones*. Available: http://biomedupdater.com/urlu8c?srk=8c8eaec03832d1c7b228d406e2d2e89353e93db0bae21181

[94] WebOfScience. (Acceso: 14/07/2015). *Citas Artículo 2 del Compendio de Publicaciones*. Available: https://apps.webofknowledge.com/full_record.do?product=UA&search_mode=GeneralSearch&qid=8&SID=T12w3LZrbl5ZH6dREgH&page=1&doc=1

[95] GoogleScholar. (Acceso: 14/07/2015). *Citas Artículo 2 del Compendio de Publicaciones*. Available: https://scholar.google.com/scholar?cites=16002539781182290289&as_sdt=2005&sciodt=0,5&hl=en

[96] MDPI. (Acceso: 14/07/2015). *Sección Physical Sensors de la revista Sensors*. Available: http://www.mdpi.com/journal/sensors/sections/physicalsensors

[97] K. Tae-Hyung and M. Ehsani, "Sensorless control of the BLDC motors from near-zero to high speeds," *Power Electronics, IEEE Transactions on*, vol. 19, pp. 1635-1645, 2004.

[98] P. P. Acarnley and J. F. Watson, "Review of position-sensorless operation of brushless permanent-magnet machines," *Industrial Electronics, IEEE Transactions on*, vol. 53, pp. 352-362, 2006.

[99] T. M. Jahns and W. L. Soong, "Pulsating torque minimization techniques for permanent magnet AC motor drives-a review," *Industrial Electronics, IEEE Transactions on*, vol. 43, pp. 321-330, 1996.

[100] E. J. Carmona-Suárez, "Tutorial sobre Máquinas de Vectores Soporte (SVM)," *Dept. of Artificial Intelligence, E.T.S. of Computing Engineering, Universidad Nacional de Educación a Distancia (UNED), Spain*, pp. 1-25, 2014.

[101] IEEE. (Acceso: 15/07/2015). *Objetivos y ámbito de la revista IEEE Transactions on Industrial Electronics*. Available: http://ieeexplore.ieee.org/xpl/aboutJournal.jsp?reload=true&punumber=41

[102] J. Ma and S. Weiss, "Motor Pulse Extraction System," US 4684858 Patent, 1987.

[103] JEET. (Acceso: 15/07/2015). *Ámbito de la revista Journal of Electrical Engineering and Technology*. Available: http://home.jeet.or.kr/submission/info_authors.asp

[104] P. Damodharan and K. Vasudevan, "Sensorless Brushless DC Motor Drive Based on the Zero-Crossing Detection of Back Electromotive Force (EMF) From the Line Voltage Difference," *Energy Conversion, IEEE Transactions on*, vol. 25, pp. 661-668, 2010.

[105] J. X. Shen and S. Iwasaki, "Sensorless control of ultrahigh-speed PM brushless motor using PLL and third harmonic back EMF," *Industrial Electronics, IEEE Transactions on*, vol. 53, pp. 421-428, 2006.

[106] C.-L. Cham and Z. B. Samad, "Brushless DC Motor Electromagnetic Torque Estimation with Single-Phase Current Sensing," *Journal of Electrical Engineering & Technology*, vol. 9, pp. 866-872, 2014.

[107] R. Flórez-López and J. M. Fernández-Fernández, *Las Redes Neuronales Artificiales*, First ed., 2008.

[108] IEICE. (Acceso: 15/07/2015). *Revista IEICE Transactions on Fundamentals of Electronics, Communications and Computer Sciences*. Available: https://www.jstage.jst.go.jp/browse/transfun

[109] M. Yasser, *et al.*, "A Method of Simple Adaptive Control for Nonlinear Systems Using Neural Networks," *IEICE Transactions on Fundamentals of Electronics, Communications and Computer Sciences*, vol. E89-A, pp. 2009-2018, 2010.

[110] R. Krishnan, *et al.*, "Neural control of high performance drives: an application to the PM synchronous motor drive," in *Industrial Electronics, Control, and Instrumentation, 1995., Proceedings of the 1995 IEEE IECON 21st International Conference on*, 1995, pp. 38-43 vol.1.

[111] M. A. El-Sharkawi, "Neural network application to high performance electric drives systems," in *Industrial Electronics, Control, and Instrumentation, 1995., Proceedings of the 1995 IEEE IECON 21st International Conference on*, 1995, pp. 44-49 vol.1.

[112] H. Li, *et al.*, "A neural-network-based adaptive estimator of rotor position and speed for permanent magnet synchronous motor," in *Electrical Machines and Systems, 2001. ICEMS 2001. Proceedings of the Fifth International Conference on*, 2001, pp. 735-738 vol.2.

[113] W. Juan, *et al.*, "A New Minimum Torque-ripple and Sensorless Control Scheme of BLDC Motors Based on RBF Networks," in *Power Electronics and Motion Control Conference, 2006. IPEMC 2006. CES/IEEE 5th International*, 2006, pp. 1-4.

[114] H. Fengtai and T. Dapeng, "A neural network approach to position sensorless control of brushless DC motors," in *Industrial Electronics, Control, and Instrumentation, 1996., Proceedings of the 1996 IEEE IECON 22nd International Conference on*, 1996, pp. 1167-1170 vol.2.

Anexo A: Documentación de otras aportaciones científicas relacionadas con la tesis

A continuación se incluyen otras aportaciones científicas dentro del campo de investigación de la tesis, como la colaboración en una patente de invención para el desarrollo de una técnica de medida de la velocidad de un motor *brushed* DC.

A.1. Patente de invención

TITULO: Método para determinar la velocidad angular en un motor conmutado mecánicamente midiendo únicamente la corriente que circula por el mismo.

AUTORES: Ernesto Vázquez Sánchez, Jaime Gómez Gil, José Fernando Díez Higuera, José Carlos Gamazo Real, y Javier García Martín.

TIPO: Patente.

FECHA DE SOLICITUD: 5 de noviembre de 2009.

NÚMERO DE SOLICITUD: P 200902143.

FECHA DE CONCESIÓN: 26 de enero de 2011.

FECHA DE CONCESIÓN: ES2334551 A1.

CLASIFICACIÓN INTERNACIONAL: G01P 3/48 (2006.01).

REFERENCIA: [37]

A continuación se incluye un extracto del documento de que sido aceptado como patente de invención española.

(19) OFICINA ESPAÑOLA DE PATENTES Y MARCAS

ESPAÑA

(11) Número de publicación: **2 334 551**

(21) Número de solicitud: 200902143

(51) Int. Cl.:

G01P 3/48 (2006.01)

H02P 6/18 (2006.01)

H02P 7/28 (2006.01)

(12) PATENTE DE INVENCIÓN B1

(22) Fecha de presentación: **05.11.2009**

(43) Fecha de publicación de la solicitud: **11.03.2010**

Fecha de la concesión: **26.01.2011**

(45) Fecha de anuncio de la concesión: **07.02.2011**

(45) Fecha de publicación del folleto de la patente: **07.02.2011**

(73) Titular/es: **Universidad de Valladolid**
Plaza de Santa Cruz, 5 - Bajo
47002 Valladolid, ES

(72) Inventor/es: **Vázquez Sánchez, Ernesto;**
García Martín, Javier;
Díez Higuera, José Fernando;
Gómez Gil, Jaime y
Gamazo Real, José Carlos

(74) Agente: **No consta**

(54) Título: **Método para determinar la velocidad angular en un motor conmutado mecánicamente midiendo únicamente la corriente que circula por el mismo.**

(57) Resumen:
Método para la determinar la velocidad angular en un motor conmutado mecánicamente midiendo únicamente la corriente que circula por el mismo. El método se basa en la determinación de los instantes en los que se van produciendo las ondulaciones de la componente alterna. Con esta información estima el valor de la frecuencia ripple con ella el valor de la velocidad angular del motor. Ambas magnitudes están directamente relacionadas debido a que por cada giro del motor se producen un número concreto de ondulaciones en la corriente que depende del número de polos y delgas del motor, entendiendo como ondulación a cada periodo de la componente alterna de la corriente. La detección de la ondulación se realiza mediante un registro de desplazamiento de longitud w en el que se van almacenando las últimas w muestras de la corriente del motor. Si se cumple que el valor máximo de la corriente se encuentra en la posición central del registro se supone que se acaba de detectar el pico y por tanto se detecta la ondulación registrando el instante en el que se ha producido la detección. Dependiendo del valor de w se consigue filtrar en mayor o menor medida el ruido que aparece en la corriente.

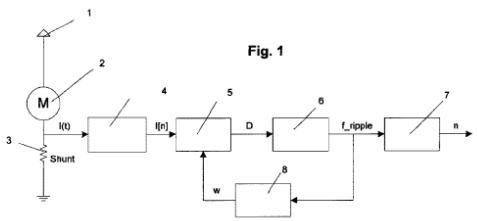

Fig. 1

ES 2 334 551 B1

ES 2 334 551 B1

DESCRIPCIÓN

Método para determinar la velocidad angular en un motor conmutado mecánicamente midiendo únicamente la corriente que circula por el mismo.

Sector de la técnica

La invención pertenece al campo de la detección de la velocidad angular en un motor de corriente continua conmutado mecánicamente mediante delgas y escobillas. La técnica objeto de invención se encuadra dentro de las técnicas de detección *sensorless* y aprovecha el rizado que aparece en la corriente que circula por el motor. La ventaja que presenta este nuevo método es la de filtrar el ruido que aparece junto a la corriente mediante una ventana de observación de las muestras de la corriente cuyo tamaño es variable.

Antecedentes de la invención

En un motor de corriente continua, la corriente que circula está compuesta por una componente de encargada de suministrar la potencia y una componente ac. La componente ac, también conocida como componente *ripple*, es debida al efecto conjunto de que la fuerza electromotriz inducida (f.e.m.) en las bobinas del rotor no es constante sino que tienen una forma sinusoidal y a que esta no es rectificada de forma perfecta en el colector de delgas. Además de esto, en el colector de delgas tiene lugar el proceso de conmutación de delga por parte de la escobillas. En el proceso de conmutación, justo en el momento en el que las escobillas se posicionan entre dos delgas, se cortocircuita la bobina unida a esas dos delgas produciendo un incremento de la corriente.

La frecuencia de dicha componente alterna de la corriente está relacionada con la velocidad de giro del motor, según lo comentado anteriormente, y con algunos parámetros constructivos como son el número de delgas del rotor y el número de polos del motor. Es por ello, que si se consigue detectar la frecuencia de esta componente se puede obtener la velocidad angular del motor.

Cada periodo de la componente alterna de la corriente es conocida en la literatura con el nombre de ondulación. Por lo general, el problema de detectar la frecuencia de la componente alterna se reduce al problema de detectar todas y cada una de las ondulaciones y medir la distancia temporal entre las mismas. Esta no es una tarea trivial, pues todo el ruido presente en la alimentación del motor es reflejado en la corriente. A todo este ruido hay que sumar el ruido generado y las interferencias captadas por el propio motor. Todo ello hace que muchas ondulaciones no puedan ser detectadas (ondulaciones fusionadas) y que aparezcan ondulaciones que no debieran (ondulaciones fantasmas). Lo que provoca imprecisiones en la determinación de la frecuencia ripple y con ello en la velocidad angular.

Mecanismos basados en la detección de la frecuencia de la componente alterna, conocida como frecuencia *ripple*, los podemos encontrar en documentos como son US 3 346 752, US 5 524 168 y US 6 172 473 B1. El problema de estas invenciones es que no tienen en cuenta explícitamente el problema del ruido. Por otro lado hay otras invenciones como son ES 2 190 011 T3, US 6 839 653 B2 y US 5 581 178 que si que tienen en cuenta el ruido y las posibles ondulaciones fantasmas y fusionadas. El problema que tienen éstas es el alto coste computacional que conllevan. Algunas de ellas requieren realizar la FFT. Por esta razón se propone un nuevo método que tenga en cuenta el ruido y no tenga un excesivo coste computacional.

Descripción de la invención

La invención se basa en la detección de las ondulaciones de la componente alterna de la corriente para determinar la velocidad angular de un motor de corriente continua conmutado mecánicamente. Por ello, en primer lugar lo que se hace es medir la corriente mediante un sensor resistivo tipo shunt. Posteriormente se digitaliza mediante un convertidor analógico/digital con una frecuencia de muestreo adecuada. A partir de este momento se procesa la señal de la corriente en el dominio digital mediante un microcontrolador, DSP o DSC.

Según se van recibiendo las muestras digitales de la corriente se van almacenando las últimas w muestras de forma consecutivas en una memoria configurada como un registro de desplazamiento. Este registro de desplazamiento tiene numeradas todas sus posiciones de 0 a w-1, de forma que la posición 0 corresponde a la última muestra capturada, la posición 1 a la muestra anterior y así sucesivamente. Para determinar si se ha producido o no una ondulación se mira si en la posición central del registro de desplazamiento, (w-1)/2, se encuentra almacenado el valor máximo de la corriente de entre todos los valores almacenados en el registro de desplazamiento. Si la respuesta es afirmativa, quiere decir que se ha detectado una ondulación. Para filtrar más o menos ruido, es decir, detectar las ondulaciones fusionadas y eliminar las ondulaciones fantasmas, basta con ajustar de forma adecuada el valor w. Este parámetro tiene que tener un valor impar y debe ser mayor o igual que 3 para que el método funcione correctamente. El valor de w se puede tomar de forma fija o de forma que sea proporcional al periodo de la componente alterna de la corriente. Hay que denotar que en todas las situaciones w debe ser menor estrictamente que el número de muestras que entran en un periodo de la componente alterna. Una elección u otra en el valor de w dependerá de la complejidad y del nivel de ruido presente.

Una vez en la que se han detectado las ondulaciones y se conoce la distancia temporal entre muestras, se procede a calcular el valor de la frecuencia de la componente alterna, o frecuencia ripple, como el inverso de la distancia entre ondulaciones detectadas. Finalmente, esta frecuencia hallada, se convierte en velocidad del motor.

Descripción de las figuras

La descripción de la invención se acompaña de una serie de figuras con el fin ayudar su compresión.

La figura 1 muestra el diagrama de bloques del método propuesto para la detección de la velocidad angular.

La figura 2 muestra esquemáticamente una posible implementación del bloque Detector de Máximo (5).

Descripción de un ejemplo de realización de la invención

En la figura 1 se muestra el diagrama de bloques del método objeto de invención. En él aparecen el sistema de alimentación del motor (1), el propio motor (2), el sensor de corriente tipo shunt (3). El siguiente bloque (4) es el convertidor analógico/digital que se encarga de digitaliza la corriente con una frecuencia de muestreo fs adecuada. El Detector de Máximo (5) detecta si se ha producido o no una ondulación, este bloque se explicará más adelante con mayor detalle. Al detector de frecuencia (6) le llega en cada instante discreto un valor lógico del Detector de Máximo (5) que le indica si en el instante actual se ha detectado una ondulación o por el contrario si no se ha detectado. Si no se ha detectado ninguna no hace nada. Si por el contrario se ha detectado una ondulación registra el instante actual como instante de detección de ondulación. Con esa información obtiene la frecuencia de la componente alterna o frecuencia ripple. Para ello se utiliza la siguiente ecuación:

$$f_{ripple} = \frac{1}{T_k - T_{k-1}}$$

Donde T_k es el instante en el que se detectó la última ondulación y T_{k-1} el instante de la ondulación anterior. Una vez obtenida la frecuencia ripple se pasa al bloque Convertidor Frecuencia-Velocidad (7). En este bloque tiene lugar la conversión de frecuencia ripple a la velocidad angular del motor. Estas dos magnitudes están relacionadas según la siguiente ecuación:

$$n = \frac{60 \cdot \eta \cdot f_{ripple}}{2p \cdot k}$$

En dicha ecuación 2p es el número de polos del motor, p es el número de pares de polos, k es el número de delgas del colector, n es la velocidad angular del motor en r.p.m. y f_{ripple} la frecuencia ripple en Hz. El parámetro η es el máximo común divisor de 2p y k tal como se indica en la siguiente ecuación:

$$\eta = m.c.d.\{2p, k\}$$

El último bloque es el estimador de ventana (8). Este bloque se encarga de obtener el parámetro w que es utilizado en el bloque Detector de Máximo. Este parámetro debe cumplir que sea impar y mayor o igual que 3 y menor que el número de muestras que ocupa un periodo de la componente alterna f_{ripple}/f_s, donde f_s es la frecuencia de muestreo. Teniendo en cuenta esto se puede tomar con valor fijo, o lo que es más recomendable calcularlo de forma dinámica en función de la frecuencia ripple. En el caso de obtenerlo de la frecuencia ripple se puede obtener como un valor proporcional al periodo ripple, es decir, del inverso de la frecuencia ripple. El cálculo de forma dinámica se puede hacer de la siguiente forma:

$$w = 2\left[c \cdot \frac{f_s}{f_{ripple}}\right] + 1 \qquad \frac{f_{ripple}}{f_s} < c < \frac{1}{2}\left(1 - \frac{f_{ripple}}{f_s}\right)$$

Donde el operador [·] es el operador parte entera y c es el factor de proporcionalidad comprendido entre los límites indicados para cumplir con las especificaciones de w. Para frecuencias de muestreo mucho mayor a la frecuencia ripple se puede decir que c debe estar comprendido entre 0 y 0.5.

En la figura 2 se muestra el esquema del bloque Detector de Máximo. El bloque se compone de un registro de desplazamiento (9) donde van entrando los valores de la corriente discretizados. Los valores se van almacenando en el registro de la siguiente forma, la última muestra de la corriente se almacena en la posición 0, la muestra anterior en la posición 1 y así sucesivamente. El siguiente bloque es el Detector de Posición del Máximo (10), donde entran

todos los valores del registro de desplazamiento y a su salida indica la posición donde se encuentra el máximo dentro del registro de desplazamiento. Por último, el bloque Detector del Máximo en el Centro (11) comprueba si el máximo se encuentra en el centro del registro de desplazamiento. Si el máximo está en el centro a su salida pone un 1, de lo contrario pone un 0. Esto se muestra en la siguiente ecuación:

$$D = \begin{cases} 1 & si \quad M = (w-1)/2 \\ 0 & resto \end{cases}$$

El registro de desplazamiento tiene una longitud w, que es el tamaño de la ventana de observación. Esto quiere decir que en cada instante se almacenarán las últimas w muestras de la corriente en 61. Mediante el valor de w se puede hacer que el sistema filtre más o menos ruido. El valor de w viene ajustado en realidad en el bloque Estimador de Ventana en la figura 1 bloque (8).

ES 2 334 551 B1

REIVINDICACIONES

1. Método para determinar la velocidad angular en un motor conmutado mecánicamente midiendo únicamente la corriente que circula por el mismo dentro de un sistema **caracterizado** por constar de un sistema de alimentación del motor (1), un motor (2), un sensor de corriente tipo shunt (3) para medir el valor de la corriente que circula por el motor (2), un convertidor analógico/digital (4) para digitalizar el valor de la corriente a una frecuencia de muestreo f_s adecuada y un microcontrolador, DSP o DSC para el procesado de las muestras digitales de la corriente y obtención del valor de la velocidad de acuerdo con las siguientes etapas:

a) Los valores muestreados de la corriente son recogidos por el bloque Detector Máximo (4) donde son almacenados en una memoria configurada como un registro de desplazamiento de tamaño w en el que la última muestra adquirida se almacena en la posición 0, la anterior en la posición 1 y así sucesivamente. El tamaño del registro de desplazamiento w se caracteriza por ser un valor impar mayor o igual que 3 e inferior al número de muestras que entran en un periodo ripple f_{ripple}/f_s, donde f_s es la frecuencia de muestreo. Sobre el registro de desplazamiento se comprueba si el valor máximo se encuentra en la posición central del registro de desplazamiento (w-1)/2. Si es así una señal indica que se ha detectado una ondulación.

b) Cada vez que se detecta una ondulación el bloque Detector de Frecuencia (6) registra el instante temporal en el que se ha detectado. Siendo el instante de la última ondulación T_k y el de la ondulación anterior T_{k-1}. Con los instantes de las ondulaciones se obtiene el valor de la frecuencia ripple como el inverso de la diferencia entre ambos instantes.

c) Posteriormente, con la frecuencia ripple el bloque Convertidor Frecuencia-Velocidad (7) obtiene la velocidad angular del motor mediante la ecuación que relaciona ambas magnitudes:

$$n = \frac{60 \cdot \eta \cdot f_{ripple}}{2p \cdot k}$$

$$\eta = m.c.d.\{2p, k\}$$

Donde n es la velocidad angular del motor expresada en revoluciones por minutos, 2p es el número de polos del motor, k es el número de delgas del colector de delgas, η es el máximo común divisor de 2p y k y f_{ripple} es la frecuencia ripple.

2. Método para determinar la velocidad angular en un motor conmutado mecánicamente midiendo únicamente la corriente que circula por el mismo según la reivindicación 1 donde el tamaño del registro de desplazamiento w se calcula de forma dinámica, de acuerdo con los requisitos indicados en la reivindicación 1 y siendo w proporcional al periodo ripple, inverso de la frecuencia ripple:

$$w = 2\left[c \cdot \frac{f_s}{f_{ripple}}\right] + 1 \qquad \frac{f_{ripple}}{f_s} < c < \frac{1}{2}\left(1 - \frac{f_{ripple}}{f_s}\right)$$

Donde el operando [·] es la parte entera y c es un factor fijo que determina el valor de ruido a filtrar. Para frecuencias de muestreo mucho mayores que la frecuencia ripple c puede tomar valores entre 0 y 0,5.

3. Método para determinar la velocidad angular en un motor conmutado mecánicamente midiendo únicamente la corriente que circula por el mismo según la reivindicación 1 donde la indicación de que se ha producido una ondulación se lleva a cabo comprobando sobre el registro de desplazamiento si el valor mínimo, en lugar del máximo, se encuentra en la posición central del registro de desplazamiento.

4. Uso del procedimiento descrito para medir y controlar la velocidad de piezas que se mueven solidarias al eje de un motor de corriente continua conmutado mecánicamente.

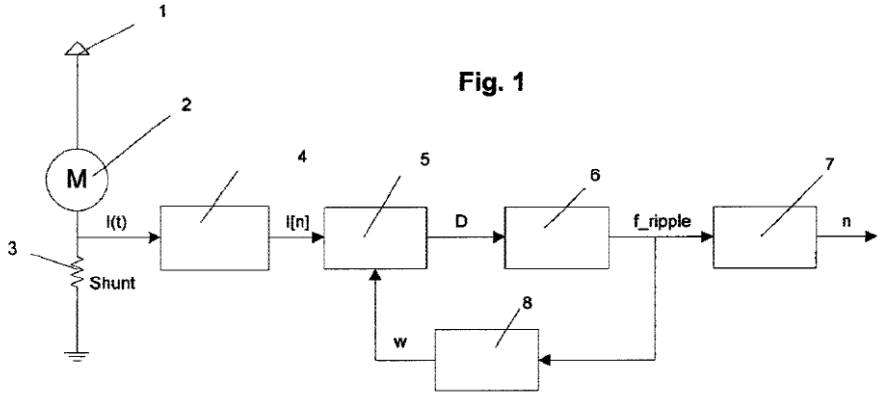
1
2
M
I(t)
3
Shunt
4
I[n]
5
D
6
f_ripple
7
n
8
w

Fig. 1

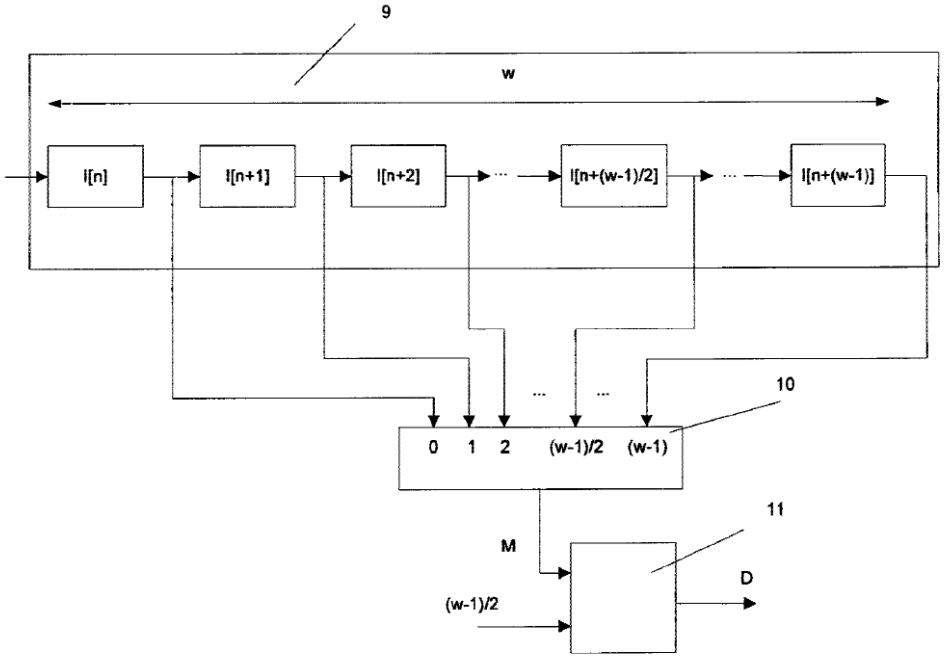
9
w
I[n]
I[n+1]
I[n+2]
I[n+(w-1)/2]
I[n+(w-1)]
10
0
1
2
(w-1)/2
(w-1)
11
M
(w-1)/2
D

Fig. 2